One-Dimensional Coordination Polymers: Complexity and Diversity in Structures, Properties, and Applications

Wei Lee Leong† and Jagadese J. Vittal*,†,‡

Department of Chemistry, National University of Singapore, Singapore 117543, and Department of Chemistry, Gyeongsang National University, Jinju 660-701, South Korea

Received May 28, 2010

Contents

1. Introduction

Crystal engineering of coordination polymers, which involves self-assembly of organic ligands with appropriate functional groups and metal ions with specific directionality

* To whom correspondence should be addressed. E-mail: chmjjv@nus.edu.sg.
† National University of Singapore.
‡ Gyeongsang National University.

10.1021/cr100160e
Published on Web 08/30/2010

Wei Lee Leong received her bachelor's degree in chemistry from Universiti Teknologi Malaysia in 2004. She joined National University of Singapore to do her PhD studies under the supervision of Professor Jagadese J. Vittal and obtained her PhD degree in 2009. Her research interests focus on inorganic materials, in particular the supramolecular chemistry of coordination polymers in the solid state and fabrication of coordination polymeric gels.

J. J. Vittal was born in Koothur, India. He received his BSc in 1975 from the University of Madras, MSc in 1977 from Madurai University, and PhD in 1982 from Indian Institute of Science, Bangalore, India. After completing his postdoctoral stint at the University of Western Ontario in Canada, he stayed there to manage the X-ray Structure Facility at the Department of Chemistry. He then moved to Singapore in 1997, and he is currently Professor in the Department of Chemistry, National University of Singapore. He is also a World Class University Chair Professor at the Department of Chemistry, Gyeongsang National University, Jinju, South Korea. J. J.'s broad research interests include inorganic materials and inorganic crystal engineering. He has been investigating solid-state supramolecular transformations, hydrogen-bonded coordination polymers, photochemical reactivity in inorganic complexes and coordination polymers, coordination polymeric gel and fiber materials, and fabrication of nanoscale materials by various routes including single molecular precursor routes.

and functionality, is one of the facile routes to produce materials of technological importance.[1] The metal−ligand coordination bonds have been widely exploited in organizing molecular building blocks into diverse supramolecular architectures, making use of the strength of coordination bonds and directionality associated with metal ions.[2] The nonmolecular compounds in which the basic building blocks containing metal ions and organic ligands assemble infinitely leading to one-, two-, and three-dimensional networks are commonly known as coordination polymers or metal−organic frameworks (MOFs).[3]

Of these one-dimensional coordination polymer (1D CP), being the simplest topological type of coordination array, is found to be ubiquitous in nature and dominating the literature. The relative simplicity of the 1D chains and their ease of formation by self-assembly allow us to incorporate functional properties at the metal centers or in the backbone of the organic linkers very easily to develop strategies for engineering multifunctional polymeric materials.[2d]

In the first ever review on coordination polymers published in 1964, Bailar Jr. discussed a few basic principles to synthesize coordination polymers along with various inorganic polymers based on cyano, hydroxo, and halo bridging, which were mainly characterized by noncrystallographic techniques.[4] Since then several comprehensive and excellent reviews offered a wide range of topics in the area of 1D CPs over the past two decades based on the metal ions, spacer ligands, or particular structures.[5] To our knowledge, the last review mainly dealing with this 1D CP was by Chen and Suslick in 1993.[5a] Since then significant progress has been made in the structural and functional aspects of coordination polymers or MOFs in general. This has been attributed to the recent advancements in the X-ray crystallographic techniques that made the structural characterization of highly crystalline coordination polymers easier than ever before.

Reflecting this fact, the number of publications in this area of coordination polymers has grown from 515 hits until the end of 1993 to more than 5800 hits according to the recent SciFinder database search. Hence, it is not the intension of this review to provide a comprehensive collection of literature. Therefore, we attempt to cover literature from 1993 until the end of 2009. Of these, the major portion is occupied by the linear and zigzag 1D CPs. Inevitably, a number of structures will be excluded in this review. For this reason, this review rather focuses on the recent progress made on these two types of structures emphasizing on unusual packing and interesting properties with selected examples from the literature. At the outset we sincerely apologize to the authors for any omission of their contributions on 1D CPs.

2. Construction and Structural Motifs of 1D CPs

For the past two decades research in the coordination polymers with specific topologies is making excellent progress by virtue of the possible design of materials with specific electronic, optic, magnetic and catalytic properties. Despite a few cases wherein the molecules are assembled in a predetermined fashion, prediction of the connectivity of the metal ions and spacer ligands is largely considered to be serendipitous. This could be attributed to the poor understanding of the role played by various experimental conditions employed for the growth of the particular crystal, and other subtle attractive or repulsive forces that prevail in the crystal lattice. Coordination polymers of various structural motifs of 1D, 2D, and 3D are known to exist.[1] Of these, 1D CPs are considered to be the least interesting structurally, nevertheless they have been found to have interesting magnetic, electrical, mechanical, and optical properties. Moreover, noncovalent interactions between such 1D infinite chains can lead to the formation of interesting architectures. Some of the most common structural features of the 1D CPs are shown in Figure 1. The structural features of 1D CPs based on this classification are discussed in this review along with their properties, if any.

2.1. Linear Polymers

At a glance, it may be realized that the 1D linear CPs can easily be synthesized by design from linear spacer ligands coordinated to the metal ions in a linear (trans) fashion, and

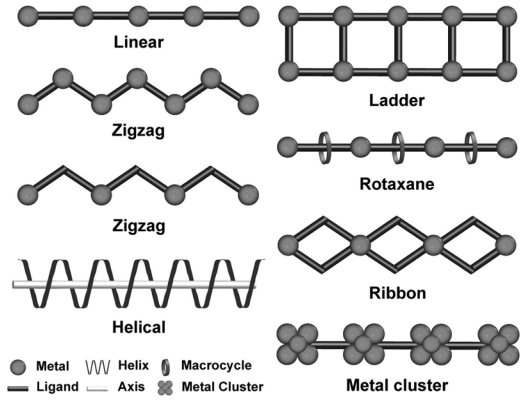

Figure 1. Various common conformations of 1D CPs.

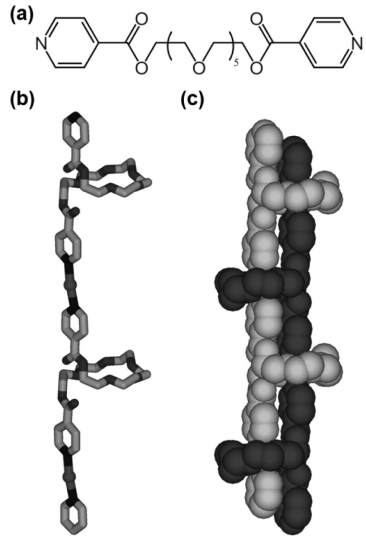

Figure 2. (a) Ligand structure. (b) Linear CP containing pseudocrown ether structure. (c) Double-stranded 1D chains hugging each other.

it is not surprising that there are numerous examples available in the literature on the linear CP structures.[6] Hence, we discuss how the packing of simple and common linear chains can result various fascinating structures and interesting functional properties of linear CPs in this section. As we mentioned earlier, it is not our intention to cover this area comprehensively.

2.1.1. Packing of Linear Chains

Hosseini et al. have reported few examples of linear CPs.[7] Of these only selected CPs with interesting packing are discussed here. In the double-stranded linear chain [AgL(ClO_4)] (L is shown in Figure 2a) the pyridyl groups of two different ligands with almost parallel and coplanar conformation coordinated to Ag(I) ions to form linear CP (Figure 2b). The hexaethylene glycol moieties adopt circular conformation and form a pseudocrown ether structure. Remarkably, all pseudocrown ether moieties are located on the same side of the CP chain. The disposition of the polyethylene glycol loops promotes interactions between Ag(I) ions of one strand and selected ether oxygen atoms of the other strand. As a result, two adjacent linear chains are hugging each other leading to a double stranded structure as shown in Figure 2c.[8]

An unsymmetrical ligand, 4-(2-(2,6-bis(methylthio)pyridin-4-yl)ethynyl) pyridine, has been shown to direct linear packing in parallel fashion but oriented in opposite directions

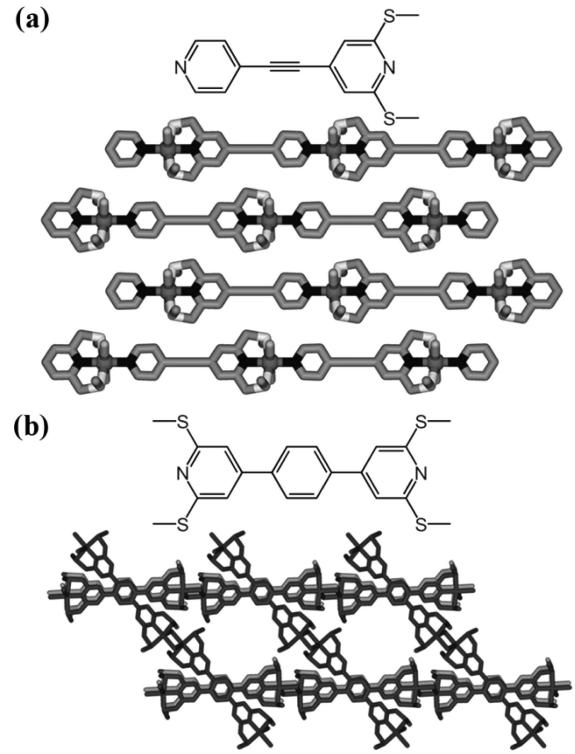

Figure 3. Structure of the ligands and packing of linear chains in (a) parallel and (b) inclined fashion.

(Figure 3a). Thus, the overall system is packed in a centrosymmetric fashion.[9] Another similar ligand, 4-(4-(2,6-bis(methylthio)pyridin-4-yl)phenyl)-2,6-bis(methylthio)pyridine, also forms linear CP with Hg(II) and pack in a parallel fashion into a layer. For consecutive layers, the 1D chains are tilted by 30° and generated large channels with a diameter of ~10.8 Å occupied by BF_4^- anions (Figure 3b).[10]

The [Cu(4,4′-bpy)] linear strands in [Cu(H_3hip)$_2$(4,4′-bpy)] (H_3hip = 5-hydroxyisophthalic acid; 4,4′-bpy = 4,4′-bipyridine) are heavily hydrogen-bonded through the H_2hip^- ligands forming ribbons. The ribbons run along two differently inclined directions related by the 2-fold rotation axes in the [Cu(4,4′-bpy)] chains. Because many different [Cu(4,4′-bpy)] chains contribute their H_2hip^- ligands to occupy each interchain space, the ribbons formed by H_2hip^- stack tightly, with three per cell along the *b*-direction and ribbon-to-ribbon spacing of 3.40 Å. Thus, along the *c*-axis, sheets of [Cu(4,4′-bpy)] chains alternate with sheets of stacked H_2hip^- ribbons, which themselves alternate in their direction of inclination (Figure 4).[11]

The linear polymeric chain in the complex [Ag(sebn)](AsF_6) (sebn = sebaconitrile/1,10-decanedinitrile) extend in three different noncoplanar directions generated by the 3-fold crystallographic axes to form 3D arrangement. It may be noted that there is no plane that can separate the whole array into two halves without breaking bonds, and only on slipping the chains the 3D arrangement can be disentangled.[12]

In [Cu(4,4′-bpy)(H_2O)$_3$(SO_4)]·2H_2O, the linear cationic chains are arranged in parallel and the adjacent layers are rotated by 60° to produce virtual hexagonal cavities in projection along the *c*-axis. The weakly coordinated sulfate anions occupy interchain positions and provide the appropriate charge balance. The water molecules of crystallization occupy these hexagonal channels (Figure 5).[13]

The linear chains of [Ag(pytz)(NO_3)] (pytz = 3,6-di(4-pyridyl)-l,2,4,5-tetrazine) are aligned in a parallel fashion

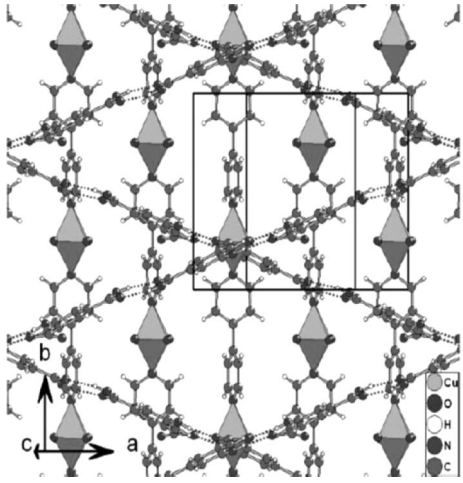

Figure 4. Inclined packing of linear ribbon chains. Reproduced with permission from ref 11. Copyright 2008 The Royal Society of Chemistry.

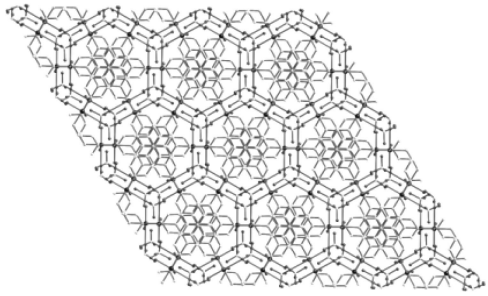

Figure 5. Stacking of polymeric chains to produce hexagonal cavities accommodating the 4,4′-bpy rings and lattice water molecules.

to form 2D sheets that stack along a 6_1 screw axis to give a helical staircase motif. The NO_3^- anions bridge adjacent chains through two of their oxygen atoms; each chain is related to the next by a 60° rotation and by a step of 5.18 Å, to generate the helical staircase motif. The point at which the chains cross each other one may consider these as the center of the helix, which corresponds to overlapping pyridine units. The corresponding PF_6^- and BF_4^- complexes exhibit ladder structures with the linear chains forming pairs that further linked through Ag···Ag and $\pi-\pi$ interactions between adjacent pytz ligands.[14]

Complex $[Co(bpbd)(NO_3)_2(H_2O)_2\cdot 2H_2O]$ (bpbd = 1,4-bis(4-pyridyl)butadiyne) displays a linear CP structure with two bpbd ligands coordinated in trans fashion. The linear chains are associated by hydrogen bonding interactions between the aqua ligand and nitrate anion of the other chains into pairs of chains. The side-by-side chain pairs do not interact and stack to form a layer. Interestingly, the pairs of chains crisscross in perpendicular fashion to pack as shown in Figure 6. Other related Cu(II), Co(II), and Cd(II) complexes exhibit 2D CP networks.[15]

The 1D linear chains in complex [Ni(hactdde)(1,4-btc)]·$4H_2O$ (hactdde = 1,3,5,8,10,12-hexaazacyclotetradecane-3,10-diethanol; 1,4-H_2bdc = 1,4-benzenedicarboxylic acid) are formed by Ni(II) macrocyclic complex and btc dianion. Interestingly, the linear 1D CPs are stacked and linked together by the hydrogen-bonding interactions between the pendent hydroxyl groups of the macrocycles belonging to one polymer chain and the secondary amines of the macrocycles belonging to the other polymer chain to give rise to

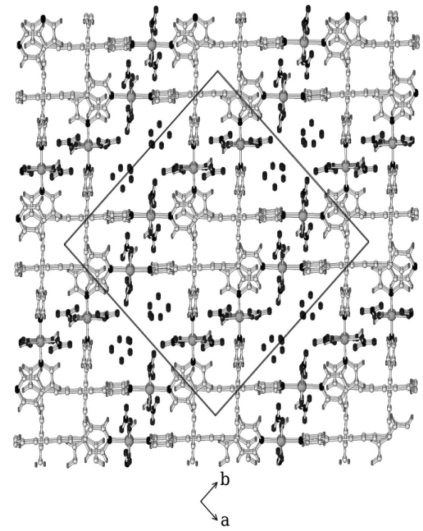

Figure 6. Packing diagram showing two crisscrossing layers of double chains in $[Co(bpbd)(NO_3)_2(H_2O)_2\cdot 2H_2O]$. Disordered water molecules located in the cavities are shown as isolated circles.

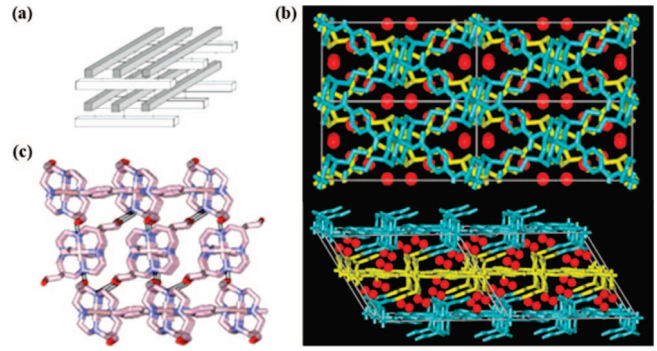

Figure 7. (a) Schematic diagram of the 3D network constructed from 1D chains (rods) by hydrogen bonding (dashed lines); (b) Views of [Ni(hactdde)(1,4-btc)]·$4H_2O$ in *ab*-plane (top) and *ac*-plane (bottom). The two different series of 1D chains are indicated in blue and yellow colors. Water molecules included in the network are represented as red spheres in CPK style; (c) Hydrogen-bonding interactions between two polymers. Adapted with permission from ref 16. Copyright 1999 American Chemical Society.

a 3D network. Figure 7 shows the hydrogen bonding interactions between CPs in the 3D network.[16]

Jin et al. have described a very unusual and interesting pipelike 1D polymer $[Ni_4(oba)_4(4,4'\text{-bpy})_4(H_2O)_4]\cdot(4,4'\text{-bpy})_2$ in which four linear 1D chains [Ni(oba)] (H_2oba = 4,4′-oxybis(benzoic acid)) are joined together by 4,4′-bpy ligands to form $[Ni_4(4,4'\text{-bpy})_4]$ square based hollow pipes. Hence, each Ni(II) is bonded to two oba ligands in trans manner, two 4,4′-bpy ligands in cis fashion, and terminated by two aqua ligands. The empty channel is filled by the uncoordinated bpy ligand. These pipes are further hydrogen-bonded with two more adjacent pipes between the water molecules and the carboxylate groups.[17] Unusual "sugar-coated" one-dimensional chiral CPs containing α-D-glucose-1-phosphate bridged by tetracopper(II) units have been described.[18]

2.1.2. Inclusion of Guest Molecules between the Linear Chains

Many types of guest molecules can be incorporated into the void space created by linear polymeric chains including solvent, anions, cations, and metal oxide clusters. Complexes $[\{Cu(4,4'\text{-bpy})\}_4Mo_8O_{26}]$ and $[Cu(4,4'\text{-bpy})_4Mo_{15}O_{47}]\cdot 8H_2O$

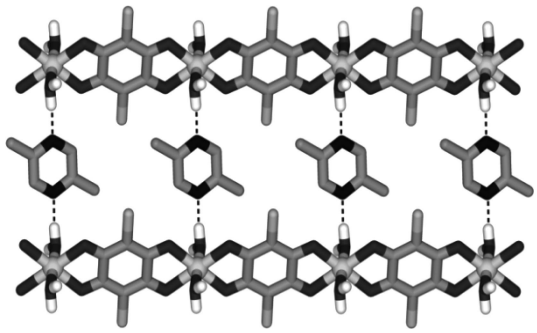

Figure 8. Intercalation of 2,5-dimethylpyrazine guest molecules with linear CP through N···H_2O bondings.

exhibit linear CP structures afforded by [Cu(4,4′-bpy)] and [$Cu(H_2O)_2$(4,4′-bpy)$_2$] units, respectively. The polyoxomolybdate clusters are sandwiched between the linear chains. The terminal oxo groups of [Mo_8O_{26}] display weak interactions with metal ions in polymeric chains. A related zigzag polymer [{$Ni(H_2O)_2$(4,4′-bpy)$_2$}$_2$$Mo_8O_{26}$] is found to encapsulate polyoxomolybdate clusters by forming covalent bonding between terminal oxo group and Ni(II) ions to generate a 2D framework.[19]

Kitagawa and co-workers have shown that [$Cu(ca)(H_2O)_2$] (H_2ca = chloranilic acid) polymeric chain is a good motif to control the intercalation of guest molecules such as 2,5-dimethylpyrazine and phenazine. The nearly coplanar linear chain is composed of Cu(II) bridging via bis-chelating ca. ligands. These chains are linked by hydrogen bonds between the coordinated water and the oxygen atoms of the ca ligand on the adjacent chain, forming extended layers, with guest molecules intercalated and supported with N···H_2O hydrogen bonding (Figure 8).[20]

An ion-pair 1D CP of [$Mn(H_2O)_{4.5}(CH_3OH)_{1.5}]_2$-{$Mn_2$(muia)$_2$}{$Mn_2$(muia)$_2(H_2O)_2$}·5$H_2O$ (H_3muia = 4-methylumbelliferone-8-methyleneiminodiacetic acid) has been reported to encapusulate solvated Mn(II) within the polymeric chains. The cations fall within the 1D anionic coordination polymeric strands and hold firmly through hydrogen bonding interactions (Figure 9a).[21] Another related Co(II) CP, [{$Co(H_2O)_4$}{Co_2(muia)$_2$ $(H_2O)_2$}]·11H_2O has been found encapuslated a hexameric water cluster within the polymeric chains. The 1D CP strands interact with neighboring strands and water molecules through hydrogen bonding to furnish a 2D network. Interestingly, a chairlike conformation $(H_2O)_6$ water cluster comprised of four lattice water molecules and two aqua ligands of $[Co(H_2O)_4]^{2+}$ is encapsulated within the crystal lattice between the 1D CP (Figure 9b). The cooperative interactions of cation−anion and hydrogen bonding have assisted such stabilization of water cluster in solid state.[22]

Reaction of 1,4-bis(4-pyridyl)anthracene with $Cu(NO_3)_2$ resulted in the formation of linear CP as a minor product and zigzag CP as the major product in one pot reaction. In the linear CP, two pyridyl groups and two nitrates are coordinated in a trans fashion at equatorial positions and one MeOH at apical position. The linear chains are linked together via O−H···O hydrogen bonds, between coordinated MeOH, encapsulated MeOH, and nitrate anion, to form a rectangular 2D grid network. The grid cavities are occupied by benzene molecules that are sandwiched between two anthracene moieties by edge-to-face aromatic interactions. Whereas, when pyridyl groups and nitrates are coordinated in cis fashion, a zigzag CP with a 2D hydrogen-bonded sheet

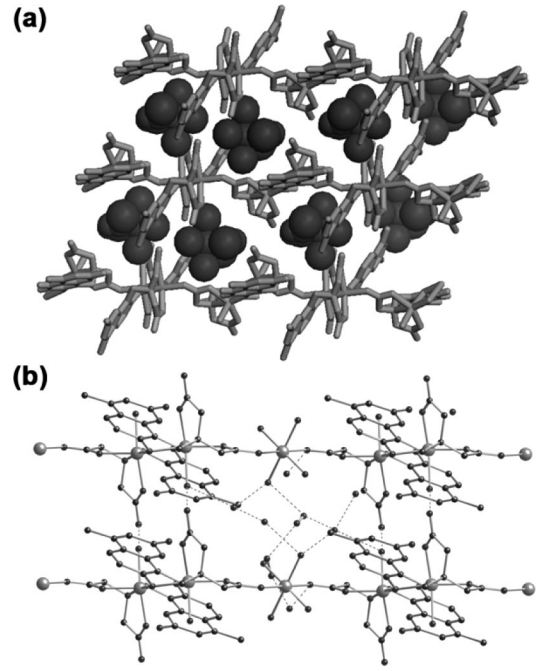

Figure 9. (a) Encapsulation of solvated Mn(II) cations within the 1D anionic polymeric strands. (b) Hexameric water cluster encapsulated in the 2D hydrogen-bonded network.

structure without encapsulated guest molecules is obtained. A similar reaction with $Ni(NO_3)_2$ afforded a mutually interpenetrated 2D grid structure.[23] In the 1D polymer [$Fe(btzx)_3$]X_2 (X = PF_6, CF_3SO_3 and ClO_4; btzx = *m*-xylylenebis(tetrazole) the building block is composed of three xylene-bis(tetrazole) ligands bridging two metal ions forming a cage where a number of counterions have been trapped. The influence of counterions on the spin-transition properties has been explored.[24]

On the other hand, 1D linear chains have been found to reside within the cavities constructed by various types of host modules. An inclusion complex [$(C_4AS)_2Ag_3$(μ−2,2′-bpy)$_2$(2,2′-bpy)$_2$] [Ag_5(μ-2,2′-bpy)$_4$(2,2′-bpy)$_4$]·20H_2O (2,2′-bpy = 2,2′-bipyridine, C_4AS = *p*-sulfonatocalix[4]arene) contains 1D linear polymeric chains of [Ag_5(μ-2,2′-bpy)$_4$(2,2′-bpy)$_4$] encapsulated within cavities built by *p*-sulfonatocalix-[4]arene-trisilver blocks. The trisilver blocks are composed of two calixarene units linked by trinuclear Ag_3(μ-2,2′-bpy)$_2$(2,2′-bpy)$_2$], and these trisilver blocks further forms hydrophobic layer. The intriguing feature is that the 1D polymer of [Ag_5(μ-2,2′-bpy)$_4$(2,2′-bpy)$_4$] is formed as counterion and occupies the cavities of trisilver blocks (Figure 10). Lattice water molecules form 1D infinite water belts parallel to 1D CP chains and serve as fences to entrap the CP. Since there is no $\pi-\pi$ stacking interactions observed here, such inclusion is likely due to the electrostatic and van der Waals interactions.[25] More examples of inclusion of linear CP will be discussed in sections 2.6 (rotaxane) and 6 (interpenetration).

2.1.3. Properties of Linear Chains

A linear polymer [$Zn(hfac)_2$(bmptfcp)] (bmptfcp = 1,2-bis[2-methyl-5-(4-pyridyl)-3-thienyl]-perfluorocyclopentene) shows an interesting photochromism in solid state attributed to the photoswitching ability of the ligand (Figure 11). In the complex, the distance between reactive carbons of bmptfcp is 3.557 Å and suitable for photoreaction. Upon irradiation with 366 nm light, single crystals of the complex turned blue because of the formation of the closed-ring

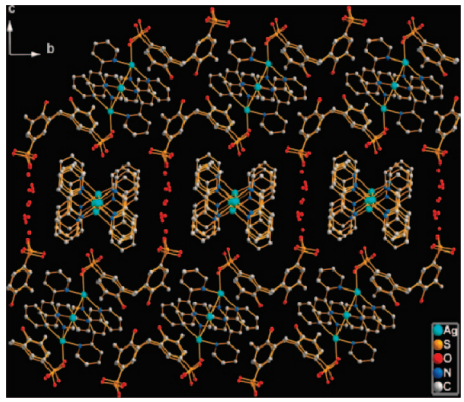

Figure 10. Clathrate-like structure, where the water belts acting as fences, isolate every two C4AS cavities into clathrate-like units, and then the 1D silver(I) chains reside in there. Reproduced with permission from ref 25. Copyright 2009 The Royal Society of Chemistry.

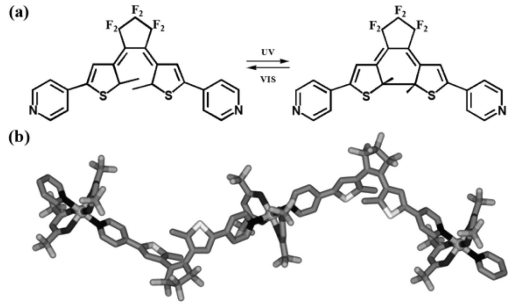

Figure 11. (a) Photochromism of bmptfcp ligand. (b) A view of linear polymer chain of open-ring form of $[Zn(hfac)_2(bmptfcp)]$.

isomer. Upon irradiation with 578 nm light, the blue color disappeared. It should be noted that there is no absorbance difference between the free ligand and the complex in solution state, but in the single-crystalline phase the absorption maximum of the complex showed a bathochromic shift attributed to an increase in the strain upon complexation.[26]

Suh's laboratory reported an interesting linear CP, $[Ni(cyclam)(bpydc)]\cdot 5H_2O$ (cyclam = 1,4,8,11-tetraazacyclotetradecane; H_2bpydc = 2,2′-bipyridyl-5,5′-dicarboxylic acid), that displays SCSC (single crystal to single crystal) transformation upon dehydration, accompanied by a fast color change of the crystal and hydrogen sorption properties. The bpydc ligand coordinated to marcocyclic Ni(II) ions in a bis-monodentate mode in trans position to form linear chains (Figure 12a). Three linear chains sustained by C−H···π and hydrogen bonding interactions are arranged into a framework with 1D channels having honeycomb-like openings (Figure 12b and c). Interestingly, this complex retains its single crystal nature after removal of the guest water molecules and turned pink color, while the porous framework structure remains intact, with slight changes on coordination spheres of Ni(II) center. When the dehydrated crystal was exposed to air or water vapor for few minutes, the structure transformed back to the original framework together with the color change. It is noted that the framework has high porosity, hydrogen storage ability and selective guest-binding ability. The complex also selectively binds with ethanol, phenol, pyridine, and benzene in isooctane, which are guests that can form hydrogen bonds with carbonyl groups that are exposed to the channels.[27] Another interesting linear 1D CP $[Ni(cyclam)(bpdc)]\cdot 2py\cdot 6H_2O$ (cyclam = 1,4,6,8,11,13-hexaaza-6,13-dimethylcyclotetra-decane; H_2bpdc = 4,4′-biphenyl-dicarboxylic acid) shows permanent porosity and promotes the room-temperature formation of both silver nanoparticle/matrix composites as a redox catalyst.[28]

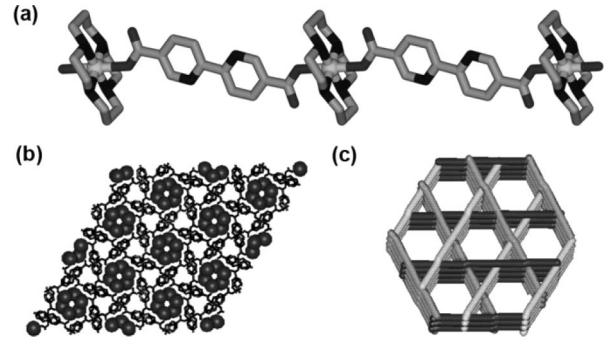

Figure 12. (a) Portion of linear chain in $[Ni(cyclam)(bpydc)]\cdot 5H_2O$. (b) Linear polymer chains extended in chains extending in three directions to generate channels to accommodate water guest molecules. (c) Schematic representation of stacking of the linear chains, which generates 1D channels.

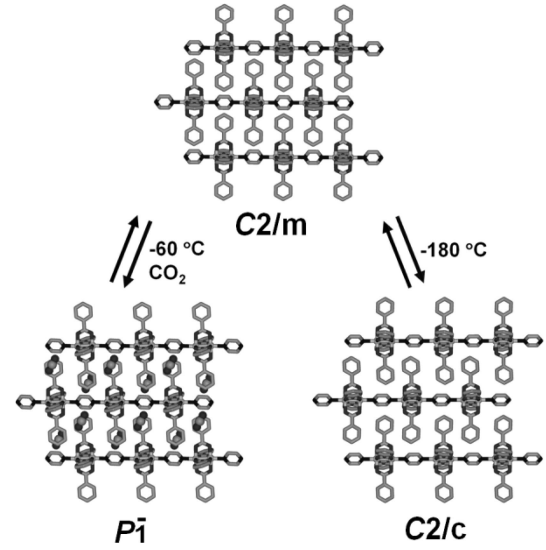

Figure 13. Schematic diagram showing the transformation of complex $[Rh_2(O_2CPh)_4(pyz)]$ upon inclusion of CO_2.

Complex $[Rh_2(O_2CPh)_4(pyz)]$ (pyz = pyrazine) features an interesting structural transformation upon inclusion of CO_2 (Figure 13). The polymer contains a paddle-wheel repeating unit of $[Rh_2(O_2CPh)_4]$ bridged by the pyrazine group in the axial positions. At 20 °C, the complex crystallizes in the monoclinic space group *C*2/*m*, and there are no channel structures sufficient to hold guest molecules, but rather, there are empty cages with dimensions of 9 × 4 × 3 Å^3. On cooling samples to −60 °C in a CO_2 atmosphere, the crystal underwent a phase transition to the triclinic space group $P\bar{1}$, and generated the 1D channels. The cages are transformed into channels by a slippage of the chain skeletons along the chain vector. External CO_2 is incorporated into the channels in the form of molecular wires. The large Brunauer−Emmett−Teller (BET) surface area of 274.1 m^2 g^{-1} indicates that CO_2 gas is adsorbed on the crystal surface and inside the crystal. Under conditions in which CO_2 is absent, the space-group symmetry changes from *C*2/*m* to *C*2/*c* on cooling to −180 °C, and the crystal exhibits a channel structure with a narrow neck of ∼2 Å diameter, which is too narrow for atmospheric gas to be adsorbed. However, the *C*2/*c* crystal can smoothly adsorb N_2 gas in the microporous region at 77 K with a large BET surface area of 352.5 m^2 g^{-1}. It is proposed that on

depressing thermal vibration as the temperature decreases, a perfect face-to-face overlap of the benzene planes in the α phase changes to an offset configuration with tilting of the rings in phases β ($P\bar{1}$) and γ ($C2/c$) favored.[29a] The similar strategy has been adopted for the inclusion of O_2 in another report.[29b]

A 1D rigid linear CP $[Cu(pySO_3)_2(4,4'\text{-bpy})]\cdot H_2O$ ($HpySO_3$ = 2-pyridine-sulfonic acid) has been shown to exhibit SCSC transformation and reversible small guest molecules exchange. The adjacent linear chains run parallel and interdigitated to form 2D grid structure through $\pi-\pi$ stacking and C−H···π interactions. These layers are further stacked into a 3D framework with 1D channels through C−H···O interactions. As evidenced by single-crystal X-ray diffraction studies, the porous structure is architecturally robust when it reversibly uptakes water molecules and exchanges small guest molecules (MeOH, *i*-PrOH) from solution. Moreover, the solid displays irreversible benzene and toluene vapor sorption behaviors because of a widening of the channel cross-section, resulting from the dynamic and "soft" supramolecular framework.[30]

In the 1D CP structure of a pink copper(II) bispyrazolate, $Cu(pyz)_2\cdot H_2O$ as determined by ab intio X-ray powder diffraction methods revealed the presence of square planar CuN_4 core with very weakly perturbed by Cu···O contacts from lattice water. This geometry at Cu(II) has been maintained even when the water is removed by heating, and the beige β-$Cu(pyz)_2$ instead of transforming to the previously known green α-$Cu(pyz)_2$ with tetrahedral CuN_4 core. Interestingly, when β-$Cu(pyz)_2$ was exposed to the vapors of NH_3, $MeNH_2$, CH_3CN, pyridine, MeOH, or EtOH, the corresponding solvates are formed.[31]

The magnetic properties of 1D chains have been very well explored by laboratories of Miller, Gao, Yamashita, and others. For example, a linear 1D polymer formed between *meso*-tetraphenylporphinatomanganese(II), and tetrachloro-1,4-benzoquinone shows ferromagnetic behavior.[32] A similar system also shows the same behavior in addition to a second-order phase transition.[33] There are a number of publications dealing with magnetic properties of 1D polymers.[34]

Gao et al. investigated the magnetic property of an interesting (μ-nitrido-diruthenium)-bridged 1D CP formed between $K_5[Ru_2N(CN)_{10}]$ and $[Cu(en)_2](ClO_4)_2$ (en = 1,2-diaminoethane), which exhibits a weak ferromagnetic interaction between the Cu(II) ions.[35] Whereas structural and magnetic studies on a series of hydrogencyanamide bridged 1D CPs built from Mn(III) and various tetradentate Schiff base ligands show that the asymmetric NCNH bridge transmits antiferromagnetic interaction between Mn(III) ions and favors the weak ferromagnetism caused by spin canting. However, these complexes exhibit different magnetic behaviors at low temperatures.[36]

Linear CP $[Fe(aqin)_2(4,4'\text{-bpy})](ClO_4)_2\cdot 2EtOH$ (aqin = 8-aminoquinoline) shows spin crossover phenomena when cooled down from room temperature to −193 °C. At 20 °C, the rigid 4,4′-bpy ligands link the Fe centers with Fe···Fe distance of 11.485 Å. The adjacent polymeric chains are linked via hydrogen-bonding interactions between perchlorate anions and aqin ligands and packed into sheets with slight interchain $\pi-\pi$ stacking interactions (3.74 Å). Upon cooling to −193 °C, a high spin−low spin (HS-LS) conversion is occurred and the main structure of the complex is retained. Nonetheless, the Fe−N bonds are shorter by about 0.2 Å, Fe−Fe distances become shorter (11.47 Å), and unit cell volume is decreased by 6.63%. Variable-temperature magnetic susceptibility measurements revealed a relatively abrupt HS-LS spin transition, with $T_{1/2} = -53$ °C (temperature for which the HS fraction is equal to 0.5).[37] Such spin crossover properties have been observed in 1D CPs also.[38,39]

The bromo-bridged linear CP $[Ni(S,S\text{-bn})_2Br]Br_2$ (*S*,*S*-bn = 2*S*,3*S*-diaminobutane) displays a strong antiferromagnetic interactions and spin-Peierls transition below −153 °C, which was shown by magnetic susceptibility and ^{81}Br nuclear quadruple resonance spectroscopy. Electrostatic carrier doping has been achieved by using a field-effect transistor (FET) device. This compound also showed *n*-type semiconductor behavior, which can be rationalized by the existence of a small amount of Ni(II) impurities acting as conductive carriers.[40] Such 1D CPs are known as quantum wires as they possess properties such as spin density wave (SDW) and charge density wave (CDW) in organic conductors, solitons, polarons, and bipolarons in p-conjugated polymers, gigantic third-order nonlinear optical properties.[41] The structural and spectroscopic characterization of a carboxylate-bridged uranium(VI) linear CP that possesses a rare bent (cis) dioxido unit with an extraordinarily acute (70°) O═U═O bond angle was described by Duval and co-workers. Interestingly, the *cis*-dioxido geometry confers different electrochemical, photochemical, and solubility behavior. This cis-dioxido geometry is expected to contribute to new separations strategies.[42]

Leznoff reported the synthesis and structures of a series of CPs of the form $[M(terpy)M'(CN)_{2\ 2}]\cdot xH_2O$ (M = Pb, Mn; M′ = Ag, Au; terpy) = 2,2′;6′2″-terpyridine; × = 0, 0.5) showing high birefringence (the nonzero difference in the refractive index of a crystal in two perpendicular directions), with Δn values exceeding twice that of calcite. Of these, Mn(II) derivative is linear 1D CP with face-to-face alignment of the terpy molecules.[43]

An interesting semiconducting 1D CPs based on bi(dithiolato) ligand, $C_4S_6^{2-}$ was reported by Rauchfuss and co-workers.[6w] Among a series of Te−Ru−Cu carbonyl complexes reported by Shieh et al., a rare −Cu−Cu−Cl-connected Te−Ru infinite chain polymer, $[PPh_4]_2[Te_2Ru_4(CO)_{10}Cu_4Br_2Cl_2]\cdot$THF has semiconducting properties with a small band gap of approximately 0.37 eV.[6x]

2.2. Zigzag Polymers

Zigzag type conformation is also ubiquitous in 1D CPs. The construction of zigzag CPs stemmed from flexible exoditopic ligands and linear or cis-coordinated octahedral metal centers or tetrahedral metal ions. Simple zigzag chains can be transformed into higher dimensional aggregates through supramolecular interactions, such as hydrogen bonding, $\pi-\pi$ stacking and argentophilic interactions. Sometimes, counteranions also link the adjacent polymeric chains into 2D and 3D aggregates. Several examples are shown in this section to demonstrate how 1D zigzag CPs can furnish supramolecular 2D and 3D network structures.

2.2.1. Packing of Zigzag Chains

Morsali and co-workers have reported a series of zigzag Zn(II) CPs of rigid and flexible organic nitrogen donor-based ligands including 4,4′-bpy, 1,2-bis(4-pyridyl)ethane (dpe), 1,2-bis(4-pyridyl)ethene (bpe), 1,3-di(4-pyridyl)propane (bpp), 1,4-bis(4-pyridyl)-2,3-diaza-1,3-butadiene (4-bpdb), and 1,4-bis(3-pyridyl)-2,3-diaza-1,3-butadiene (3-bpdb). It has been

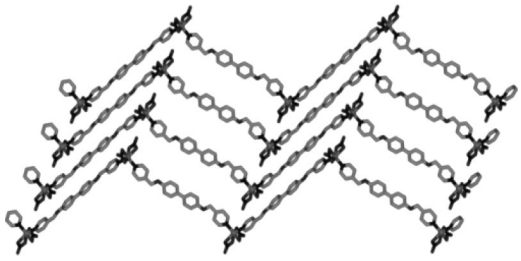

Figure 14. View of a two-dimensional layer in $[Co(bpmbp)(NO_3)_2]$ formed via $\pi-\pi$ stacking interactions.

shown that the nitrite anion may be suitable choice for preparing 1D CPs because higher-dimensional CPs have been reported for Zn(II) with these ligand but with different anions.[44]

A zigzag CP $[Co(bpmbp)(NO_3)_2]$ (bpmbp = 4,4′-bis(pyridin-4-ylmethoxy)biphenyl) composed of two types of bridging bpmbp ligands with different conformations alternately. The aromatic rings of first type of ligands are almost perpendicular, while in the second one they are almost parallel to the plane of the zigzag chain with dihedral angles of 81.5° and 4.3°. A 2D layer is formed via $\pi-\pi$ stacking interactions involving the former type of ligands as shown in Figure 14.[45]

Complex $[Mn(bda)(phen)(H_2O)]\cdot n py\cdot nH_2O$ (H_2bda = 4,4′-biphenyldicarboxylic acid; phen = 1,10-phenanthroline; py = pyridine) displays zigzag polymeric structure with each bda located on the inversion center and joins two Mn(II) into zigzag chain. The adjacent zigzag chains are arranged in an antiparallel fashion and cross-linked by interchain hydrogen bonding interaction between aqua ligands and carboxylate groups to generate a 2D hydrogen-bonded corrugated layer. The 2D layers are further stabilized through $\pi-\pi$ stacking interactions between interlayer phen rings into 3D framework. On the other hand, the reaction in piperazine has resulted in a linear CP with inclusion of piperazine guest molecules. The intrachain Mn atoms are in the linear form and phen ligands are decorated on the same side of CP chain.[46]

Complex $[Ag_2(dps)_2](ClO_4)_2\cdot MeCN$ (dps = 4,4′-dipyridylsulfide) exhibits zigzag polymeric structure. The adjacent polymeric chains are aligned parallel by facial $\pi-\pi$ interactions (centroid-to-centroid distance, 3.68 Å). The weak Ag···O and Ag···S interactions seem to neutralize the charge on Ag(I) ions to bring them closer with moderate Ag···Ag distance of 3.24 Å. Interestingly, the Ag···Ag interactions afford a zigzag double-stranded structure. The adjacent double-stranded chains are bridged by perchlorate anions via Ag···O interactions and further stabilized by alternate Ag···S interactions to form a sheet-like structure. A pseudosupramolecular polymorph shows double-stranded zigzag chain structure through acetonitrile bridging. There is only weak $\pi-\pi$ interactions (centroid-to-centroid distance: 3.835 Å) and no Ag···Ag and Ag···S interactions between polymeric chains. Analogous $[Zn(dpds)(CH_3COO)_2]$ exhibits single stranded zigzag chain structure and form 2D sheet via hydrogen bonding interactions.[47] The Ag−Ag interaction has been observed between zigzag CP chains to furnish 2D sheet structures.[48]

Puddephatt and co-workers have reported an interesting packing of zigzag CP $[Pd(dppp)(dpbdc)](CF_3SO_3)_2$ (dpbdc = *N*,*N*′-di(4-pyridyl)-1,3-benzenedicarboxamide, dppp = 1,3-bis(diphenylphosphino)propane) into a laminated sheet. The bridging ligand dpbdc adopts an unusual conformation in which the amide groups are displaced to opposite sides of the central C_6H_4 group to give a stretched conformation. There exist a short-range helicity induced by the bridging ligands dpbdc and, though all palladium atoms are crystallographically equivalent, neighboring centers have opposite chirality so that the polymer has the unusual syndiotactic structure. Adjacent polymer chains are arranged with all NH groups directed inward and CO groups directed outward, such that direct CNO···HN hydrogen bonding between adjacent chains is not possible. Instead one triflate anion bridges between two NH groups from neighboring chains. The second triflate anion is not involved in hydrogen bonding. By symmetry, two chains cross each bridging ligand, and the overall result is a laminated sheet structure with the triflate ions sandwiched in the center.[49]

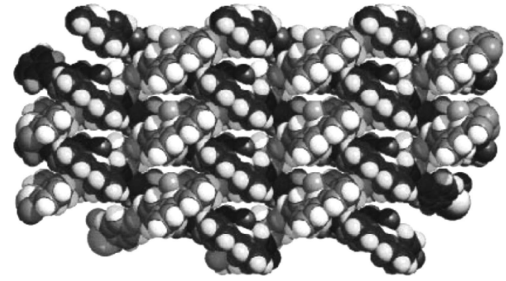

Figure 15. Warp-and-woof sheet in $[Cu(2,2'\text{-bpy})(azpy)(H_2O)]\cdot NO_3\cdot H_2O$. Reproduced with permission from ref 51. Copyright 2000 The Royal Society of Chemistry.

In complex $[Zn(2,2'\text{-bpy})(1,4\text{-bdc})]\cdot(2,2'\text{-bpy})$, each 1,4-bdc group acts in a bis-bidentate mode and bridges two zinc atoms, resulting in zigzag CP chains with additional 2,2′-bpy ligands found alternately on both sides. Two strong complementary C−H···O hydrogen bonds form a double-linked C−H···O hydrogen bond interaction which further extends CP chains into undulating layer with all lateral 2,2′-bpy ligands parallelly displaced and intercalated in a zipperlike mode. The undulating layers further extends into a 3D supramolecular network featuring 1D nanosized saddle-like channels through C−H···O hydrogen bond. The guest 2,2′-bpy molecules reside in the channels and exhibit an intermolecular parallel-displaced stacking geometry (3.5 Å) between themselves.[50]

2.2.2. Entanglement of Zigzag Chains

Ciani and co-workers have investigated the construction of CPs using $[Cu(2,2'\text{-bpy})]^{2+}$ with different dipyridyl-based spacer ligands including 4,4′-bpy, *trans*-4,4′-azobis(pyridine) (azpy), dpe, bpe, bpp, pyz, and *iso*-nicotinatic acid (Hnic). Depending on the length of the rod-like spacer ligands, the zigzag chains propagate with varied periods. The zigzag CPs can be extended into higher dimensional architectures via hydrogen bonding and $\pi-\pi$ stacking interactions. More interestingly, they also discovered the first example of 1O/1U (one over/one under) interwoven 2D structure in a 1D rigid zigzag CP, $[Cu(2,2'\text{-bpy})(azpy)(H_2O)]\cdot NO_3\cdot H_2O$. The zigzag polymeric chains propagate along [110] and $[1\bar{1}0]$ directions to generate warp-and-woof like 2D sheet as shown in Figure 15. The warp-and-woof layers are superimposed along the [001] direction with an ABAB sequence, and each layer is interdigitated with the two adjacent (upper and lower) ones, giving $\pi-\pi$ stacking interactions involving the 2,2′-bpy ligands to generate a 3D array.[51]

Later, Loye et al. reported the first 2O/2U interwoven 2D network assembled from 1D zigzag chains in complex

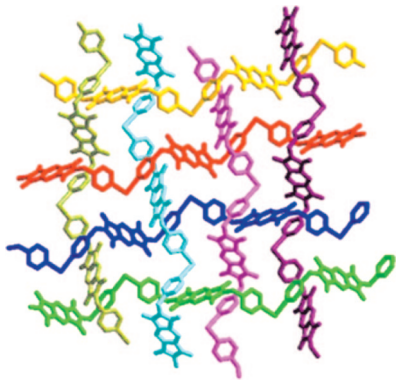

Figure 16. View of 2O/2U interwoven 2D network in [HgI_2(bpmbpt)]. The independent chains are distinguished by different colors. Reproduced with permission from ref 52. Copyright 2003 The Royal Society of Chemistry.

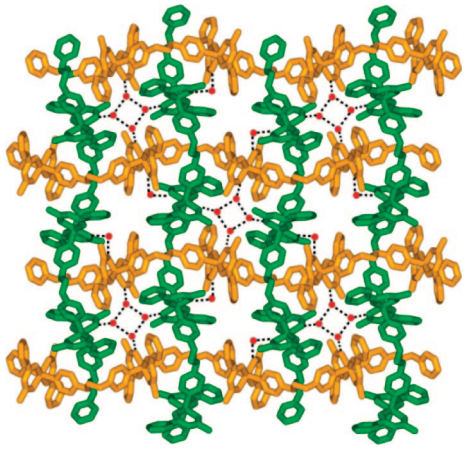

Figure 17. View of hydrogen bonding interactions between 2D interwoven network and guest water molecules.

[HgI_2(bpmbpt)] (bpmbpt = 2,6-bis(4-pyridinylmethyl)-benzo[1,2-*c*:4,5-*c*′]dipyrrole-1,3,5,7(2H,6H)-tetrone). The zigzag chains propagate in perpendicular directions to interweave in a 2O/2U fashion to generate cloth-like sheet structure as shown in Figure 16. At each Hg(II) ion, the two coordinated arms of the ligands pass either both above or both below two other perpendicular 1D chains.[52]

Another example of 2D interwoven network of zigzag chains has been observed in [$Zn(bac)_2(bpp)$]·1.5H_2O (bac = 1-benzoylacetone). Here, the zigzag conformation stems from the ligand, rather than the metal center geometry. Indeed two bac ligands chelate the Zn(II) to form a plane and the bpp ligands bridge the metal center in trans manner but resulted in a flexible zigzag CP. The zigzag chains propagate in two nearly perpendicular directions, which enable them to interweave to generate 2D entangled network. Fascinatingly, the presence of square $(H_2O)_4$ clusters and lattice water molecules enforce the interwoven network through hydrogen bonding interactions (Figure 17). The warp-and-woof layers are superimposed with an ABAB sequence, and the stacking of all layers generates a 3D extended array with 1D channels.[53]

Another spiral 1D CP of [Pb(bpe)(CH_3COO)(CF_3COO)] has been shown to deliver a interwoven fabric structure in "warp and weft" fashion as shown in Figure 18. The spiral chains are approximately in parallel but crossing over the C═C bond in perpendicular directions. Since the middle of C═C bond in bpe also serves as inversion center, these bpe ligands are interlaced. All of the polymeric strands are laid

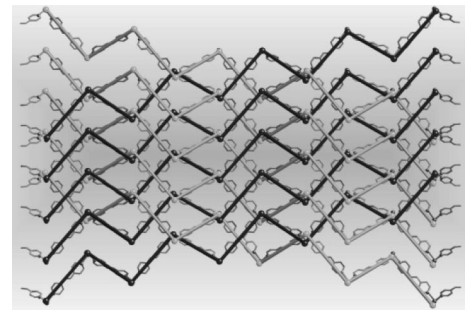

Figure 18. View of interwoven fabric structure in [Pb(bpe)-(CH_3COO)(CF_3COO)]. The polymeric chains are simplified in black and gray colors.

one over the other alternately with no observable weak interactions between the interlaced CP strands. This may be considered as the genuine molecular fabric structure without any weak interactions between the strands in the interwoven structure.[54]

The following is a rare example of 3D entanglement of zigzag 1D CPs containing channels. Complex [Zn(phen)(sdc)] (H_2sdc = *trans*-stilbene-4,4′-dicarboxylic acid) displays 1D zigzag polymeric structure through sdc ligands bridging. In this context, zigzag chains are holding together around the crystallographic 4-fold axes by $\pi-\pi$ interactions and propagate in four noncoplanar directions (Figure 19a−c). Two chains are interwoven into the warps-and-woofs cloth-like 2D sheet. Furthermore, two sets of 2D sheets are interlocked in perpendicular fashion to generate a 3D entangled framework with 1D channels (Figure 19d and e). The zigzag shape of polymeric chains are essential for the formation of 2D interwoven motif, while the aromatic groups in the ligands are responsible for 3D entanglement of the chains through $\pi-\pi$ stacking interactions.[55] Utilization of other terminal ligands such as pyridine, 2,2′-bpy and 2,2′-biquinoline also have resulted zigzag CPs which displayed hydrogen bonding or $\pi-\pi$ stacking interactions that assembled the zigzag chains into higher dimensional interpenetration or catenation.[56] Other related complexes [$Cu(sdc)(H_2O)(py)_2$]·2py and [$Cd(sdc)(phen)(H_2O)$]·H_2O display 1D linear[57] and zigzag[58] polymeric structures, respectively.

2.2.3. Properties of Zigzag Chains

Recently, zigzag 1D CP of [Zn(bepsac)]·guest (guest = benzene and toluene; H_2bepsac = (*R*,*R*)-(−)-*N*,*N*′-bis(3-*tert*-butyl-5-(4-ethynylpyridyl)salicylidene)-1,2-diamino-cyclohexane) with 3D supramolecular pores has been demonstrated as materials to separate aromatic−aliphatic mixtures, namely, benzene and cyclohexane, which are tedious to separate by conventional methods. Furthermore, this complex undergoes structural transformation in a reversible SCSC manner upon heating at 100 °C in the presence of guest vapors or guest exchange. The polymeric chains are stretchable because of the flexibility of [Zn(bepsac)] units and the distortable coordination geometry of the metal centers. The 1D polymeric chains are arranged in parallel fashion by strong interchain $\pi-\pi$ interactions to form 2D neutral rhombohedral grid which further stacked into 3D porous supramolecular structures to accommodate the guest molecules in the empty channels by weak guest−host CH···π and hydrophobic interactions. More interestingly, sorption studies revealed that these compounds are selective to benzene compared to cyclohexane despite their comparable molecule sizes, since cyclohexane unable to form strong

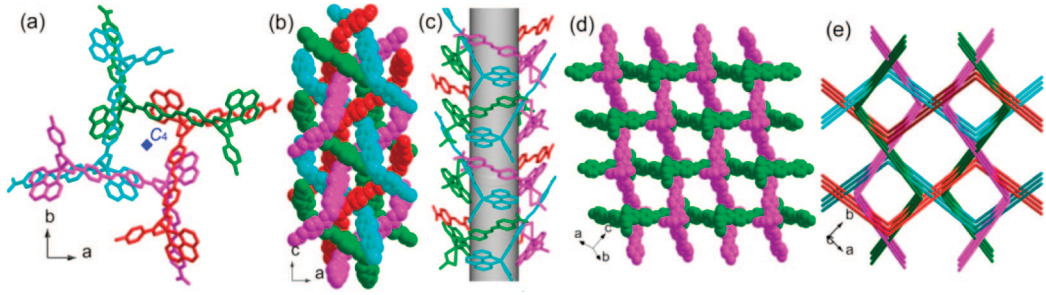

Figure 19. (a) Four 1D zigzag chains arranged around a 4-fold axis. (b) Entanglement of the chains. (c) $\pi-\pi$ stacking interactions around a channel. (d) View of 2D warp-and-woof weave sheet. (e) 3D entanglement of the 2D sheets.

enough supramolecular interactions with the hydrophobic pore surface.[59]

A zigzag 1D CP [Cu(H_2btec)(2,2′-bipy)] (H_4btec = 1,2,4,5-benzenetetracarboxylic acid) has been tested as a heterogeneous catalyst for the oxidation of cyclohexene and styrene, with *tert*-butyl hydroperoxide (tbhp) as oxidant. The catalytic activity for 24 h and at 75 °C shows a high value for the conversion of cyclohexene (64.5%), and a lower one for styrene (23.7%). The 1D CP seems to be efficient and selective from the high turnover frequency (TOF) values for the epoxide products.[60]

Xiong and co-workers have shown that a homochiral 1D wavelike CP, [(Hqa)($ZnCl_2$)(2.5H_2O)] (Hqa = 6-methoxyl-(8*S*,9*R*)-cinchonan-9-ol-3-carboxylic acid), exhibits a high dielectric constant (ε_0 = 37.3) and dielectric loss characteristic of a relaxation process. The complex displays a zwitterionic form with the *N* atom of the quinicludine ring is protonated. As a result of packing of wavelike chain produce the dipolar moment. Furthermore, the compound that belongs to polar point group (C_1, space group *P*1) shows second-harmonic-generation (SHG) active and exhibits a response that is approximately 20 times greater than that reported for KDP. Such a strong SHG response could be due to the presence of intramolecular charge separation, which could be due to the zwitterionic moiety generating a large dipole moment. In addition, the compound also shows a relaxation process in the dielectric loss measurement.[61] Complex [Cu(PPh_3)(ppma)]·ClO_4 (ppma = *N,N*-(2-pyridyl)(4-pyridylmethyl)amine), which crystallizes in a noncentrosymmetric space group (*Cc*), shows SHG active with an estimation of 1.5 times than that of urea. It is worth noting that free ligand fails to display SHG response, indicating that the packing may be in centrosymmetric space group, and more importantly, the coordination the free ligand to copper(I) results in the formation of acentric packing.[62]

Spin crossover behavior in a series of iron(II) zigzag coordination polymeric chains have been investigated.[63] Further, there are several examples of zigzag polymers dealing with different properties reported in the literature.[64]

2.3. Helical Polymers

Infinite helical structural motif has special place in supramolecular chemistry because of its similarities in biological systems and enantioselective catalysis. Generally, utilization of flexible or chiral ligands is a facile approach to achieve helical CPs, while many successful examples of spontaneous chirality induction from achiral ligands also have been widespread in the literature. Helical coordination polymers have been assembled from chiral or achiral building blocks. When achiral building blocks are used, usually both right- and left-handed helices have been obtained in equal amounts as racemates. In other cases, spontaneous resolution into enantiomeric chiral crystals has been achieved. In this section, helical CPs including single-, double-, triple-, and multiple-stranded are discussed in detail. We restrict our discussion to helical CPs only and finite helicates are not covered here. Excellent reviews on helicates are available elsewhere.[65] The design strategy of construction of helical CPs based on different types of bridging ligands has been discussed in an excellent review by Hong.[5c] Here, we will only highlight the literature published after this review and selected examples with unusual features. Recently, Lu has highlighted the general approaches for the construction of helical coordination compounds and correlation between the chirality of building blocks and the helicity of 1D chains, as well as the chirality transfer among the helices.[66a] In the context of helicity and chirality, the supramolecular interactions in the 1D CPs formed by the biomolecules including nucleic acids are very important. This was addressed in a book chapter by Zamora et al.[66b]

2.3.1. Single-Stranded Helices

Zaworotko and co-workers synthesized homochiral helical CP from the linear spacers 4,4′-bpy bonded to Ni(II) ions in a cis-geometry, [Ni(4,4′-bipy)($PhCOO)_2$($MeOH)_2$]·(guest)$_x$. They demonstrated the ability of helical coordination polymers with large chiral channels to host a series of organic guest molecules and showed that chiral crystals can be obtained from achiral components.[67,68]

Similarly, an achiral anthracene-pyrimidine derivative, namely, (5-(9-anthracenyl)pyrimidine (ap), forms homochiral helical strands with Cd(II) in [Cd(ap)($NO_3)_2$(H_2O)(EtOH)] in which the metal ion is hexacoordinated with two pyrimidine ligands occupying cis positions and with water and ethanol in equatorial cis geometry, and the axial positions are occupied by two nitrate ions. Interestingly all the crystals from each batch of crystallization were found to be homochiral as supported by circular dichroism measurements in Nujol mull. But the handedness changes with different crystallization badges. On the other hand, [Cd(ap)($NO_3)_2$(H_2O)].2H_2O having nonhelical zigzag chains due to trans geometry of the two pyrimidine ligands around the metal center. Further, this zigzag polymer can be converted to the chiral helical polymer upon exchange of water by ethanol or by seeding.[69] Similar helical chains obtained from achiral components have been realized in several other compounds also.[70] In a number of cases, both *P* (right) and *M* (left) helices have been found in lattice.[71]

The thermodynamically controlled formation of coordination polymers from racemic (*R*/*S*) ligands has yielded crystals containing either homochiral (isotactic or *S*,*S*,*S*/*R*,*R*,*R*) or heterochiral (syndiotactic or *R*,*S*,*R*,*S*) architectures. However, the heterotactic (*R*,*R*,*S*,*S*) architecture seems to be scarce in

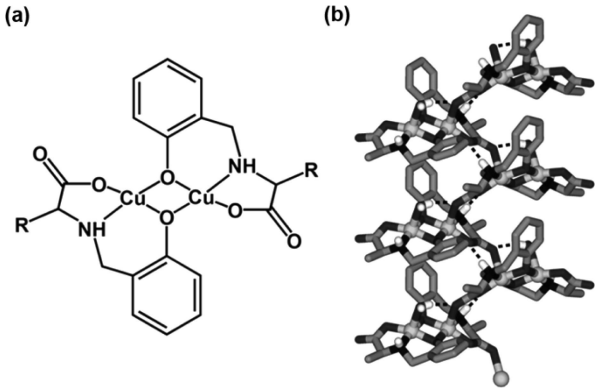

Figure 20. (a) Schematic diagram of the dinuclear building block. (b) Portion of the helical polymeric chain constituted by dinuclear building blocks.

coordination polymers. Wheaton and Puddephatt reported the heterotactic architecture in a gold(I) CP $[Au_2(binap)(4,4'\text{-bpy})](X)_2$, (binap = 2,2′-bis(diphenylphosphino)-1,1′-binaphthyl. For isotactic, *S*-binap and X = $CF_3CO_2^-$; for syndiotactic *R*/*S*-binap and X = $CF_3CO_2^-$; and for heterotactic, *R*/*S*-binap and X = NO_3) as well as the first direct structural comparison with the isotactic, syndiotactic, and heterotactic architectures. The switch from syndiotactic to heterotactic architecture is dependent on the anion used (trifluoroacetate versus nitrate).[72] There are some other examples available on such isotactic, syndiotactic to heterotactic chirality also.[73]

Reduced Schiff base ligands derived from salicyaldehye and amino acids have been found as good chelating ligands for Cu(II) ions. The reaction in molar ratio 1:1 often afforded dinuclear units through phenolate bridging through carboxylate oxygen atoms (Figure 20a). Further, these dinuclear building blocks can be self-assembled into helical CPs which are further sustained by O−H···O and N−H···O hydrogen bonds (Figure 20b). In the dinuclear moiety, one axial site is occupied by water while the other by an oxygen atom of the carboxylate group from the adjacent dimer to form 1D helical polymer.[74] Ternary complex of [Cu(2,2′-bpy)(Hsgly)]Cl·$2H_2O$ and [Cu(2,2′-bpy)(Hsala)]$(NO_3)\cdot 2H_2O$ also shows helical CP structures.[75]

Mak and co-workers have shown that the pitch length of the helical chains can be fine-tuned by the metal ions and counteranions. A series of complexes of 2-pyridinyl-3-pyridinylmethanone (ppm) have been structurally characterized, and these polymers displayed single-stranded helical

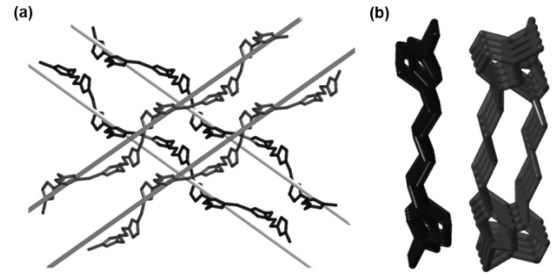

Figure 22. (a) View of the 1D helical chains in perpendicular arrangement. (b) Side view two helices with flat zigzag and spiral tube motifs. Adapted with permission from ref 77. Copyright 2008 American Chemical Society.

structures (Figure 21). The Ag(I) centers adopt linear coordination geometry with ppm ligands in bidentate anti bridging mode. The counteranions in the 2_1 helical Ag(I) complexes [Ag(ppm)X] (X = NO_3, PF_6, BF_4, ClO_4, CF_3CO_2, CF_3SO_3) are fully or partially embedded into the grooves of the helices. The pitch length depends on the size of the anion and its manner of docking into the groove of the helix. On the other hand, Cu(II), Co(II), and Zn(II) complexes display distorted octahedral geometries with ppm ligand in tridentate syn or anti bridging mode along with coordinated anion and solvent molecules. In Cu(II) complex, the helical chain is stabilized by intramolecular hydrogen bonding interactions between ClO_4^- and aqua ligand. In Co(II) and Zn(II) complexes, helical chains without anion embedment suggest that the pitch lengths are dominated by the size of the metal cations.[76]

Complex $[Cu_2(bimb)_2Cl_2]$ (bimb = 1,4-bis(imidazol-1-yl)-butane) contains left- and right-handed helical chains arranged in perpendicular directions (Figure 22a). This is unprecedented as compared to the common parallel arrangement of opposite handedness helical chains. Complex $[Co(mb)_2(bimb)]$ (Hmb = 4-methoxybenzoic acid) displays an unusual two distinct types of helical chains. Both types of helical chains have racemic enantiomers with same pitch length of 15.09 Å. The salient feature is that one helical shows an almost flat zigzag type motif, while the other exhibits a more spiral tube motif (Figure 22b).[77]

The cucurbituril (CB6) has been joined by two different Cu(II) complexes to form helical coordination polymers namely, $[Na_2(CB6)(H_2O)_2][Cu(I_2sal)(Hqs)]\cdot 6.5H_2O$ and $[Na_2(CB6)(H_2O)_2][Cu(Ibz)(Hqs)Cl]\cdot 5.5H_2O$ (H_2I_2sal = 3,5-diiodosalicylic acid, HIbz = 3-iodobenzoic acid, H_2qs = 8-hydroxyquinoline-5-sulfonic acid) with the assistance of

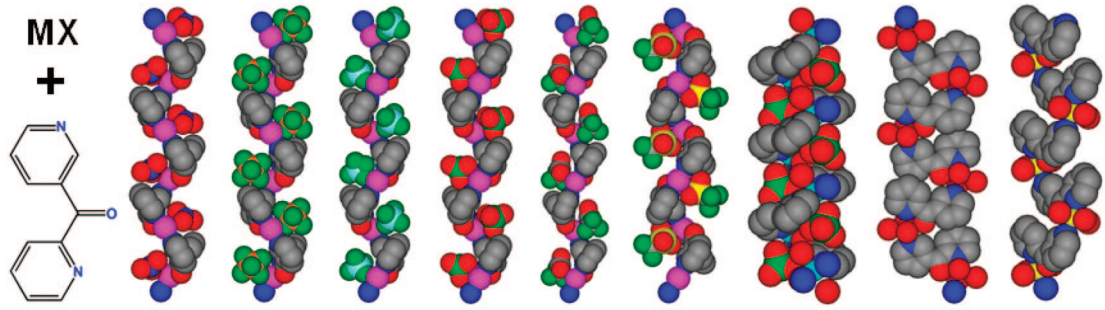

Metal (M)	Ag	Ag	Ag	Ag	Ag	Ag	Cu	Co	Zn
Anion (X)	NO_3	PF_6	BF_4	ClO_4	CF_3CO_2	CF_3SO_3	ClO_4	ClO_4	CF_3SO_3
Pitch (Å)	12.116	12.193	12.407	12.513	13.636	12.444	8.216	11.158	11.578

Figure 21. Tuning of helical pitch length by variation of counteranions.

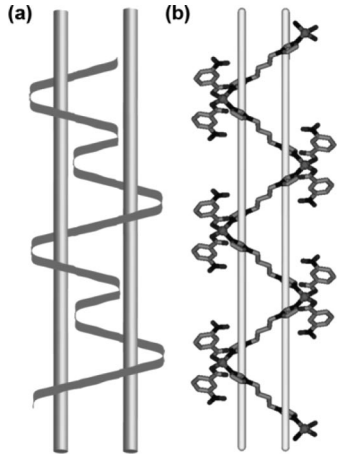

Figure 23. (a) Schematic diagram of a meso-helix. (b) Portion of meso-helical network in $[Co(nba)_2(bimb)]$.

iodo substituents. The iodine atoms at the backbone of the ligands appear to play an important role through selective shape matching interactions in the formation of helical structure.[78]

Apart from simple single helical strands, few examples of meso-helix CPs are also found in literature,[79] and some even furnish multiple stranded helices.[80] Just like circle can be converted into a helix by transforming it in the third dimension a meso-helix is a three-dimensional presentation of a lemniscate (Figure 23a). The ternary Co(II) and Ni(II) complexes of bimb or bix (bix = 1,4-bis(imidazol-1-yl-methyl)benzene) and substituted benzoic acid display similar meso-helical structures. The neighboring metal centers are bridged together via *trans* bis(imidazole) ligands, affording extraordinary meso-helical chains. These chains contain both left- and right-handed helical loops in each chain, and display a "∞" shape. Figure 23b shows a typical meso-helical network in $[Co(nba)_2(bimb)]$ (Hnba = 4-nitrobenzoic acid).[77]

Packing and interactions between helical chains often lead to interesting architectures, as well as higher-dimensional network structures. For instance, complex $[Ag(binn)(H_2O)]_3 \cdot (BF_4)_3 \cdot 2CHCl_3$ (binn = (*R*)-6,6′-dibromo-2,2′-bis(isonicotinoyl)-1,1′-binaphthalene) shows a rare packing mode in which the single-stranded helical chains are packed in the cubic crystallographic space group $I2_13$ near-neighboring helical rods arranged in an orthogonal disposition to one another (Figure 24).[81]

In the following sections, we will discuss how helical chains interact with each other to form multiple strand helices.

2.3.2. Double-Stranded Helices

There are double-helices without any observable intermolecular interactions between them. For example, in $[Ag(L)(PF_6)_2]$ (L is shown in Figure 25a), no $\pi-\pi$ stacking or hydrogen-bonding interactions between the two intertwined strands; however, these two chains are topologically inseparable (Figure 25b). On the other hand, $\pi-\pi$ stacking interactions between neighboring double helices and the electrostatic attractions between the cationic polymer and the anions facilitate molecular packing.[82] Similar double helices with no supramolecular contacts was formed in $\{[Zn_2I_4(tmdp)_2]\text{-}[Zn_2I_4(tmdp)_2]\}$ (tmdp = 4,4-trimethylenedipyridine), but the double helix is chiral although the tmdp ligand is achiral.[83] In the double helical polymer $[Ag(NO_2)(pdsi)]$ (pdsi = bis(4-

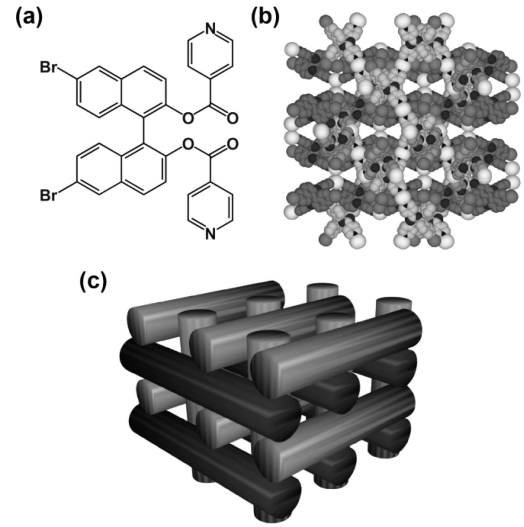

Figure 24. (a) Ligand structure. (b) Portion of the packed structure of the 1D helical network. (c) Schematic representation using cylindrical rods. Adapted with permission from ref 81. Copyright 2006 The Royal Society of Chemistry.

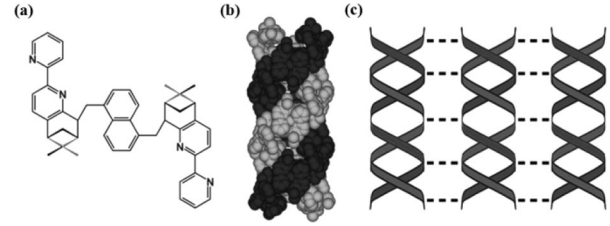

Figure 25. (a) Ligand structure. (b) Side view of double helical with no interactions between two strands. (c) Schematic representation of Ag···Ag interactions (shown in dashed lines) between double helices.

pyridyl)dimethylsilane), there is no observable supramolecular interactions between the strands. However the double helices are glued to each other through Ag···Ag interaction (3.002 Å) to form a sheet (Figure 25c). The Ag(I) ion is chelated by nitrite anion, two pyridyl groups in the helical chain, and Ag···Ag interaction.[84]

Intermolecular interactions have been successfully used to bring the single-stranded helices close to each other to create multiple-stranded helices. Chen et al. have exploited the $\pi-\pi$ interactions between aromatic rings of single-stranded helices to direct the formation of double-stranded helices. Complex $[Cu(1,3\text{-bdc})(2,2'\text{-bpy})] \cdot 2H_2O$ (1,3-H_2bdc = 1,3-benzenedicarboxylic acid) exhibits a single-stranded helical structure, while the phen analogue $[Cu_2(1,3\text{-bdc})_2(phen)_2(H_2O)]$ exhibits double-stranded helical structure through $\pi-\pi$ stacking. The phen ligands, which alternately attach to both sides of a single-stranded helical chain, are approximately in parallel and perpendicular fashion alternately. The perpendicular orientation of the phen ligands allows pairing of two centrosymmetrically related single-stranded helical chains through $\pi-\pi$ interactions to generate doubles-stranded zipper-like chain (Figure 26a). In another related double-stranded helical polymer [Cu(oba)(phen)] (H_2oba = 4,4′-oxybisbenzoic acid), the phen ligands are extended in a parallel fashion at both sides of a single-stranded chain with a face-to-face distance of 6.84 Å. Interestingly, two adjacent helical chains intertwine into a double-stranded helix through $\pi-\pi$ interactions between the phen ligands (Figure 26b) The distance between interstrand phen ligands in the double helix is 3.42 Å.[85] Nonetheless,

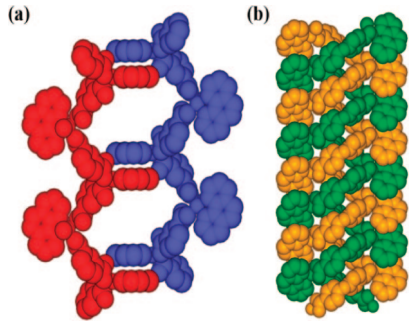

Figure 26. Formation of double-stranded helix through face-to-face $\pi-\pi$ interactions in (a) $[Cu_2(1,3\text{-bdc})_2(phen)_2(H_2O)]$ and (b) [Cu(oba)(phen)].

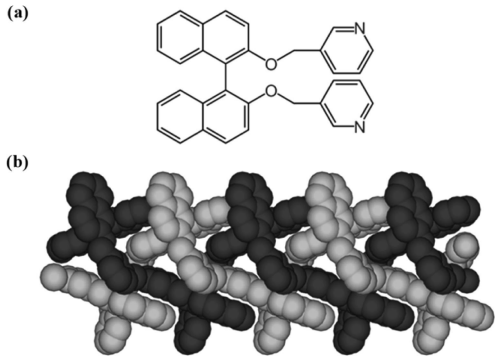

Figure 27. View of of double helical structure in $[Ag(bpmbn)(NO_3)\cdot H_2O]$.

not all $\pi-\pi$ interactions between adjacent helical chains produce double-stranded helix. For instance, the analogue Co(II) and Ni(II) helical CPs furnished wavy 2D layers by $\pi-\pi$ stacking.[86] The Zn(II) and Cd(II) complexes of 1,3-bdc exhibit 1D helical ribbon-like structures which further assembled into 3D networks by $\pi-\pi$ stacking interactions.[87]

The helical chain of complex $[Ag(bpmbn)(NO_3)\cdot H_2O]$ (bpmbn = (*S*)-2,2′-bis(3-pyridylmethyleneoxy)-1,1′-binaphthalene) also forms a double helical structure through $\pi-\pi$ stacking interactions between the pyridyl and naphthyl rings (3.84 Å). Such intermolecular $\pi-\pi$ stacking interactions stabilize the helical framework and furnish a double-helical structure with an adjacent Ag···Ag separation of 4.29 Å between different helical chains (Figure 27). Variation of nitrogen atom to 4-position has resulted another helical CP. In this case, the naphthyl rings on the same side of polymeric chains are separated by 7.12 Å. Hence, the adjacent polymeric chains are interdigitated in an alternate fashion which effectively fills in the voids.[88] The same ligand forms similar monohelical structure with Cd(II) in$[Cd(pbmbn)Cl_2(H_2O)]\cdot 0.5H_2O$, while a zigzag conformation in $[Zn(bpmbn)Cl_2]\cdot 0.5DMF\cdot 0.5H_2O]$.[89]

In complex $[Zn_2(tma)_2(H_2O)_6]$ (L-H_2tma = terephthaloyl-monoalanine), each [Zn(tma)] helical chain is twisted around another in a left-handed manner. Two such 1D helical chains are self-assembled into double helices through hydrogen bonds and $\pi-\pi$ interactions and adjacent double helices are further linked by hydrogen bonds between amide carbonyl and aqua ligand. It is worth noting that the helical folding pattern of [Zn(tma)] chains also is observed in the Cd(II) analogue, which displays a with 4-fold type [2 + 2] interpenetration diamondoid network.[90]

Hydrothermal reactions of $ZnCl_2$ with achiral 2,6-bis(imidazol-1-yl)pyridine (bip) afforded both spontaneous left- and right-handed resolved double helical motifs in $[Zn(bip)Cl_2]\cdot 0.5H_2O$ with enantiomorphic space groups of $P3_221$ and $P3_121$. It has been found that the formation of left-handed helices is higher than the right-handed counterpart with ratio 7:3. In the left-handed helices, the bip ligand coordinated to Zn in syn−syn conformation via imidazole N atoms to form an infinite 3_2 helices with a large helical pitch of ∼25.3 Å. Further, these helical polymeric chains are paired to generate a unique double helical structure through hydrogen bonding interactions with guest water molecules (C−H···O 3.319 and 3.648 Å) and $\pi-\pi$ stacking interactions between pyridine rings on the two strands (3.57 Å). Figure 28 shows the packing of double helices along *c*-axis. Similar spontaneous left- and right-handed helices also have been observed in $Zn(bip)Br_2\cdot 0.25H_2O$. On the other hand, solvothermal reaction in dried and wet DMF afforded two achiral supramolecular isomers of $[Zn(bip)Cl_2]$. The isomer obtained from dried DMF crystallized in $P2_1/n$ space group and displays zigzag CP structure with bip ligands in syn−anti conformation. Another supramolecular isomer isolated from wet DMF exhibits helical CP structure. The bip ligand coordinated to Zn(II) centers in anti−anti conformation and propagate into 2_1 helical chains with helical pitch of 9.45 Å. This complex is packed in a centrosymmetric unit cell and hence the helical chains are related by inversion symmetry.[91]

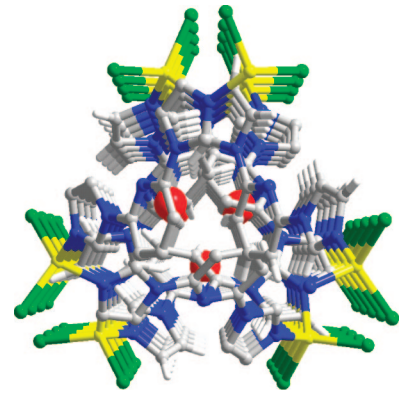

Figure 28. Packing of double helices along the *c*-axis direction. Reproduced with permission from ref 91. Copyright 2007 American Chemical Society.

A divergent bis-3-pyridinecarboxylate bridged by a 1,3,4-oxadiazole ring ligand with a "Σ-shaped" angular directional conformation forms helical structures with trigonal Ag(I) ions. The helical chains of $[Ag(L)(EtOH)]\cdot X$ (L is shown in Figure 29a; X = ClO_4, BF_4) are arranged in a zipperlike double helices structure with two right-handed single strands are offset by one-half of a pitch. The polymeric chains intertwine together to generate a right-handed double-stranded helix (but different from double helix) through $\pi-\pi$ stacking interactions between the oxadiazole−phenyl and phenyl−phenyl rings (Figure 29b). The corresponding complex with $CF_3SO_3^-$ anion displays a helical structure with both *M*- and *P*- helical chains present resulting from the existing *R*- and *S*-configuration of ligands. The left- and right-handed chains are arranged alternatively in the solid state and linked through $CF_3SO_3^-$ anions into a one-dimensional ladder-like chain (Figure 29c). These complexes exhibit fluorescence in solid state around 540 nm.[92]

The argentophilic interactions also assemble the helical chains into double-stranded helices.[93] (See section 4.1 for details.) Complex $[Au(dppb)\cdot 0.25CH_2Cl_2]$ (Hdppb = 4-diphenylphosphino benzoic acid) contains helical polymeric chain

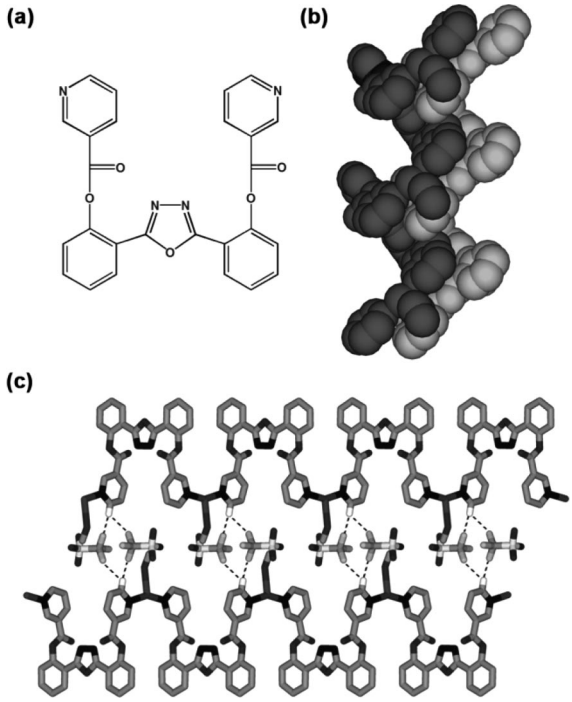

Figure 29. (a) Ligand structure. (b) Double-stranded helix generated by the intertwining of two single helical chains through the interchain $\pi-\pi$ interactions. (c) $CF_3SO_3^-$ anions are located between left- and right-handed helical chains.

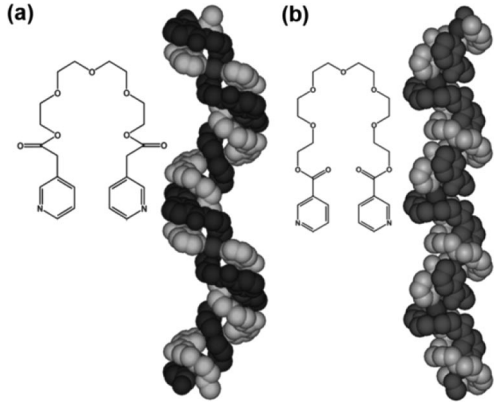

Figure 30. Perspective view of the double helices formed between two single stranded helices using two different ligands (a and b).

due to the propeller-like arrangement of phenyl groups at the phosphorus centers, and all units within the same polymer chain have the same helicity, *P* or *M*. It is worthwhile to mention that the polymer chains associate in pairs primarily through Au−Au contacts (3.16 Å) to give a racemic double-helical structure.[94]

Apart from intermolecular interactions, sharing the connectors between helical chains also can led to the formation of double-helical structures. For example, two adjacent helical chains in [AgL(PF_6)] (L is shown in Figure 30a) form infinite double helices through charge−dipole interactions between oxygen atoms of the tetraethyleneglycol units of one strand with Ag(I) of the other strand with same chirality (Figure 30a). The consecutive double helices are of opposite chirality and packed in a parallel fashion leading to a racemate. Extension in spacer chain length to hexaethylene glycol also has resulted in a pseudo-crown-type arrangement that leads to a double helical arrangement with the same chirality for both strands (Figure 30b). The packing of

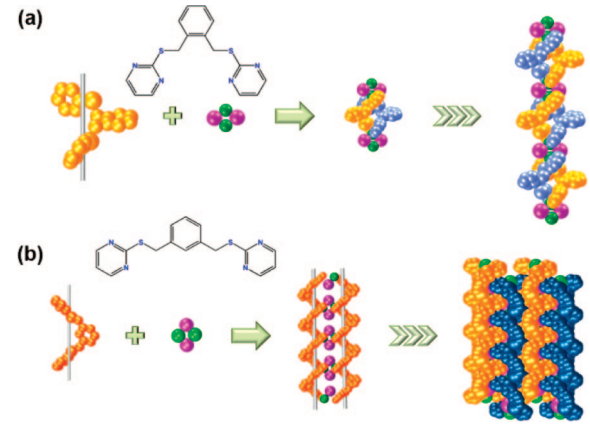

Figure 31. Schematic representation of the formation of 1D chains with (a) 1,2-bis-(2-pyrimidinesulfanylmethyl)benzene and (b) 1,3-bis-(2-pyrimidinesulfanylmethyl)benzene.

consecutive double helices bearing opposite chirality is again parallel and led to a racemic mixture.[95] The Ag(I) metal ions appear to serve as a crossover points to link the nitrogen bases.

Halide ions have been utilized to link the single-stranded helices into double stranded chains. In [Cu_2(bpsmb)$_2I_2$·CH_3CN] (bpsmb = 1,2-bis-(2-pyrimidinesulfanylmethyl)-benzene), two bis-monodentate ligands are linked to the Cu_2I_2 rhomboid dimers to generate the [Cu_2(bpsmb)$_2$] double-helical subunit as shown in Figure 31a. It is interesting that the bridging bpsmb ligands bring two single-stranded helical chains together to form fused double helix. Variation of pendant arm in 1,3-positions afforded another type double helical structure. Two single-stranded helical chains with the same handedness are linked through Cu_2I_2 units to form a double-stranded fused helix (Figure 31b). It is worthwhile to note that the adjacent chiral helices are racemically packed through intercalation of the lateral pyrimidine rings into 2D layers, which is further extended into the final 3D networks through strong $\pi-\pi$ interactions.[96]

A di-Schiff base ligand formed between 3-acetylpyridine and 1,2-diaminoethane forms a 1:1 complex with $AgNO_3$ with an interesting double helical structure. The two helices are placed side by side but connected to each other by tetrahedrally coordinated Ag(I) ions.[97] The structure is different from the double helical structure found in another Ag(I) salt of di-Schiff base formed between 2-pyridylcarboxaldehyde and 1,2-diaminocyclohexane.[98] Complex [Zn(cmb)(bbi)·H_2O] (H_2cmb = 4-carboxymethylbenzoic acid, bbi = 1,10-(1,4-butanediyl)bis(imidazole)) displays a heterostranded double-helical structure with two different flexible ligands forms helical CP chains by sharing the Zn(II) centers. Double helices are arranged in a parallel channel and accommodate lattice water molecules.[99] Strictly speaking, this is a 2D sheet made up of fused double helices. In another example, the polymers [M(pbbt)$_2$($NCS)_2$]·H_2O (M = Ni or Co, pbbt = 1,1′-(1,3-propylene)bis-1*H*-benzotriazole) are not independent helices but fused through the metal ions.[100] In fact, a number of such 2D and 3D network structures have been described in terms of fused helical chains in the literature.

2.3.3. Triple-Stranded Helices and Braids

Lin et al. have reported an elegant homochiral triple helical CP, [Ni(acac)$_2$(mnvp)]·($CH_3OH)_{1.5}$·H_2O (mnvp = 2,2′-dimethoxy-1,1′-binaphthyl-3,3′-bis(4-vinylpyridine)). Be-

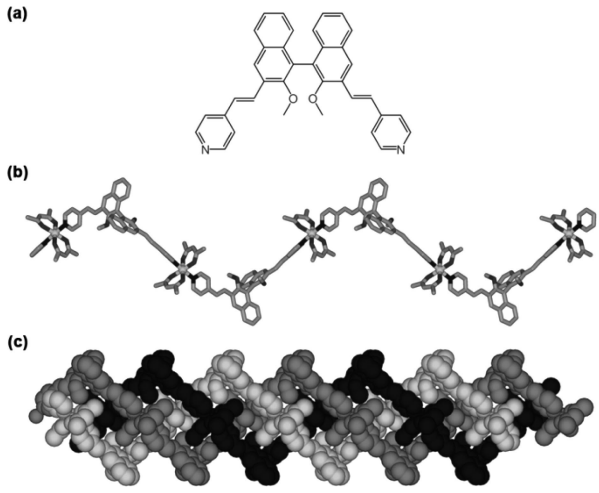

Figure 32. (a) Ligand structure. (b) View of a left-handed 2_1 helix. (c) Interwoven of three adjacent chains into triple helix structure.

cause of the nearly linear coordination of pyridyl groups to Ni(II) and perpendicular conformation of binaphthyl rings, a helical CP structure is obtained here (Figure 32a). It is noted that the naphthol rings are positioned away from the helical axis, and this allowed the self-recognition of aromatic rings through $\pi-\pi$ stacking, which leads to the interwoven of helical polymers. Three left-handed helical strands shown in Figure 32b further interwine in a nonparallel fashion with the nearest C−C distance of 3.35 Å to generate a 2D network. The 2D porous structure acts as host for the inclusion of methanol and lattice water molecules.[101] On the other hand, reaction with $AgNO_3$ or $AgClO_4$ furnished luminescent homochiral lamellar coordination polymers, which are built from linking helical chains by Ag(I) atoms as hinges.[102] Reaction with Cd(II) resulted in the formation of zigzag and ribbon-like CPs.[103] The elongated (*S*)-2,2′-diethoxy-1,1′-binaphthyl-6,6′-bis(4-vinylpyridine) ligand formed 1D CP chains and 2D rhombic structures.[104] Another binaphthol derivative, (*S*)-2,2′-dihydroxy-1,1′-binaphthalene-6,6′-dicarboxylic acid gave 1D CPs with carboxylate bridging, while hydroxyl groups formed higher dimensional hydrogen-bonded networks.[105]

Another complex, $[HgLCl_2]$ (L is shown in Figure 33a) also forms an interesting triple-stranded helices through $\pi-\pi$ stacking interactions between pyridine of different strands (~3.73 Å). The triple-stranded helical units (Figure 33b) are arranged in a parallel fashion and further linked through very weak bonds (2.93 Å) between the O atoms of the carbonyl group of ester groups and Hg(II) into a 3D network (Figure 33c).[106]

Triple-stranded helices have been constructed through hydrogen bonding interactions between the polymeric chains. Complex $[Cu_4(bpp)_4(maa)_8(H_2O)_2]\cdot 2H_2O$ (Hmaa = 2-methylacrylic acid) forms helical CP with alternating handedness through the flexible bpp ligands bridging. It is worth highlighting that this single-stranded chain is not a "real" helix because of the presence of inversion center. Nonetheless, the hydrogen bonding interactions between three single-stranded chains have given rise to an interesting interlaced triple-stranded braid as described by the authors. Three single-stranded chains interweave with the Cu(II) of the alternate helical parts located in a line in the middle of the braid.[80a] In a later study, the same researchers adopt a linear rigid ligand, biphenyl-4,4′-dicarboxylic acid (H_2bpdc) to

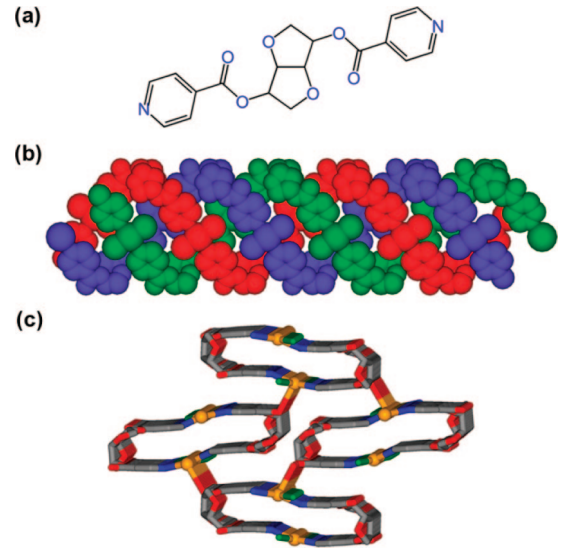

Figure 33. (a) Ligand structure. (b) Portion of the triple-stranded helix formed between three single-stranded helices through aromatic/aromatic interactions. (c) Parallel view on the lateral packing of enantiomerically pure triple stranded helices and their interconnection through O−Hg bonding leading to a 3-D coordination network.

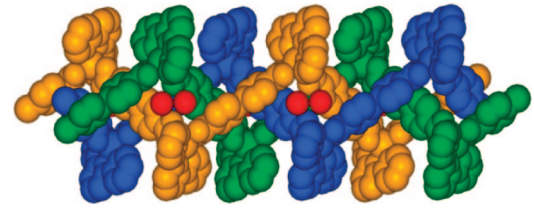

Figure 34. Triple-stranded helix in $[Cd(bpdc)(tpy)]\cdot H_2O$ showing that water dimers linking two helical chains (orange and green colors).

construct molecular braid. The linear bpdc ligands link the Cd(II) centers with alternate bis-chelating and bis-monodentate fashion to generate a meso-helix of $[Cd(bpdc)(tpy)]\cdot H_2O$ (tpy = 2,2′:6′,2″-terpyridine). Interestingly, the neutral, interlaced, triple-stranded-braided network is self-assembled by the interweaving of three single-stranded meso-helices (Figure 34). The presence of water dimers between the twisted single-stranded chains helps to stabilize the structure of the molecular braid.[80b]

Complex $[Cu_2(pcp)_2(bpp)_2(H_2O)_2]$ (pcp = 1,3-bis(4-carboxy-phenoxy)propane) represents the first example of 1D → 1D parallel interpenetrating network containing three double-stranded meso helical chains directed by covalent interactions, which involve more than two interpenetrating networks. The pcp and bpp ligands bridged the Cu(II) centers to construct a double-stranded chain with large windows, which are further interpenetrated by two other identical chains. The three interpenetrating chains propagate in the same direction to form a 3-fold 1D parallel interpenetration. In the three double-stranded chains, two types of triple-stranded molecular braids present. The first type is made up of bpp ligands bridging the copper centers, while in the second type of triple-stranded molecular braid is created by the pcp ligands bridging the copper centers (Figure 35a and b). Each triple-stranded molecular braid further interlocks the other type of triple-stranded molecular braid to form an exceptional sextuple-stranded molecular braid (Figure 35c). The two types of braids are interconnected via the shared Cu atoms to give the double stranded 1D chains.[107]

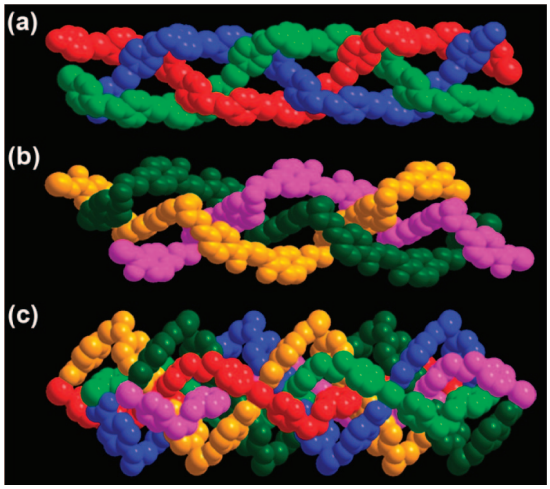

Figure 35. Space-filling view of (a) the first type of triple-stranded molecular braid. (b) Second type of triple-stranded molecular braid. (c) Sextuple-stranded molecular braid. Adapted with permission from ref 107. Copyright 2009 The Royal Society of Chemistry.

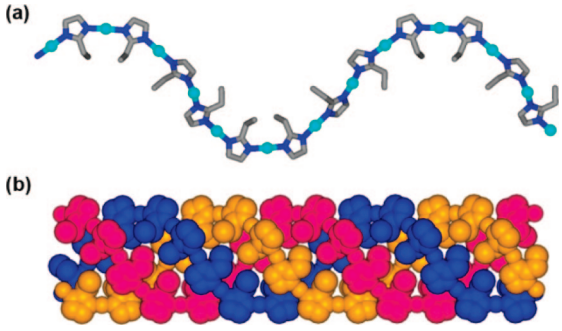

Figure 36. (a) View of helical chain in [Cu(eim)]. (b) Intertwined of three helices to form triple stranded helix.

On the other hand, a triple-stranded helix structure can also be stabilized by hydrophobic interactions. In complex [Cu(eim)] (eim = 2-ethylimidazole), every three helices are intertwined to form a triple-stranded helix with ethyl groups of eim ligands are inside the channel (Figure 36). Such triple helices formation is attributed to the hydrophobic nature of the ethyl groups in the relatively polar media. The helices with the same helicity are associated through short Cu···Cu contacts (2.83 Å) to generate homochiral layers, and these layers with opposite helicity are further alternatively interacting through longer Cu···Cu contacts (3.03 Å) to yield the final racemic and ligand-unsupported cuprophilicity 3D supramolecular architecture.[108]

Complex $[Ni(tren)]_3[Mo(CN)_8](ClO_4)_2 \cdot 5H_2O$ (tren = tris(2-aminoethyl)amine) displays an exceptional left-handed triple-helix structure with one right- and two left-handed helices. The three single-stranded helices intersect at Mo(IV) twisting into a complex triple-stranded chain. Because of the different properties of the alkyl group of the capping tren ligand and terminal CN group, hydrophobic and hydrophilic areas on the surface are formed. Water molecules are found to fill the hydrophilic pits on the chains.[70b] A triple-stranded helical compound $[\{M(bpp)_3\}_2\{M_3(OH)\}](SCN)_3 \cdot 6H_2O$ (M = Ni^{2+} or Zn^{2+} and Hbpp = 3,5-bis(2-pyridyl)pyrazole) and CuSCN in the presence of PPh_3 led to CPs $[\{M(L)_3\}_2\{M_3(OH)\}][Cu_{12}(CN)_{11}(SCN)_4]$. The latter compound could also be obtained in a solvothermal reaction in acetonitrile by the one-pot reaction of CuSCN, Ni^{2+} or Zn^{2+}, Hbpp, and PPh_3. The structure of this compound has been found to have double helical strands trapped inside a 3D anionic framerwork of

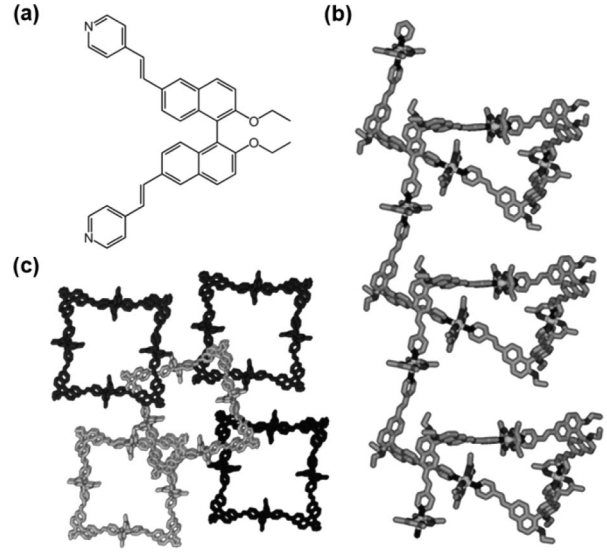

Figure 37. (a) Ligand structure. (b) Perspective view of left-handed 4_1 helical chain. (c) Interlocking of quintuple helices.

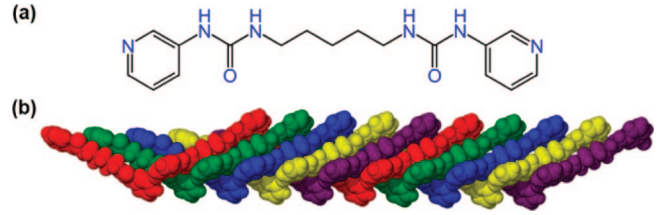

Figure 38. (a) Ligand structure. (b) Quintuple helical molecular braid.

$[Cu_{12}(CN)_{11}(SCN)_4]$. The double-helical strands has been thought to be formed because of template effect of the triple-helical structure.[109] Triple helical structures also have been observed in other complexes.[70b,110]

2.3.4. Higher-Dimensional CPs from Interactions between Helices

An interesting interlocked quintuple-helices has been reported in $[Ni(acac)_2(envp)] \cdot 3CH_3CN \cdot 6H_2O$ (envp = (*S*)-2,2′-diethoxy-1,1′-binaphthyl-6,6′-bis(4-vinyl-pyridine)). The $Ni(acac)_2$ units are bridged by binaphthyl pyridyl ligands (Figure 37a) to form a left-handed helical CP (Figure 37b). The naphythyl rings are placed away from the helical axis to generate a hollow cylinder. The intriguing feature of this complex is that five infinite helical chains associated in parallel to form the wall of a tetragonal nanotube with 2 × 2 nm cavities. Each helix further interwines with four other helices from four different nanotubes to give interlocked quintuple-helices (Figure 37c). The helices are stabilized by $\pi-\pi$ interactions between vinylnaphthyl moieties. Interlocking of nanotubes furnishes a 3D framework that encapsulated CH_3CN and water molecules. Similar structure also has been observed in a related crown ether analogue.[111]

A combination of bifunctional rigid bis(pyridylurea) ligand (shown in Figure 38a) and linear two-coordinate silver(I) ion can assemble either in a planar arrangement or a twisted helical chain based on the freedom of rotation along Ag−N bond. However, only helical conformation has been found to dominate because of the influence of hydrogen bonds between the ligand, BF_4^- anions, and THF solvent molecules. The mutually near-orthogonal arrangement of the ligands within the stacks because of orthogonal interstack interactions

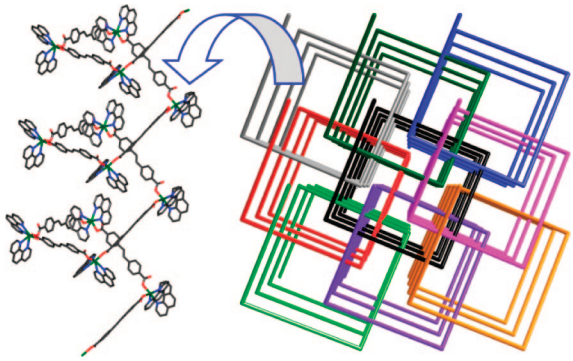

Figure 39. Schematic representation of the 9-fold interlocked homochiral helices from left-handed helical chains.

of the BF_4^- anions lead to the helical conformation. The space available in the helical confirmation by the long pentamethylene chain results in the intertwining of five such helices thus yields a quintuple helical molecular braid (Figure 38b).[112] On the other hand, the nitrate anion and water molecules nestled between the offset pairs of ligands causes the ligand in $[Ag(L)]NO_3 \cdot MeCN \cdot 1.75H_2O$ to have planar arrangement with the pyridyl nitrogen atoms in anticonformation.

Nine-fold interlocked helices were observed in complex $[Cd(sdc)(phen)_2]$. The left-handed 4_1 helix is generated by bridging the $[Cd(phen)_2]^{2+}$ units through long linear sdc spacer ligands. Each pair of nearly perpendicular phen ligands are arranged away from the helical axis and leads to the formation of a tetragonal nanotube with channels about 1.8 × 1.8 nm. Further, each helical chain is interlocked by eight equivalent helices to furnish an infinite interlocked array from 9-fold interwoven homochiral helices (Figure 39). The framework is stabilized by strong $\pi-\pi$ stacking interactions between the interwoven aryl rings.[113] This is similar to the previous example in which the orientation of bulky groups directed the nanotube open channel formation and the adjacent helices interlocked within the cavities. This may suggest a general route to generate higher order interlocked helices.

2D and 3D solid-state structures quite often explained as fused helices or self-catenated aggregates.[114,115] For example, the 3D structure $[Cd(1,2\text{-bdc})(dpa)(H_2O)] \cdot 4H_2O$ (1,2-H_2bdc = 1,2-benzenedicarboxylic acid; dpa = 4,4′-dipyridylamine) has been interpreted as self-catenated chiral topology made up of homochiral $[Cd(H_2O)(dpa)]^{2+}$ double helices and [Cd(1,2-bdc)] mono helices.[116] Similarly, another 3D network structure $[Zn_4(bptc)_2(4,4'\text{-bpy})_4] \cdot (C_5H_3N) \cdot 4H_2O$ (H_4bptc = 3,3′,4,4′-benzophenone-tetracarboxylic acid) has been described as self-penetrating structure in terms of quintuple-stranded molecular braid, 9-fold meso-helices, and 17-fold interwoven helices, but they are indeed 3D network structures.[117] Such higher dimensional fused helices are not discussed here since they are beyond the scope of this review.

2.4. Ladder Polymers

Ladders can be generated by metal ions as nodes and spacer ligands as rails and rungs in 1:1.5 ratio to form "T-shaped" building blocks. The cavities formed by ladders are defined by the length, shape, and orientation of spacer ligands. Hence, one can envisage the construction of a desired ladder structure by judicious choice of these components. Excellent reviews on molecular ladders dealing with interesting and diversified architectures are available in the literature.[5e,118] In this section, we describe 1D ladder structures based on their building blocks, unusual molecular ladder motifs, and interpenetrated network.

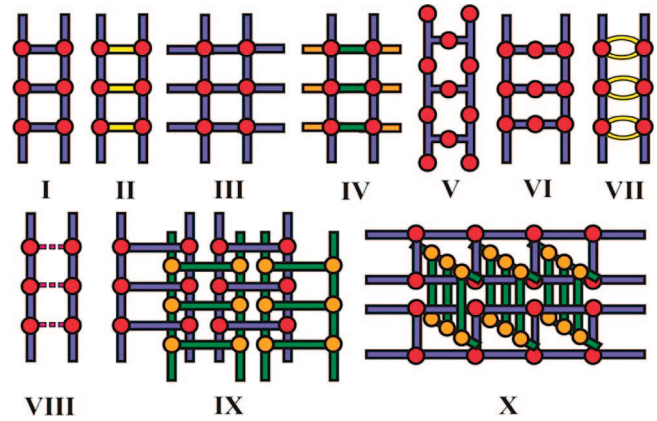

Figure 40. Schematic representation of different types of common molecular ladder motifs. Red and yellow balls represent metal nodes; long rods represent spacer ligands. Different kinds of spacers are shown in different colors. Metallophilic bonds are represented as dashed lines.

2.4.1. Common Motifs of Noninterpenetrated Ladders

Figure 40 displays the nine categories of common ladder motifs including same spacers for rails and rungs (Type I), different spacers for rails and rungs (Type II), same spacers for rails, rungs, and lateral arms (Type III), different spacer lateral arms where the rails and rungs may be the same spacer or different (Type IV), T-shaped or dendritic shaped spacers (Type V), another metal node in the rung (Type VI), two bridging spacers for rungs (Type VII), metallophilic interactions as rungs (Type VIII), parallel interpenetration (Type IX), and inclined interpenetration (Type X). Table 1 summarizes CPs that belong to each category. Selected examples for each category are discussed briefly.

Type I ladder represents the most basic and common ladder structure in which bifunctional linear spacers bridged the metal ions to form side rails and rungs. These molecular ladders have square shape as expected, and the cavities are predetermined by the chain length of spacers. In the early stage of crystal engineering, many ladder structures were reported from $ML_{1.5}(NO_3)_2$ building blocks.[118a] Zaworotko et al. reported the first example of noninterpenetrated molecular ladder $[Co(NO_3)_2(4,4'\text{-bpy})_{1.5}]$ with large square hydrophobic cavities (Figure 41a).[119] Since the spacers are different in Type II ladders, the cavities have rectangular shape. Type III ladders are similar to Type I but have one more spacer coordinated to metal nodes to form lateral arms. In Type I, generally, nitrate anions are coordinating and hence block these binding sites. Whereas the anions are noncoordinating in Type III ladder, therefore an additional spacer ligand is needed to complete the coordination sphere, which further form lateral arms. Hence the nature of anions has a role to play in these structures along with M/L ratio. Examples of Type II and Type III ladders are displayed in Figure 41b and c, respectively. In most of the noninterpenerated ladders, the cavities are filled with solvent, anions or free ligand guest molecules. If the voids are empty, interpenetrated structures (Type VIII and IX) are observed in

Table 1. Various Types of Ladderlike 1D CPs

Compound	Ligand	Features	Ref.
Type I			
$[Co(4,4'\text{-bpy})_{1.5}(NO_3)_2]\cdot 0.75MeCN$ $[Co(4,4'\text{-bpy})_{1.5}(NO_3)_2]\cdot 2CHCl_3$	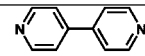	Solvent molecules are placed inside the ladder cavities Show preference for inclusion hydrophobic guests (arenes, $CHCl_3$ and MeCN) over hydrophilic guests (MeOH and H_2O)	119
$[Co(dpe)_{1.5}(NO_3)_2]$	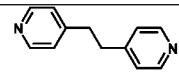	Displays supramolecular isomerism under different solvents	120
$[Co(bpe)_{1.5}(NO_3)_2\cdot 3CHCl_3]$	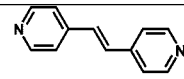	Transforms into mononuclear complex reversibly One solvate chloroform molecule sits in the square void, whereas the other two chloroform molecules are positioned outside Immediately lost partial chloroform molecules when removed from mother solution	121
$[Zn(4,4'\text{-bpy})_{1.5}(NO_3)_2]\cdot$guest Guest = benzene, toluene, *p*-xylene, and chlorobenzene	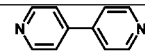	Inclusion of benzene, toluene, *p*-xylene, and chlorobenzene molecules inside ladder cavities Show exciplex fluorescence due to π-π stacking interactions	122
$[Co(bpd)_{1.5}(NO_3)_2(CH_2Cl_2)_2]$ (bpdh = 2,5-bis(4-pyridyl)-3,4-diaza-2,4-hexadiene)	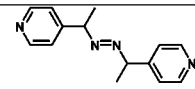	CH_2Cl_2 molecules partially fill the space between ladders	123
$[Ni(L)_{1.5}(NO_3)_2\cdot$(mesitylene)·(methanol)] L is shown in the next column	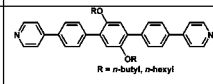	The ladder squares have dimension of *ca.* 24 x 24 Å. Inclusion of mesitylene and methanol molecules inside ladder cavities	124
$[Cd(bpmna)_{1.5}(NO_3)_2]$ bpmna = *N,N'*-bis-pyridin-4-ylmethylene-naphthalene-1,5-diamine	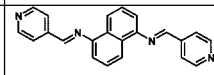	Each square is formed by four Cd(II) and four ligands and contains 76 atoms with dimensions *ca.* 20.8 x 20.8 Å	125
$[Pb(bimb)_{1.5}(NO_3)_2]\cdot$DMF bimb = 4,4'-bis(imidazol-1-methyl)-biphenyl	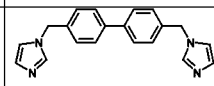	DMF molecules fill the channel formed by adjacent two ladders Exhibits strong self-defocusing behavior in third-order NLO	126
$[M_2(3,3'\text{-pytz})_3(NO_3)_4]\cdot$guest M = Cd, Zn; guest = EtOH, CH_2Cl_2 (3,3'-pytz = 3,6-bis(pyridin-3-yl)-1,2,4,5-tetrazine)	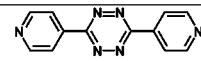	Inclusion of EtOH and CH_2Cl_2 molecules inside ladder cavities	127
$[Cd_2\{(R)\text{-Hdmpa}\}_2\{(S)\text{-Hdmpa}\}_2(bpe)_3]$ (H_2dmpa = 6,6'-dimethyl-1,1'-biphenyl-2,2'-dicarboxylic acid)	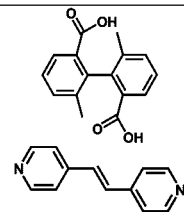	Interdigitation of Hdmpa (*R*)-Hdmpa and (*S*)-Hdmpa are coordinated to Cd(II) center, which suggests an assembly process of ligand self-discrimination, therefore, no optical activity is expected in this structure	128
$[Ag_2(bpdms)_3](CF_3SO_3)_2\cdot 2CH_3OH$ bpdms = bis(4-pyridyl)-dimethylsilane	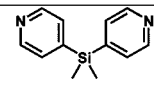	Tubular channel	129
$[M(hbs)_3(H_2O)_2]\cdot 2H_2O$ M = Tb, Er and Yb (Hhbs = 4-hydroxybenzenesulfonic acid)	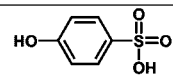	Tb(III) complex exhibits ligand-to-metal energy transfer emission	130
$[Ag(1,4\text{-pyz})_{1.5}CF_3SO_3]$ (pyz = pyrazine)		The structure does not contain any cavities	131
$[(DMF)_4EuM(CN)_4]$ M= Ni, Pt		Ladders are ionized into solvent-separated ion-pairs in solution	132

Table 1. Continued

Compound	Ligand	Features	Ref.
Type I			
{[Fe(bpca)(μ-CN)$_3$Mn(H$_2$O)$_3$]-[Fe(bpca)(CN)$_3$]}·3H$_2$O (bpca = bis(pyridylcarbonyl)amide)	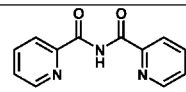	Ferrimagnetic chain with intrachain antiferromagnetic coupling between the LS Fe(III) and the HS Mn(II)	133
Mn(N$_3$)(MeOH)[Cr(2,2'-bpy)(CN)$_4$]·2H$_2$O	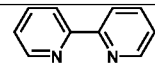	Forms 2D double layer with adjacent ladders through hydrogen bonding Exhibits antiferromagnetic and metamagnetic behaviors	134
[MCr(ox)$_3$(H$_2$O)$_4$]$_2$·12H$_2$O M = La, Ce (H$_2$ox = oxalic acid)	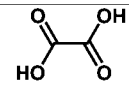	Exhibit antiferromagnetic behaviors	135
Cu$_2$(4,4'-bpdz)$_3$(CF$_3$CO$_2$)$_4$ (bpdz = 4,4'-bipyridazine)	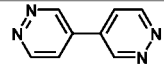	Each ring is made up of four Cu(II) and four ligands with Cu···Cu distance *ca.* 10.68 Å	136
Type II			
[Ag$_2$(hmt)$_2$(bca)(H$_2$O)$_2$]·H$_2$O (hmt = hexamethylenetetramine; H$_2$bca = 4,4'-biphenyldicarboxylic acid)	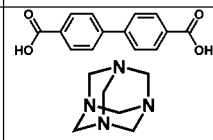	Rail: hmt; Rung: bca Forms staircase-like 2D with adjacent ladders through hydrogen bonding	137
[Zn(4,4'-bpp)(1,2-bdc)]·H$_2$O (bpp = 1,3-bis(4-pyridyl)propane)	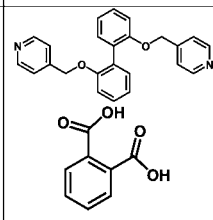	Rail: 4,4'-bpp; Rung: 1,2-bdc	138
[Cu(4,4'-bpy)]$_2$[HPMo$_{12}$O$_{40}$]	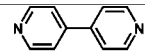	Rail: 4,4'-bpy; Rung: molydate Shows good electrocatalytic activity for the reduction of nitrite.	139
[(dien)PtBr$_2$(4,4'-bpy)Pt(dien)]Br$_4$·2H$_2$O (dien = diethylenetriamine)	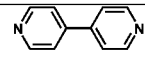	Rail: bromide; Rung: 4,4'-bpy Mixed-valence of Pt(II)-Pt(VI) Has a pair of out of phase charge-density waves within each ladder	140
[{Cu(bip)}$_2$(ox)]·6H$_2$O (Hbip = 3,3-bis(2-imidazolyl)propionic acid)	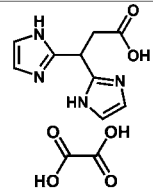	Rail: bip; Rung: ox Exhibits antiferromagnetic behavior Water molecules are placed in lattice	141
Cu$_2$(dca)$_2$(4,4'-bpy)(MeCN)$_2$·0.5(4,4'-bpy) (dca = dicyanamide)	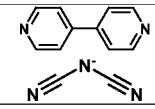	Rail: dca; Rung: 4,4'-bpy Inclusion of free 4,4'-bpy molecule	142
Type III			
Ni(4,4'-bpy)$_{2.5}$(H$_2$O)$_2$(ClO$_4$)$_2$·1.5(4,4'-bpy)·2H$_2$O	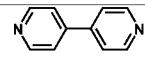	Inclusion of free 4,4'-bpy, perchlorate and lattice water molecules inside the ladder cavity	143
[Co(4,4'-bpy)$_{2.5}$(NO$_3$)$_2$]··2phenanthrene	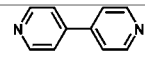	Inclusion of phenanthrene molecules inside the ladder cavity Interdigitation of lateral arms to form planar network	144

Table 1. Continued

Compound	Ligand	Features	Ref.
Type III			
$Ni(4,4'\text{-bpy})_{2.5}(H_2O)_2(ClO_4)_2 \cdot 1.5(4,4'\text{-bpy}) \cdot 2H_2O$	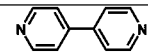	Inclusion of free 4,4'-bpy, perchlorate and lattice water molecules inside the ladder cavity	[143]
$[Co(4,4'\text{-bpy})_{2.5}(NO_3)_2] \cdot \cdot 2$phenanthrene	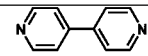	Inclusion of phenanthrene molecules inside the ladder cavity Interdigitation of lateral arms to form planar network	[144]
Type IV			
$[M_2(4,4'\text{-bpy})_3(H_2O)_2(phb)_2]\text{-}(NO_3)_2 \cdot 4H_2O$	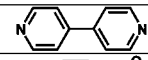	Rail: 4,4'-bpy; Rung: 4,4'-bpy; Arm: phb	[145]
M = Cu, Co (H_2phb = 4-hydroxybenzoic acid)	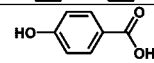	Interdigitation of lateral arms into the squares	
$[Cd(H_2bna)(bpy)_{1.5}(H_2O)_2]$ (H_4bna = 2,2'-dihydroxy-[1,1']-binaphthalene-3,3'-dicarboxylic acid)	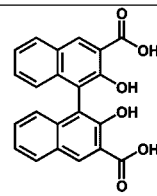	Rail: 4,4'-bpy; Rung: 4,4'-bpy; Arm: H_2bna Exhibits strong blue emission	[146]
$[\{(Cu(2,2'\text{-bpy})(H_2O)(CF_3SO_3)\}_2(pyz)]\text{-}\cdot(CF_3SO_3)_2$	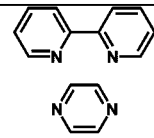	Rail: triflate; Rung: pyz; Arm: 2,2'-bpy	[51]
$[Ni_2(tppz)(dca)_4] \cdot C_2H_5OH$ (tppz = tetra-2-pyridylpyrazine, dca = dicyanamide)	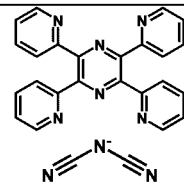	Rail: dca; Rung: tppz; Arm: dca EtOH molecules inside ladder cavity	[147]
$[Cu(pdc)(bib)_{1.5}].4H_2O$ (H_2pdc = pyridinedicarboxylic acid, bib =1,4-bis(N-imidazolyl)butane)	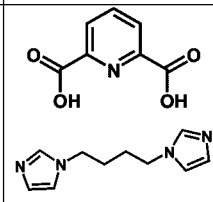	Rail: bib; Rung: bib; Arm: pdc Three lattice water molecules form pentagonal rings with pdc ligands via strong hydrogen bonds and water cluster are located inside ladder cavity	[148]
Type V			
$[Cu_5(NO_3)_{10}(dpyatriz)_2(MeCN)_2] \cdot 7MeCN$ (dpyatriz = 2,4,6-tris(dipyridin-2-ylamino)-1,3,5-triazine)	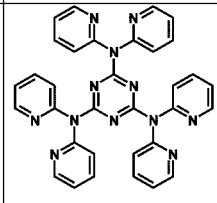	Dendritic/tripodal shape of dpyatriz	[149]
$[Pr(NO_3)_3(fafpmtmb)(H_2O)]$ (fafpmtmb = 1,3,5-tris{[(2'-furfurylaminoformyl)phenoxyl]methyl}-2,4,6-trimethylbenzene)	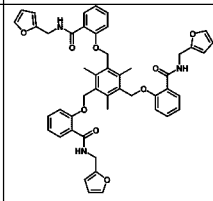	Third arm acts as the middle of the rung in the ladder	[150]
$[Ag_3(bpi)_2](OTf)_3$ (bpi = 4,4'-bipyrimidine)	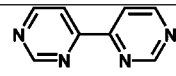	Perpendicular bridging and chelating sites of bpi	[151]

Table 1. Continued

Compound	Ligand	Features	Ref.
Type V			
$[Zn_3(peeb)_2Cl_6]\cdot 2H_2O$ (peeb = 1,3,5-tris[2-(pyridin-2-yl)ethyl]-2,4,6-triethylbenzene)	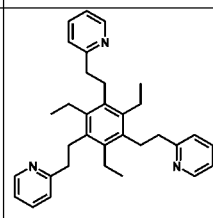	Dendritic/tripodal shape of peeb	152
$[Ba_2(chbs)_4(H_2O)_{10}]$ (H_2chbs = 3-carboxy-4-hydroxybenzenesulfonic acid)	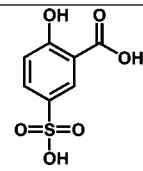	Exodentate binding sites of chbs Three types of molecular square	153
$[Co_3(1,3,5\text{-btc})_2(2,2'\text{-bpy})_2(H_2O)]\cdot 4H_2O$ $[Co_3(tpo)_2(2,2'\text{-bpy})_2(H_2O)_6]\cdot xH_2O$ (1,3,5-H_3btc = 1,3,5-benzenetricarboxylic acid; H_3tpo = tris(4-carboxylphenyl)phosphine oxide)	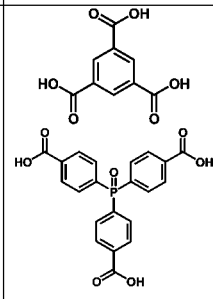	Tripodal shape of 1,3,5-btc and tpo	154
Type VI			
$[M_3(na)_4(dca)_2(H_2O)_8]\cdot 2H_2O$ M = Co, Cu (Hna = nicotinic acid, dca = dicyanamide)	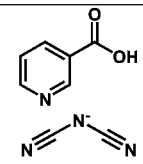	Rungs are made up of $[M(H_2O)_4(na)_2]$ units while the rails are $[M(H_2O)_2(na)(\mu\text{-dca})_2]$. No long range magnetic ordering has been observed in the case of Co(II) ladder.	155
$Co_3(tbapp)_2(hfac)_6$ (tbapp = 5-[4-(*N*-tert-butyl-*N*-aminoxyl)phenyl]pyridimine)	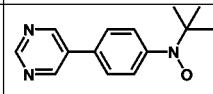	Exhibits strong antiferromagnetic exchange	156
Type VII			
$[\{(CH_3CO_2)(\mu\text{-}O_2CCH_3)Zn\}_2(bpe)_2]$ $[\{(CF_3CO_2)(\mu\text{-}O_2CCH_3)Zn\}_2(bpe)_2]$	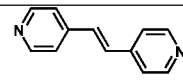	Acetate bridging Undergo [2+2] photodimerization	157
$[\{(CF_3CO_2)Ag\}_2(bpe)_2]\cdot H_2O$	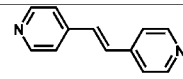	Trifluoroacetate bridging Undergo [2+2] photodimerization Ag-Ag distance: 3.15 Å	158
$[Zn_2(bpefmp)(OH)(bpe)_2](ClO_4)_2\cdot 4H_2O$ (bpefmp = 2,6-bis[*N*-(2-pyridylethyl) formimidoyl]-4-methylphenol)	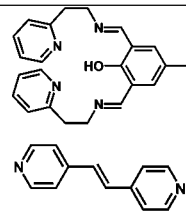	Phenoxo and hydroxyl bridging Undergo [2+2] photodimerization	159
$[Ag(4,4'\text{-bpy})(CH_3COO)]\cdot 3H_2O$	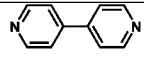	Acetate bridging Ag-Ag distance: 3.12 Å	160
$[Co(4,4'\text{-bipy})(CH_3COO)_2]$	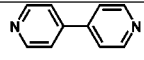	Acetate bridging	161

Table 1. Continued

Compound	Ligand	Features	Ref.
Type VII			
$[Cu(4,4'\text{-bipy})(CH_3COO)_2]\cdot 2.5H_2O$ $[Zn(4,4'\text{-bipy})(CH_3COO)_2]$	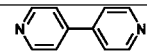	Acetate bridging Forms 2D double layer with adjacent ladders through hydrogen bonding	162
$[Cu(Hsal)_2(4,4'\text{-bipy})]\cdot DMF$ (Hsal = salicylic acid)	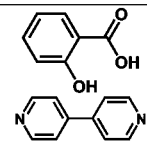	Salicylic acid bridging	163
$[M_2(bpdb)_2(CH_3COO)_4\cdot 2(MeOH)]$ M = Zn, Mn (bpdb = 1,4-bis(4-pyridyl)-2,3-diaza-1,3-butadiene)	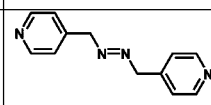	Acetate bridging Two parallel ligands interact with weak π-π interactions (3.8 Å)	164
Type VIII			
[Ag(pytz)(X)(MeCN)] X= PF_6, BF_4 (pytz = 3,6-di(4-pyridyl)-l,2,4,5-tetrazine)	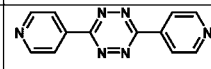	Ag-Ag distance: 3.23 and 3.31 Å	14
[Ag(cpa)(Hcpa)(4,4'-bpy)·H_2O] (Hcpa = *p*-chlorophenoxyacetic acid)	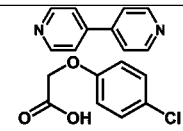	Ag-Ag distance: 3.21Å; π-π stacking interaction: 3.58 Å Exhibits intense emission due to metal-to-ligand charge transfer	165
$[Ag_2(4\text{-stilbz})_4][CF_3CO_2]_2$ (4-stilbz = *trans*-1-(4-pyridyl)-2-(phenyl)ethylene)	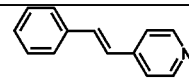	Ag-Ag distance: 3.41 Å; ; π-π stacking interaction: 3.62 Å Undergo [2+2] photodimerization	166
$[Ag_2(dp)_2(H_2O)]\cdot NO_3$ (dp = 1,2-diaminopropane)	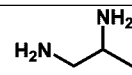	Ag-Ag distance: 3.04 Å Forms a 2D layer with the adjacent layers via short Ag···O contacts	97
$[Ag(4,4'\text{-bpy})]\cdot H_2PO_4\cdot H_3PO_4$	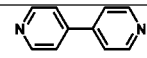	Ag-Ag distance: 3.29 Å; π-π stacking interaction: 3.44 Å	160
[Ag(im)] (Him = imidazole)		Ag-Ag distance: 3.44 Å Displays supramolecular isomerism under different solvents	167
$[Ag(pybut)]\cdot PO_2F_2\cdot MeCN$ (pybut = 1,4-bis(4-pyridyl)butadiyne)	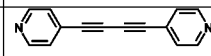	Ag-Ag distance: 3.19 Å	168
$[Ag_2(adca)(4,4'\text{-bpy})_2]$ (H_2adca = anthracene-9,10-dicarboxylic acid)	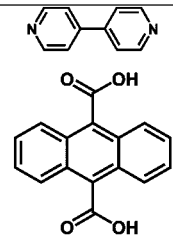	Ag-Ag distance: 3.32 Å Exhibits intense emission at 525 nm	169
Type IX			
$[Cu_2(pybut)_3(MeCN)_2]\cdot(PF_6)_2$ (pybut = 1,4-bis(4-pyridyl)butadiyne)	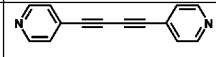	Each ladder is polycatenated by four ladders Type I ladder; 1D → 2D	170
$[Cd_2(pytz)_3(\mu\text{-}NO_3)(NO_3)_3(MeOH)]$ (pytz = 3,6-di(4-pyridyl)-l,2,4,5-tetrazine)	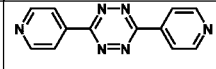	Type I ladder; 1D → 3D Polyknot structure Inclusion of MeOH molecules	171

Table 1. Continued

Compound	Ligand	Features	Ref.
Type IX			
$\{Cu_3(4,4'\text{-bpy})_3(H_2O)[PMo_{12}O_{40}\text{-}(VO)_2]\cdot 5H_2O\}$	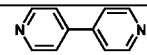	Each rectangle of the double ladder is penetrated by two other parallel double Type II ladder; 1D → 3D	172
$[Ni(bpp)_{1.5}(H_2O)(hip)]$ (bpp = 1,3-bis(4-pyridyl)propane, H_3hip = 5-hydroxyisophthalic acid)	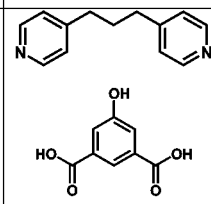	Type IV ladder; 1D → 2D; Inclination 57° Each rectangle is penetrated by two lateral arms from different ladders Polythreaded structure	173
Type X			
$[M_2(bpethy)_3(NO_3)_4]$ M = Zn, Co (bpethy = 1,2-bis(4-pyridyl)ethyne)	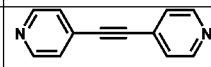	Each square of the ladder is interlocked with two squares of two adjacent ladders Type I ladder; 1D → 3D; Inclination 76°	174
$[Ag_2(bpe)_5]\cdot(BF_4)_2$	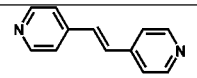	The terminal bpe ligands of each ladder are threaded into the squares of the adjacent ladders leads to mutual polythreading Type II ladder; 1D → 2D; Inclination 22°	175
$[Cd(bpmb)_{1.5}](NO_3)_2$ $[Cd(bpmb)_{1.5}](NO_3)_2\cdot C_6H_4Br_2$ (bpmb = 1,4-bis(4-pyridylmethyl)benzene)	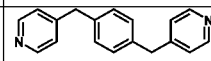	Each square of the ladder is interlocked with four squares of different ladders. Type I ladder; 1D → 2D; Inclination 71° and 86° Inclusion of *p*-dibromobenzene molecule	176
$[Cu_2(ip)(4,4'\text{-bpy}]\cdot 3.5H_2O$ (Hip = isophthalic acid)	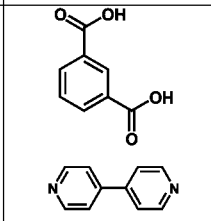	Type II ladder; 1D → 2D; Inclination 57° Inclusion of water molecules	177
$[Cd(NO_3)_2(bpethy)_{1.5}]$ (bpethy = 1,2-bis(4-pyridyl)ethyne)	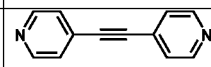	Type I ladder: the dimensions of the square ~14.25 x 14.25 Å and found to be doubly interpenetrating	178
$[Cu_3(cenep)_4(DMF)_6(H_2O)_3(ClO_4)](ClO_4)_5\cdot 10DMF\cdot 10EtOH\cdot 7H_2O$ (cenep = (*R*)-6,6′-dichloro-2,2′-diethoxyl-1,1′-binaphthyl-4,4′-bis(*p*-ethynylpyridine))	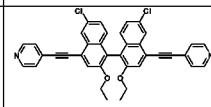	Type I ladder; 1D → 3D; Inclination 44° Interlocked and interpenetration	179

molecular ladders with large cavities. Chen et al. have reported Type IV molecular ladders containing different lateral arms. Complexes $[M_2(4,4'\text{-bpy})_3(H_2O)_2(hba)_2](NO_3)_2\cdot 4H_2O$ (M = Cu, Co; H_2hba = 4-hydroxybenzoic acid) display molecular ladder structures with metal(II) ions as the nodes, μ_2-4,4′-bpy as the inner rungs, and η_2-hba as lateral arms (Figure 42d). More interestingly, the lateral arms in each ladder are interdigitated into the $[M_4(4,4'\text{-bpy})_4]$ squares of adjacent ladders so that each square is penetrated oppositely by two phba lateral arms from two different adjacent molecular ladders.[145]

While most of the molecular ladders are composed of T-shape metal nodes, such T-shaped spacers linking the metal nodes to generate ladder structures of Type V also have been reported. Complex $[Cu_5(NO_3)_{10}(dpyatriz)_2(CH_3CN)_2]\cdot 7CH_3CN$ (dpyatriz = 2,4,6-tris(dipyridin-2-ylamino)-1,3,5-triazine) displays ladder structure owing to the dendritic shape of dpyatriz (Figure 42a). The rails of the ladder are composed of Cu(II), two dipyridylamine units and bridging nitrate anions. The other dipyridylamine unit coordinated to another Cu(II) which linked the two chains into ladder structure.[149] Complex $[Ag_3(bpi)_2](OTf)_3$ (bpi = 4,4′-bipyrimidine) exhibits ladder structure with two adjacent linear [Ag(bpi)] units linked by central Ag(I) ions as shown in Figure 42b. The bpi ligand contains bridging and chelating sites at right angles favor the formation of square or rectangular motifs. The ladders are arranged in parallel fashion with $\pi-\pi$ interactions between bipyrimidine rings.[151]

Whereas H-shaped ligands are also capable of linking the metal ions into molecular ladder structure. For instance, the 1,4,7,10,13,16,19,22-octathiacyclotetracosane ([24]aneS_8) has been shown to furnish ladder structure in complex $[Ag_2([24]aneS_8)(CF_3SO_3)_2(MeCN)_2]$.[180] In Type VI ladders, rungs are constructed by two spacers and another metal node.

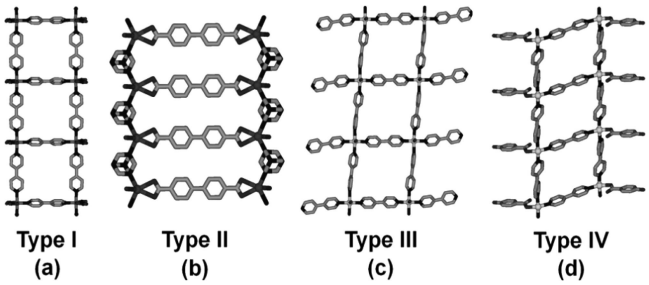

Figure 41. Perspective view of Type I−IV molecular ladder frames: (a) $[Co(NO_3)_2(4,4'\text{-bpy})_{1.5}]$, (b) $[Ag_2(hmt)_2(bca)(H_2O)_2]\cdot H_2O$, (c) Cation in $[Ni(4,4'\text{-bpy})_{2.5}(H_2O)_2](ClO_4)_2\cdot(4,4'\text{-bpy})_{1.5}\cdot(H_2O)_2$, and (d) cation in $[Cu_2(4,4'\text{-bpy})_3(H_2O)_2(hba)_2]\ (NO_3)_2\cdot 4H_2O$.

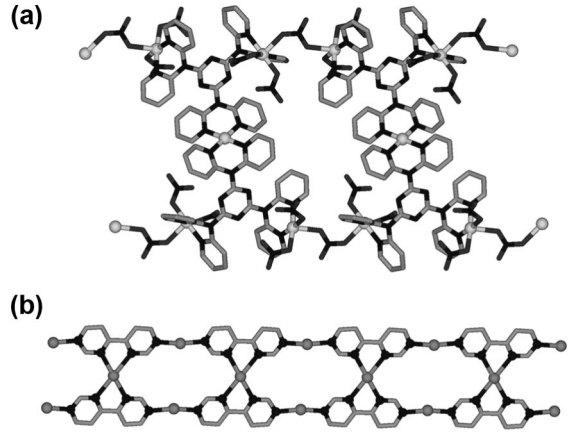

Figure 42. View of Type V ladder motifs in (a) $[Cu_5(NO_3)_{10}(dpyatriz)_2(CH_3CN)_2]\cdot 7CH_3CN$ and (b) $[Ag_3(bpi)_2](OTf)_3$.

For instance, complex $[Co_3(dca)_2(nic)_4(H_2O)_8]\cdot 2H_2O$ (dca = dicyanamide; Hnic = nicotinic acid) form ladder structure through $[Co(H_2O)_4(nic)_2]$ units linked the Co(dca) chains (Figure 43).[155a]

Type VII ladders are formed by metal−metal interactions to transform 1D polymeric chains into ladder structures. The argentophilic interactions (>sum of van der Waals radii 3.44 Å) have been found in the "ligand unsupported" ladder structures in Ag(I) complexes. The linear[14,160,166,168] and zigzag[97,167] polymeric chains are linked through Ag···Ag interactions (3.04−3.44 Å) to furnish ladder-like structures. Figure 44 shows perspective of ladder structures of linear polymer $[Ag(pytz)(PF_6)(MeCN)]$ and zigzag polymer $[Ag_2(dp)_2(H_2O)]\cdot NO_3$ (dp = 1,2-diamino-propane) reported by Schröder's laboratory.

Suh and co-workers have reported a stair-shaped infinite silver atom chain, $[Ag_4py_2]$, as the first Ag(0) coordination compound without bridging ligands (Figure 45). The compound is formed from two covalently linked 1D zigzag Ag chains, with alternating long (2.876−2.897 Å) and short (2.827−2.830 Å) Ag···Ag bonds with an average Ag···Ag distance of 2.858 Å. Here the pyridine molecules are bonded to alternating Ag(0) atoms. Theoretical calculations indicate that Ag atoms with partial positive (+0.35) and negative (−0.30) charges are alternately located with the HOMO−LUMO gap of 4.1 eV.[181]

In complex $[Cu_4I_4(mqmsta)_2]$ (mqmsta = 5-methyl-2-(8-quinolylmethylsulfanyl)-1,3,4-thiadiazole), the Cu(I) centers are bridged by mqmsta ligand and iodide anions to form zigzag chain. Two such polymeric chains are linked by iodide to form double-stranded stair-like structure as shown in Figure 46. The CP double chains are of corrugated structure

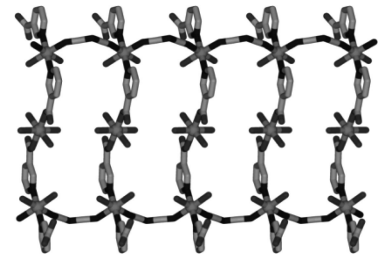

Figure 43. View of Type VI ladder structure in $[Co_3(dca)_2(nic)_4(H_2O)_8]\cdot 2H_2O$.

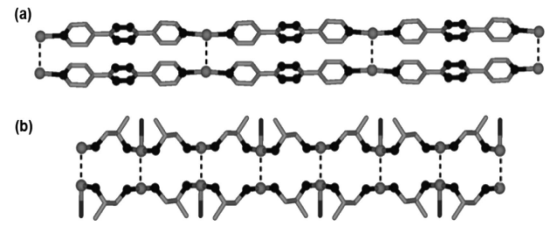

Figure 44. Type VII ladder structures in (a) $[Ag(pytz)(PF_6)(MeCN)]$; (b) $[Ag_2(dp)_2(H_2O)]\cdot NO_3$. The Ag−Ag interactions are shown as dashed lines.

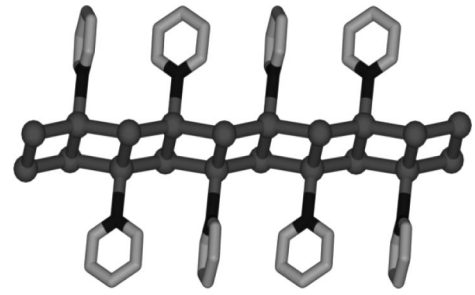

Figure 45. Portion of stair-shaped molecular Ag(0) chain.

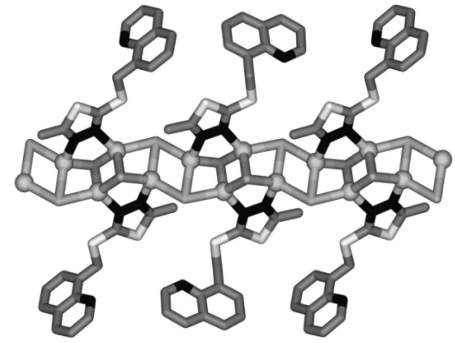

Figure 46. Perspective view of the stairlike polymeric structure in $[Cu_4I_4(mqmsta)_2]$ showing the chairlike Cu_4I_4 units.

and the stair is distorted from an "ideal ladder" (i.e., from "perfectly orthogonal" steps).[182]

2.4.2. Interpenetrated Ladders

Often large cavities of molecular squares in the ladder structures favor interpenetration/catenation. Catenation of 1D molecular ladders either in inclined or parallel fashion have been shown to generate higher dimensional CPs, such as 1D → 2D[170,175,176b] and 1D → 3D.[171,174,176a,177,183] Fujita et al. have reported 4-fold interpenetration in molecular ladder of $[Cd(bpmb)_{1.5}]\cdot(NO_3)_2$ (bpmb = 1,4-bis(4-pyridylmethyl)-benzene). Each square of the ladder interlocks three more rings of different ladders. Hence, no guest molecules were included despite the large size of the cavities (16.4 × 16.6 Å^2).[176a] However, later study by Fujita found that 1,4-

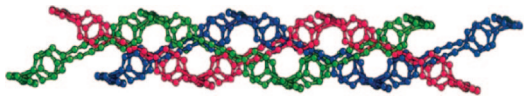

Figure 47. Interwoven structures of three flattened undulating ladders. Reproduced with permission from ref 170. Copyright 1997 The Royal Society of Chemistry.

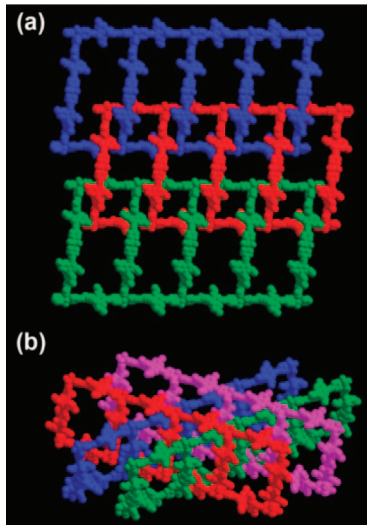

Figure 48. (a) Interlocking of the 1D ladders to form a 2D lamellar network. (b) Interlocked and interpenetrated of the 1D ladders. Adapted with permission from ref 179. Copyright 2008 American Chemical Society.

dibromobenzene molecule can be enclatharated in the middle of each cavity.[176b] Schröder and co-workers have shown polycatenation of undulating molecular ladder structure in $[Cu_2(MeCN)_2(pybut)_3](PF_6)_2$ (pybut = 1,4-bis(4-pyridyl)-butadiyne) as shown in Figure 47. Because of the tetrahedral geometry of Cu(I), the ladder structure observed here displays undulating conformation. These ladders further interweave in a parallel fashion and polycatenate to form a flattened 2D layer structure. Interestingly, each ladder is interwoven with four adjacent ladders, which resulted in a fully polycatenated net. The short C−C distance of 3.48 Å between adjacent pyridyl rings appear to stabilize the structure through $\pi-\pi$ interactions.[170]

Reaction of $Cu(NO_3)_2$ with 1,2-bis(4-pyridyl)ethyne (bpethy) in EtOH yielded blue crystals of $[Cu(bpethy)(NO_3)_2]\cdot 0.5EtOH$ with ladder structure along with a 3D network structure.[184] Complex $[Cu_3(cenep)_4(DMF)_6(H_2O)_3(ClO_4)](ClO_4)_5\cdot 10DMF\cdot 10EtOH\cdot 7H_2O$ (cenep = (*R*)-6,6′-dichloro-2,2′-diethoxyl-1,1′-binaphthyl-4,4′-bis(*p*-ethynylpyridine)) displays large rectangular grid of 24.8 × 48.6 Å^2. The neighboring ladders interlock each other with strong $\pi-\pi$ interactions between the naphthyl rings (3.51 Å) and the C≡C bond and the naphthyl ring (3.53 Å) to form a 2D lamellar framework (Figure 48a). Interestingly, the interlocked frameworks further interpenetrate with another ladder with inclination of 46.6° (Figure 48b). Hence, this ladder furnishes 3D framework structure by simultaneously interlocking and interpenetrating and the large voids are filled with ClO_4^- anions and solvent molecules.[179]

Complex $[Co(bpeb)_{1.5}(NO_3)_2]$ (bpeb = 1,4-bis[(4-pyridyl)-ethynyl]benzene) consists of mutually 2-fold interpenetrating ladders that leads to 3D architecture (Figure 49). There are two distinct sets of ladders running in two different directions ([112] and [1$\bar{1}$2]), and the ladders of one set are catenated to those of the other set and vice versa. Each square grid of a given ladder is interlocked with two squares of two adjacent ladders of the other set.[183b]

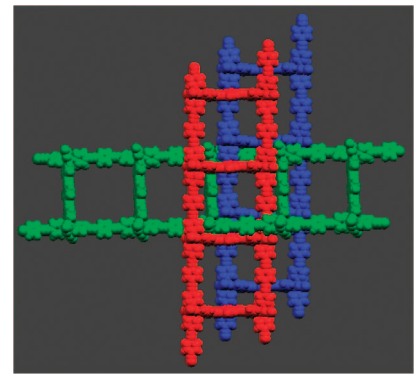

Figure 49. Perspective view of the interpenetrating polycatenated assembly in $[Co(bpeb)_{1.5}(NO_3)_2]$. Reproduced with permission from ref 183b. Copyright 2005 American Chemical Society.

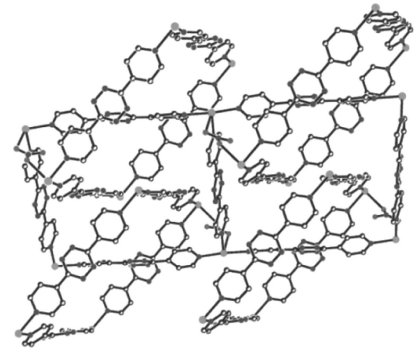

Figure 50. View of the interpenetrating ladders in $[Cd_2(pytz)_3(\mu\text{-}NO_3)(NO_3)_3(MeOH)]$ with the bridging NO_3^- anions. Reproduced with permission from ref 171. Copyright 2000 American Chemical Society.

Complex $[Ni(bpp)_{1.5}(H_2O)(hip)]$ (bpp = 1,3-bis(4-pyridyl)-propane) exhibits ladder structure arising from hip as rails and bpp with different conformations as rungs as well as lateral arms. More interestingly, the cavity of each molecular ladder is interdigitated by the flexible propane rungs. Further, each rectangle is oppositely penetrated by two lateral arms from different molecular ladders to furnish a polythreaded polymeric structure.[173] Another complex $[Cd_2(pytz)_3(\mu\text{-}NO_3)(NO_3)_3(MeOH)]$ displays a unique polycatenation of molecular ladder structure, wherein the ladders are interpenetrated in perpendicular fashion. Moreover, each Cd(II) centers at the intersections of the ladder is bridged to another Cd(II) center of the interpenetrated ladder by a coordinated NO_3^- anion (Figure 50) This connectivity resulted in the formation of a 3D polymer but the total architecture is constructed by a single unit. This single polymeric network also exhibits polycatenation which can be regarded as a fused polyknotted array or a "polyknot".[171]

In complex $[Cu(bptd)(NO_3)_2]\cdot 0.5CHCl_3$ (bptd = 2,5-bis(4-pyridyl)-1,3,4-thiadiazole), two neighboring antiparallel linear chains are linked through weak coordination interactions between the Cu(II) centers and NO_3^- anions (1.975 Å), as well as $\pi-\pi$ interactions to form a 1D double-chain or ladder motif. These double-chains extend in two directions (with respect to each other by a 36.6°) and stack along the [001] direction, leaving space occupied by the disordered $CHCl_3$ molecules.[185]

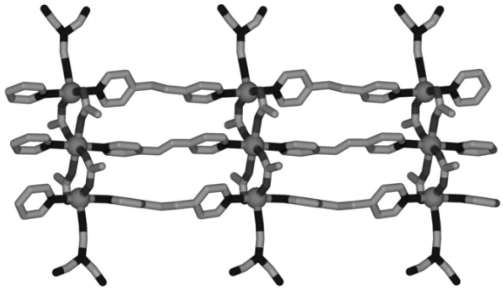

Figure 51. View of three-leg ladder structure in $[Co_3(CH_3COO)_4(dpe)_3(dca)_2]$.

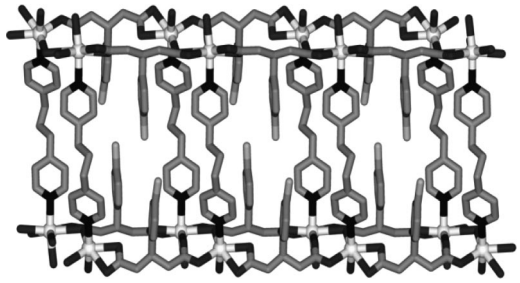

Figure 52. 1D bilayer ladder of $[Cd(bpp)(cpg)_2(H_2O)_2]$.

2.4.3. Unusual Motifs of Ladders

Apart from the common motifs of regular molecular ladders, some unusual motifs have been reported. Gao and co-workers reported the first example of three-stranded molecular ladder in $[Zn_3(CH_3COO)_4(4,4'\text{-bpy})_3\{N(CN)_2\}_2]$. The 4′4-bpy ligands bridged Zn(II) ions to form rails, while acetate anions linked the adjacent Zn(II) ions into rungs. As a result the arrangement of two rungs between three adjacent chains (rails) have yielded an unusual three-stranded ladder structure.[186] Another three-stranded ladder structure has also been observed in the complex $[Co_3(CH_3COO)_4(dpe)_3(dca)_2]$ (dpe = 1,2-bis(4-pyridyl)ethane and dca = dicyanamide). It is found that $\pi-\pi$ stacking interactions (3.75 and 3.86 Å) between the pyridyl rings stabilize the formation of the ladder (Figure 51).[187] Recently, one more triple-stranded ladder similar to the above built from Zn(II), 4,4′-bpy, and acetate has been reported.[188]

An interesting 1D bilayer ladder structure was formed in $[Cd(bpp)(cpg)_2(H_2O)_2]$ (H_2cpg = 3-(4-chlorophenyl)glutaric acid) by Cao et al. Here the glutaric acid acts as rung and is bonded to four different Cd(II) atoms, and bpp occupies the space of rung. The structure can be described as two face-to-face connected ladder structures as depicted in Figure 52.[189]

Obha and co-workers have reported interesting rope-ladder chain structures in heterobimetallic molecular ladder. The polymeric zigzag chains formed by alternate arrangement of $[M(CN)_6]^{3-}$ (M = Co, Fe) and *cis*-$[Ni(en)]^{2+}$ which are further linked by trans $[Ni(en)]^{2+}$ to generate rope-ladder chains. The complexes show antiferromagnetic intermolecular interactions. The Fe(III) complex was metamagnetic below −255 °C.[190] Other rope ladder structures have also been reported.[191] The twisted-ladder structure arise from fused $(NLi)_2$ rings has been observed in $[\{[PhCH_2N(H)Li]_2\cdot H_2NCH_2Ph\}_n]$ whereas the complex $[Cu_4(bpm)_2(N_3)_8]$ (bpm = bis(pyrazol-1-yl)methane) features a railroad-like chain with defective double cubane repeating units with azido bridges.[192]

Hardie and co-workers have described 1D CPs with distorted ladder topology from complexes of metallo-supramolecular cavitant based repeating units.[193] On the other hand, the Cu(I) centers in $[Cu_3(4,7\text{-phen})_4(PPh_3)](BF_4)_3\cdot 2(THF)$ (4,7-phen = 4,7-phenanthroline) are linked through the 4,7-phen ligands to form a ladderlike structure.[194] In the complex $[Ag_4(pdt_2)_6(H_2O)(ClO_4)](ClO_4)_3\cdot H_2O\cdot 1.5MeCN$ (pdt = 4-(2-pyridinyl)-1,2,4-triazole), the side rails are composed of pdt ligands, percholate anions and aqua ligands while two pdt ligands linked the Ag(I) ions to form rungs.[195] Furthermore, macrocycle constructed from Zn(II) and di-Schiff base furnished a ladder structure through 4,4′-bpy bridging.[196] Similar strategy has been adopted to align C=C bonds for [2 + 2] cycloaddition reactions.[159]

An unusual ladder structure has paddlewheel $[Ru_2(CF_3O_2C)_4]$ rails and $TCNQF_4$ (2,3,5,6-tetrafluoro-7,7,8,8-tetracyanoquinodimethane) rungs, which happens to be a supramolecular isomer of a 2D network structure.[197] In another "ladder" polymer [Pb(pzp)(1,3-bdc)] (pzp = pyrazino[2,3-f][1,10]phenanthroline), two $[Pb(1,3\text{-bdc})(H_2O)_{0.5}]$ rails are joined by $\pi\cdots\pi$ interactions between two pzp ligands as rungs.[198] In $(Ph_4As)_2[M_2(dca)_6(H_2O)]\cdot H_2O\cdot xCH_3OH$, (M = Co, Ni), the rails and rungs were occupied by the dicyanamide anions forming loops with metal ions.[199] While most of the ladders are constructed from T-shaped metal nodes, both the metal and ligand adopt T-shape geometries in molecular ladder of $[Co_3(pedta)_2(H_2O)_3\cdot(NO_3)_6\cdot 24H_2O]$ (pedta = 3-pyridyl-ethylenediaminetetraacetic amide).[200]

Rao and Natarajan's laboratory described a ladder structure composed of ZnO_4 and HPO_4 act as T-shaped connectors in $[teta][Zn(HPO_4)_2]_2$ (teta = triethylenetetramine). These two tetrahedral ions are edge-shared to form four-membered rings, which, in turn, form a one-dimensional chain. In other words, this has mixed T-shaped connectors.[201]

2.4.4. Properties of Ladderlike Chains

With predetermined topologies and dimensions, molecular ladders offer great opportunities to fabricate network with desired properties and framework structures for widespread applications. Since the ladders contain cavities, the first implication of the structure could be applicable for inclusion/host−guest chemistry. In general, noninterpenetration ladders enclathrate solvent and anion guest molecules. Many studies have shown that the labile inclusion of guest molecules facilitate guest exchange processes. The inclusion/host−guest assembled structures not only give rise to interesting supramolecular architectures but also can serve as functional molecular devices.

Zaworotko et al. have shown that complex $[Zn(4,4'\text{-bpy})_{1.5}(NO_3)_2]\cdot 0.5pyrene\cdot MeOH$ (Type I) exhibits strong fluorescence because of the exciplex formation between pyrene and 4,4′-bpy. The intercalated pyrene molecules form 2:1 4,4′-bpy:pyrene exciplex through $\pi-\pi$ stacking interactions. As a result, the complex displays strong fluorescence around 540 nm.[122,202] Whereas complex that belongs to ladder Type IV $[Cd(H_2bna)(4,4'\text{-bpy})_{1.5}(H_2O)_2]$ (H_4bna = 2,2′-dihydroxy-[1,1′]-binaphthalene-3,3′-dicarboxylic acid) with bna anions as lateral arms exhibits solid state photoluminescence, which may be attributed to mainly ligand-to-ligand change transfer transitions of $\pi-\pi$ from the H_2bna ligands and admixing ligand-to-metal charge-transfer transitions.[146]

A molecular ladder $[Ba(H_2O)_3(Cu(L))_2]\cdot 2H_2O$ (H_3L = glycylglycine-*N*-[1-(2-hydroxyphenyl)propylidene]) with $[Ba(H_2O)_3]$ as node displays a ferromagnetic dimer with a weak interdimer antiferromagnetic interaction.[203] In $[Co_3(dca)_2$-

$(nic)_4(H_2O)_8]\cdot 2H_2O$, the Co···Co separations are large across the nic bridges (7.3−7.4 Å) and across the dca bridges (7.2 Å) that, combined with the weak superexchange capabilities of both bridges, leads to no observable weak, short-range antiferromagnetic coupling and long-range magnetic order.[155a] The corresponding Cu(II) analogue shows antiferromagnetic behavior with $J = -0.58$ cm^{-1}.[155b] Complex $[Cu(4,4'\text{-bpy})]_2[HPMo_{12}O_{40}]$ containing polyoxometalates as rungs has been exploited to fabricate modified electrodes to catalyze the reduction of nitrite.[139]

According to Yamashita and co-workers, the band gap of unique halogen-bridged Pt(II)/Pt(IV) mixed-valence ladders, $\{(\mu\text{-bpym})[Pt^{II}(en)]_2\}\{(\mu\text{-bpym})[Pt^{IV}X_2(en)]_2\}X_2(ClO_4)_6\cdot 2H_2O$ (X = Br, Cl) and $\{(\mu\text{-bpym})[Pt^{II}(en)]_2\}\{(\mu\text{-bpym})[Pt^{IV}X_2(en)]_2\}X_8\cdot 4H_2O$ (X = I, Br) can be fine-tuned by varying the bridging halide ions.[140] The ladders are constructed from [Pt(en)] moieties and bpym ligand (bpym = 2,2′-bipyrimidine) as rungs to form binuclear $\{(\mu\text{-bpym})[Pt(en)]_2\}$ unit, which are further bridged by halide ions to form ladder structures. It is interesting to note that the mixed-valence centers in these complexes have resulted in both in-phase and out-of-phase arrangements depending on the halide ions. The bridging Br^- ions lie closer to the Pt(IV) centers, indicating the Pt(II)/Pt(IV) mixed valence or charge-density-wave state (CDWs). The nonbonded halide ions also lie closer to Pt(V) and stabilize the in-phase arrangement. On the other hand, in the iodide-bridged ladder, the compound is postulated as out-of-phase arrangement since there is no nonbonded iodide to stabilize the structure. The degree of displacement of the bridging halide ions from the midpoints between the two neighboring Pt ions indicates the electron−phonon interaction and the band gap. In this context, the distortion parameters (d) of these complexes are dependent on the bridging halide ions and increase in the order I, Br, Cl. This result suggests that the band gap was controlled by changing bridging halide ions.[204] Another mixed valence ladder $[(dien)PtBr_2(4,4'\text{-bpy})Pt(dien)]Br_4\cdot 2H_2O$ also has a pair of out of phase CDWs within each ladder and here also pairs of CDWs are ordered in the Pt(II)/Pt(IV)X-chain complexes. The CT excitation energy in the MX ladder was found to be significantly higher than that in the MX-chain, which is due to the intersite Coulomb repulsion V_{rung} along the rung.[140]

Furthermore, ladderlike CPs have been demonstrated to assemble pair of reactive olefins in the linear spacers suitable for [2 + 2] photochemical dimerizations. More detailed discussion will be given in section 7.

2.5. Rotaxane Polymers

The rotaxane molecules have been very well studied in organic chemistry and further employed for stimuli-driven molecular shuttles.[205] This structural motif has also been observed in a number of metal complexes and coordination polymers.[206,207] Conformationally flexible ligands are the key success of self-assembly of structural motifs, such as polycatenanes, helices, braids, Borromean rings and rotaxanes. In this section, several selected examples of interesting 1D CPs having this rotaxane structural motif shown in Figure 53 are presented. Type I rotaxane molecules can be obtained by combination of macrocyclic rings with axle ligands to form pseudorotaxane molecules, which further coordinate with other metal ions to assemble CPs. Type II rotaxane molecules are formed with same spacer ligands with different conformations, that is, gauche/anti and cis/trans that function as ring and rod motifs in rotaxane. Often, other polymeric strands are threaded into the macrocylic rings to furnish 2D polyrotaxane based on 1D CPs. In some cases, utilization of another type of spacer which functions as terminal ligand or lateral arm also produce rotaxane structures with the extra lateral arm threaded into marcocyclic rings to form Type III rotaxane. Type IV rotaxanes are 1D CPs that are threaded into macrocyclic rings constructed by hydrogen bonding interactions.

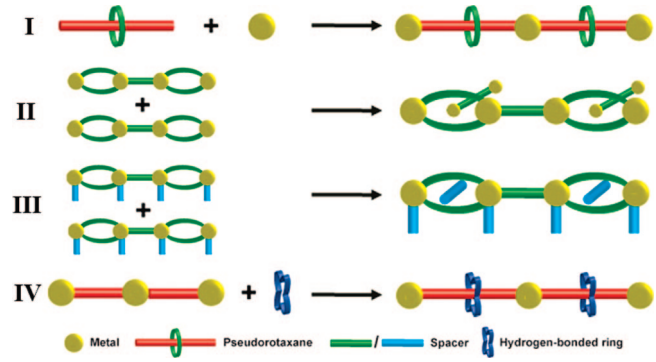

Figure 53. Different types of rotaxane structures observed in 1D CPs.

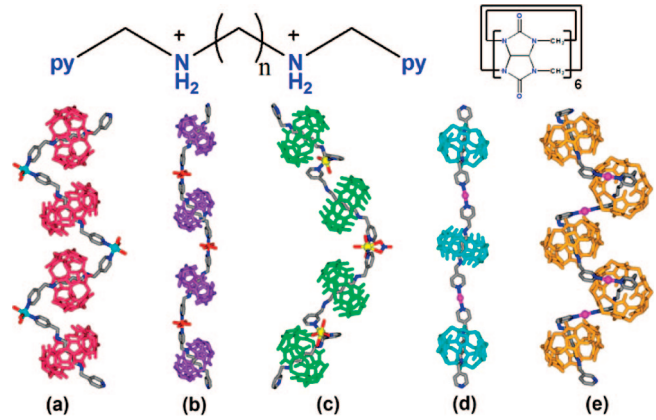

Figure 54. Polyrotaxane with different conformations: (a) zigzag, (b) square-wave shaped, (c) helical, (d) linear, and (e) helical.

2.5.1. 1D Polyrotaxanes

Type I rotaxane molecules can be obtained by using crown ether or cucurbituril derivatives as wheels while axle ligands containing coordination sites, such as pyridyl. Such strategy has led to successful construction of numerous 1D and higher-dimensional rotaxane structures. Kim et al. have shown that rotaxane structures can be achieved by threading the cucurbituril "bead" with short "string" of 1,4-diaminobutane, 1,5-diaminopentane with 4- or 3-pyridylmethyl groups and linking the amine groups with metal ions as "linkers". The strong hydrogen bonding between the protonated amine nitrogen atoms of the "string" and the oxygen atoms of cucurbituril have firmly positioned the cucurbituril "bead" at the middle of repeating unit. The overall structure of a polyrotaxane is controlled by the coordination preferences of the metal ions, size, and coordination ability of anions as summarized in Figure 54.[206d] Generally, coordination of pyridyl groups to square pyramidal and octahedral metal ions such as Cu(II), Co(II), and Ni(II) in cis conformation afforded zigzag structures while trans coordination afforded square-wave polymers. Interestingly Cd(II) complex has helical conformation and the 3-pyridyl units coordinate in trans and

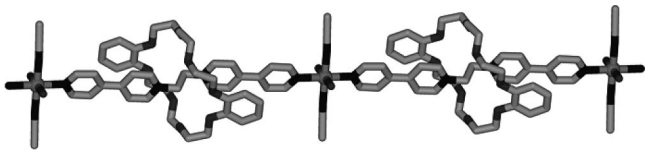

Figure 55. Portion of straight chain 1D polyrotaxane.

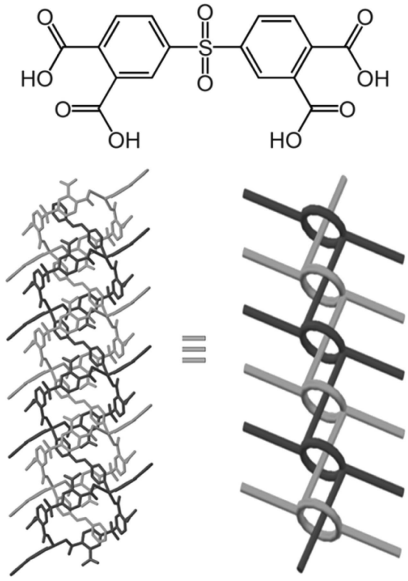

Figure 56. Structure of H_4dstc ligand (top) and the two polymeric chains interlocked and interpenetrated to form polyrotaxane (bottom).

cis positions alternately to Cd(II) centers.[208] On the other hand, the two-coordinate Ag(I) furnished both linear or helical CPs.[209] A stable [3]pseudorotaxane constructed from the self-assembly of Ni(II) and Zn(II), a phenanthroline derivative containing *N*-(3-pyridylmethyl)-1,4-butanediammonium and cucurbituril formed square-wave-shaped 1D polyrotaxane.[210] Such interplay of metal ion geometry and shape of the axle ligands has been exploited to produce similar 1D polyrotaxanes with β-cyclodextrin and other organic rings; and the structures are further confirmed by various spectroscopic and microscopic techniques.[211]

Loeb and co-workers have reported 1D CP rotaxane structures using another type of [2]pseudorotaxane obtained by threading the dipyridinium axle into dibenzo-[24] crown-8 ether. The Co(II) and Zn(II) CPs display octahedral coordination geometry comprising of two [2]pseudorotaxane ligands, two MeCN and two water molecules all in trans orientations (Figure 55). The infinite 1D channels are formed between the polymer strands and are filled with the BF_4^- anions and water molecules. By changing to noncoordinating solvents, the corresponding Cd(II) complex can be obtained as square-grid 2D polyrotaxanes.[206c,212] Recently, two related [2]pseudorotaxane ligands resulted from disulfonated-dibenzo-[24]crown-8 ether and dicationic 1,2-bis(pyridinium)ethane and 1,4-bis(4-pyridyl)-benzene have been shown to form 1D CP rotaxane structures.[213]

Complex $[Zn(H_2dstc)(dpe)_{1.5}]$ (H_4dstc = 3,3′,4,4′-diphenylsulfonetetracarboxylic acid, shown on top in Figure 56) features Type III polyrotaxane structures facilitated by two different spacers. Two Zn(II) atoms are bridged by two H_2dstc ligands to form a 30-membered molecular ring with dimension of 11.2 × 12 Å^2. Of two dpe ligands, one links the rings into polymeric chains, while the other one coordinates to Zn(II) in terminal fashion as arm and arranged

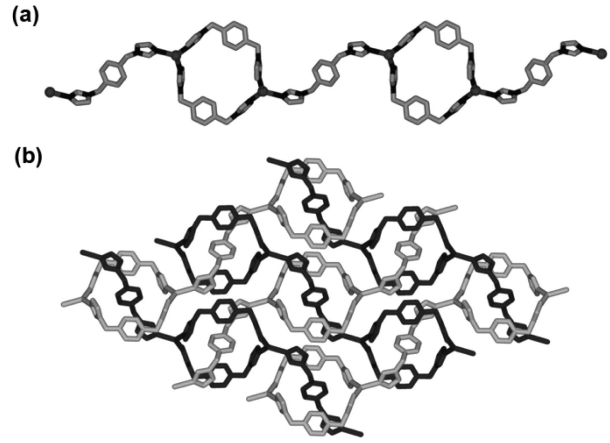

Figure 57. (a) View of the ligand and $[Ag_2(bix)_2]^{2+}$ polymeric chains. (b) 2D polyrotaxane network.

alternately at two sides of chains. These identical polymeric chains are entangled in pairs to form a 1D armed-polyrotaxane structure with the dpe rods threaded into the macrocyclic rings of $[Zn_2(H_2dstc)_2]$ (bottom of Figure 56). Further, the polyrotaxane polymeric chains form a 2D hydrogen-bonded network stabilized by weak $\pi-\pi$ interactions between dpe arms (3.77 Å).[214]

Complex $[Cu(bph)_3(H_2O)(NO_3)][Cu(bph)_2(H_2O)(NO_3)]_2 \cdot (NO_3)_2 \cdot EtOH$ (bph = 1,6-bis(4-pyridyl)-hexane) contains two different types of infinite 1D chains. In the single-stranded 1D chain of $[Cu(bph)_3(H_2O)_2(NO_3)_2]$ (A) contains two bridging pbh ligand and two monocoordinated dangling ligands, whereas in $[Cu(bph)_2(H_2O)(NO_3)]$ (B), the metal centers are doubly bridged by the ligands forming 30-membered $Cu_2(bph)_2$ rings. The two motifs (A and B), exhibiting a 1:2 ratio, are entangled to give 2D layers. The A chains are threaded into the rings of the B ribbons, in such a way that each Cu−bph−Cu segment penetrates two loops of two adjacent ribbons. Neighboring A chains show a relative displacement.[215]

2.5.2. 2D Polyrotaxanes

Type II rotaxanes are formed by spacer ligands with flexible backbone that can function as both ring and rod components. Complex $[Ag_2(bix)_3(NO_3)_2]$ has been found to have an infinite 2D polyrotaxane structure arising from 1D polymeric chains. As shown in Figure 57a, two Ag(I) ions and two bix ligands form a macrocyclic ring which further linked by another bix ligand into 1D linear CP. Interestingly, closer look at the structure reveals that these individual chains associate to produce 2D polyrotaxane in a inclined fashion as displayed in Figure 57b. Edge-to-face interactions between phenylene and imidazole rings have been found as 2.77 and 2.68 Å, while no observable face-to-face $\pi-\pi$ interaction between the aromatic rings.[216]

In a later study, Ciani and co-workers have achieved a parallel 2D polyrotaxane in $[Zn_2(bix)_3(SO_4)_2] \cdot 8H_2O$. In this case, the polymeric chains are highly undulated because of the gauche conformation of bix, and all the chains are interlaced with two adjacent rings, generating a parallel 2D polyrotaxane layer with interlayer distance of 13.5 Å (Figure 58). Another related $[Cd_2(bix)_3(SO_4)_2]$ analogue also exhibits 2D network similar to the aforementioned $[Ag_2(bix)_3] \cdot (NO_3)_2$. Herein, the bix ligands adopt anti conformation and lead to "straighter" chains structure. The adjacent chains are interlaced to give an inclined 2D layer.[217] The Zn(II)

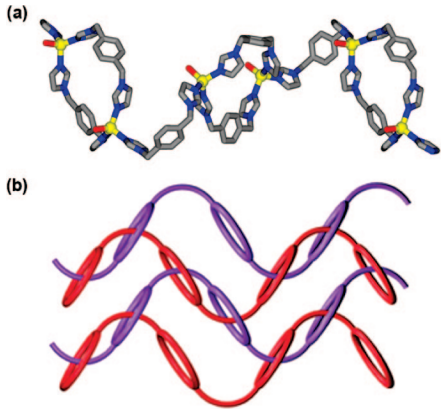

Figure 58. (a) Portion of polymeric chain. (b) Schematic diagram of entanglement. Adapted with permission from ref 217. Copyright 2005 American Chemical Society.

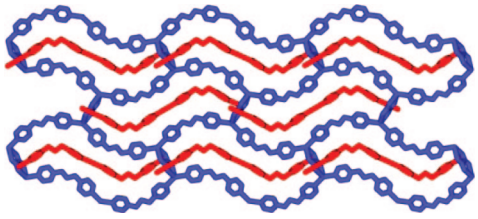

Figure 59. View of 3D pseudo-polyrotaxane structure in $[Ag(bpp)][Ag_2(bpp)_2(ox)]\cdot NO_3$.

analogue displays another type of 2D rotaxane structure.[218] Other 2D polyrotaxane structures also have been observed with structurally related spacer ligand, 1,4-bis(4-pyridylmethyl)-2,3,5,6-tetrafluorobenzene.[219]

2.5.3. 3D Polyrotaxanes

Complex $[Ag(bpp)][Ag_2(bpp)_2(ox)]\cdot NO_3$ is a 3D pseudo-polyrotaxane generated by the interpenetration of 1D chains and 2D layers (Figure 59). In the 2D anionic sheets, the tetrahedral Ag(I) atoms are connected by bridging bpp and bis-chelated oxalate to furnish a 2D (6,3) hexagonal topology. The 2D anionic layers are almost coplanar and adjacent sheets are stacked in an offset fashion along the *a*-axis in such a way that hexagonal cavities are divided into two identical halves. Further the Ag(bpp) 1D cationic polymeric chains interpenetrate into the 2D sheets in an inclined fashion to generate a rare 3D pseudo-polyrotaxane.[220]

Another Type III rotaxane is observed in complex $[Cd(1,4\text{-bdc})(bpybc)_{1.5}]\cdot 10H_2O$ (bpybc = 1,1′-bis(4-carboxybenzyl)-4,4′-bipyridinium, shown in Figure 60a) which displays a polythreaded network containing both polyrotaxane and polypseudopolyrotaxane features. The 1D loop chain is composed of a ring formed by two Cd(II) bridging two bpydc in cis conformation with a window of 17.6 × 14.5 Å which are further linked through another bpybc in trans conformation (Figure 60b). In these 1D chains, the rods penetrate into the macrocyclic rings to form a 2D polyrotaxane network. The monodentate 1,4-bdc ligands reside both sides of the chain and act as lateral arms in these 2D polyrotaxane layers and thread into the remaining voids of the adjacent layers to generate a 3D polypseudorotaxane array (Figure 60c and d). The entanglement is sustained by charge transfer interaction occurs between the electron-rich 1,4-bdc and the electron-deficient bipyridinium cation. Further, this complex exhibits photo- and thermochromic behaviors because of the reduction of bipyridinium molecules to blue bipyridinium radicals.[221]

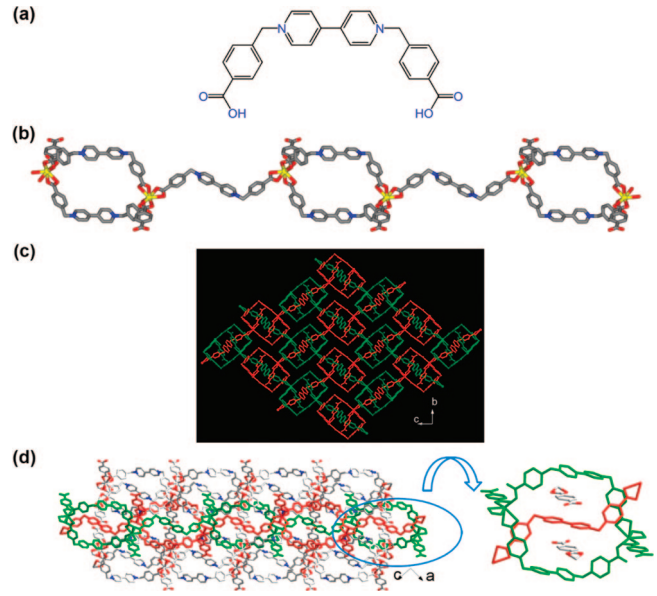

Figure 60. (a) Ligand structure. (b) Portion of 1D polymeric chain. (c) Perspective view of polyrotaxane sheet. (d) Perspective view of 3D polypseudorotaxane comprised of mutual polythreading of three adjacent polyrotaxane sheets.

2.5.4. Hydrogen-Bonded Polyrotaxanes

Type IV rotaxane molecules contain 1D CPs threaded into macrocyclic rings that are formed through hydrogen bonding interactions. Self-assembly of $Zn(CH_3COO)_2\cdot 2H_2O$ and dpe has led to the formation of hydrogen-bonded polyrotaxane-like structure in $[Zn(CH_3COO)_2(dpe)]\cdot 2H_2O$. The oxygen atoms of acetate groups from two different adjacent polymeric chains are O−H···O hydrogen-bonded to four lattice water molecules to form a 24-membered ring. The dpe ligands of the adjacent [Zn(dpe)] polymeric chains "thread" through the center of the hydrogen-bonded ring. Such hydrogen-bonded polyrotaxane-like structure has resulted in a sheetlike structure. These hydrogen-bonded rings are further fused with two eight-membered rings formed by the water tetramer to generate a 3D supramolecular network (Figure 61).[222]

Wang and co-workers have reported polythreading of 1D CPs into hydrogen-bonded network. In complex $[Co(4,4'\text{-bpy})(H_2O)_4]\cdot(H_2bptc)\cdot 2H_2O$ (H_4bptc = 3,3′,4,4′-biphenyltetracarboxylic acid), the zigzag CP $[Co(4,4'\text{-bpy})(H_2O)_4]$ are threaded into hydrogen-bonded anionic ladder constructed by the uncoordinated H_2bptc anions and lattice water molecules (Figure 62a). The aqua ligands of 1D zigzag chain form hydrogen bonding interactions with carboxylate groups and lattice water molecules of 1D ladder which further stabilize the whole entangled array. The related $[Ni(4,4'\text{-bpy})(H_2O)_4]\cdot 0.5(1,2,4,5\text{-btc})\cdot H_2O$ (1,2,4,5-H_4btc = 1,2,4,5-benzenetetracarboxylate acid) also displays pseudorotaxane structure. Two linear polymeric chains which extend in two different directions (rotated by 120°) threaded into the 2D (4,4) hydrogen-bonded network formed by lattice water molecules and carboxylate anions (Figure 62b).[223]

In complex $[Cu(NO_3)_2(H_2O)(bmimb)_{1.5}\cdot 4H_2O]$ (bmimb = 1,4-bis[(2-methylimidazol-1-yl)methyl]benzene), two bmimb ligands bridged the Cu(II) centers into 1D CP via two imidazole moieties, while another two bmimb ligands only are coordinated to the metal centers via one of its imidazole groups. Interestingly, the uncoordinated imidazole group is hydrogen bonded to a lattice water molecule which in turn

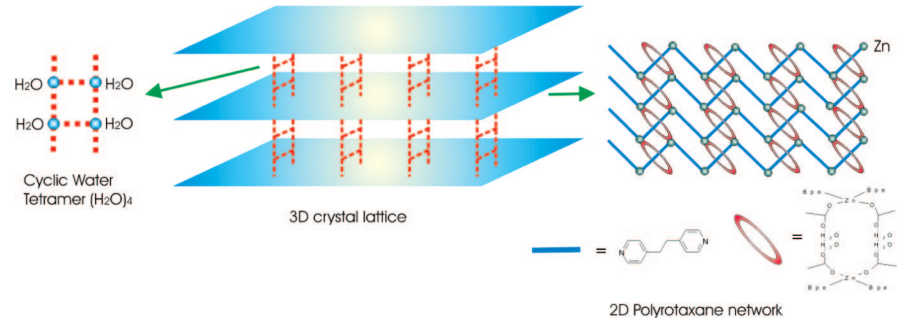

Figure 61. Schematic digram of the crystal structure involving hydrogen-bonded polyrotaxane.

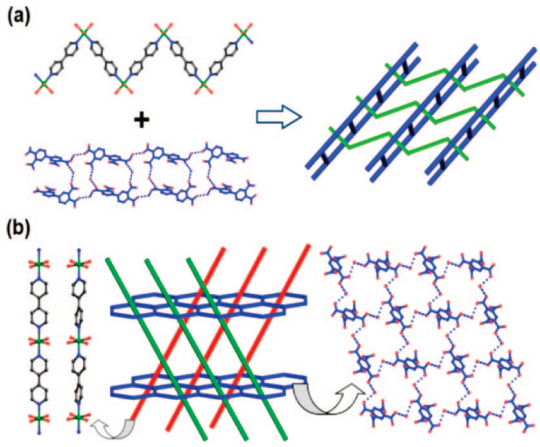

Figure 62. (a) Polythreading of 1D zigzag chains into the hydrogen-bonded ladders; (b) 3D poly(pseudorotaxane) array constructed from linear chains and hydrogen-bonded 2D layer.

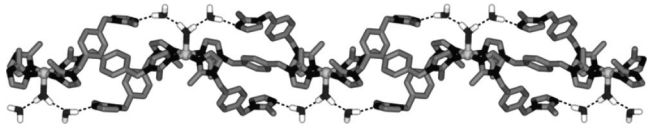

Figure 63. Portion of pseudo-polyrotaxane constructed by hydrogen-bonded marcocycle and 1D CP.

hydrogen bonded to an aqua ligand. As a result, the appended bmimb ligands form a hydrogen-bonded 34-membered ring and the 1D chain of [Cu(bmimb)] is threaded through to form a pseudo-polyrotaxane structure as shown in Figure 63.[224]

2.6. Ribbon/Tape Polymers

Generally, ribbon or tape-like polymers are obtained from flexible ligand backbone in bent/gauche conformations which interconnected through metal nodes to form macrocycle. In some cases, solvent or anions are accommodated in the rings (cavities). These double-bridged 1D polymers or "ring polymers" are of special interest in the coordination networks. Apart from their 1D nature, they also contain cavities/pores which may facilitate encapsulation of guest molecules, gas adsorption, interpenetration of other polymers, etc. as in higher dimensional CPs. Some interesting examples of rotaxane and interpenetrated structures arising 1D CPs are discussed in sections 2.6 and 6.1, respectively. In this section, few selected ribbon-like polymers are highlighted.

A series of flexible guest-binding ribbon CPs, $[Cu(dpe)_2(guest)_2](PF_6)_2 \cdot n$guest have been reported by Noro and co-workers. The Cu(II) ion has an elongated octahedral environment with four dpe nitrogen atoms in the equatorial plane and two axial positions occupied by a variety of Lewis base guest molecules. While guests such as acetone, DMF,

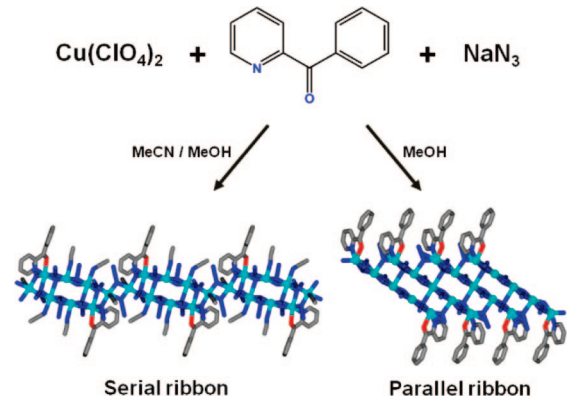

Figure 64. Formation of two types of ribbon polymers by the variation of solvents.

H_2O or MeCN are directly bound at the Cu(II) centers, THF, dioxane, and 2-PrOH cannot coordinate to the Cu(II) centers probably because of steric hindrance. Instead, these noncoordinated guests are incorporated into the host framework by hydrogen bonding and van der Waals interactions. It is worthwhile to note that complex $[Cu(dpe)_2(acetone)_2](PF_6)_2$ undergoes crystal-to-crystal transformation under thermal treatment, in which the PF_6^- anions are coordinated in during the desolvation process.[225] Recently, the desolvated compound $[Cu(dpe)_2(PF_6)_2]$ with weak and flexible Cu−PF_6 has been shown to be highly selective CO_2 adsorption for CO_2 and C_2H_2 with three-step structural transformations. The results of the temperature-dependent IR spectra under CO_2 flow, calculations, and adsorption isotherms of CO_2 and C_2H_2, indicate that the specific adsorption sites may be on the surface of PF_6^- anions, which have the strongest polarity in the framework. Interestingly, the CO_2 adsorption properties can be regulated by modifying the axial ligands PF_6^-, BF_4^-, and DMF.[226]

Self-assembly of $Cu(ClO_4)_2$, 2-benzoylpyridyl (bzp), and NaN_3 in methanol/acetonitrile and methanol afforded two 1D ribbons with serial and parallel azido-bridged eight-membered copper rings, respectively (Figure 64). In complex $[Cu_4(N_3)_8(CH_3CN)_3(bzp)_2]$, the metal ions are bridged by eight azido groups to form the eight-membered copper ring and the adjacent rings are further linked in a serial mode to an exotic 1D chain by double azido bridges. Whereas in complex $[Cu_5(N_3)_{10}(bzp)_2]$, the five copper ions are bridged by double azides to form a linear unit. The parallel neighboring units are further connected to a tape through another azido bridge.[227]

Flexible coordination networks are desired to enclathrate organic guests that can be induced-fit by guest molecules. However, if the ligands are flexible, the networks are in general constricted or interpenetrated leaving no void space

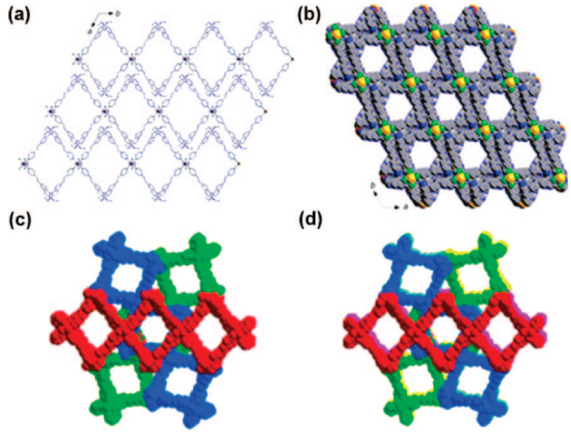

Figure 65. (a) View of the packing of the ring polyemeric chains. (b) Space-filling model of the 1D hexagonal channels. (c) Space-filling model of the 6_2-helical arrangement of the 1D polymeric chains before structural transformation. (d) Space-filling model of the 6_1-helical arrangement of the 1D polymeric chains after benzene exchange. Adapted from ref 229. Copyright 2005 Wiley Interscience.

in the solid for enclathrating guests. To solve this, Fujita and co-workers developed networks to favor "hetero-recognition" (enclathration) rather than "self-recognition" (constriction or interpenetration). In one of their findings, they have found a 1D CP $[Cd(bpmtfb)_2](NO_3)_2$ (bpmtfb = 1,4-bis(4-pyridylmethyl)-2,3,5,6-tetrafluorobenzene) to contain *tert*-butylbenzene in each cyclic cavity.[228]

A ribbon polymer, $[Cd(envp)_2(ClO_4)_2]\cdot 11EtOH\cdot 6H_2O$ exhibits high permanent porosity and undergoes SCSC transformation induced by solvent exchange. As shown in Figure 65a, all the 1D chains interdigitate and lie parallel to each other in the *ab*-plane to form layers through strong $\pi-\pi$ stacking interactions (3.36 Å). The 1D chains in the adjacent layers along the *c*-axis are rotated by 120° with respect to each other to create chiral, 1D pseudohexagonal channels of 16.77 Å in dimension (Figure 65b). The 6_2 operation generates an ···ABCABC··· stacking pattern for all the 1D chains along the *c*-axis, as shown in Figure 65c. More interestingly, the compound undergoes reversible SCSC transformation in the presence of benzene vapor as monitored by X-ray diffraction and ^{1}H NMR techniques. It is notable that the relative orientation of the ethoxy groups of the envp ligands, coordinating perchlorate groups and the relative orientation of the 1D polymeric chains are changed significantly during the structural transformation. As a result, the 1D polymeric chains stack in an ···ABCDEFABCDEF··· pattern along the *c*-axis with the marcocycle planes slightly tilted away from the ab plane (Figure 65d).[229]

Double-stranded 1D chains with rectangular-shaped cavities have been found in $[CoCl_2(4\text{-pmna})_2]$, $[Co(NCS)_2(4\text{-pmna})_2]\cdot 2Me_2CO$, and $\{[Co(4\text{-pmna})_2(H_2O)_2](NO_3)_2\cdot 2CH_3OH$ (4-pmna = *N*-(pyridin-4-ylmethyl)nicotinamide). In the first compound, each chain slips and obstructs the neighboring cavities so that there are no guest-incorporated pores, whereas the cavities in the latter two polymers have been filled with a guest molecule. The chain with nitrate anion shows a reversible structural rearrangement during adsorption and desorption.[230] Many other rings containing 1D structures have been reported in the literature.[103,231] They are also involved in the interpenetration/catenation and supramolecular isomerism (see sections 5 and 6).

Furthermore, apart from common motifs which described earlier, some unusual 1D CPs with similar morphologies are reported as well. For example, in complex $[Ni_2(oba)_2(4,4'\text{-bpy})_2(H_2O)_2]\cdot 4,4'\text{-bpy}$ (H_2oba = 4,4′-oxybis(benzoic acid)), oba ligands linked two Ni(II) centers into binuclear building units which further joined by bpy to construct a 1D train-like box that contain free bpy ligands. Each box is entangled with another two adjacent boxes.[17] An interesting tubular 1D CP with its wall made of edge-sharing hexagons, topologically similar to that of carbon nanotubes has been described by Gao et al. This is prepared from 2,2′-bipyridine-3,3′-dicarboxylate-1,1′-dioxide and Cu(II) ions under hydrothermal conditions.[232]

Complex $[Ag_7(tpst)_4(ClO_4)_2(NO_3)_5(DMF)_2]$ (tpst = 2,4,6-tris[(4-pyridyl)methyl-sulfanyl]-1,3,5-triazine) displays an interesting 1D chain structure containing nanotubes. Each Ag(I) ion is coordinated to the pyridyl groups of two tpst ligands and each tridendate tpst ligand in turn binds to three Ag(I) centers to form an $[Ag_3(tpst)_2]$ nanosized ring. These rings are further linked by Ag−N and Ag−S bonds from one N and one S atom of the trithiocyanuric spacer to form the basic nanosized tube unit with the dimensions of 1.35 × 0.96 × 0.89 nm, which accommodates two DMF molecules and two perchlorate anions. The tube units share Ag(I) ions by Ag−N and Ag−S bonds to form an infinite chain. The nitrate anions are located near the Ag(I) centers and embedded in the polymer chain regions.[233] Several other 1D tubular CPs are also reported.[93,155b,234]

2.7. Metal Cluster As Building Blocks for 1D CP

In the past two decades, there is an enormous interest in the properties of the CPs particularly magnetism. Numerous complexes ranging from discrete to 3D CPs have been designed, synthesized and reported for their exceptional magnetic properties.[235] Oligonuclear clusters or single molecule magnets (SMMs) can be tailored into 1D CPs, which may also feature single chain magnet (SCM) behaviors. One can refer to the recent reviews on the synthetic strategies and magnetism of oligonuclear clusters and SMMs that form 1D CPs.[235f−i] In this section, we describe how the metal carboxylates, metal halides, metal chacogenides and SMMs can be utilized as building blocks for the construction of 1D CPs.

2.7.1. Metal Carboxylate Clusters

A 1D linear CP of $[Zn_7(\mu_4\text{-}O)_2(CH_3COO)_{10}(dpe)]$ is formed by the self-assembly of a heptanuclear zinc cluster $[Zn_7(\mu_4\text{-}O)_2(CH_3COO)_{10}]$ linked by the dpe as shown in Figure 66a. Interestingly, by changing the backbone of the dinitrogen spacer ligand from $-CH_2-CH_2-$ group to $-S-S-$ group, that is, 4,4-dipyridyldisulfide (dpds), the shape of the 1D CP varies from quasi-linear to zigzag chain.

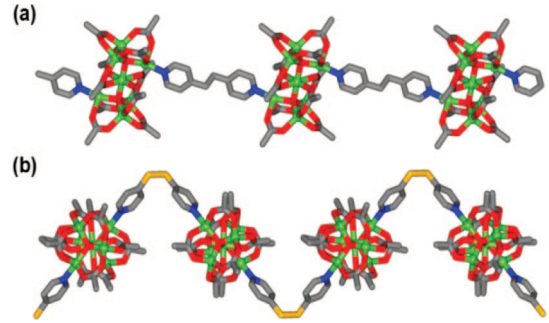

Figure 66. 1D CPs comprising $[Zn_7(\mu_4\text{-}O)_2(CH_3COO)_{10}]$ with (a) linear and (b) zigzag conformations.

The related compound $[Zn_7(\mu_4\text{-}O)_2(CH_3COO)_{10}(dpds)]$ has similar geometry, coordination as well as packing of the polymeric chains in the crystal lattice with the former, yet exhibits different structural motif (Figure 66b). The torsion angle of two methylene carbon atoms in bpe is 180° in the former compound, while 61.8(5)° for C−S−S−C bond in the latter. Such drastic difference in torsion angles has directed the linear chain of the CP into wavy conformation. As a result, the interplanar angles between the two pyridine rings in both compounds have been found of 0° and 89.4(4)°, respectively.[236]

Complex $[Zn_6(sas)_4(H_2O)_8]\cdot 5H_2O$ (H_3sas = *N*-(2-hydroxybenzyl)-*L*-aspartic acid) displays 1D structure with hydrated Zn(II) cations linking $[Zn_5(sas)_4(H_2O)_4]^{2-}$ anions. The Zn(II) ions dimerized through bridging of two carboxylate groups to form Zn_2O_2 ring and four phenolate oxygen atoms from these two dimers further bonded to another Zn(II) center to form a pentazinc cluster. This is quite distinct from the other metal complexes containing *N*-(2-hydroxybenzyl)-amino acid ligands where the phenolate oxygen atoms are involved in the formation of dimer.[74a] The other four free carboxylate groups link to $[Zn(H_2O)_4]^{2+}$ units to generate CP structure. On the other hand, the related Cu(II) complex shows 1D zigzag CP structure with mononuclear building units.[237]

A 1D CP, $[Co_8(H_2O)_2(CH_3COO)_7(ampd)_6]$ (H_2ampd = 2-amino-2-methyl-1,3-propanediol), which is composed of alternating discrete hepta- and mononuclear moieties bridged by acetate ligands, shows ferromagnetic exchange within the heptanuclear unit and negligible interactions along the chain between the hepta- and mononuclear fragments.[238] Complex $[Mn_3(1,3\text{-}bdc)_2(Hbdc)_2(2,2'\text{-}bpy)_2]\cdot 2.5H_2O$ contains isophthalato-bridged trimanganese cluster building units further linked by isophthalato ligands in 1D ladder-like network with the linear trimanganese units function as the parallel rungs. The complex shows antiferromagnetic behavior with intratrimanganese cluster coupling interactions which behave like other discrete trimanganese clusters.[239]

Reaction of pyrazole (Hpz) with copper(II) formate gives a 1D zigzag CP, $[Cu_3(\mu_3\text{-}OH)(pz)_3(HCOO)_2(Hpz)_2]$ in which the triangular trinuclear units are connected through single formate bridges. Whereas reaction with copper propionate afforded complex $[Cu_3(\mu_3\text{-}OH)(pz)_3(C_2H_5COO)_2(EtOH)]$ with two oxygen atoms of two carboxylate ions doubly bridge two copper atoms of different triangles, thus generating hexanuclear units. Interestingly, two other propionate ions link together two hexanuclear units yielding a 12-membered cycle and giving rise to 1D CP.[240] Reaction of copper(II) acrylate and methacrylate with pyrazole afforded 1D CPs in which triangular trinuclear units $[Cu_3(OH)(pz)_3]$ are connected through carboxylate bridging to form hexanuclear clusters, which are further connected through carboxylate bridging into CPs. Furthermore, these complexes are valuable catalysts in the peroxidative oxidation with aqueous H_2O_2, in MeCN at 25 °C, of cycloalkanes to the corresponding ketones and alcohols.[241]

In $[Mn_{17}O_8(N_3)_5(CH_3COO)_4(pd)_{10}(py)_6]$ (H_2pd = 1,3-propanediol), the $Mn^{III}_{11}Mn^{II}_6$ core is held together by eight $\mu_4\text{-}O^{2-}$ and four $\mu_3\text{-}N_3^-$ bridging ligands. The structures also contain 10 pd^{2-} and two carboxylate bridging ligands, while the six terminal pyridine, two chelating acetate, and one $\mu\text{-}N_3^-$ ligands act as peripheral ligands. The azide bridged the Mn_{17} units into 1D CP structure as shown in Figure 67. The complex exhibits ferromagnetic interaction and giant ground-state spin for the Mn_{17} units. There are numerous 1D CPs comprised through azide bridging and exhibit interesting magnetism.[242]

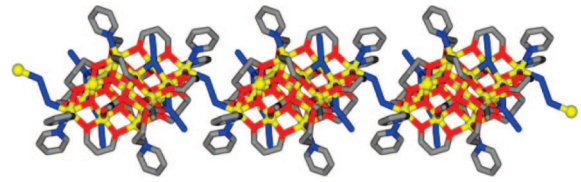

Figure 67. Portion of azide bridged Mn_{17} cluster CP.

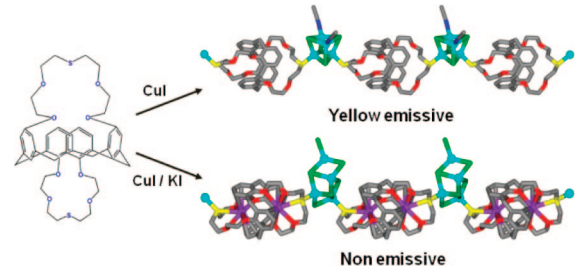

Figure 68. Isolation of two 1D CPs containing copper halide clusters.

Sequential assembly of the linear trimetallic cluster, $[Cd_3(bhnq)_3(H_2O)_2]\cdot DMF\cdot 3H_2O$ (bhnq = 2,2′-bis(3-hydroxy-1,4-naphthoquinone) with rigid covalent linker has resulted in a 1D hybrid cluster-based CP, $[Cd_3(bhnq)_3(4,4'\text{-}bipy)]\cdot DMF\cdot 3H_2O$. The presence of a sticky surface based on the π conjugation is responsible for further 3D MOF containing solvent-filled cavity.[243] Complex $[CuI_3(pymt)_3]$ (pymt = pyrimidine-2-thiolate) is obtained from solvothermal reaction along with the reduction of Cu(II) to Cu(I). Each pymt ligand acts as a μ_3-bridge to link three copper atoms through S and N donors and three Cu atoms form a slightly distorted isosceles triangle via two Cu−Cu interactions. The trinuclear units further extend into an infinite 1D CP via pymt bridging.[244] There are many other 1D CPs comprised of metal carboxylate clusters in the literature.[245]

2.7.2. Metal Halide Clusters

The copper-halide type clusters have been demonstrated as building blocks for 1D CP in many cases. A recent review by Li on copper(I) halides describes the assembly of the clusters into zero to 3D CPs.[246] Selected examples of CPs contaiing metal halide clusters are illustrated in this section.

The Cu(I) complexes of calix[4]-bis-dithiacrown-based ligands features 1D CP structures through copper halide cluster linking (Figure 68). Complex $[(Cu_4I_4)L(CH_3CN)_2]$ (L is shown in Figure 68) forms 1D CP through cubane-type Cu_4I_4 linking units. The complex exhibits bright yellow emission because of a cluster-centered excited state with mixed halide-to-metal charge transfer character. More interestingly, removal of acetonitrile molecule from Cu(I) centers lead the structural change which induced the photoluminescence switching from yellow to red emission. Another 1D polymer with K^+ encapsulated in calix[4]-bis-dithiacrown marcocyclic is also obtained with scoop-type $Cu_4I_6^{2-}$ cluster linking.[247]

Solvothermal reaction of 5,10,10-trimethyl-bicyclo[2.2.1]-heptano-2-phenyl imidazole (Htbhpi) with CuBr as a catalyst gave a 1D polymer, $\{[(cis\text{-}(2C\text{-}2C)bi\text{-}tbhpi)_2(trans\text{-}(2C\text{-}2C)bi\text{-}tbhpi)](Cu_2Br_2)(Cu_4Br_4)\}$. In the crystal structure, the 1D chain is composed of both cis and trans coupling isomers of in situ formed (2C-2C)bi-tbhpi ligand.[248]

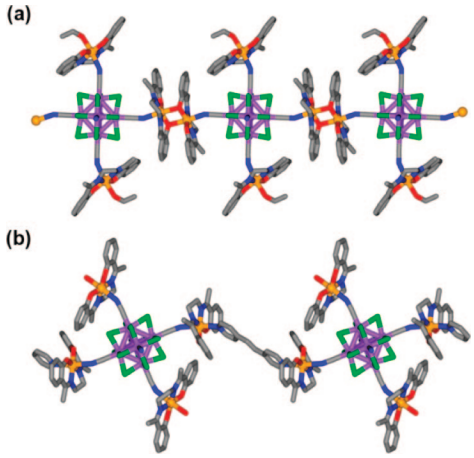

Figure 69. View of the two polymers (a) with and (b) without bpe as bridging ligand.

$[Mn(7\text{-Me-salen})]_2[Mn(7\text{-Me-salen})(EtOH)]_2[Nb_6Cl_{12}(CN)_6]$ (salen = *N,N′*-ethylene bis-(salicylidene)imine) is composed of heteropentamers linked through phenoxo bridges between the $[Mn(salen)]^+$ complexes (Figure 69a). Each pentamer is comprised of an octahedral cluster $[Nb_6Cl_{12}(CN)_6]^{4-}$ connected to two $[Mn(salen)]^+$ and two $[(Mn(salen)(EtOH)]^+$ complexes through four CN^- ligands located in equatorial positions. Addition of bpe resulted in the formation of extended 1D CP, $\{[(Mn(salen)(bpe)Mn(salen)][\{Mn(salen)(H_2O)\}_2\{Nb_6Cl_{12}(CN)_6\}]$, in which the heteropentamers are linked through the bpe ligands (Figure 69b). The location of the cyanide and bpe ligands on the same side of the $N_{CN}-Mn-N_{bpe}$ axis leads to chains with sinusoidal wavelike structures. Hydrogen bonds between nonbridging cyanide groups and aqua ligands connect the chains into layers that held together through hydrogen bonding with the water molecules. The complexes show intradimer antiferromagnetic and paramagnetic coupling respectively.[249] In a zigzag CP, $(Me_4N)_3\{[Mn(5\text{-MeO-salen})][Nb_6Cl_{12}(CN)_6]\}\cdot 1.5MeOH\cdot 0.5H_2O$, each cluster is trans-coordinated by two $[Mn(5\text{-MeO-salen})]^+$ complexes via CN^- ligands and each Mn complex links two clusters to give anionic chains that stack perfectly parallel to each other to form layers that are separated by ammonium cations.[250]

2.7.3. Metal Chalcogenide Clusters

Chalcogenide clusters display properties such as microporosity, fast ion conductivity, and photoluminescence to narrow and tunable electronic band gaps,[251] and these properties have been incorporated in 1D CPs through rigid ligand bridging. For instance, penta-supertetrahedral clusters form homo- and heterobimetallic 1D CPs via bpe and bpp bridging. The complexes show optical transitions with band gaps of 3.44−3.54 eV.[252]

Zheng and co-workers have shown that hexanuclear rhenium selenide clusters can be employed as the fundamental building units to create a wide variety of preprogrammed architectures such as molecular squares, stars and trees.[253] Cluster complexes possessing additional pyridyl *N* atoms are capable of further metal coordination and allow the construction of CPs. 1D CPs with a repeating unit consisting of a single *trans*-$[Re_6(\mu_3\text{-}Se)_8(PEt_3)_4(4,4'\text{-bpy})_2]$ unit bound to a M(II) (M = Cd, Zn, Co) ion via the open nitrogen of a single 4,4′-bpy ligand. In Cd(II) and Co(II) complexes, the neighboring chains have their cluster and M(II) units shifted slightly with respect to one another,

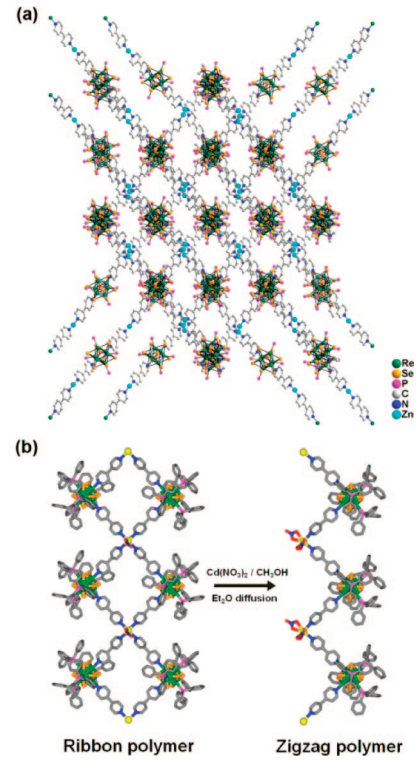

Figure 70. (a) Interpenetration of zigzag polymeric chains; (b) Conversion of ribbon to zigzag polymer.

leading to alternating layers of opposing "phases". However, in Cd(II) complex, the adjacent chains are arranged in parallel fashion and held together by hydrophobic and hydrophilic interactions at the cluster and Cd(II) positions, respectively to furnish a large channel. The zigzag Zn(II) polymer chains are also arranged in parallel to form layers, which are interpenetrated. (Figure 70a).[254]

On the other hand, the corresponding *cis*-$[Re_6(\mu_3\text{-}Se)_8(PEt_3)_4(4,4'\text{-bpy})_2]$ cluster with an enforced right angle between the two dipyridyl ligands forms another type of 1D CPs. From the reaction in 1:1 cluster/Cd molar ratio, a 2:1 cluster/Cd complex is obtained as a 1D CP with corner-sharing squares/ribbon. Usage of large amount of excess of $Cd(NO_3)_2$ has afforded a zigzag CP with 1:1 cluster/Cd ratio (Figure 70b). The zigzag chain structure can be formally considered to be derived from ribbon polymer by replacing the cluster on one side of the squares with a nitrato ligand. The formation of these polymeric structures may be rationalized in terms of two competing thermodynamic factors controlling crystal density/close packing of the multicluster arrays and maximization of Cd(II) pyridyl coordination. The corner fused square represents a compromise between optimal Cd(II) coordination and structural density and is the favored structure for the higher concentration of the cluster complex. The presence of excess Cd(II), however, favors the zigzag. Interestingly, when methanol solution of the ribbonlike CP is reacted with a large excess of Cd(II), crystals of the zigzag CP is obtained in quantitative yields.[255]

In the complex $[\{Cu_4(OH)_4(NH_3)_7\}_2\{Re_6Se_8(CN)_6\}]\text{-}[Re_6Se_8(CN)_6]\cdot 2H_2O$, the cyano groups of the rhenium clusters are coordinated to the Cu(II) atoms of the cubane units to form CP structure as shown in Figure 71. It is worthwhile to note that the hexarhenium cluster-supported $Cu_4(OH)_4$ cubane compound can function as an efficient heterogeneous catalyst with high catalytic activity in the

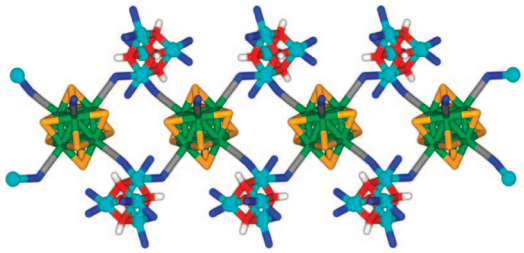

Figure 71. Portion of cationic rhenium supported Cu(II) cubane polymer. The anionic rhenium clusters are omitted for clarity.

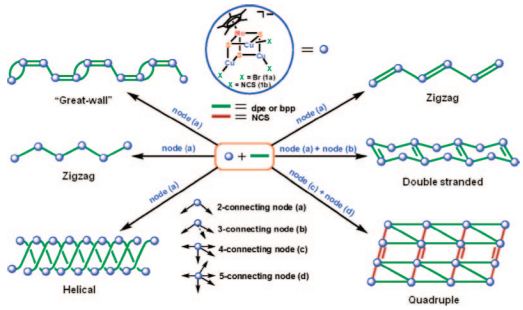

Figure 72. Schematic diagram showing various 1D structures from $[(\eta_5\text{-}C_5Me_5)MoS_3Cu_3]$ building blocks. Reproduced with permission from ref 257. Copyright 2008 American Chemical Society.

transesterification of a range of esters with methanol under the mild conditions.[256]

Lang and co-workers have shown that the metal cluster in $[PPh_4][(\eta_5\text{-}C_5Me_5)MoS_3(CuBr)_3]$ and $[PPh_4][(\eta_5\text{-}C_5Me_5)MoS_3Cu_3(NCS)_3]$ can be employed as the building blocks in the 1D CPs along with bridging ligands such as dpe and bpp. A series of interesting cluster-based 1D CP have been obtained and display "Great Wall"-like, zigzag, double-stranded, helical, and quadruple chain structures, as well as good third-order NLO properties in solution (Figure 72).[257]

A number of chalcogenide nanoclusters such as $Cd_{32}S_{14}(SPh)_{36}L_4$ $Cd_{32}S_{14}(SPh)_{38}L_2^{2-}$ $Cd_{17}S_4(SPh)_{26}L_2$, and $Cd_8S(SPh)_{14}L_2$ by several spacer ligands forming 1D chains under solvothermal conditions by reacting $Cd(SPh)_2$ or $(NMe_4)_2[Cd_4(SPh)_{10}]$ and thiourea or $Na_2S_2O_3$ in CH_3CN and H_2O.[258]

In the complex $[Ag_6(CF_3CO_2)_3(bmtm)_3(SCH_3)_3]$ (bmtm = bis(methylthio)methane), two centrosymmetrically related units generate an *atlas*-sphere cluster with 12-silver nuclear complex. These clusters are linked through the bmtm spacers and form a 1D CP. The Ag atoms present different coordination modes, from 5 to 7, and Ag···Ag interactions, with distance range from 2.93 to 3.36 Å. The 12 Ag atoms of the cluster are situated at the corners of a distorted cuboctahedron and bridging via uncommon μ_4-SCH_3 ligands. The polymeric chains are held only by van der Waals forces and pack in a hexagonal manner. The analogue Ag(I) pentafluoropropionate complex also contains a $Ag_{12}S_6$ cluster but with two water aqua ligands, which are strongly hydrogen bonded to the oxygen atoms of two pentafluoropropionate groups within the cluster and in an adjacent chain to form a 2D hydrogen-bonded network.[259a]

Under solvothermal microwave conditions, the reaction between $Cu(BF_4)_2 \cdot H_2O$ and 2,2′-dipyridyldisulfide (2-dpds) give rise to an interesting 1D CP $[Cu_9(2\text{-dpds})_8(SH)_8](BF_4)$ as one of the products. The Cu_9 cluster cage repeating unit resulted from the unusual cleavage of C−S and S−S bonds of the 2,2′-dipyridyldisulfide ligand during the synthesis.[259b]

2.7.4. Polyoxometalate Clusters

Self-assembly of oxo-centered Fe cluster, $[Fe_3(\mu_3\text{-}O)(CH_2{=}CHCOO)_6]$ with acrylate as the bridging ligand and hexamolybdate in acetonitrile gives rise to spontaneous resolution and resulted in the formation of helical CP $[(Fe_3(\mu_3\text{-}O)(CH_2{=}CHCOO)_6(H_2O))(MoO_4)(Fe_3(\mu_3\text{-}O)(CH_2{=}CHCOO)_6(H_2O)_2)] \cdot 2CH_3CN \cdot H_2O$. During the assembly process, $[Mo_6O_{19}]^{2-}$ anions are slowly decomposed to $[MoO_4]^{2-}$, and water ligands coordinated to $[Fe_3O(CH_2{=}CHCOO)_6]^+$ are removed and replaced by molybdate oxo ligands. The magnetic properties of the helical CP are dominated by intratriangle antiferromagnetic coupling similar to that of the isolated $[Fe_3(\mu_3\text{-}O)(CH_2{=}CHCOO)_6]$ species, whereas the coupling between neighboring triangles via the molybdate bridges is weaker.[260]

In the complex $[\{Cu(pz)(H_2O)\}\{Cu(pz)_3(H_2O)\}\{Cu(pz)_4\}\{P_2Mo_5O_{23}\}]$, the distorted octahedral $[Cu(pz)_3(H_2O)O_2]$ and trigonal bipyramidal $[Cu(pz)(H_2O)O_3]$ complex units are covalently link adjacent P_2Mo_5 clusters into linear chains; each cluster is also capped by $\{Cu_3(pz)_4O\}$. Higher pyrazole molar ratio afforded another 1D double-chain CP, $[\{Cu(pz)_4\}_3\{Cu(pz)_3(H_2O)\}_2\{HP_2Mo_5O_{23}\}_2] \cdot 7H_2O$. It is noted that the chains do not extend into 2D sheets as the coordinated water molecules are involved in the formation of a novel hexadecameric water cluster.[261]

A zigzag CP $[\{Ag_3(2,2'\text{-bpy})_4\}\{PMo_{12}O_{40}\}] \cdot 2H_2O$ and complex $[\{Ag(2,2'\text{-bpy})\}_2\{Ag_4(2,2'\text{-bpy})_6\}\{PMo_{11}VO_{40}\}][\{Ag(2,2'\text{-bpy})\}_2\{PMo_{11}VO_{40}\}]$ consist of isolated $[\{Ag(2,2'\text{-bpy})\}_2\{PMo_{11}VO_{40}\}]^{2-}$ anions and infinite 1D cationic chains $[\{Ag(2,2'\text{-bpy})\}_2\{Ag_4(2,2'\text{-bpy})_6\}\{PMo_{11}VO_{40}\}]^{2+}$ show good electrocatalytic activity toward the reduction of the nitrite. Furthermore, Ag···Ag interactions exist in the clusters and the complexes exhibit photoluminescence with emission maximum ~410 nm because of the ligand-to-metal−metal charge-transfer.[262] Higher nuclear polyoxometalate, Mo_{36}-polyoxo-metalate $[Mo_{36}O_{108}(NO)_4(H_2O)_{16}]_{12}^-$ anion has also been used to generate 1D CPs.[263]

Complex $[Cu^I_6(2,3'\text{-bpy})_6(2,3'\text{-bpy-}2'\text{-}O)_2][V^{IV}_2Mo^V_5Mo^{VI}_7O_{38}(PO_4)]$ (2,3′-bpy-2′-OH = 3-(pyridin-2-yl)pyridin-2-ol) containing the bicapped Keggin mixed molybdenum−vanadium polyoxoanions exhibits 1D ribbon CP structure through 3-(pyridin-2-yl)pyridin-2-ol bridging. The mixed molybdenum−vanadium heteropolyoxoanion is made up of α-Keggin structure of $[Mo_{12}O_{36}(PO_4)]^{8-}$ with two capping five-coordinated terminal $[VO]^{2+}$ units,and four internally edge-shared triads (Mo_3O_{13}) that are corner-shared to each other. The polyoxoanions and the trinuclear copper(I) clusters $[Cu^I_3(2,3'\text{-bpy})_3(2,3'\text{-bpy-}2'\text{-}O)]^{2+}$ link to each other to generate the 1D CP ribbon. These chains are arranged in parallel to furnish layer structure via the strong $\pi-\pi$ stacking interactions between the pyridine rings in 2,3′-bpy terminal ligands (3.2−3.6 Å) from neighboring strands.[264]

Anderson-type heteropolyanion, $[Al(OH)_6Mo_6O_{18}]^{3-}$, which consists of seven edge shared octahedra, six of which are molybdenum octahedra arranged hexagonally around the central octahedron of Al(III) has been reported to form 1D CPs linked by rare earth[265] and transition metal ions.[266] Another Anderson-type polyoxometallate has been linked to form 1D CP in $(C_6H_5NO_2)_4[(H_2O)_{14}Cd_3(CrMo_6H_6O_{24})_2]$ ($C_6H_5NO_2$ = pyridine-4-carboxylic acid), which is made up of $[CrMo_6H_6O_{24}]^{3-}$ polyoxoanions.[267] On the other hand, a 1D CP made up of a double-Dawson type polyoxoanion $Na_8H_2L(H_2enMe)_4\{Mn(H_2O)_2[(W_4Mn_4O_{12})(P_2W_{14}O_{54})_2]\} \cdot 17H_2O$, (enMe = 1,2-diaminopropane) was obtained by

hydrothermal reaction between $K_{12}[H_2P_2W_{12}O_{48}]\cdot 24H_2O$ and $Mn(NO_3)_2$. This polymer has been found to show catalytic activity toward the reduction of nitrite.[268] Similarly, a Wells−Dawson-based 1D CP $(H_2(bbi)_{0.5}[Ni(phen)(bbi)_2]_2-[P_2W_{18}O_{62}]$ (bbi = 1,1′-(1,4-butanediyl)bis(imidazole)) was also prepared from hydrothermal method.[269] In the polyoxotungstate 1D CP, $(NH_4)_7[Bi(H_2W_{12}O_{42})]\cdot 20H_2O$, the $[H_2W_{12}O_{42}]^{10-}$ anions are linked by the trivalent main group atom Bi(III) into a 1D chainlike structure.[270] Other polyoxoanion clusters also have been used to furnish 1D CPs.[271]

2.7.5. Single Molecular Magnets as Building Blocks

Polynuclear clusters are versatile frameworks for the generation of numerous molecular magnetic arrays. Moreover, some of them can behave as single molecule magnets (SMMs).[272] However, despite the characterization of many new polynuclear complexes including those which behave as SMMs, similar works to build CPs exhibiting magnetic properties through linking of individual metal clusters is not prevalent in the literature. Networks of metal clusters bridged by multifunctional ligands can, indeed, result in more desirable magnetic properties than individual clusters in isolation. There are several reviews available on this subject.[235f−i] A few representative examples are highlighted in this section.

The first 1D chain is composed of mixed-valence trinuclear Mn_3O or nonanuclear Mn_9O_7 cluster blocks and 4,4′-bpy linkers.[273a] There are few more examples of 1D CPs constructed from Mn_3O units showing interesting SCM properties.[273b−d] The mixed-valence Mn_6 cluster, $[Mn_6O_2(t\text{-}BuCO_2)_{10}(t\text{-}BuCO_2H)_4]$ gave a 1D CP structure through 4,4′-bpy bridging as "nano-dots-wires". The overall magnetic

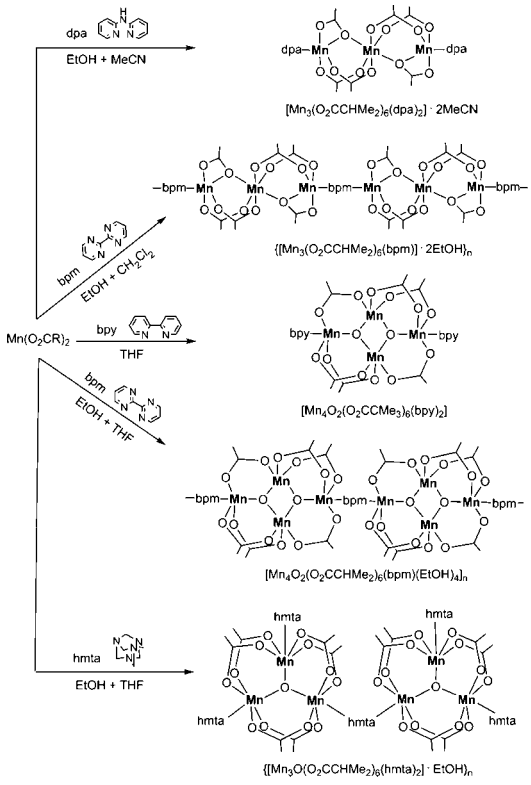

Figure 73. Self-assembly of manganese(II) isobutyrate or manganese(II) pivalate with appropriate N-containing ligands. Reproduced with permission from ref 275. Copyright 2008 American Chemical Society.

behavior of CP chain is nearly identical to that of the parent cluster; hence, the intercluster magnetic interaction, which arises from both intrachain and interchain magnetic interactions, is negligible.[274]

The trinuclear $[Mn(II)_3(O_2CCHMe_2)_6(dpa)_2]\cdot 2MeCN$ (dpa = 2,2′-dipyridylamine) and tetranuclear $[Mn(II)_2Mn(III)_2O_2(O_2CCMe_3)_6(2,2'\text{-bpy})$ clusters with SMM properties have been incorporated into 1D CPs through bridging of 2,2′-bipyrimidine (bpm) or hexamethylentetramine (hmta) ligands (Figure 73). The magnetic properties of the CP composed of trinuclear cluster have been elucidated by approximating the system to a dimer of trimers through a combination of vector coupling and full-matrix diagonalization methods.[275]

Another report showed that when SMMs are interconnected into 1D CPs magnetization relaxation has occurred as in $[Mn_4(hmp)_6Cl_2](ClO_4)_2$ (hmp = 2-hydroxymethylpyridine), which is composed of $[Mn_4(hmp)_6]^{4+}$ units bridged by chloride ions. The magnetization hysteresis loops for this polymer are similar to those for an SMM and further show significant coercive field along with steps at regular magnetic intervals. Spin-canted antiferromagnetic coupling because of misalignment of easy axes of neighboring Mn_4 units is also observed in the crystal.[276]

3. Interpenetration/Catenation Involving 1D CPs

Batten and Robson had given detailed and excellent account on the interpenetration of coordination polymers.[206b,277] The interpenetration/catenation of 1D CPs with same motifs, that is, linear with linear, zigzag with zigzag, ladder with ladder, to form higher dimensional network have been discussed in sections 2.2.2 and 2.4.2. In this section, interpenetration/catenation of 1D CP with different motifs and higher dimensional CP are discussed.

3.1. Interpenetration of 1D CPs

Apart from interwoven of similar types of polymeric strands, different motifs of 1D polymer strands have also been reported to form interpenetration. For instance, in $[Cu(bpeb)(solv)(NO_3)_2]$ $[Cu(bpeb)_{1.5}(NO_3)_2]\cdot 2solv$ (bpeb = 1,4-bis[(4′-pyridylethynyl) benzene]; solv = methanol or ethanol), the ladders and linear 1D CPs are present in the same crystal and further interpenetrate to form unprecedented network structure with each square channel of ladders are filled by bundles of four chains as shown in Figure 74. Such interpenetration has facilitated the formation of 3D network structure.[278]

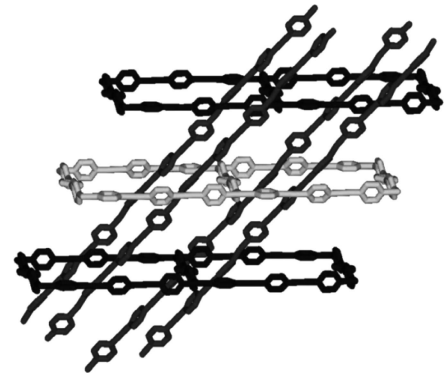

Figure 74. Interpenetration of chains into terraced stacks of ladders.

3.2. Interpenetration of 1D CPs into 2D Structures

Most of the interpenetration/catenation of 1D polymeric chains are observed with 2D polymers in which linear, ribbon, and zigzag polymers into 2D grids. Ciani and coworkers have reported the first example of interpenetration involving 1D and 2D polymers. Complex $[Cu_2(bpp)_8(SO_4)_4(EtOH)(H_2O)_5](SO_4)\cdot EtOH\cdot 25.5H_2O$ contains two different polymeric motifs, namely, 1D ribbons of rings and (4,4) nets. The 1D ribbon consists of $[Cu_4(bpp)]$ rings fused by Cu(II) atoms. The intriguing feature of this complex is that the ribbons and the 2D layers are entangled into 3D structure. Each ring of the ribbon locks two adjacent layers and each "square" mesh of the layers is catenated by two rings of different ribbons.[279]

Another complex $[Cu_3(cenep)_5(DMF)_8](ClO_4)_6\cdot 6DMF\cdot 8EtOH\cdot Et_2O\cdot 6H_2O$ features interpenetration of 1D polymer into 2D coordination square grids. The 1D polymer is comprised of Cu(II) ions bridged by cenep ligands (Figure 75a), while Cu(II) centers are linked by cenep ligands to generate a 2D lamellar framework (Figure 75b). The adjacent 2D networks form a double lamellar pair through strong $\pi-\pi$ interactions between two neighboring naphthyl rings (3.42 Å) as shown in Figure 75c. Each lamellar pair is separated about 8.1 Å and form 13.8 × 20.8 Å open channels which are occupied by 1D linear CPs stabilized by strong $\pi-\pi$ interactions between the naphthyl rings, pyridyl rings and C≡C bonds. The voids are still large enough to accommodate perchlorate anions and solvent molecules.[179]

Another example of 1D + 2D interpenetration is observed in complex $[Cd(dpe)(DMF)_4]\ [Cd(dpe)(\alpha\text{-}Mo_8O_{26})]\cdot 2DMF$. The anionic 2D $[Cd(dpe)(\alpha\text{-}Mo_8O_{26})]^{2-}$ framework (Figure 76a) is penetrated at an angle of 64.7° by cationic 1D $[Cd(dpe)(DMF)_4]$ chains (Figure 76b). The 2D framework contain windows constructed by dpe and $[\alpha\text{-}Mo_8O_{26}]^{2-}$ with dimension of 13.3 × 11.9 Å and the spacing between two parallel layers is 12.1 Å. This has allowed the threading of 1D chains into the grid and $\pi-\pi$ interactions between the pyridyl rings (3.51 Å) of two motifs help to stabilize the network (Figure 76c).[280]

Complex $[Hg_2(bpdh)(SCN)_4][Hg_2(bpdh)(SCN)_4]_2$ (bpdh = 2,5-bis(3-pyridyl)-3,4-diaza-2,4-hexadiene) exhibits 1D + 2D polycatenation. In the 2D motif, two SCN^- ligands doubly bridged two Hg(II) ions via both *N* and *S* atoms to form linear chains and these chains are further linked by bidentate bridging bpdh ligands to furnish a 2D network. On the other hand, in the 1D motif, linear chains of $[Hg(SCN)_2]$ building blocks are linked by bridging bpdh to generate ladder structure. The 2D net is polycatenated by the ladder as shown in Figure 77.[281]

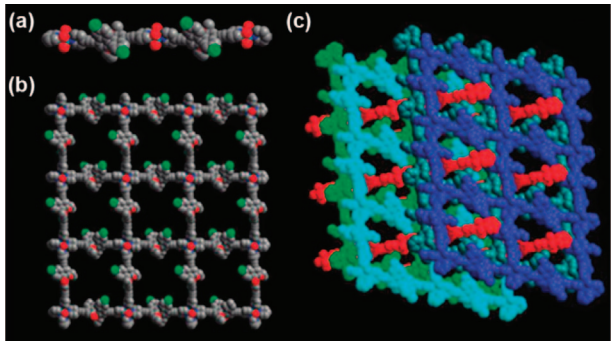

Figure 75. (a) View of the square grid network. (b) View of the 1D CP. (c) Threading of the 2D lamellar by 1D CPs. Adpated with permission from ref 179. Copyright 2008 American Chemical Society.

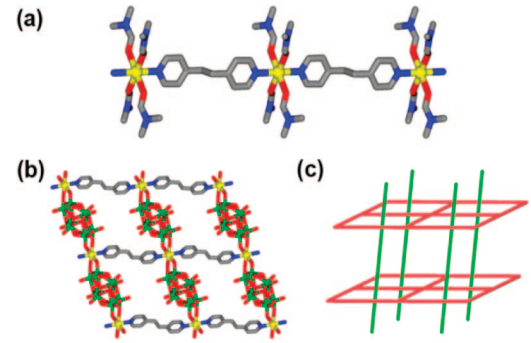

Figure 76. (a) Portion of 1D polymeric chain. (b) View of 2D network. (c) Schematic representation of interpenetration of 1D chains into 2D grids.

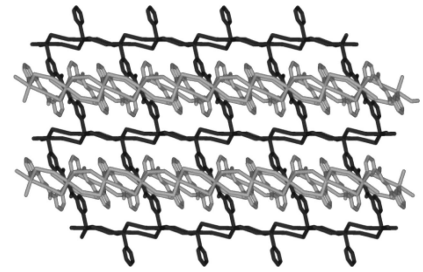

Figure 77. Polycatenation of the ladder and 2D CPs.

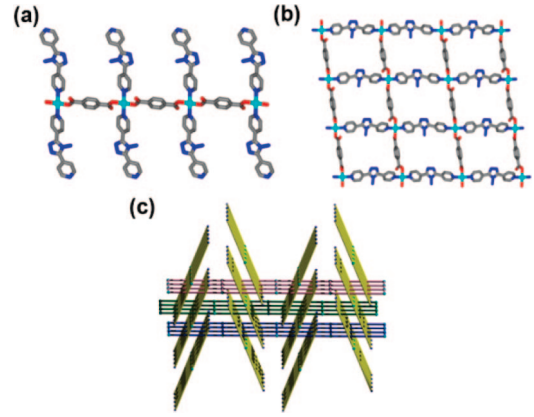

Figure 78. (a) Portion of 1D linear polymeric chains with bpt side arms. (b) View of 2D (4,4) nets. (c) Schematic representation of interdigitated polythreading of the 1D chains and 2D layers.

Complex $\{[Cu(1,4\text{-}bdc)(bpt)(H_2O)]_2[Cu(bpt)_2(tp)]\cdot 2H_2O$ (bpt = bis(4-pyridyl)-4-amino-1,2,4-triazole) displays an intriguing 1D + 2D → 3D polythreaded network. One of the motifs, $[Cu(bpt)_2(1,4\text{-}bdc)]$ exhibits a linear 1D CP structure with the bpt ligands decorated as side arms (Figure 78a). Another polymeric motif is [Cu(bpt)(1,4-bdc)] with a planar 2D (4,4) framework as shown in Figure 78b. The salient feature of this structure is that the side arms of the 1D CP intercalate the grids of the 2D sheets in an inclined fashion and lead to 3D polythreaded network (Figure 78c).[282]

Complex $[Ag(L)_2](PF_6)$ (L is shown in Figure 79a) features a ribbon-like $[AgL_2]_2$-metallacycle with a cavity of ~9.2 × 17.2 Å. This cavity is large enough to allow the insertion of two other ligands, one from a neighboring chain below and the other from above (Figure 79b and c). The structure can be described as parallel chains of 1D polycatenates, fused via the silver cations to yield the 2D overall motif. In

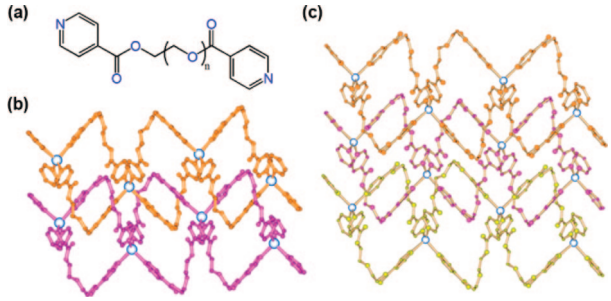

Figure 79. (a) Ligand structure. (b) 1D structure of Ag-fused metallacycles. (c) Interpenetration of 1D chains to yield 2D polycatenanes.

addition, this complex also can be obtained when a related discrete metallacycle compound left in mother liquor for two months.[283] Other interpenetration of 1D CPs into 2D polymers are reported also.[284]

3.3. Interpenetration of 1D into 3D Structures

Complex $[Co(bix)_2(H_2O)_2](SO_4)\cdot 7H_2O$ is the first example of an inextricable 1D + 3D array. These are two independent motifs, namely 1D ribbon polymeric chain and 3D network have the same stoichiometry. In the 1D polymer, two Co(II) atoms, two bix ligands and two aqua ligands constitute ribbons of 26-membered cycles along *b*-axis. As for the 3D network, the coordination geometries of Co(II) is similar to the 1D polymer; however, the bix ligands bridge both "horizontal" and "vertical" edges to form $(6^5\cdot 8)$ $CdSO_4$ topology network. Interestingly, the penetrating ribbons are inextricably entangled with the 3D frame via catenation. All the rings of the ribbons are threaded by one vertical edge of the net, as shown in Figure 80.[285] Other complexes of bix have been reported by same research group later.[231g,286]

A linear 1D CP cation $[Cu(4,4'\text{-bpy})(H_2O)_4]^{2+}$ was found to be hosted by an interpenetrating 3D network anionic structure in $[Cu(4,4'\text{-bpy})(H_2O)_4]^{2+}[Cu_2(mel)(4,4'\text{-bpy})(H_2O)_2]^{2-}$ (Hmel = mellitic acid, benzene-1,2,3,4,5,6-hexacarboxylic acid) from the hydrothermal reaction of mellitic acid, 4,4′-bpy and $[Cu_2(CH_3CO_2)(H_2O)_2$.[287] Interwoven of linear CP into 3D network of double helical host is observed in $[Cu_6(CN)_6(dmtrz)]_2[Cu_2(CN)_2(dmtrz)_2]$ (dmtrz = 4-amino-3,5-dimethyl-1,2,4-triazole). The 1D CP $[Cu_2(CN)_2(dmtrz)_2$ is composed of two Cu(II) ions bridged by two dmtrz which further linked through cyanide anions as cable-like linear chains (Figure 81a). On the other hand, in the double helical host, two kinds of helical chains are present. Six Cu(II) centers bridged by six cyanide ions form a honeycomb-shaped helical chain with left- and right-handed chiralities (Figure 81b). These helices are coupled with each other in forming helical tubes. Another hexagonal helical chain composed of 22 Cu(II) ions, 22 cyanide ions, and four dmtrz ligands furnish helical channels of 42.26 × 4.99 Å^2 with opposite chirality. Furthermore, two chemically independent polymers interweave to form a 3D architecture with double-stranded helical channels along two spiral directions. The salient feature is that the linear CP chains are interwoven into the helical channels of large hexagonal helical chains with opposite chirality (Figure 81c and d).[288]

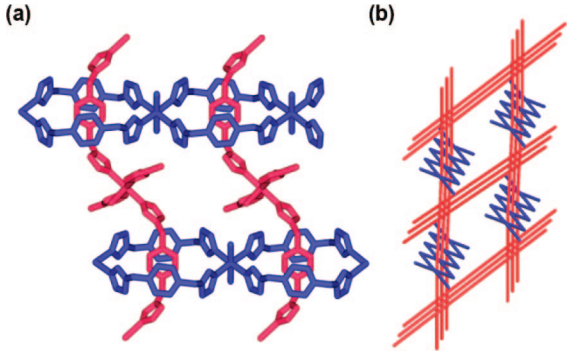

Figure 80. (a) Perspective view of 1D and 3D motifs in $[Co(bix)_2(H_2O)_2](SO_4)\cdot 7H_2O$. (b) Catenation of ribbons into 3D structure.

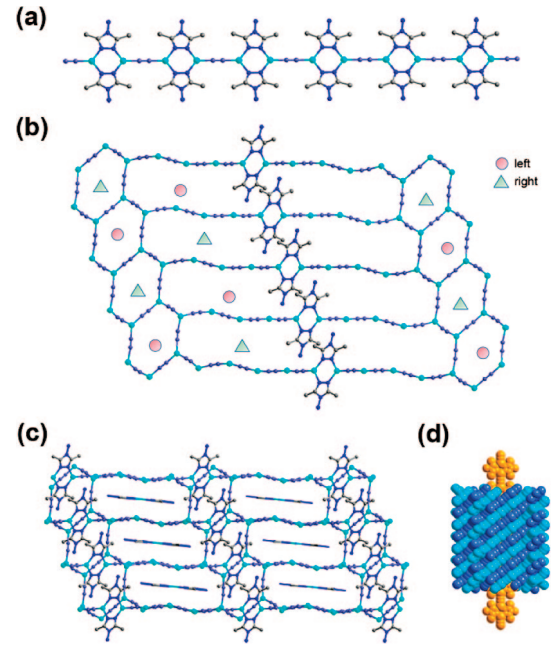

Figure 81. (a) Portion of linear polymer. (b) 3D network comprised of left- and right-handed helical chains. (c) View of 3D + 1D structure with the 1D polymer filled in the two independent helical 3D polymers. (d) 1D polymer chain filled in the helical channel of 3D polymer.

3.4. Interpenetration of 1D, 1D′, and 2D Structures

Biradha and Fujita demonstrated an interesting structure consisting of interpenetration of three types of CP networks. Three CPs consists of a square grid $[Cd(bpbp)_2(NO_3)_2]$ (A) (bpbp = 4,4′-bis(4-pyridyl)biphenyl), ladder $[Cd_4(bpbp)_4(NO_3)_6(MeOH)_6]$ (B), and linear chain $[Cd(bpbp)(NO_3)_3]_2$ (C) composed the complex with molecular formula of $[(A)(B)(C)NO_3\cdot(mesitylene)_2\cdot(MeOH)_3]$ (Figure 82a−c). In polymer A, linear spacer bpbp ligands linked the adjacent Cd atoms to form square grid network with channels of 10 × 20 Å. Such large cavities have afforded the interpenetration of polymer B and C. In polymer B, Cd atoms form linear chains with bpbp ligands and nitrate anions bridged two neighboring chains into ladder structure. These molecular ladders are accommodated in the channels that are formed across the packing of grid A to form a 3D-polyrotaxane type arrangement. Linear polymer C comprised of Cd atoms, bpbp ligands and chelating nitrate anions. These linear chains are packed between the 2D layers of polymer A and perpendicular to the polymer B. Figure 82d shows the interpenetration of three polymers. The mesitylene, MeOH molecules, and nitrate occupied the cavities.[289] In few more cases, the interdigitation of 1D CP[290] and 1D with higher D CPs are observed.[291]

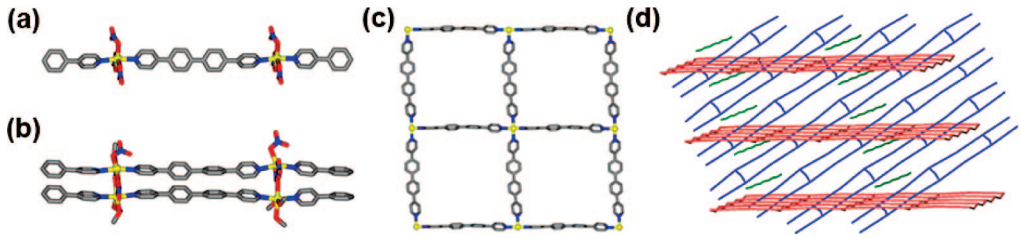

Figure 82. Perspective view of (a) linear polymer, (b) ladder polymer, (c) 2D grid polymers, and (d) interpenetration of three CPs.

4. Influence of Various Factors on the CP Architectures

It is well-known that the conformation, connectivity, metal−ligand ratio, dimensionality, and packing in the final product depend on the experimental conditions, such as solvents, concentration, temperature, crystallization vessel surface, pressure (solvothermal), time, impurities, and metal−ligand ratio, among other things. Apart from thermodynamic and kinetic products as well as crystal structures, predictability of these informations in the final outcome of crystallization is a major problem in this area even for this simple connectivity in 1D CPs. This section scrutinizes all these factors dealt in the literature.

4.1. Influence of Metal Ions

The 4,4′-dipyridyldisulfide ligand (dpds) has been utilized for assembling both discrete molecule and a CP based on its potentially 90° angle between binding sites with two different metal ions. Complex $[Pt(dpds)(Et_3P)_2(NO_3)_2]_2$ exhibits a chair-like structure with two dpds ligands in gauche conformation (Figure 83a). Interestingly, same reaction conditions with Cu(II) has afforded $[Cu(dpds)(hfacac)_2]$ as racemic helical CP though the dpds ligands are also in gauche conformation (Figure 83b). It appears that the more inert Pt-pyridyl bond resulted in the formation of closed system, while the more labile Cu−pyridyl bond drove the formation of CP.[292]

Self-assembly of peeb with Pd(II), Cu(II), Co(II), and Zn(II) resulted in the diverse supramolecular architectures depending on the nature of metal(II) ions (Figure 84). Complex $[Pd_3(peeb)_2Cl_6]\cdot 2H_2O$ exhibits a capsule-type supramolecular complex with square planar Pd(II) centers with the N_2Cl_2 donor set, where the two pyridine nitrogen atoms possess the trans configuration. In the complex $[Cu(peeb)Cl_2]\cdot EtOH$, each ligand is connected by $CuCl_2$ through the coordination of two of the three pyridine nitrogens, yielding a 1D zigzag CP. The remaining pyridine group does not participate in the metal coordination. The Cu(II) ion also has a square planar structure with the N_2Cl_2 donor set having trans configuration with respect to the pyridine nitrogen. The relative strength of the Pd(II)−N_{Py} bonds appear to dictate capsule versus polymer structure. Here, the stronger Pd(II)−N_{Py} bond may be practically irreversible and thus provides a kinetically capsule-type

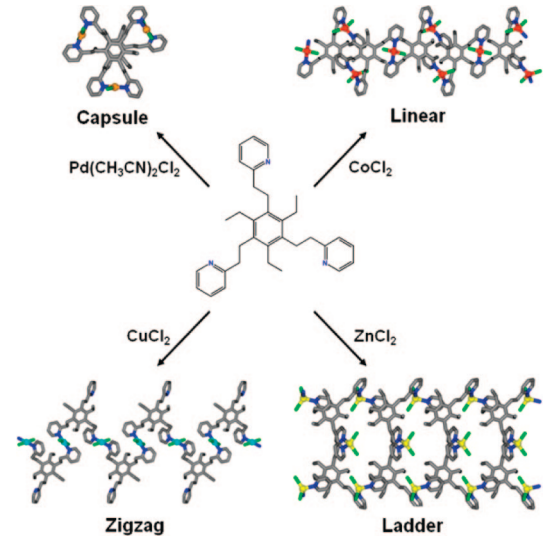

Figure 84. Self-assembly of peeb with different metal chloride salts.

trinuclear complex, while the weaker Cu(II)−N_{Py} bond, which may be reversible, can afford a thermodynamically more stable polymer complex. In the complex $[Co_3(peeb)_2Cl_6]\cdot 2CH_2Cl_2$, all three pyridine ligands participate in the metal coordination to yield the triangular building blocks that extends into 1D linear polymer. The structural difference in Cu(II) and Co(II) complexes is the coordination geometry of metal(II) ions. The tetrahedral geometry of the cobalt center brings the neighboring ligands closer to each other, making it possible to furnish the triangular shape, whereas the square planar geometry of the copper ion cannot adapt such arrangement. Hence, the Zn(II) complex, $[Zn_3(peeb)_2Cl_6]\cdot 2H_2O$, exhibits a ladder polymer structure, in which the three pyridine rings of each ligand bind to a different Zn(II) ion exhibiting a tetrahedral geometry.[152]

Self-assembly of a tetrakis ligand (shown in the inset of Figure 85a) with $HgCl_2$ leads to the formation of 1D coordination network. In this polymer, two Cl^- anions are bonded to Hg(II) while four pyridyl groups of the ligand are coordinated to four different Hg(II) nodes to provide a tetrahedral geometry (Figure 85b). When Co(II) is used, four coordination sites of the ligand occupied the equatorial positions of Co(II) while two Cl^- anions resided the axial positions. Therefore, a 2D coordination network as shown

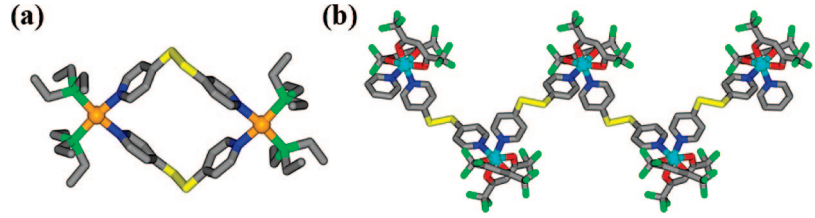

Figure 83. (a) Perspective view of Pt(II) marcocylcle. (b) Portion of helical Cu(II) polymer.

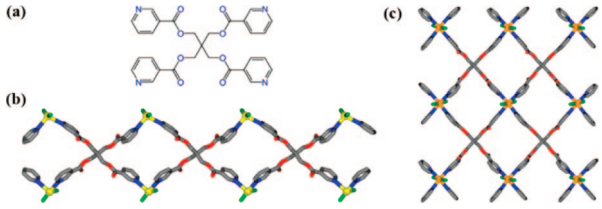

Figure 85. (a) Ligand structure. (b) Ribbon polymer constructed from square planar ligand node. (c) 2D polymer constructed from square planar ligand node.

in Figure 85c is obtained. In other words, the ligand acts as a square planar node in both the structures. By changing the N atoms to 4-position of pyridyl rings the ligand functions as pseudo tetrahedron tecton. Reactions with $HgCl_2$ and $CoCl_2$ have resulted in the 2D network structures.[293]

Self-assembly of Co(II), Fe(II), and Ag(I) with a number of crown ether-based ligands, *N,N'*-bis(4-pyridyl-methyl)-diaza-18-crown-6 (bpmdc), afforded a series of 1D CPs with a range of ligand conformations and bridging lengths, which are dependent on the presence and nature of crown-based guests. Encapsulation of guest molecules such as K(I), Ba(II), Ca(II), and Ag(I) within the crown ether leading to the disruption of hydrogen bonding interactions. As a result, the ligand lengths in 1D CPs can be varied over a large range.[294]

The oxidation states of metal ions determine the coordination geometry of metal centers that also influences the conformation of CP structures. For instance, solvothermal reaction at high temperature resulted the reduction of Cu(II) with square pyramidal to Cu(I) tetrahedral coordination geometries. As a result, the pyrazine complexes vary from linear to zigzag CP structures.[295] The influence of metal coordination geometry has been investigated in metal(II)−benzoate complexes with 4,4′-bpy co-ligand. Here systematic changes in the coordination geometries of the metal ions have been achieved from a tetrahedron (Zn), a trigonal-bipyramid (Zn), an octahedron (Co, Ni, Mn, Cu, Zn) to a pentagonal-bipyramid (Cd). Because of the difference in coordination geometries of metal ions and coordination modes of benzoate, these complexes display diverse structural features ranging from ladder, helical, chain containing paddle-wheel units, zigzag to 2D sheet. Further, these complexes have been shown to catalyze the transesterification of a variety of esters with the non-redox-metal-containing compounds (Zn and Cd) and show better activity than the redox-active metal containing compounds (Mn, Cu, Co and Ni).[296]

Self-assembly of metal halides, MX_2 (M = Cd, Hg, Pb; X = Br, I), with free base tetrapyridylporphyrin (TPyP) form predictable 1D or 2D coordination networks depending upon the coordination geometry of the metal. The 1D polymer is formed with each HgI_2 units is tetrahedrally coordinated with a pyridyl moiety of two TPyP molecules. The coordination of four pyridyl moieties to octahedral metal ions such as Pb(II) and Cd(II) resulted in the formation of 2D CPs. Interestingly, metal cations can be selectively inserted into the porphyrin cavities in these crystalline networks and may also be selectively stripped by exploiting the discrepancies in their acid stability constants.[297] There are similar observations reported in the literature on the influence of metal coordination geometry on the polymeric architectures.[298]

4.2. Influence of Ligands

Ligand flexibility is also a deciding factor on the final structure of the 1D CPs. This is illustrated in the isolation of three azide-bridged complexes $[M(dpa)(N_3)_2]$ (M = Cu, Co,) and $[Ni(dpa)(CH_3COO)_{0.5}(N_3)_{1.5}(H_2O)]$ (dpa = 2,2′-dipyridylamine). The Cu(II) polymer has an EO-N_3 bridged chain (EO = end-on), where, as in the Co(II) polymer, the metal ions are linked by two EO-N_3 and two EE-N_3 bridges alternatingly (EE = end-to-end). Interestingly, the Ni(II) complex is a zigzag chain linked alternatively by one EE-N_3 and a novel 3-fold bridge, which is composed of two EO-N_3 and one acetate group. The flexibility of the dpa ligand seems to have an important role in directing the structures of the final products. Magnetic studies reveal dominant intrachain antiferromagnetic couplings in Cu(II) polymer, but Co(II) and Ni(II) are weak ferromagnets due to the spin canting, with critical temperatures of −260 and −241 °C, respectively.[299]

A conformationally labile ditopic ligand, 1,3-bis(4-pyridylthio)propan-2-one (bptp) displays various conformations as shown in Figure 86a. The Ni(II) and Co(II) centers acts as square-planar nodes to form 3D networks. Whereas assembly of bptp with linear node Ag(I) produced a 1D U-like polymer (Figure 86b). The ligands are in E conformation with higher steric energy than that of isomers A and D. It is noted that the nitrate ions located in "U" chains stabilize the E conformation of bptp. The Ag(I) complex displays two weaker blue emission bands at λ = 416 and 442 nm and one stronger, broad, green emission band at λ_{max} = 541 nm because of a Ag(I)-perturbed intraligand transition and charge transfer transition.[300]

Chen et al. have reported the assembly of Ag(hmt) (hmt = hexamethylenetetramine) polymer to be mainly dependent on the nature of the anionic co-ligands. Figure 87 displays the schematic diagram of various CP structures generated by various co-ligands including 4-hydroxybenzoic acid, 4-aminobenzoic acid, 4,4′-biphenyldicarboxylic acid, isonicotinic acid, benzenesulfinic acid, and 1,4-butanedioic acid. As expected, the monocarboxylate co-ligands generated 1D zigzag CPs while dicarboxylate ligands linked the zigzag chains into ladderlike structure. The isonicotinate co-ligand with two binding sites coordinated to Ag(I) ions to furnish 2D grid network. Benzenesulfinate and 1,4-butanedioate ligands formed double-chain-like CPs.[301]

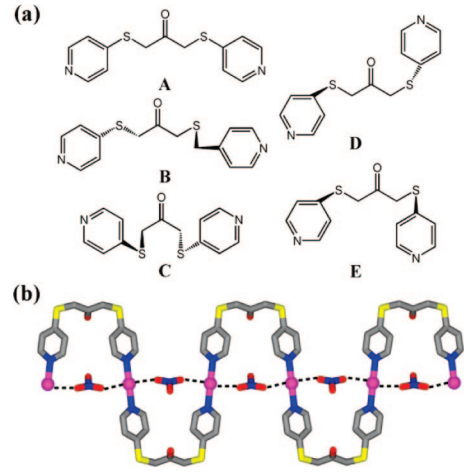

Figure 86. (a) Conformational isomers of bptp. (b) Portion of U-like polymer.

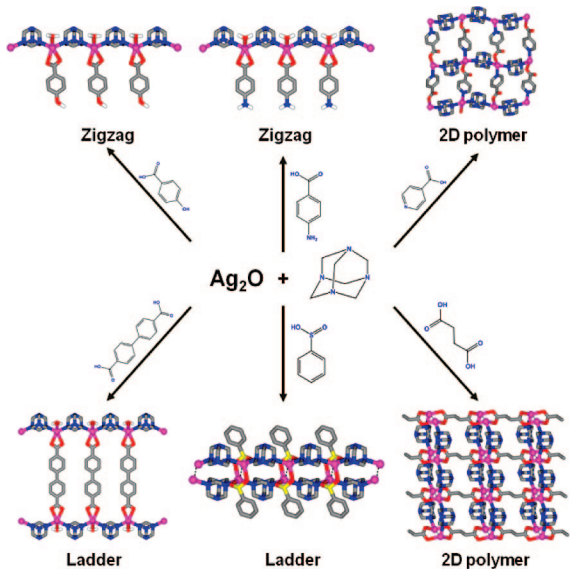

Figure 87. Various CP structures generated by linking [Ag(hmt)] chains with different co-ligands.

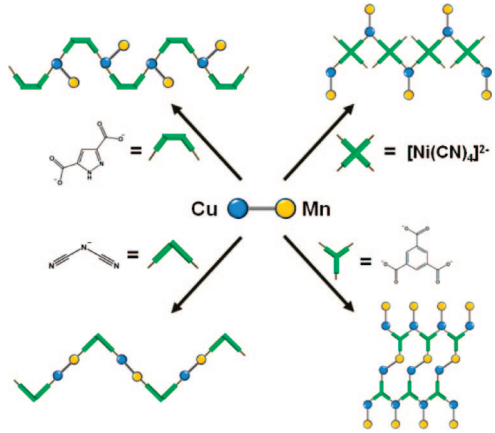

Figure 88. Construction of CPs by combination of heterobimetallic nodes with various spacer ligands.

The reaction between the mononuclear complex [Cu(pbmsi)] (pbmsi = *N*,*N*′-propylene-bis-(3-methoxysalycilideneiminato)), cobalt(II) acetate, and KSCN forms zigzag chains made up of alternating up and down dinuclear [(pbmsi)CuCo] units linked by thiocyanato bridges.[302] The heterometallic [Cu(II)Mn(II)] and [Cu(II)Co(II)] nodes can be further employed to generate CPs with various anionic spacers including pyrazole-3,5-dicarboxylic acid (H_2pzdc), 1,3,5-H_3btc, tetracyanonickelate(II) anion ($[Ni(CN)_4]^{2-}$), dicyanosilverate(I) anion $[Ag(CN)_2]^-$, and dicyanamide anion as illustrated in Figure 88.[303] More examples of the influence of ligand in the final structures of the complexes may be found in the literature.[304]

4.3. Influence of Counterions

Most of the CPs are in general neutral and cationic in nature because of the presence of metal ions, and the influence of anions have been studied extensively. However the influence of cations on 1D structure are limited.[294] Structural investigation of Zn(II), Cu(II), and Pb(II) complexes of *N*-(2-pyridylmethyl)-amino acids (glycine = Hpgly and alanine = Hpala) revealed that 1D CP structures are anion-dependent. The presence of semicoordinating anions such as perchlorate and coordinating anion, such as acetate,

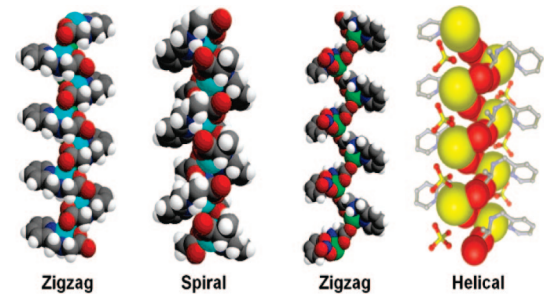

Figure 89. Influence of anions on the CP conformation of complexes of *N*-(2-pyridylmethyl)-alanine.

chloride, and nitrate, have been found to greatly influence CP conformations in the solid state. Figure 89 shows the 1D CP structures of complexes of Hpala with different anions. Complex [Pb(pala)(ClO_4)] shows single-stranded helical structure, pillared by Pb···O···Pb interactions from perchlorate anions.[305] Complexes [Cu(pgly)Cl]·H_2O and [Cu(pala)Cl]·H_2O display 1D zigzag CP structures through unsymmetrical Cl−Cu−Cl bridging and sustained by N−H···O═C interactions. Interestingly, hydrogen-bonded single-stranded water chains have been hosted by the hydrophilic channels guided by C═O···H−O−H hydrogen bonds. Acetate and nitrate anions have participated in the bridging metal centers and generated a 1D spiral CP [Cu(pala)(CH_3COO)]·0.75H_2O and 1D zigzag polymer [Zn(pgly)(NO_3)], respectively.[306]

Schröder and co-workers have evaluated the relative coordinating ability of the anions and the tendency of the N-donor ligand to adopt intermolecular aromatic interactions by studying the self-assembly of AgX with 2,7-diazapyrene (diaz); (X = BF_4, NO_3), pybut (pybut = 1,4-bis(4-pyridyl)-butadiyne; X = BF_4, NO_3, PF_6 or CH_3CO_2), 4,4′-bpy (X = BF_4), or 1,4-bis(4-pyridylethynyl)phenylene (pyphe); (X = PF_6). These complexes display 1D CP structures with general formula of [Ag(ligand)]·X and exhibit intermolecular interactions including $\pi-\pi$ stacking, Ag···Ag, Ag···aromatic, and Ag···anion interactions depending on the anions. When the noncoordinating anion, such as BF_4^-, is used, the linear CP is obtained with Ag(I) ions adopt linear coordination geometry and the diaz ligands show offset face-to-face $\pi-\pi$ stacking interactions. The chelating coordination of the NO_3^- anion to the Ag(I) resulted in a strongly distorted tetrahedral geometry of Ag(I) with altered the CP into zigzag conformation. On the other hand, the rod-like pybut ligand allows the linear chains of [Ag(pybut)]·BF_4·MeCN arranged in a parallel fashion where the ligand molecules are shifted relative to each other so that the shortest interchain Ag···Ag distance is 7.147 Å. The utilization of bidentate anions, such as $PO_2F_2^-$ and $CH_3CO_2^-$ coordinated more strongly and can significantly mediate the interchain interactions with shorter Ag···Ag distance. Hence the complexes exhibit infinite ladder structure with Ag−Ag bond as rungs.[168]

The reaction of AgX (X = CF_3CO_2, NO_3, CF_3SO_3, PF_6, ClO_4) with 2,2′,3″-tripyridylamine (tpa) afforded a series of 1D CPs with different modes of coordination, depending upon the counterion present in the compound (Figure 90). When $CF_3CO_2^-$ is used, two pyridyl groups of tpa ligands coordinated to Ag(I) with endo conformation to form the dimer which further linked through bridging trifluoroacetate anion into 1D CP, [Ag(tpa)(CF_3CO_2)], while the remaining pyridyl ring does not involve in coordination. In the complex [Ag(tpa)(CH_3CN)(NO_3)], the NO_3^- anion does not involve in bridging and the tpa ligand adopts an *exo* bridging

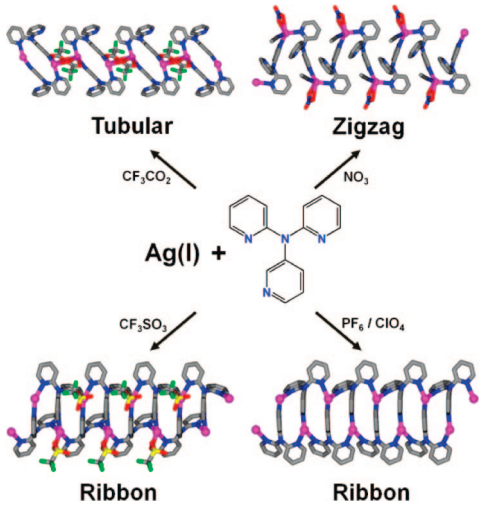

Figure 90. Anion-dependent isolation of different 1D structures.

conformation, resulting in the formation of a zigzag 1D chain polymer. Though triflate usually functions as a noncoordinating anion, here it is coordinated to the Ag(I) center as a terminal ligand in complex [Ag(tpa)(CF_3SO_3)] and, in fact, forms a shorter bond to Ag(I) than nitrate and trifluoroacetate ligands. The lack of chelation from the triflate counterion appears to leave more room around the metal center, allowing the third pyridyl group of the tpa ligand to coordinate to Ag(I) ion in a rare η_3-bridging mode to form an interesting ribbonlike 1D CP. Changing to the other counteranions such as BF_4^- and ClO_4^- have resulted in the formation of similar ribbon-like CPs. All these complexes are luminescent in acetonitrile solution, with emission maxima in the near-UV region ~367 nm. At −196 °C, the emission maxima are red-shifted to ~452 nm. Interestingly, the presence of the Ag(I) ion in solution cause fluorescence quenching attributed to the heavy atom affect, which may be useful for the detection of Ag(I) ions.[307]

Self-assembly of AgX (X = NO_2, NO_3, CF_3SO_3, and PF_6) and bis(4-pyridyl)dimethylsilane (bpdms) clearly exemplifies the effect of anions on the molecular construction since the resulting complexes were not significantly affected by the mole ratio or solvent. The noncoordinating PF_6^- and $CF_3SO_3^-$ anions afforded adducts with higher ligand ratio and resulted in 2D grid and 1D ladder structures. In the case of coordinating NO_3^-, a 2 nm thick interwoven sheet structure consisting of nanotubes $[Ag_3(bpdms)_4](NO_3)_3$ is obtained. A relatively more coordinating anion NO_2^- produces a double helix, [Ag(NO_2)(bpdms)], which are connected to each other via the Ag···Ag interactions (3.00 Å) to form a unique sheet. Such structural motif may be attributed to the chelating mode of the nitrite, which acts as a chelating ligand and cause the N−Ag−N angles more bent (127°). A linear relationship between the ratio of ligand to metal and the coordinating ability of anions is established where the ligand to metal ratios increase with decreasing order of coordinating ability as shown in Figure 91.[308] The similar trend also has been observed Ag(I) complexes of 2,4′-thiobis(pyridine).[309]

Structures of Ag(I) complexes of 2-aminomethylpyridine-dipropionitrile (2-ampdpn) are depend on the counteranions. When the noncoordinating $CF_3SO_3^-$ is used, a ladder structure has resulted with the anions occupying the empty spaces. Incorporation of weakly coordinating ClO_4^- has

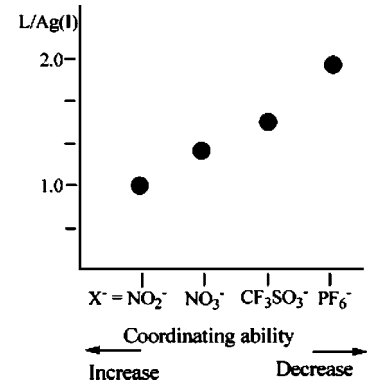

Figure 91. Correlation between the Ag(I)/ligand ratio and the coordination ability of the anions. Reproduced with permission from ref 308a. Copyright 2005 American Chemical Society.

afforded an isomorphous structure as the former except for the weak Ag−Ag interactions (3.3 Å) between the polymeric chains. The NO_3^- anions bridge the Ag(I) centers along with pyridyl ligands resulted in a racemic 2_1 helical CP.[310] Self-assembly of 2,3-diarylpyrazines with Ag(I) salts is also modulated by the anions. The noncoordinating anion, BF_4^- facilitates the formation of a linear pyrazine-silver-pyrazine bond (173°), whereas coordinating anion, CF_3COO^-, enforces nonlinear pyrazine-silver-pyrazine bond (111°) thereby facilitating a helical structure. In the case of triflate anion, the pyrazine-silverpyrazine bond is more bent (166°) compared to BF_4^- anion.[311]

Reaction of $AgNO_3$ in MeCN and pyz in CH_2Cl_2 afforded linear CP [Ag(pyz)(NO_3)] through pyz bridging. The polymeric chains are aligned in a parallel fashion with weakly bridging nitrate anions to form a 2D sheet. It is noted that the bridging nitrate anions also help to stack the polymeric chains in a helical staircase motif with 6-fold symmetry. Similar reactions with PF_6^- and BF_4^- afforded isomorphous linear CPs [Ag(pyz)(PF_6)(MeCN)] and [Ag(pyz)(BF_4)-(MeCN)]. But the linear CP chains are linked through Ag···Ag interactions (3.23 and 3.31 Å, respectively) and $\pi-\pi$ interactions between adjacent pyz ligands into ladder-like structure and no observable interactions between adjacent ladders.[14]

The ambidentate ligand 5,5′-dicyano-2,2′-bipyridine (dcbpy) displayed as a bi-, tri-, or tetradentate chelate or chelate/bridging ligand in the coordination of silver ions depending on the anion and crystallization conditions (Figure 92). When coordinating anions such as NO_3^- and $CF_3SO_3^-$ were used, the anions coordinated to Ag(I) ions through one of the oxygen atoms and serve as terminal ligands. The dcbpy ligand chelates a silver atom through the bipyridine moiety and bridges to a neighboring silver center through one of the exodentate cyano groups leading to 2_1 helical and spiral CPs. It is noted that in the helical CP, adjacent strands interdigitated $\pi-\pi$ stacking interactions between pyridyl rings (3.47 Å). Interchain nonbonding Ag···O, Ag−pyridine, or electrostatic cation−π interactions appear to stabilize the structure. When weakly coordinating anions such as BF_4^- and PF_6^-, only the endodentate bipyridine nitrogen atoms serve as donor atoms toward silver; the exodentate cyano groups are not involved in coordination, hence resulted in monomeric complexes. By changing the solvent system, a 2D CP is obtained in which the dcbpy ligand chelates a silver ion and bridges to two other metal centers with both of the exodentate cyano groups.[312]

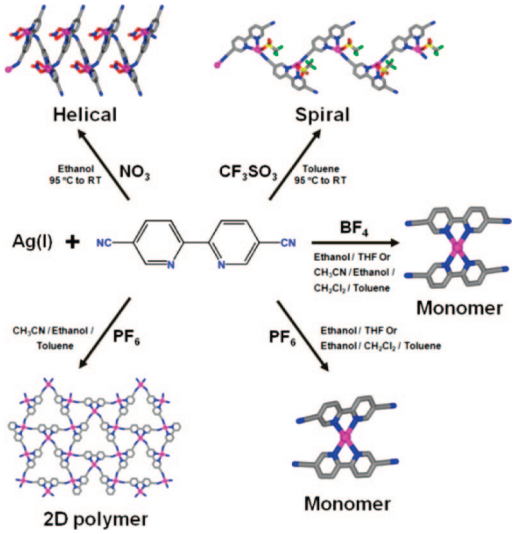

Figure 92. Influence of anions and crystallization conditions on self-assembly of Ag(I) and dcbpy.

Self-assembly of bis(methylthio)methane (bmm) and AgX (X = NO_3, ClO_4, p-TsO, CF_3CO_2, $CF_3CF_2CF_2CO_2$, CF_3SO_3, $C_6H_5CO_2$, CH_3SO_3, and $HO_2CCF_2CF_2CO_2$) demonstrates the effect of the size of the anions on the structure adopted by the supramolecular coordination network. In the presence of small and elongated anions, the 2D layers are made up of [Ag(bmm)], in which the anions complete the tetrahedral coordination of the silver atoms. A 1D CP is formed by the benzoate anions, and in two such adjacent polymers, the Ag(I) ions are further bridged by two benzoate groups to form the dimeric units that linked by four bmm ligands to generate a ladder-like 1D CP. This complex also may be described as a corrugated ribbon of adjacent 10-membered rings, in which $[Ag_4(bmm)_2]$ shares Ag···Ag edges, whereas the two benzoate groups coordinated to the silver atoms are in a direction nearly perpendicular to the ribbon axis. In contrast to perfluorocarboxylate, the benzoate groups favored the $\pi-\pi$ stacking between the benzoate groups from adjacent chains that lead to a 2D. This fact clearly shows the influence of the shape of the coordinating anions upon the supramolecular network. When $CH_3SO_3^-$ is used, two Ag(I) ions are bound by two bmm ligands to construct the dimers, which are further bridged by four methanesulfonate anions to form 1D CP. The dimers are almost perpendicular to the ribbon that constitutes the polymeric chain. There are weak hydrogen-bond interactions between the sulfonate oxygen atoms that are not engaged with the Ag(I) atoms of one polymer, and a methylene hydrogen of the bmm ligands of another chain.[313]

Self-assembly of tetrahedral Cu(I) with thia-oxa macrocycle, ligand, has been found depend on the counteranions (Figure 93a). In the presence of CN^-, the linear polymeric CuCN chains are bridged by macrocyclic units to form a puckered square-grid framework. Whereas, the iodide analogue displays a double-stranded polymeric chain structure with macrocycles bridging a dinuclear iodobridged copper unit. An alternating arrangement of a pair of macrocycles and a square-dimeric $Cu-(I)_2-Cu$ unit forms a large cyclic dimer, corresponding to a 22-membered ring.[314] Another isostructural compound can be obtained from CuCl. Changing one donor atom in the thiamacrocycle to S and NH afforded a dimer and 2D polymer respectively.[315] Self-assembly of Ag(I) with another similar thiamacrocycle afforded 1D single and double-stranded CP depending on

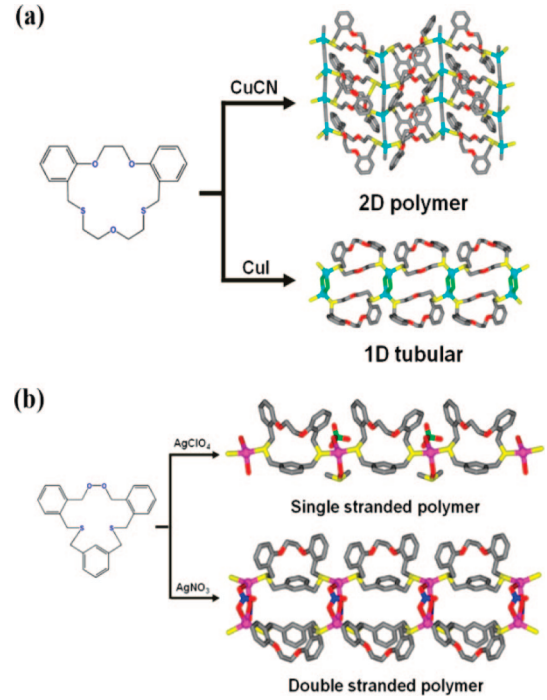

Figure 93. Self-assembly of thiamacrocycles with (a) Cu(I) and (b) Ag(I) with different anions.

counteranions (Figure 93b). When ClO_4^- is used, S atoms from two marcocyles are coordinated to a tetrahedral Ag(I) center along with one monodentate ClO_4^- and DMSO molecule. In the case of NO_3^-, Ag(I) center is coordinated by two S donors from two adjacent marcocycles, a monodentate NO_3^- and a bidentate NO_3^- to form an infinite poly(cyclic dimer) structure. It is noted that in both polymers, macrocycles are arranged side by side with interligand $\pi-\pi$ stacking between two benzo-groups in adjacent ligands, which could be reason for the preference for the 1D array.[316]

There are few more examples where the shape of anions directed the assemblies of supramolecules in the literature. For example, reaction of $AgNO_3$ with 1,2-bis[(2-pyrimidinyl)-sulfanylmethyl]benzene (bpsb) afforded a single-stranded helix of $[Ag_4(bpsb)_2(NO_3)_4]$ owing to the template effect of nitrate anions that embedded in the interior and flank of the helix. Whereas reaction with $AgClO_4$ under the same conditions gave rise to a 2D lamellar polymer $[Ag_2(bpsb)_3(ClO_4)_2]$ containing crown-like cavities. The poorly coordinating ClO_4^- anions are partly encapsulated inside the cavity and weakly bound to the Ag(I) of another layer.[70h]

The Cu(II) complexes of dipyrromethene derivatives furnish different structures depending on counteranions. When acetylacetonate (acac) is used, the complexes form 1D zigzag CPs. In contrast, the introduction of the perfluorinated spectator ligand, hexafluoroacetylactonate (hfacac), is found to have a large influence on the resulting supramolecular structures. In the 1D CP, the perfluoromethyl groups from the ancillary hfacac ligand are directed toward the outside of the helical structures in such a way that each perfluoromethyl group interacts with four neighboring hfacac groups of adjacent chains with F···F distances of 2.9−3.5 Å. Other hfacac complexes exhibit discrete six-membered rings that display perfluoromethyl groups at their periphery.[317] Self-assembly of *N*,*N*′-bis(3-pyridylmethyl)thiourea (bpt) with $ZnCl_2$ and $CdCl_2$ in the presence and absence of KSCN yielded macrocyclic, helical, double-helical structures. The

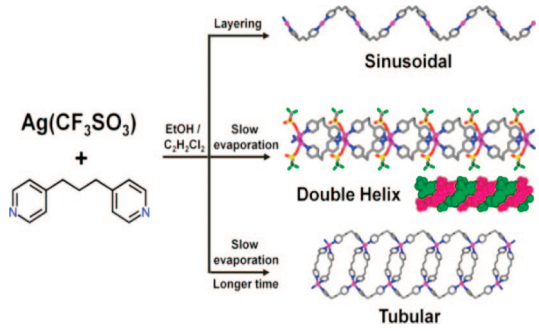

Figure 94. Schematic representation of self-assembly of Ag(I) with bpp under different conditions.

presence of NCS^- anion was found to favor the formation of helical structure in $[Zn(bpt)(NCS)_2]$ and double helical structure in $[Cd(bpt)_2Cl_2 \cdot 2CH_3OH]$, while Cl^- anion driven the macrocyclic formation in $[Zn(bpt)_2Cl_2]$.[318] The influence of anions on the formation of discrete complexes, 1D and higher D polymers has also been noted in other systems.[319]

4.4. Influence of Crystallization Techniques

Reaction of $Ag(CF_3SO_3)$ with bpp clearly illustrates the effect of crystallization conditions on the supramolecular architectures (Figure 94). Layering of CH_2Cl_2 solution of ligand and ethanolic solution of Ag(I) salt yielded $[Ag(bpp)](CF_3SO_3) \cdot EtOH$ as 1D sinusoidal CP. Whereas slow evaporation of the same solution mixture afforded a helical CP of $[Ag(bpp)](CF_3SO_3)$. The helical CP shows racemic double-stranded helical structure. The left- and right-handed helical chains interact via Ag···Ag contacts with distance of 3.09 Å. Slow evaporation of the same solution on longer time furnished a tubular CP $[Ag_2(bpp)_4](CF_3SO_3)_2 \cdot bpp$ in which the $[Ag_2(bpp)_2]$ rings form a 24-membered macrocyle interlinked by two other bpp ligands. Notably, the solvated bpp molecules threaded into these macrocycle rings to form pseudorotaxane. It appears that the facile reversible dissociation of the Ag−N bonds in these polymers may be the key for the conversion of structures.[93] Crystallization in H-tube also can afford two different products in different arms (see section 5).[320]

When $AgBF_4$ was reacted with pyz in ethanol in a 1:1 molar ratio, an immediate precipitation of a linear CP $[Ag(pyz)](BF_4)$ was observed. The same reaction with a 1:2 salt/pyz molar ratio afforded immediate precipitation of linear CP and upon leaving the solution for few days, the precipitate is completely transformed to $[Ag_2(pyz)_3](BF_4)_2$. The transformation also can be observed when the 1D CP suspended in ethanol with an equimolar ethanolic solution of the pyz and on leaving the reaction mixture to stand for a few days. Interestingly, layering of the same reactants in a test tube gave rise to the needle-shaped crystals of 1D linear CP in the bottom, as well as distorted cubical shape and rhombohedra crystals, at the interface. These two products are supramolecular isomers and display 2D CP structures with cationic sheets composed of six-membered rings of pyz-bridged Ag(I) folded in chair conformation and interpenetrating 3D framework, respectively. Reactions in 1:4 molar ratios generated the 1D linear CP immediately, 2D CP after several days along with a 1D zigzag CP, $[Ag(pyz)_3]BF_4$.[321]

4.5. Influence of Other Factors

Schröder et al. have shown that the solvent coordinating ability can control the formation of extended structures. Three alcoholic solvents, MeOH, EtOH, and *i*-PrOH have been used in the reaction of Cd(II) and Zn(II) with 3,3′-pytz. It has been found that the strong coordinated MeOH molecules have blocked the binding sites hence allow only two pyridyl ligands coordinated in trans positions and resulted in a 1D zigzag CP. Whereas more ligands bind to metal ions and lead to the formation of molecular ladders in less coordinating solvent EtOH and *i*-PrOH.[127]

Recrystallization of a discrete dinuclear metallocycle with two acetone as guest molecules, $[Cu_2Cl_4(bmimb)_2] \cdot 2(acetone)$[322] (Figure 95a) from a variety of common solvents has exemplified the effect of solvent templation on the resulting structures. The formation of the cyclic structures are observed with acetone, MeCN, dichloromethane, THF, DMSO, ethyl acetate, chloroform, and 1,4-dioxane as guest template. There is no clear pattern to predict the conformation of guest molecules since the solvent molecules accommodate inside the cavity of marcocycles with different amount, conformation, weak and no intermolecular interactions. Interestingly, recrystallization in 1,2-dichloroethane gave rise to a 1D wavelike CP structure (Figure 95b). Packing of adjacent strands furnished the semicircular apertures as guest pockets, and each pocket is occupied by only one guest molecule. On the other hand, DMF molecules coordinate to the copper ions and thus cause the formation of 1D CP as shown in Figure 95c, although other coordinating solvents, such as THF and DMSO resulted in the formation of cyclic complexes.[323] By varying the solvents, the reaction of $Cu_2(CH_3CO_2)_4 \cdot 2H_2O$, 4,4′-bpy, and salicylic acid by layered-solution approach yielded three 1-D CPs bearing a $[Cu(Hsal)_2(4,4\text{-bp})]$ motif, namely, *trans*-$[Cu(Hsal)_2(4,4'\text{-bpy})](DMF)$, *cis*-$[Cu(Hsal)_2(4,4'\text{-bpy})] \cdot 2H_2O$, and $[Cu_2(Hsal)_4(4,4'\text{-bpy})]$, with ladder, zigzag, and linear structures, respectively.[324]

In some cases, crystallization at various temperatures has been used to control the self-assembly and hence the conformation of flexible ligands and, consequently, the topology of the metal−organic frameworks. For instance, reaction of $AgBF_4$ and L at 0 °C afforded $[Ag_2L(H_2O)](BF_4)_2$ (L is shown in Figure 96), a highly corrugated 2D sheet with the ligand in trans conformation. Crystallization at 30 °C resulted in the formation of a 1D nanosized tube, $[AgLBF_4] \cdot 0.5(C_6H_6)$ with ligands in the cis conformation.

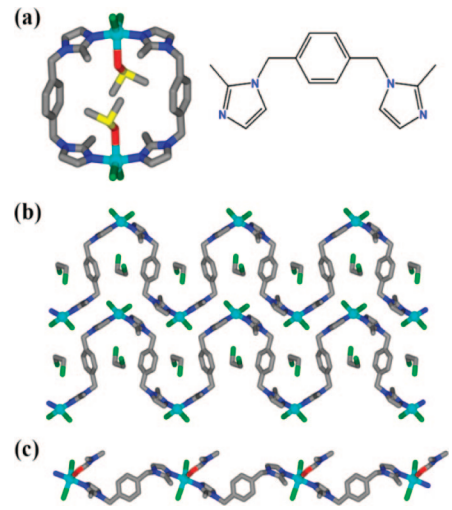

Figure 95. (a) View of metallocycle of $[Cu_2Cl_4(bmimb)_2] \cdot 2(acetone)$ (left) and ligand structure (right). (b) Wavelike CP obtained from 1,2-dichloroethane. (c) CP obtained from DMF.

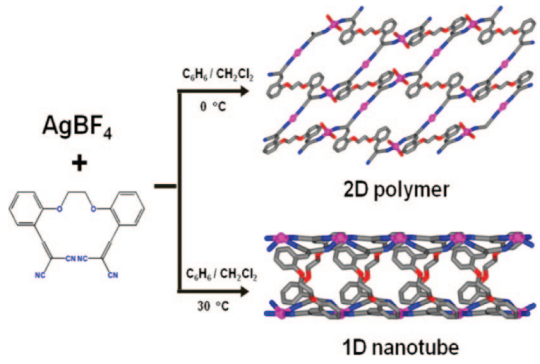

Figure 96. 1D nanotube and 2D polymer obtained from different temperatures.

Two of the 1D planar chains are connected to form a 1D tube motif with a internal dimensions of ~8.2 × 12 Å. It is interesting to note that the tube walls of are full of oxygen and nitrogen atoms, which is comparable to a crown-ether-like nanoscale tube. The nanotubes are completely empty, while the weak interactions between the silver ions and the intercalated benzene molecules linked the tubes to form layer. DFT calculations showed that higher temperature enhances the tendency for the transformation from the trans to cis conformation since the transformation barrier is relatively small and hence the transformation process is very fast.[325]

Jacobson and co-workers studied the self-assembly of Ni(II), 1,4-bdc and chelating amine coligands, such as 2,2′-bpy and phen. The Ni(II) complexes display zigzag CP structures through 1,4-bdc ligands bridging as shown in Table 2. In this polymer, the Ni−Ni−Ni angles are defined by the orientations of the two 1,4-bdc ligands in the Ni(1,4-bdc)$_2$(coligand), which in turn determine the conformation of CP chains, as well as intermolecular interactions between the chains. For instance, when the 1,4-bdc ligands are coordinated in chelating modes, the CP chains are in idealized zigzag conformations with Ni−Ni−Ni angles close to 120°. The incorporation of a coordinating water molecule into a trans position to one of the nitrogen atoms, resulted in the change of coordination mode of one of the two 1,4-bdc ligands from chelating to monodentate and an increase in the Ni−Ni−Ni angle to 135° leading to less bent chains. When the aqua ligand is coordinated in cis position with respect to the amine ligand, the Ni(II) centers are bridged by alternating bis-chelating and bis-monodentate ligands. The CP chain becomes more bent with Ni−Ni−Ni angle of 90°, hence crankshaft rather than zigzag conformation. This may

Table 2. Structures and Synthesis Conditions of the Polymers

Compound[a]	Reaction conditions[b]
[Ni(1,4-bdc)(1,10-phen)] 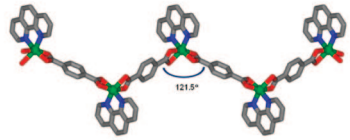	1:1.5:4:1 165-210°C, pH 8
[Ni(1,4-bdc)(2,2'-bpy)]·0.75H_2bdc 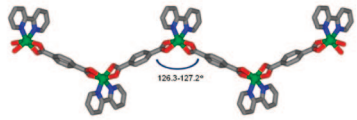	1:1.2:1.8:1 160°C, pH 5
[Ni(1,4-bdc)(1,10-phen)(H_2O)] 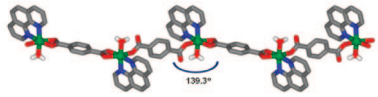	1:1.5:4:1 150-165°C, pH 8.5
[Ni(1,4-bdc)(1,10-phen)(H_2O)]·0.5H_2bdc 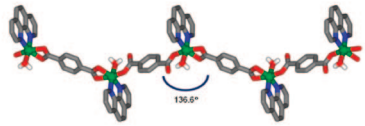	1:1.2:1.8:1 140-200°C, pH 4
[Ni(1,4-bdc)(2,2'-bpy) (H_2O)] 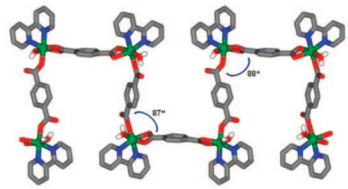	1:1.5:4:1 150-200°C, pH 8.5

[a] Angles shown in the figure correspond to Ni−Ni−Ni angles. [b] Molar ratio of reactants ($NiCl_2$/1,4-H_2bdc/KOH/amine).

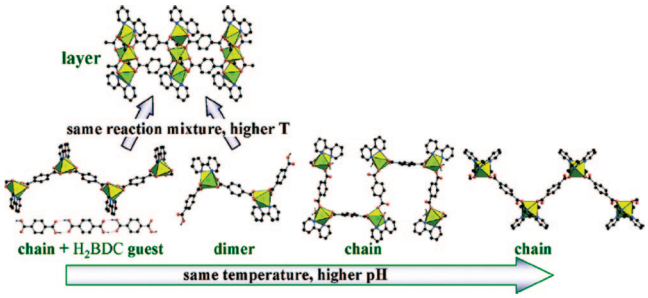

Figure 97. Self-assembly of Ni(II), 1,4-bdc, and 2,2′-bpy under different temperatures and pH. Reproduced with permission from ref 327. Copyright 2005 American Chemical Society.

be attributed to the preferred optimization of interchain noncovalent interactions and packing considerations.[326]

In a later study, Jacobson and co-workers elucidated the effect of pH and temperature on the assembled structures of ternary complexes Ni(II)/1,4-bdc/2,2′-bpy (Figure 97). Complex [Ni(1,4-bdc)(2,2′-bpy)]·(0.75)1,4-H_2bdc obtained from reaction mixture in pH 4 at 160 °C displays a zigzag CP structure. A slight increase in pH to 4.75 has resulted a protonated and noncoordinating 1,4-bdc ligand in [Ni_2(1,4-bdc)(1,4-Hbdc)$_2$(2,2′-bpy)$_2$]; hence, this complex exhibits a discrete dimeric structure. Reactions at higher temperature and the same pH lead to the transformation of zigzag CP and dinuclear compound into the 2D layered trinuclear compound [Ni_3(1,4-bdc)$_3$(2,2′-bipy)$_2$], where all 1,4-bdc ligands are deprotonated and bridging. As the pH is increased to 5.25, a crankshaft CP, [Ni(1,4-bdc)(2,2′-bpy)(H_2O)] is obtained. Increasing either the pH to 8.5 or the 2,2′-bpy content led to incorporation of the second chelating 2,2′-bpy into the chain and the formation of a 1D zigzag CP, [Ni(1,4-bdc)(2,2-bpy)$_2$]·2H_2O.[327]

Barbour and co-workers have studied the influence of the metal-to-ligand molar ratio on the formation of the final product using three copper(II) salts with a chloride, bromide, or nitrate counterion in combination with 1,3-bis(imidazol-1-ylmethyl)benzene (bimb). They observed that the use of excess ligand leads to the formation of extended 1D or 2D polymeric systems. The relative high metal-to-ligand ratio of 4:1 resulted in dinuclear complexes with an overall metal-to-ligand ratio of 1:1. When the metal-to-ligand is low, that is, 1:4, infinite 1D ribbon polymers with metal-to-ligand 1:2 are obtained. Two bimb ligands bridged the Cu(II) centers, while the apical positions are occupied by either chloride ions which are hydrogen bonded to noncoordinated methanol or water molecules that hydrogen bond to noncoordinated bromide ions. In the case of nitrate ion, metal-to-ligand ratio of 1:4 and 1:1 both exhibited concomitant polymorphism and produced two different crystal forms with 1D ribbon and 2D layer structures.[328]

Self-assembly of Cu(ClO_4)$_2$ and Hphis (Hphis = *N*-(2-pyridylmethyl)-*L*-histidine) has been shown to depend on the cations and pH. In the acidic pH, a 1D zigzag CP of [Cu(Hphis)(H_2O)](ClO_4)$_2$ is obtained through carboxylate bridging. When the potassium salt of phis was used, a trinuclear metallacrown [Cu_3(phis)$_3$](ClO_4)$_3$·2H_2O with unsymmetrical Cu···Cu distance is formed. Two carboxylate groups from different phis ligands coordinated to the equatorial and apical positions, respectively, to generate cyclization in trinuclear structure. When an equimolar of $LiClO_4$ was added, compound [(ClO_4)Li{Cu_3(phis)$_3$}](ClO_4)$_3$·3H_2O is isolated as a metallocrown encapsulated with lithium cation. The same product can also be obtained

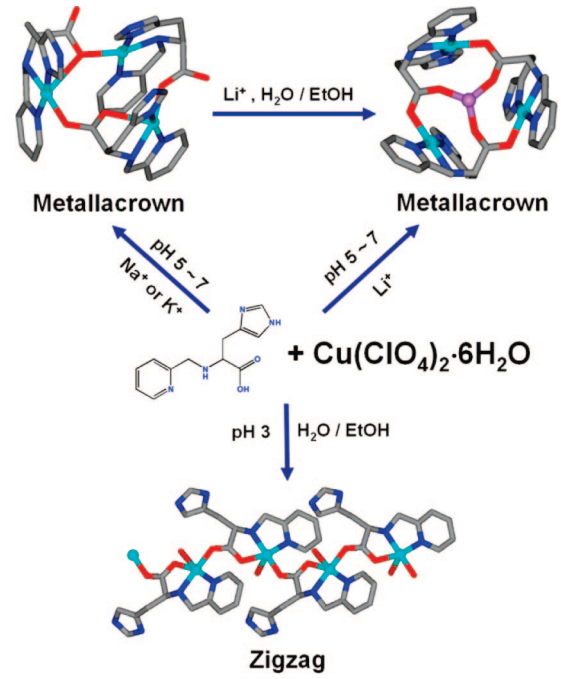

Figure 98. Formation of metallocrown and zigzag polymer under different conditions.

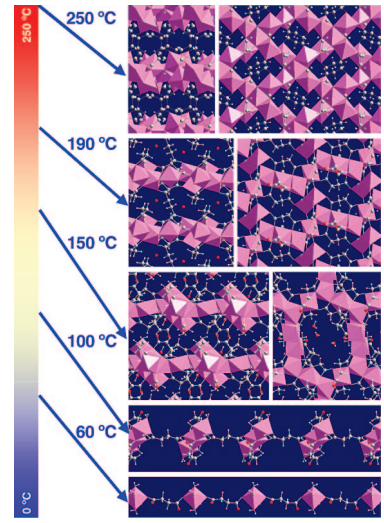

Figure 99. Graphical summary of cobalt succinate structures that form at the different temperatures studied. Purple polyhedra are drawn around cobalt centers, and oxygen atoms are colored red, carbon atoms gray, and hydrogen atoms white. Reproduced with permission from ref 330. Copyright 2004 The Royal Society of Chemistry.

from reaction of lithium salt of phis and Cu(II). The cone shape [Cu_3(phis)$_3$]$^{3+}$ cation accommodates the lithium cations through carboxylate coordination. On the other hand, the formation of 1D CP is favorable in the absence of base. Figure 98 shows schematic representation of isolation of these complexes under different conditions.[329]

Férey, Cheetam, and co-workers have reported the influence of temperature in the synthesis of metal−organic hybrid materials using cobalt succinates as an example (Figure 99).[330] Slow evaporation of the reaction mixture resulted in the formation of 1D CP with Co(H_2O)$_4$ units bridged by succinates ligands.[331] Another 1D CP with edge-sharing trimer clusters link through succinate ligands is obtained under reflux condition.[330] Higher temperature and hydrothermal conditions resulted in 2D sheets and 3D network.[332]

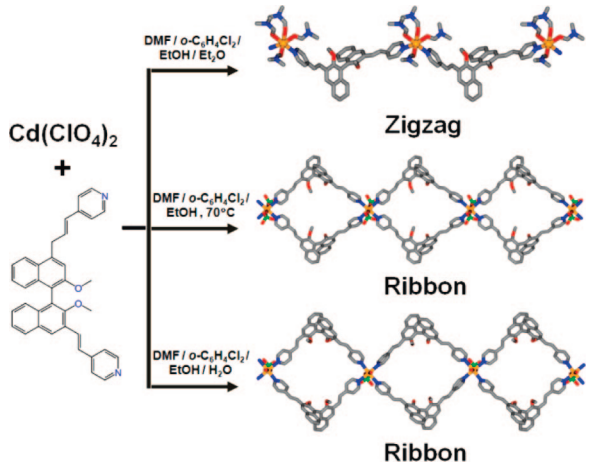

Figure 100. Reaction scheme of $Cd(ClO_4)_2$ with mnvp under different conditions.

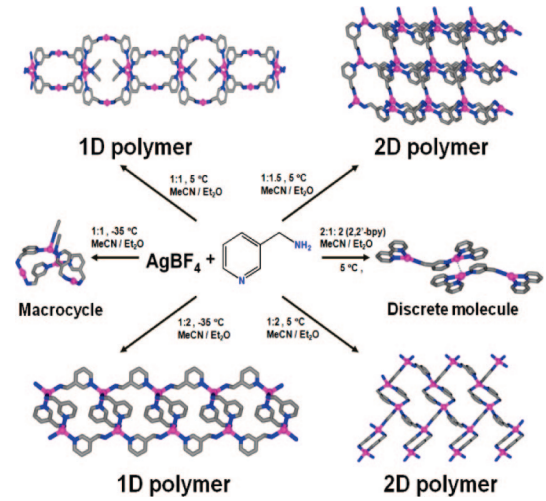

Figure 101. Self-assembly of $AgBF_4$ and 3-A under various experimental conditions.

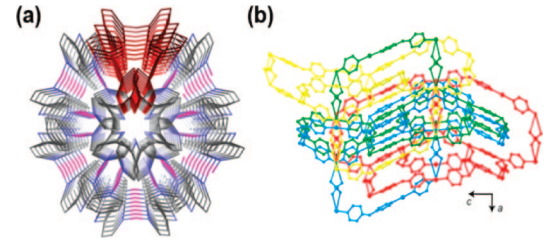

Figure 102. (a) View of packing of adjacent helices with lack of free volume. One helix is highlighted in red. (b) View of the 4-fold interpenetrated net of helices. Reproduced with permission from ref 335. Copyright 2006 American Chemical Society.

It is reasonable to assume that the amount of water decreases with increasing temperature; hence, the coordination sites in the cobalt atoms are more available for carboxylate groups. These trends favor higher overall dimensionality as well as M−O−M dimensionality of the structures. Further, decrease of dielectric constant of water under hydrothermal conditions may also favor higher coordination numbers for carboxylate groups.

Reaction of $Cd(ClO_4)_2$ with (*S*)-2,2′-dimethoxy-1,1′-binaphthyl-3,3′-bis(4-vinylpyridine) (mnvp) under different conditions gave rise to various 1D structures (Figure 100). Reaction in DMF/*o*-$C_6H_4Cl_2$/EtOH yielded a zigzag polymer, $[Cd(mnvp)(DMF)_4](ClO_4)_2 \cdot EtOH \cdot 0.5H_2O$, with two mnvp ligands coordinated to Cd(II) centers in cis positions. The neighboring chains are linked to each other via $\pi-\pi$ stacking interactions (3.47 Å) to lead to a 3D supramolecular framework with 1D chiral channel. The same reaction at 70 °C afforded a ribbon-like polymer, $[Cd(mnvp)_2(ClO_4)_2] \cdot 3EtOH \cdot H_2O$, with 38-membered macrocycles formed by four mnvp ligands in the equatorial plane and two perchlorate anions on the axial positions. Addition of small amount of water into reaction mixture afforded a similar ribbon polymer $[Cd(mnvp)_2(ClO_4)(H_2O)] \cdot (ClO_4) \cdot 1.5(o\text{-}C_6H_4Cl_2) \cdot 3EtOH \cdot 6H_2O$ with perchlorate anions at the axial positions. It is noted that the ribbon-like CPs lose their crystallinity upon the removal of included solvent molecules by heating under vacuum, but their crystallinity can be restored by immersing the evacuated compounds in EtOH.[103]

The reaction of 3-aminomethylpyridine (3-A) ligand with $AgBF_4$ produces an array of structural motifs that depend on the ratio of the reactants and cystallization temperature (Figure 101). An equimolar ratio of 3-A to Ag(I) furnished a 1D CP after several days at −35 °C. The CP chain is linked to another strand through Ag···Ag interaction to form a chain-like structure with alternating circular and oval "links" joined at every other metal center. Interestingly, rapid crystallization within several hours at 5 °C furnished a folded macrocycle with similar structure of the polymer. At a 3:2 ratio, a 2D CP is formed regardless of temperature of crystallization. With a 2:1 ratio, another 2D CP with box in box structure is obtained at 5 °C. When the solution mixture is kept at −35 °C, the lower temperatures cause a constriction in the size of the larger ring that is formed by the bridging 3-A. This smaller, more constrained bridge preferentially grows into a 1D CP as opposed to the former 2D network. When 2,2′-bpy is added in at least a 1:1 ratio with silver in solutions of 3-A and $AgBF_4$, it effectively stops the formation of the other structural motifs by capping each of the silvers to form discrete molecule.[333]

The neutral square-planar Pt(II) complexes $[Pt(RNH_2)_2(NHCO^tBu)_2]$ (R = H, Et) and [Pt(dach)(NHCO^{t}Bu)$_2$] (dach = 1,2-diaminocyclohexane) act as metalloligands and react with TlX (X = NO_3, ClO_4, PF_6, and $Cp_2Fe(CO_2)_2^{2-}$) forming 1D and 2D CPs with heterobimetallic backbones. The structures of the Pt−Tl compounds depend on both counteranions and the amine substituents. The compounds $[Pt(NH_3)_2(NHCO^tBu)_2Tl]X$ (X = NO_3, ClO_4^-) adopt 1D zigzag chain structures comprising of alternating $[Pt(NH_3)^{2-}(NHCO^tBu)_2Tl]^+$ units, whereas $[\{Pt(NH_3)_2(NHCO^tBu)_2\}_2Tl_2]X_2$ (X = PF_6^-) consists of a helical chain. Others are regular 1D CPs.[334]

Layering of bis(4-pyridyl)amine (bpa) solution with AgX (X = CF_3SO_3, PF_6, ClO_4) furnished 1D polymers with zigzag conformations. However, hydrothermal reaction using $AgClO_4$ and $AgNO_3$ resulted in the formation of single-stranded helical CPs with 4-fold interpenetrated 3D networks (Figure 102a). The helical CP chain in $[Ag(bpa)]ClO_4$ propagated along the 3_2 screw axes with pitch of 33.35 Å. The helices are packed closely together resulting in the formation of a strongly interacting $\pi-\pi$ stack (3.56 Å). The helices further held together in a 3D array by a number of other supramolecular interactions between helical chains and ClO_4^- anions in addition to $\pi-\pi$ stack interactions (Figure 102b). The crystal is made up of one enantiomer of the helix probably because of the $\pi-\pi$ stacking, which is likely to pack more efficiently than a racemic mixture of M and P helices. In complex $[Ag(bpa)]NO_3$, the helical chain propagated along the 3_1 screw axes with pitch of 34.56 Å, but there were no

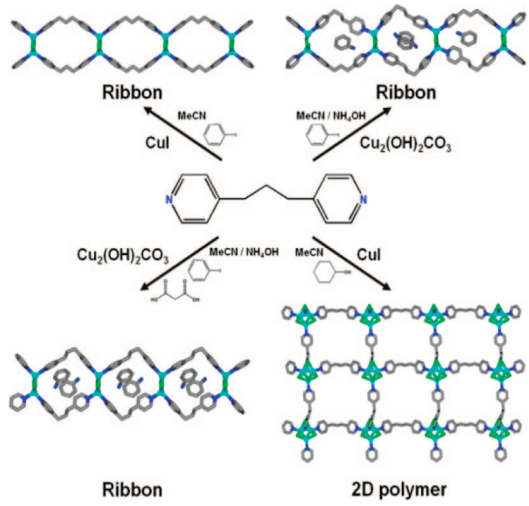

Figure 103. Schematic diagram showing the formation of different structures from bpp ligand.

$\pi-\pi$ interactions. Consequently the helices were held together to form a 3D network by a number of weaker interactions involving the NO_3^- anions.[335]

A schematic digram detailing the self-assembly of Cu(I) with bpp under different experimental conditions shown in Figure 103 contains the formation of three 1D double chain structures and a 2D CP.[336] The shape and size of the macrocycle in the 1D chain structures change because of inclusion of solvents used and in situ formed solvents in the cavities.

Recently, Uemura and co-workers reported a series of 1D CP of Ag(I) with amide containing ligands with different anions including PF_6^-, ClO_4^-, BF_4^-, and NO_3^-. When *N*-(4-pyridyl)isonicotinamide (4-pia) is used, the 1D chains display wavy conformation, and the anions are hydrogen bonded to amide moieties thus prevent the formation of amide···amide hydrogen bonds. The 1D CP formed by the reaction of $AgPF_6$ with *N*-(pyridin-4-ylmethyl)isonicotinamide (4-pmia) shows zigzag CP structure. The adjacent chains are aligned and formed wave sheets through C═O···Ag interactions. In the case of ClO_4^- and NO_3^-, the oxygen atoms of amide moieties form hydrogen bond with water molecules. Changing the nitrogen atom to 3-position of pyridyl group resulted in zigzag CP structure with complementary amide bonding lead to the formation of β-sheet like network. Coordination of Ag(I) with *N*-(pyridin-4-ylmethyl)nicotinamide (4-pmna) furnished left-handed helical CP with 4_3 axis. The helical column is interdigitated with adjacent columns by weak association between the oxygen atom of the amide moiety and the Ag(I) atom in the adjacent chain. It is interesting to note that two kinds of biomimetic structure, β-sheet and helix, can be constructed by slight change of ligand orientation.[337]

Pyridine-2,4,6-tricarboxylic acid (H_3ptc) readily reacts with a Zn(II) salt at room temperature to form different products depending upon the presence or absence of pyridine in the reaction mixture. In the presence of pyridine, the ligand breaks to form infinitely zigzag CP $[Zn(ox)(py)_2]\cdot H_2O$. Stability of the product and its insolubility in the reaction medium seem to be responsible for the breakage of the ligand and drive the reaction forward. In absence of pyridine, the ligand remains intact and forms a mixture of a 3D CP and a discrete 12-membered metallomacrocycle.[338]

Self-assembly of 1,3-bis(4,5-dihydro-1H-imidazol-2-yl)-benzene (bib) with silver(I) salt in a 1:1 molar ratio generated a [2 + 2] metallocyclic complex in the presence of different counteranions, such as SCN^-, NO_3^-, BrO_3^-, ClO_3^-, and ClO_4^-.[339] On the other hand, the metallocycles undergo ring-opening polymerization to form 1D CPs upon the addition of competing ligands/counterions. When $C_2O_4^{2-}$, NO_2^- and VO_3^- were used, the bib ligand adopts trans configuration that resulted in the formation of helical chains. When 1,2-diaminoethane (en) and 1,3-diaminopropane (pn) is used, ribbonlike polymers containing [2 + 2] metallocycles with bib ligands in cis configuration is formed.[340]

The structural changes influenced from ligand protonation upon stepwise crystallization have rarely been investigated. Here the reaction of $Zn(NO_3)_2$, 1,3,5-H_3btc, and 1,2,4-triazole (Htrz) under hydrothermal conditions yielded three compounds from crystallization of the reaction mixture and evaporation of the filtrate. Complex $[Zn_{2.5}(trz)_2(btc)(H_2O)]\cdot 2H_2O$ with 3D microporous framework structure is obtained directly from hydrothermal reaction at pH 3.6, and both its ligands are completely deprotonated. Slow evaporation of the filtrate with pH 3.4 afforded another 3D structure, $[Zn_{2.5}(trz)(Hbtc)_2(H_2O)_2]$, which contains monodeprotonated trz and doubly deprotonated Hbtc. Upon further evaporation, complex $[Zn(Htrz)(Hbtc)(H_2O)]\cdot 2H_2O$ with neutral Htrz and doubly deprotonated Hbtc is produced at pH 3.5−3.9 with the infinite chain motif bridged by Hbtc anions, while the Htrz act as terminal ligands.[341] Influence of experimental conditions on the self-assembly of CPs has been further explored.[185,234a,342]

5. Supramolecular Isomerism Involving 1D CPs

In many syntheses, self-assembly of CPs can result in the formation of more than one structural motif with identical formula.[1] The flexible ligands that adopt a variety of conformations can impart to CP and lead to unexpected, novel, and interesting supramolecular isomerism. However, in 1D CP, such diverse structural variations observed in 2D and 3D structures, are not possible because of the nature of dimensionality. These supramolecular isomers have also been induced by the presence of solvents in the lattice. These isomers with varying solvent guest molecules are commonly known as pseudo-supramolecular isomers.

5.1. Cyclic and Acyclic Structures

Two supramolecular isomers of Cu(II) complexes of 5-nitro-1,3-benzenedicarboxylic acid have been found as discrete molecular hexagon and zigzag CP in concomitant crystallization. The hexagon is composed of six ligands, six Cu(II) cations with effective outer diameter of 3.14 nm, but the internal cavity has an effective diameter of ~0.8 nm (Figure 104). The zigzag polymeric chains are packed efficiently and sustained by hydrogen bonding and $\pi-\pi$ stacking interactions. According to Zaworotko et al., the closed discrete structure is thermodynamically favored over the open polymeric supramolecular isomer.[343]

The reactions of HgI_2 with the 1,3-bis(benzimidazol-1-ylmethyl)-2,4,6-trimethylbenzene (bbimms) afforded three complexes with different structures depending on reactant ratio and amount of solvent (Figure 105). It is interesting that the macrocyclic ring and helical CP are supramolecular isomers, and both are related to the triply bridged binuclear precursor via the addition of one more ligand in a ring-opening process, which also termed as "ring-opening isomerism" by the authors.[344]

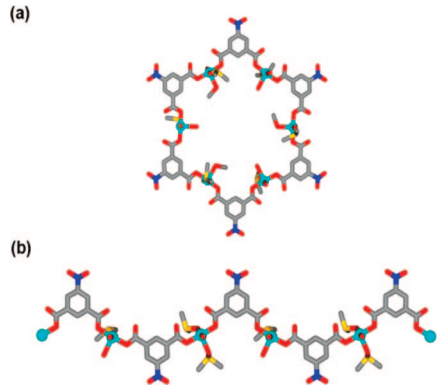

Figure 104. Two supramolecular isomers: (a) hexagon marcocyclic ring and (b) zigzag polymer.

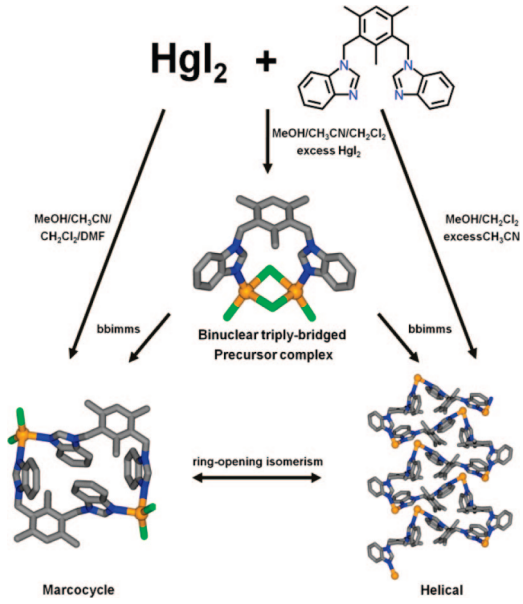

Figure 105. Schematic diagram of ring-opening isomerism.

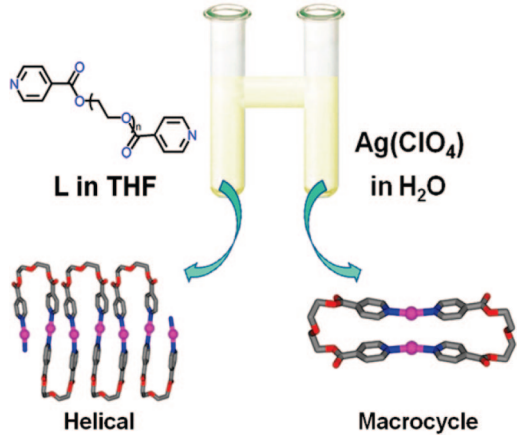

Figure 106. Two supramolecular isomers obtained from two different concentrations.

Self-assembly of $Ag(ClO_4)$ with L (L is shown in Figure 108) in an H-tube afforded two supramolecular isomers in the same solution mixture, depending on the concentration of the reactants (Figure 106). In the arm-containing excess Ag(I) salt, an oval-shape macrocycle ring with dimension 3.15×20 Å^2 composed of two Ag(I) ions bridged by two ligands is obtained. Another single-stranded helical CP with three ligands coordinated to two Ag(I) cations is obtained from the other arm-containing excess L solution. The

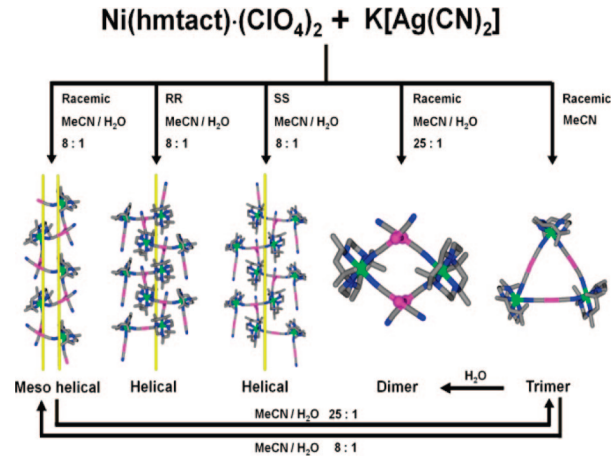

Figure 107. Formation of supramolecular isomers based on solvent and chirality.

U-shaped helical conformation of the polymeric chains does not exhibit Ag···Ag or $\pi-\pi$ interactions. The helical polymer is a kinetic product, while the ring is thermodynamically more stable.[320]

The reactions of [Ni(α-*rac*-hmtact)]$(ClO_4)_2$, [Ni(α-*SS*-hmtact)]$(ClO_4)_2$, and [Ni(α-*RR*-hmtact)]$(ClO_4)_2$ (hmtact = 5,5,7,12,12,14-hexamethyl-1,4,8,11-tetraazacyclo tetradecane) with $K[Ag(CN)_2]$ in a molar ratio of 1:2 in acetonitrile/water (8:1) afford a 1D meso-helical, [Ni(*f*-*rac*-hmtact)]-$[Ag(CN)_2]_2$ and two supramolecular stereoisomers with homochiral right- and left-handed helical motifs, [Ni(*f*-*SS*-hmtact)]$_2[Ag(CN)_2]_4$ and Ni(*f*-*RR*-hmtact)]$_2[Ag(CN)_2]_4$, respectively. Reactions of [Ni(α-*rac*-hmtact)]$(ClO_4)_2$ with $K[Ag(CN)_2]$ in the same molar ratio in acetonitrile/water (25:1) and pure acetonitrile generated a dimer, [Ni(*f*-*rac*-hmtact)]$[Ag(CN)_2]_2$ and trimer, [Ni(*f*-*rac*-hmtact)Ag-$(CN)_2]_3(ClO_4)_3$, respectively. Figure 107 shows the formation of supramolecular isomers and transformation under different conditions. In the meso-helical structure, the [Ni(*f*-*RR*-hmtact)]$[Ag(CN)_2]_2$ enantiomers are alternately connected to [Ni(*f*-*SS*-hmtact)]$[Ag(CN)_2]_2$ enantiomers through intermolecular argentophilic interactions (~3 Å) to form a 1D achiral meso-helical chain. The salient feature is that the meso helix can be converted reversibly to another supramolecular isomer, a dimer which is constructed from a pair of enantiomers that are connected through argentophilic interactions (3.25 Å) by changing the solvent mixture ratio. This has been described as ring-opening polymerization or ring-opening isomerism. These two helices are supramolecular stereoisomers. Another related trimer complex has been found to transform to the dimeric structure because of the introduction of atmospheric moisture into the solution.[79e]

Self-assembly of Ni(II) with 5,5,7,12,12,-14-hexamethyl-1,4,8,11-tetraazacyclo tetradecane (hmtatd) under different reaction conditions gave rise to a coordination complex, a molecular square, and 1D helical CP (Figure 108). The 1D helical chains are packed in an alternating right- and left-handed chirality because of the oppositely twisted arrangements of two adjacent $[Ni(CN)_4]^{2-}$ anions. It is worth mentioning that the coordination complex is a metastable compound, which can be converted to the helical CP in a MeCN/MeOH solution. Furthermore, the molecular square and helical CP are supramolecular isomers with same formula of {*cis*-[Ni(*f*-*rac*-hmtatd)][Ni(CN)$_4$]}. More interstingly, the helical CP can be considered to be formed by the ring-opening polymerization of the molecular square precursor.[345]

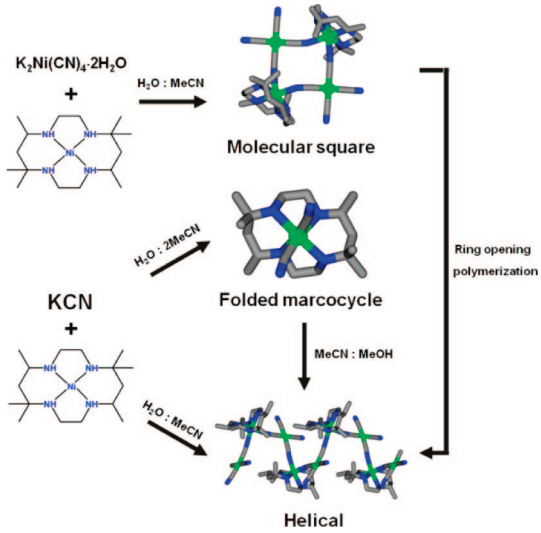

Figure 108. Supramocular isomers obtained from ring-opening polymerization.

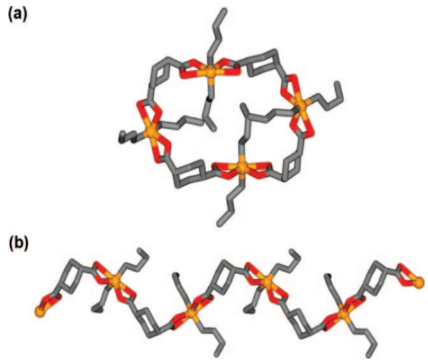

Figure 109. (a) Perspective view of marcocylic ring. (b) Portion of zigzag CP chain.

Complex [{nBu$_2$Sn(*cis*-1,4-chdca)}$_4$][{nBu$_2$Sn(*cis*-1,4-chdca)}$_n$] (*cis*-1,4-H$_2$chdca = *cis*-1,4-cyclohexanedicarboxylic acid) contains two different supramolecular isomers with cyclotetramer and zigzag CP in the same crystal lattice (Figure 109). The coordination geometries of the tin atoms and the conformations of the carboxylate ligands are similar in both cyclic and the polymeric structure. In the CP, *cis*-1,4-chdca bridged tin ions to form zigzag CP chains. In the 36-membered cyclotetramer ring the cavity is occupied by half of the nBu groups.[346]

A triply bridged Ag(I) cage complex [Ag$_2$(dppa)$_3$](CF$_3$SO$_3$)$_2$ (dppa = bis(diphenylphosphino)acetylene), when stored in its supernatant for 16 weeks, is converted to its supermolecular isomeric coordination polymer [Ag(dppa)$_2$Ag(dppa)-(CF$_3$SO$_3$)$_2$]. This polymer a structure is composed of ten-membered Ag$_2$(dppa)$_2$ rings linked into infinite one-dimensional chains by a third dppa unit.[347]

5.2. Different 1D Structures

The 1D CP [Cu$_2$(sval)$_2$(H$_2$O)$_3$] features an interesting supramolecular isomerism in which recrystallization of the dehydrated compound from different solvents furnished different supramolecular isomers as shown in Figure 110. Products obtained from 2-propanol and 1-butanol are pseudosupramolecular isomers. It is surprising that the basic building block, [Cu$_2$(sval)$_2$], can be linked in different ways to form 1D CPs.[348]

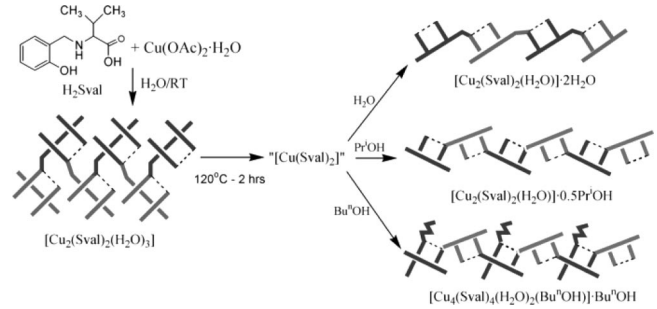

Figure 110. Recrystallization of dehydrated [Cu$_2$(sval)$_2$] leading to supramolecular isomerism. Reproduced with permission from ref 348. Copyright 2004 American Chemical Society.

The reactions of *N*,*N*′-bis(3-pyridinecarboxamide)-1,2-ethane (bpce) with AgX (X = ClO_4^-, $CF_3SO_3^-$ or NO_3^-), Zn(ClO$_4$)$_2$·6H$_2$O, and Cd(ClO$_4$)$_2$·6H$_2$O produced zigzag 1D CPs, which further form corrugated sheets via complementary amide hydrogen bonds. Of these [Ag(bpce)](ClO$_4$) exhibits supramolecular isomerism, which arose from two rotamers in which the bpce ligand was in syn and anti orientations.[349]

Chen and co-workers came across supramolecular isomerism in a series of Ag(I) and Cu(I) complexes of imidazolate (im) derivatives. Simple imidazolate derivatives are bent exobidentate ligands that are expected to show a linear or slightly bent im-M-im geometry and CuI-imidazolates furnished only 1D CPs as expected. On the other hand, supramolecular isomers from the 1:1 metal/ligand ratio may be generated by utilizing an angular ligand (M−L−M ≈ 135−145°) and a linear two-coordinate metal ion as polygons, helices, and zigzag chains.

As shown in Figure 111a, self-assembly of Cu(I) with 2-methylimidazolate (mim) afforded three supramolecular isomers from different solvents. It has been shown that the hydrophilic solvent facilitated the formation of chain-like structure while hydrophobic, circular solvents favored the ring structures since mim methyl groups are pointing inward the ring. Discrete supramolecular isomers (0D) were suggested to be thermodynamically favored compared with the chain ones.[350] Furthermore, the analogue [Ag(mim)] complex displays pseudosupramolecular isomerism under different solvent diffusion conditions as shown in Figure. 111b. These isomers feature 1D CP structures with different motifs. In the helical CP, the mim ligands bonded to Ag(I) in syn fashion, and the polymeric chain propagates with all the methyl groups pointing toward the channel of the helix having 8_1 screw axis which does not exist as a crystallographic symmetry. Another complex [Ag$_4$(mim)$_4$(C$_8$H$_{10}$)] shows a *S*-shaped 1D CP structure with each four mim ligands orientated in anti fashion. Orientation of all mim ligands alternating in anti fashion has resulted in a zigzag chain.[351] In a later study, the analogous [Cu(eim)] (eim = 2-ethylimidazolate) has been obtained from water and water-cyclohexane solution mixture as helical and zigzag CPs, respectively (Figure 111c). The former isomer displays a triple-stranded helix structure and has been discussed in section 2.4.3. It has been found that a water medium favors the aggregation of the hydrophobic ethyl groups, while the nonpolar solvent cyclohexane has opposite effect.[108] Similar such supramolecular isomers have been reported in the literature.[167]

Self-assembly of CuI and dpds in different solvents also afforded two supramolecular isomers in the same reaction

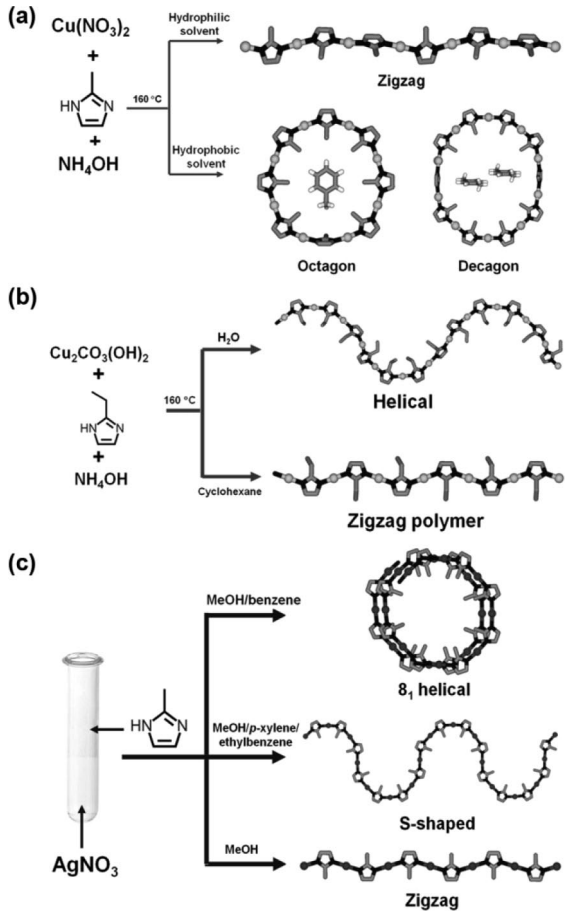

Figure 111. Supramolecular isomerism of (a) [Cu(mim)], (b) [Ag(mim)], and (c) [Cu(eim)].

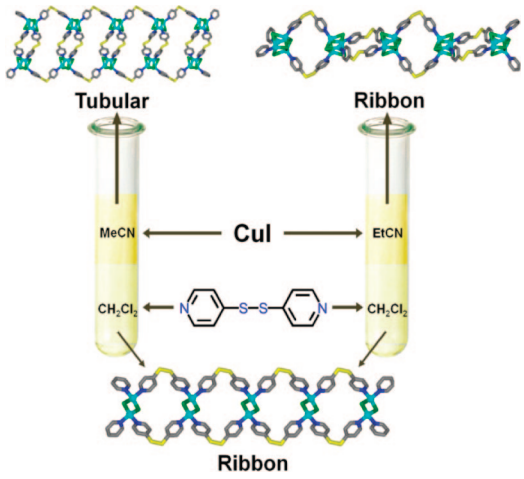

Figure 112. Schematic diagram of self-assembly of CuI and dpds in different solvents.

solution but depending on the concentration of the reactants and regardless of the metal-to-ligand ratios used (Figure 112). Crystallization in $MeCN/CH_2Cl_2$ or $EtCN/CH_2Cl_2$ yielded yellow needles of ribbon-like 1D CP, [CuI(dpds)], in the ligand-rich region of the solution. Another complex $[(CuI)_2(dpds)]$ with two different structural motifs is obtained in the metal-rich region depending on the solvent. Complex obtained from $EtCN/CH_2Cl_2$ contains tetrahedral Cu_4I_4 cubane units alternately bonded to pairs of dpds ligands that are orientated perpendicular to each other in adjacent links of the necklace. Crystallization in $MeCN/CH_2Cl_2$ resulted in another structural isomer based on Cu_4I_4 cubane units that

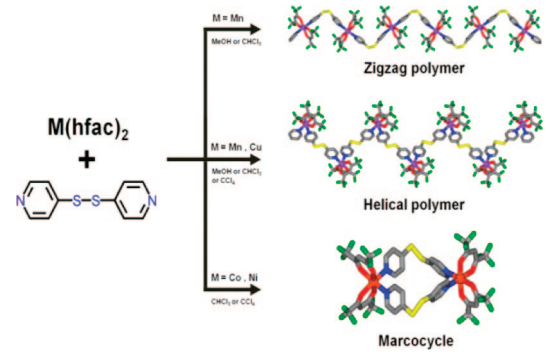

Figure 113. Supramolecular isomersim of $M(hfac)_2(dpds)$ complexes under different conditions.

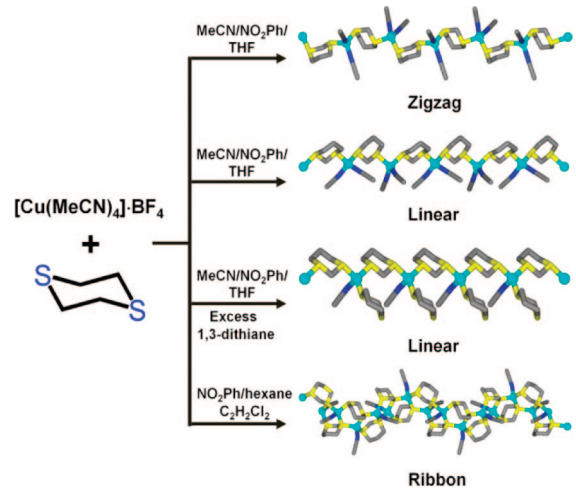

Figure 114. Supramolecular isomerism of Cu(I) complexes of 1,4-dithiane.

interlink dpds ligands to form a tubular polymer. These isomers are termed as topological isomers with different topology and connectivity of polymorphs.[352]

Similarly, self-assembly of $M(hfac)_2$ (M = Cu, Co, and Ni) with dpds also depends on the metal ions and crystallization solvents (Figure 113). Complex $[Mn(hfac)_2(dpds)]$ can be obtained as zigzag or helical CPs when crystallized in MeOH or $CHCl_3$ and CCl_4, respectively. It has been noted that coordination of dpds to Mn(II) in trans positions resulted zigzag CP, while helical CP is obtained when dpds coordinated in cis positions. However, coordination of dpds in cis positions provided helical CP regardless of crystallization solvents. On the other hand, when Co(II) and Ni(II) were employed, marcocyclic complexes were obtained regardless of the crystallization conditions.[353]

Four Cu(I) complexes of 1,4-dithiane obtained from different solvents exhibit supramolecular isomerism with unique bonding modes for the 1,4-dithiane ligands in each isomer (Figure 114). From the same solvent system, different coordination mode of 1,4-dithiane ligands yielded two supramolecular stereoisomers with different 1D structures and chiralities. Furthermore, other crystallization conditions such as amount of ligand and solvent also determine the 1D CP structures.[354]

Self-assembly of [Cu(2-pytz)] (2-Hpytz = 3,5-di-(2-pyridyl)-1,2,4-triazole) provides interesting supramolecular isomers under different experimental conditions (Figure 115). The isomer obtained from $Cu_2(OH)_2CO_3$/aqueous solution displays a centrosymmetric, chairlike tetrameric structure containing both cis−cis and cis−trans 2-pytz ligands. Similar

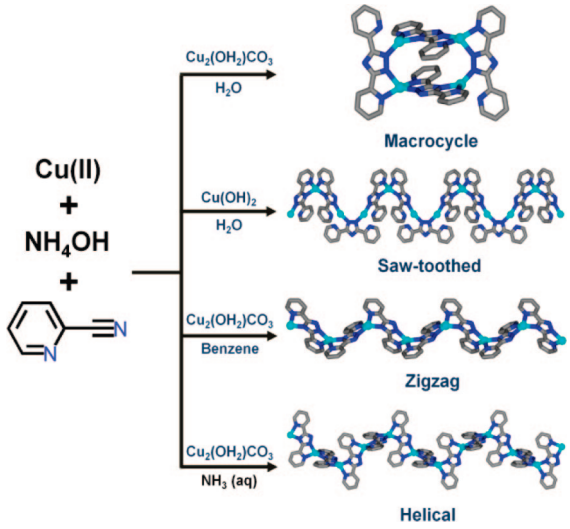

Figure 115. Supramolecular isomerism [Cu(2-pytz)] under different reaction conditions.

reaction with $Cu(OH)_2$ yielded a 1D CP with one cis−trans and half cis−cis 2-pytz ligand in the asymmetric unit and propagates with an unexpected sawtoothed geometry. More interestingly, these polymeric chains dimerized to form a zipperlike double chain through face-to-face $\pi-\pi$ interactions (3.43 Å). Reaction in benzene afforded 1D zigzag CP structure generated by Cu(I) ions and cis−trans ligands. The antiparallel chains stack with each other via $\pi-\pi$, C−H$\cdots\pi$, and C−H$\cdots$N interactions and resulted in centrosymmetric packing. In addition, reaction of $Cu_2(OH)_2CO_3$ with 2-cyanopyridine in aqueous ammonia resulted in helical CP. These are examples of conformational supramolecular isomers.[355]

5.3. 1D and Higher-D Structures

A simple dpe ligand with gauche (angular) and anti (linear) conformations can give rise to three distinct supramolecular isomers of $[Co(NO_3)_2(dpe)_{1.5}]$. Figure 116 displays the schematic representation of crystallization conditions and polymeric architectures of these supramolecular isomers. The first isomer is composed of two gauche spacers that link Co(II) centers to a form square structure and another anti spacer bridging to form linear chains. This compound is isostructural to the previously reported Cd analogue.[356] The isomer obtained in the same solvent mixture but, with ferrocene as template, has bilayer structure that contains two anti spacers for every gauche spacer. Third isomer is a

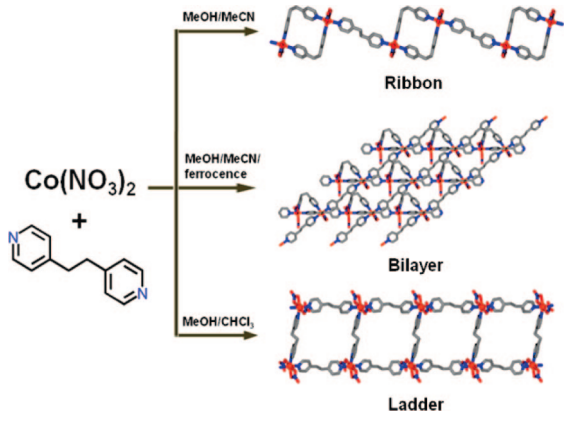

Figure 116. Supramolecular isomerism in $[Co(NO_3)_2(dpe)_{1.5}]$.

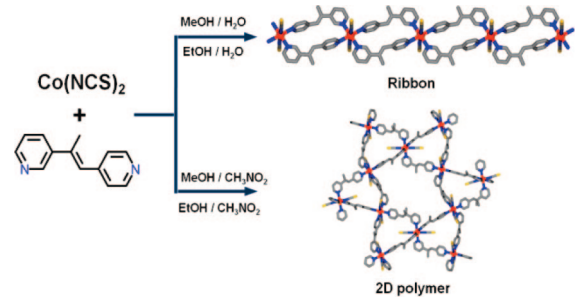

Figure 117. Formation of two supramolecular isomers from different solution mixture.

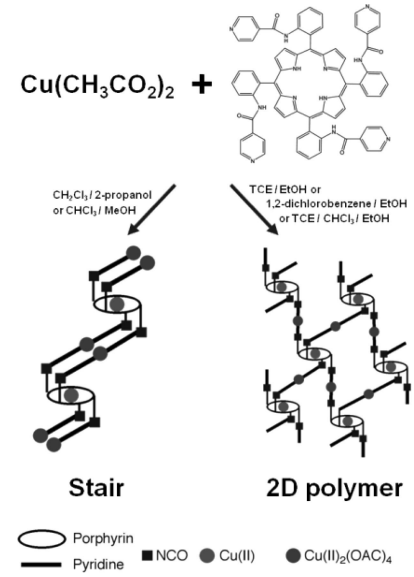

Figure 118. Two supramolecular isomers in different solvent systems.

molecular ladder in which all spacer ligands adopt anti conformations.[357]

Self-assembly of $Co(NCS)_2$ with 1-methyl-1′-(3-pyridyl)-2-(4-pyridyl)ethene (mppe) yielded $[Co(mppe)_2(NCS)_2]$ as chain or 2D CP sturctures depending on the solvent combination used as shown in Figure 117. The supramolecular isomerism is attributed to the different orientations of the unsymmetrical ligands around the metal center.[358]

Reaction of $Cu(CH_3COO)_2$ with *meso*-tetrakis(*o*-isonicotinoylamidophenyl)porphyrin demonstrates another example of supramolecular isomerism in porphyrin complexes (Figure 118). Crystallization in $CHCl_3$/*i*-PrOH or $CHCl_3$/MeOH afforded a 1D stair-type CP in which Cu-porphyrin units are linked together via all four isonicotinoyl moieties of four neutral $Cu_2(CH_3COO)_4$ dimers. The pyridine units are located on the same face of the porphyrin ring are oriented almost parallel to each other. On the other hand, crystallization in 1,1′,2,2′-tetrachloroethane (TCE)/EtOH, 1,2-dichloro benzene/EtOH, or a TCE/$CHCl_3$/EtOH give rise to 2D CP. In this context, one of the two pyridine rings is almost perpendicular to the porphyrin plane, while the other one is strongly tilted. Therefore, the Cu-porphyrin building blocks are joined through isonicotinoyl moieties of four neutral $Cu_2(CH_3COO)_4$ dimers leading to a 2D network.[359]

Redox reaction between $[Cu_2(CH_3COO)_4(H_2O)_2]$ as oxidant and hydroquinone as reductant in EtOH afforded a organometallic building block $[Cu^{I}_2(bq)(CH_3COO)_2]$ (bq = *p*-benzoquinone), which has two types of supramolecular synthons on coordination that lead to three supramolecular

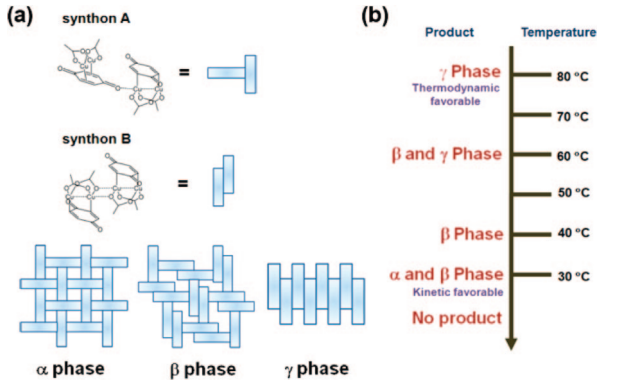

Figure 119. (a) Top: Two types of supramolecular synthon on coordination between two dicopper building blocks. Bottom: Schematic representation of three supramolecular isomers. (b) Schematic diagram showing temperature-dependent supramolecular isomerism.

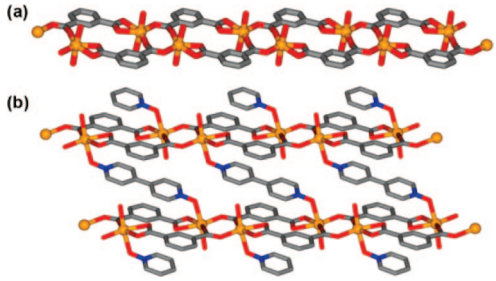

Figure 120. (a) Portion of 1D polymeric chain in colorless compound. (b) Perspective view of 2D network in pink compound.

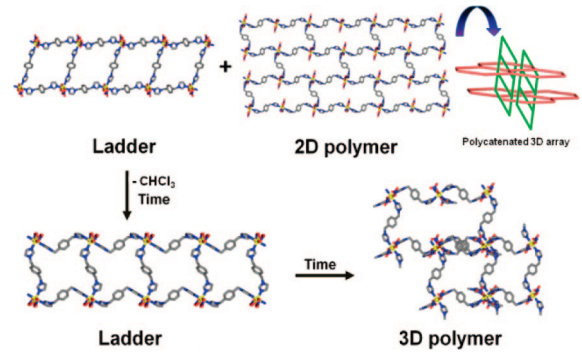

Figure 121. Supramolecular isomerism upon guest removal.

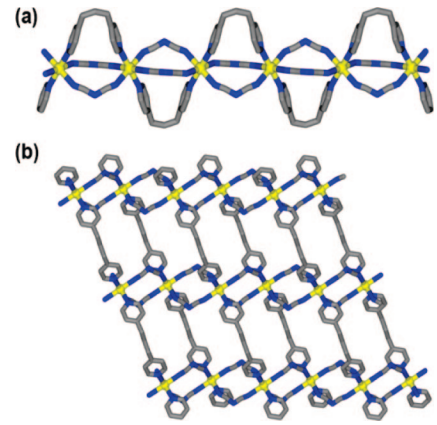

Figure 122. (a) View of 1D CP chain of kinetic product. (b) View of 2D network of thermodynamic product.

isomers with different phases (Figure 119a). The α- and β-phase products display 2D network, while γ-phase product is a 1D CP. It is noted that three supramolecular isomers were crystallized in the same solvent and pure phases can be obtained by varying the reaction temperature and concentration (Figure 119b). High-temperature reaction conditions and a low concentration of the molecular building block produced the thermodynamically favorable γ-phase product. Further decreasing of temperature facilitated the formation of the kinetically favored β-phase and eventually α-phase product.[360]

Reaction of $MnCl_2$, disodium isophthalate (Na_2isop) and 4,4′-dipyridyl-*N*,*N*′-dioxide (dpyo) on refluxing in H_2O/MeOH yielded two pseudosupramolecular isomers concomitantly as colorless $[Mn(isop)(H_2O)_2]\cdot dpyo\cdot H_2O$ and pink $[Mn(isop)(H_2O)(dpyo)_{0.5}]$ $(dpyo)_{0.5}(H_2O)$ complexes. The colorless compound features a ribbon-like CP chain structure composed of alternate 8- and 16-membered rings (Figure 120a). The 8-membered ring is formed by two symmetry-related bridging isop ligands and two Mn(II) ions while 16-membered ring is furnished by two Mn(II) ions, two chelating and bridging isop ligands. The neighboring polymeric chains are stacked in a stair-like fashion with $\pi-\pi$ stacking interactions between aromatic isop rings (3.51 Å). The dpyo ligands remained uncoordinated. In another supramolecular isomer, one of the aqua ligand is replaced by dpyo ligand and resulted in a 2D CP (Figure 120b).[361]

Depending on the crystallization time, reaction of $Mn(NO_3)_2\cdot 4H_2O$ with bix afforded three products (Figure 121). The kinetic product, $[Mn_2(bix)_3(NO_3)_4]\cdot 2CHCl_3$ is obtained in one or two days. Two distinct motifs, i.e., 1D ladder polymers and 2D brickwall layers as supramolecular isomers are present in the same compound; the ladders cross the brickwall layers in an inclined fashion at an angle of 30°. Each ring is interpenetrated by three ladders and each ring in the ladders is catenated by two brickwall layers. Such 1D + 2D catenation leads to 3D polycatenated architecture. More interestingly, when the same solution is left for longer times, the crystals dissolved and recrystallized to form just a molecular ladder $[Mn(bix)_{1.5}(NO_3)_2]$ with no guest molecules. It has been suggested that chloroform is important to template the product formation. Further prolonged of crystallization time resulted in a thermodynamic product, $[Mn(bix)_2(NO_3)_2]$, with interpenetrated 3D network.[362]

Reaction of [Na(dca)], $Cd(NO_3)_2\cdot 6H_2O$ and bpp in MeOH/H_2O yielded two types of crystals of different shapes but identical stoichiometry, $[Cd(dca)_2(bpp)]$. When the crystals were allowed to remain in the solution, the kinetic product, column-shaped crystals disappeared and transformed into the thermodynamic product as block crystals. If mixture of both compounds were recrystallized from MeOH, only the block crystals were obtained. The kinetic product shows a sinusoidal ribbon-like polymeric structure in which two bpp ligands with gauche, gauche conformations coordinated to Cd(II) in trans positions (Figure 122a). The adjacent chains are aligned in parallel and interdigitated with the $(CH_2)_3$ groups overlapping to generate a 2D sheet. As for the thermodynamic product, the bpp ligands with transoid, transoid conformations coordinated to Cd(II) centers in cis positions and thus lead to zigzag CP chain of $Cd(dca)_2$ (Figure 122b). The arc-shaped bpp ligands linked the parallel adjacent zigzag chains to furnish an undulating 2D layer with a (4,4) network.[363]

Reaction of $Ag(CF_3SO_3)$ and 1,1′-bis(diphenylphosphino)-ferrocene (dppf) in $CHCl_3$ afforded $[Ag_4(CF_3SO_3)_4(dppf)_2]$ in three supramolecular isomers depending on the reaction

time. Short reaction time of 1.5 h gave rise to a mixture of 2D polymer comprising a tetra-silver basic unit and a linear polymer based on a di-silver building block. Longer reaction time of 15 h resulted in the formation of a discrete tetra-silver framework and a linear polymer. The linear polymer consists of eight-membered $[Ag_2S_2O_4]$ macrocyclic ring connected by bridging dppf. This coordination polymer is further strengthened by an unusually short (and presumably significant) nonbonding Ag···C interactions (2.489 Å) between the phenyl ring and Ag(I).[364] The analogous complex $[Ag(CF_3CO_2)(dppf)]$ also displays 1D CP structure through dppf bridging.[365]

Reaction of $Cu(ClO_4)_2$ with $KAu(CN)_2$ in DMSO produced two polymorphs, $Cu[Au(CN)_2]_2(DMSO)_2$, depending on the total concentration of starting reagents. In dilute solution, green crystals of 1D CP is formed slowly, whereas blue crystals of 2D corrugated CP is obtained rapidly in a highly concentrated solution. The color difference between the two polymorphs can be attributed to the different coordination number and geometry around the Cu(II) centers. In the 1D CP, the five-coordinate Cu(II) centers are bridged by two $[Au(CN)_2]^-$ units to form a zigzag chain with another dangling $[Au(CN)_2]^-$ unit. The chains are stacked with offset to allow interdigitation of the dangling $[Au(CN)_2]^-$ units. Interestingly, each chain is connected to the four neighboring chains through Au···Au interactions of 3.22 Å between the dangling group and the chain backbone. Whereas the 2D layers comprising the distorted octahedral Cu(II) with two DMSO molecules and four bridging $[Au(CN)_2]^-$ units are stacked and held together by weak Au···Au interactions of 3.42 Å. Interestingly, despite significantly different solid-state structures, both isomers show identical vapochromic properties when exposed to a variety of other donor solvent vapors including H_2O, MeCN, dioxane, DMF, pyridine, NH_3. The vapochromism can be readily observed both by visible color changes and large IR changes for CN bands. The solvent molecules adsorbed by $Cu[Au(CN)_2]_2$ bind to the Cu(II) centers, thereby altering the visible spectrum associated with the Cu(II) chromophores and the number and frequency of the CN as well.[366] Other supramolecular isomers are also reported in the literature.[231d,367]

6. Structural Transformations Involving 1D CP

Structural transformation of one structure to another is particularly interesting because it is fundamentally important to understand the solid state reactivity. Such structural modifications can render significant chemical rearrangement involving breaking and forming covalent bonds in 1D CPs and change the chemical and physical properties of the compounds. Topochemical reactions of the compounds facilitate the structural transformation with minimal movement of atoms. Single-crystal to single-crystal (SCSC) transformation without loss of single crystallinity makes possible to monitor the structural change by X-ray crystallography. Various factors have been found to influence the structural transformation, including thermal, solvent, and UV irradiation. An extensive account on structural transformation involving supramolecular structures in the solid state was reviewed in 2007.[368] Here, we focused on structural transformation involving 1D CPs both in solid and solution.

6.1. Structural Transformations in Solid State

Recently a number of interesting structural rearrangements involving 1D CPs in the solid state has been discovered.[368] Of these many of them can be predicted based on the packing and supramolecular interactions present in the polymeric architectures and several unexpected structural changes were encountered serendipitously. A few interesting structural transformations are discussed in detail in this section.

6.1.1. Transformation Induced by Heat and Desolvation

Here is an example of a structural conversion from a hydrogen-bonded helical CP to 3D CP with chiral channels. A single-stranded helical CP $[Cu_2(sala)_2(H_2O)]$ (H_2sala = *N*-(2-hydroxybenzyl)-alanine) is obtained through bridging of dimeric $Cu_2(sala)_2$ unit by carboxylate group to the axial position of one of the Cu(II) centers whereas an aqua ligand occupies the axial position of the second Cu(II) center. This carboxylate bridging generates helical conformation of the 1D coordination polymer. Further all the strands are aligned parallel and are sustained by O−H···O and N−H···O hydrogen bonding. A closer examination of coordination sites of Cu(II) centers discloses that it is possible when the aqua ligand at one of the Cu(II) center is removed, the carboxylate group can be coordinated to the metal center because of the short Cu···O distance (3.70 Å). This geometric proximity of the carboxylate groups and Cu(II) center appears to be favorable for topochemical reaction. Indeed, when the aqua ligand is removed by thermal dehydration (115 °C for 2 h), an anhydrous $[Cu_2(sala)_2]$ compound is obtained and the process is irreversible (Figure 123). The X-ray crystallography of the anhydrous product revealed that it has porous honeycomb-like 3D network structure similar to the Zn(II) analogue.[369] This solid-state structural transformation is the first example of the use of a helical CP as the building block for a 3D coordination framework with chiral channels.[370]

Compound $[Ag_4(tmp)_3\{O_2C(CF_2)_3CF_3\}_4(EtOH)_2]$ (tmp = tetramethylpyrazine) displays a zigzag chain conformation with pairs of tmp ligands link the $[Ag_2\{O_2C(CF_2)_3CF_3\}_2(EtOH)]$ units, which are further connected by another tmp as shown in Figure 124. It is worth noting that an EtOH molecule is coordinated to one of the Ag(I) centers and hydrogen-bonded to one of the cabroxylate groups. Interestingly, upon thermal desolvation (47 °C for 48 h), the structure is transformed into $[Ag_4(tmp)_3\{O_2C(CF_2)_3CF_3\}_4]$ in SCSC manner. The overall 1D tape structure is maintained, but the dimeric unit has changed to simple silver carboxylate dimer $[Ag_2\{O_2C(CF_2)_3CF_3\}_2]$ accompanied by the change in coordination geometry of Ag(I) from tetrahedral to trigonal planar. In this context, the structural transformation is possible owing to the flexibility of Ag coordination. The relatively weak Ag−O bonds allow facile insertion and elimination of ethanol molecules through the fluoroalkyl chain.[371]

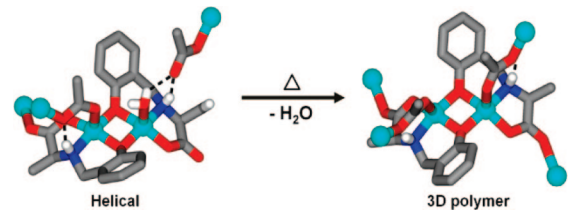

Figure 123. Schematic diagram of structural transformation upon thermal dehydration.

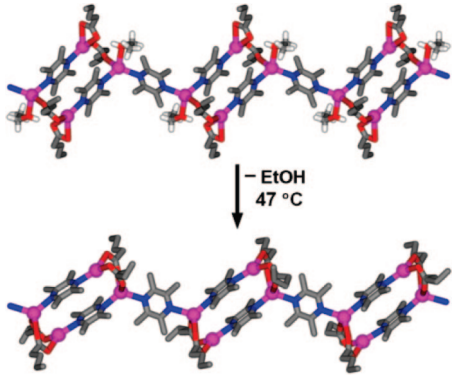

Figure 124. Thermal-induced SCSC reaction involving loss of coordinated ethanol molecule. Fluorine atoms are omitted for clarity.

A 1D ribbon polymer of cobalt citrate cubanes, $\{Cs_2[Co_7(citr)_4(H_2O)_{13.5}]\}$, has been shown to undergo structural transformation to 2D polymer $[Co(H_2O)_6]\{Cs_2[Co_{6.5}(citr)_4(H_2O)_9]\}_2 \cdot 3H_2O$ upon increasing the temperature from 5 to 30 °C in dry nitrogen atmosphere (Figure 125). In the former compound, the basic unit of the polymer has two segments, singly and doubly bridged pair of cubanes. Surprisingly, upon sitting for a day at 30 °C, the crystal undergoes structural transformation into a 2D polymeric net of cobalt cubanes. The Co atoms of two neighboring chains broke the Co−H_2O bonds and formed new bonds with carboxylate oxygen from citrate with the adjacent chains to furnish a 2D network structure.[372]

A 1D meso-helical CP, $EuAg(pda)_2(H_2O)_3 \cdot 3H_2O$ (H_2pda = pyridine-2,6-dicarboxylic acid) can be transformed into racemic helix upon thermal dehydration. The meso-helical structure consists of two adjacent three-stranded single-helical *P* and *M* chains connected through Ag−O bonds (left Figure 126). Interestingly, heating the single crystals to 120 °C resulted in the cleavage of interchain Ag−O coordination bonds that simultaneously induce the conversion of the helical arrangement in SCSC manner. The single crystals heated at 70 °C for 5 h have the same monoclinic space group $P2_1/n$ with the original crystals and the cell volume decreased 170 $Å^3$ attributed to the loss of two uncoordinated water molecules. Because of the increased molecular movement as a result of heating of the crystal, the Ag−O bond distance between two adjacent *P* and *M* chains increased from 2.635 to 2.832 Å, accompanied by a reduction of the O−Ag−O bond angles from 100° to 96° (middle Figure 126). Further heating of the crystals at 120 °C for 2 h afforded single crystals with monoclinic space group *C*2/*c* and racemic helical structure (right Figure 126). The crystal volume was reduced by 11% compared to the initial crystals and the remaining uncoordinated water molecule was removed. Owing to the vibrations induced by heating, the

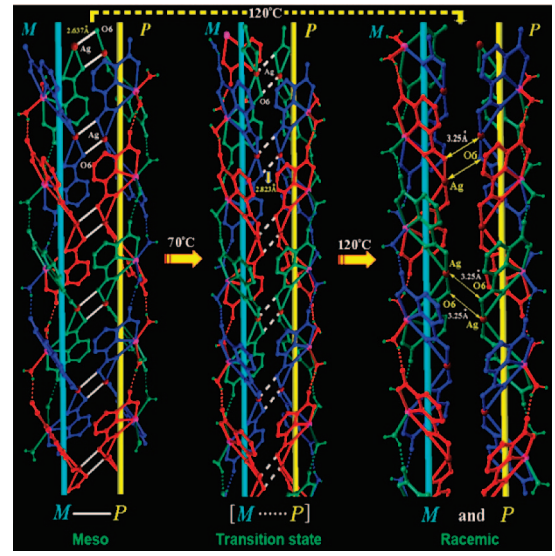

Figure 126. Temperature-driven conversion of meso into racemic helix. Reproduced with permission from ref 373. Copyright 2009 American Chemical Society.

two adjacent helical chains are further separated with Ag−O distance of 3.251 Å and therefore resulted in the formation of racemic helical chains. Moreover, the helices may be considered as selective luminescent probes for Mg(II) since the luminescence intensities increased significantly when Mg(II) was added. The Mg(II) ions may be coordinated with the carboxylic groups and coordinated water molecules located on Eu(III).[373]

Structural transformation also has been observed in aluminophosphate. Compound $[C_5H_9NH_3]_5[Al_3P_5O_{20}H]$ with 1D chain structure is converted into a 2D CP of $[C_5H_9NH_3]_2 \cdot [Al_2P_3O_{12}H]$ upon heating at 200 °C. The transformation is evidenced by X-ray crystallography and XPRD.[374] In another example, complex $[ZnCl_2(4,4'\text{-bpy})]$ exhibits zigzag polymeric structure with 4,4′-bpy bridging. The chloride ligands are toward the adjacent polymeric chains. However, when the temperature is cooled down to below −143 °C, the single crystal is transformed into 2D CP $[ZnCl_2(4,4'\text{-bpy})]$ by chloro ligand bridging (Figure 127). The reaction is reversible in which the 2D CP converts back to 1D chain at temperatures above 87 °C.[375] In another case, prolonged heating of the 1D CP $[Ce(btz)_3(Hbtz)]$ (Hbtz = 1H-benzotriazole) in a sealed system has resulted in the removal of btz ligand and transformed into 3D CP $[Ce(btz)_3)]$.[376]

The removal of benzene guest molecules that is involved in weak π interactions with the ligand in the 1D CP of $[Rh_2(CF_3COO)_4(dcb)_2] \cdot 0.5CH_2Cl_2 \cdot 1.75C_6H_6$ (dcb = 1,3-dicyanobenzene) has triggered the collective irreversible reorientation of the polymeric chains and resulted in a new

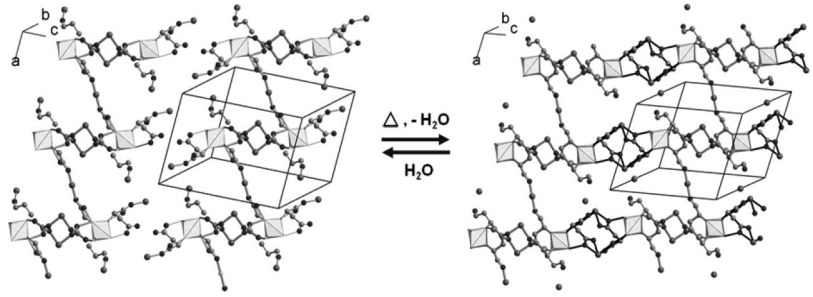

Figure 125. Transformation from 1D to 2D cobalt cubanes.

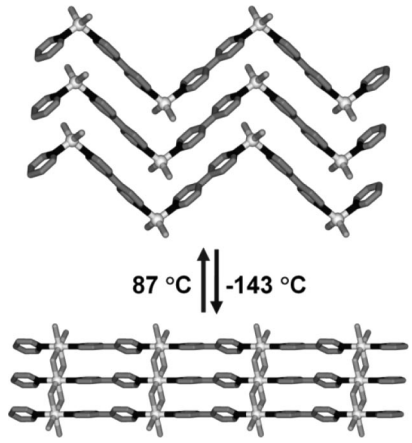

Figure 127. Temperature-dependent transformation from 1D zigzag chains into 2D network.

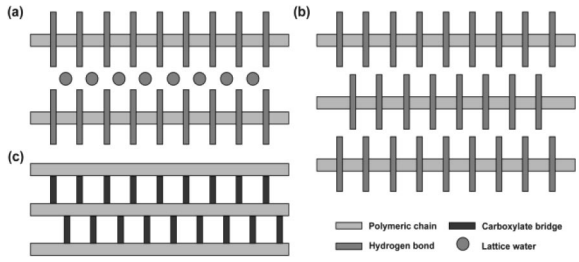

Figure 128. Schematic representations of the conversion of 1D CPs (a and b) to 2D CP (c) by thermal dehydration for Cu(II).

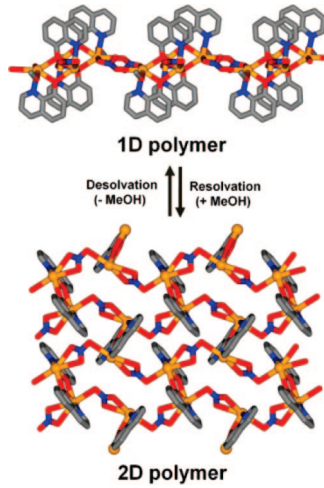

Figure 129. Structural transformation from 1D to 2D CP by thermal desolvation.

CP, $[Rh_2(CF_3COO)_4(dcb)_2]$.[377] A combination of ab initio X-ray powder diffraction methods with in situ thermodiffractometry and thermal analyses has been utilized to track reversible transformation of the $[M(pmdc)(H_2O)_2]\cdot H_2O$ compounds (M = Fe, Co, Ni, Cu; H_2pmdc = pyrimidine-4,6-dicarboxylic acid) into the $[M(pmdc)(H_2O)_2]$ followed by an irreversible transformation into anhydrous 2D CP as shown in Figure 128.[378]

A brown 1D CP of $[Pb_2(8\text{-quin})_2(NO_3)_2(MeOH)]$ (8-quin = 8-hydroxyquinoline) is transformed into a yellow 2D CP, $[Pb(8\text{-quin})(NO_3)]$ by heating at 165−170 °C (Figure 129). The 1D CP is comprised of tetrameric building block of $[Pb_4(8\text{-quin})_4(MeOH)_2]$ bridged through nitrate anions. The close nonbonding contacts (3.37 Å) between the O atom of unbridging nitrate and its neighboring Pb(II) atoms has been utilized to facilitate the structural transformation. Upon

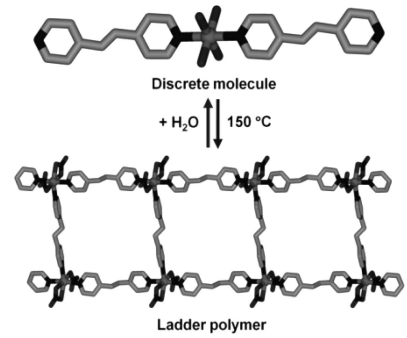

Figure 130. Temperature- and moisture-dependent interconversion between discrete and ladder structures.

removal of methanol molecule by heating, the dimeric units of $[Pb_2(8\text{-quin})_2]$ units are doubly bridged by nitrate anions to form a 2D infinite network. The new bond formation between Pb and nitrate take place along with removal of methanol; hence, the coordination number of the Pb atoms remains unchanged. The reaction is reversible by resolvation of the 2D polymer with methanol.[379]

The structural transformation between ladder CP $[Co(NO_3)_2(bpe)_{1.5}\cdot 3CHCl_3]$ and discrete mononuclear complex $[Co(H_2O)_4(bpe)_2](NO_3)_2\cdot 8/3H_2O\cdot 2/3$bpe is found to be depended on solvent and temperature (Figure 130). It is postulated that the aqua ligands in the mononuclear complex are evaporated at high temperature and then immediately replaced by nitrate groups to form ladder structure. The ladder structure also can slowly convert back to the mononuclear complex on standing at sufficient moisture condition.[121] A CP $[Ni(NO_3)_2(pym)(MeCN)_2]$ (pym = pyrimidine) is readily converted into a more stable zigzag CP, $[Ni(NO_3)_2(pym)(H_2O)_2]$ in atmospheric moisture by replacing the MeCN with water molecules. It has been shown that the presence of water allows hydrogen bonding interactions between adjacent chains and strengthens the CP.[380]

6.1.2. Transformation Induced by Photodimerization

In the solid-state organic chemistry, [2 + 2] cycloaddition reactions are of immense interest and important. Since the seminal work of Schmidt, a plethora of these photodimerization reactions have been studied. Supramolecular interactions including hydrogen bonds have been successfully employed to orient the C═C bonds in functional ligand congenial for cycloaddition reactions to synthesize stereo- and regiospecific cyclobutane derivatives, ladderanes, in one step without the use of organic solvents. Of these 1,2-bis(4-pyridyl)ethylene (bpe) is the most studied compound because of its ease of controlling the disposition of double bonds through the use of pyridyl functional groups. Of the 1D CPs, ladder structures are the most suitable to bring the photoreactive double bonds in the bpe ligands closer. The double bonds of the bpe ligands in two 1D CPs [M(bpe)] can be aligned by suitable bridging ligands, such as carboxylate, nitrate, and halides. Metallophilic interactions have also been exploited for this purpose. This section deals with such photoreactive CPs.[381]

6.1.2.1. 0D → 1D. MacGillivray et al. have reported the 100% [2 + 2] photodimerization of $[Ag_2(4\text{-stilbz})_4]\text{-}[CF_3CO_2]_2$ accompanied by SCSC transformation to 1D coordinating polymer sustained by Ag···π interactions (Figure 131). The discrete Ag(I) complex displays a dinuclear structure sustained by Ag···Ag interactions of 3.41 Å and the C═C bonds are separated by 3.82 Å in criss-cross

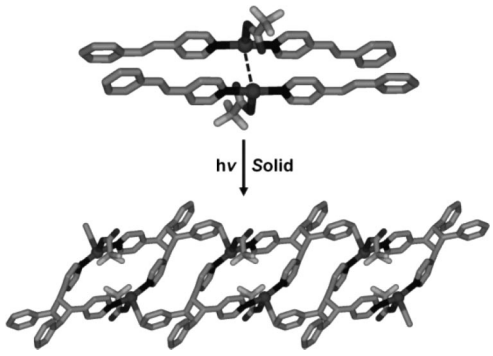

Figure 131. SCSC transformation of 0D to 1D CP upon photodimerization.

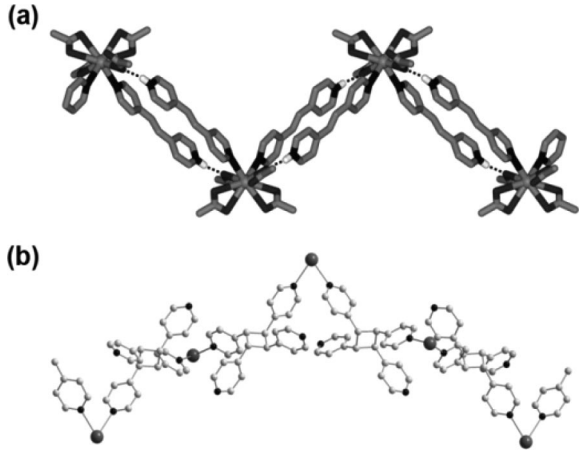

Figure 132. (a) Portion of the zigzag hydrogen-bonded polymer. (b) Portion of the 1D coordination polymeric structure of cyclobutane CP.

manner. UV irradiation for 18 h leads to the reorientation and successful photodimerization of olefins accompanied by breaking of Ag···Ag interactions and formation of Ag···C(phenyl) interactions to yield a linear CP structure.[166]

6.1.2.2. 1D → 1D. The 1D hydrogen-bonded zwitterionic Pb(II) complex, $[Pb(bpe\text{-}H)_2(CF_3CO_2)_4]$ as shown in Figure 132a with favorable alignment of adjacent C═C bonds with a distance of 3.63 Å undergoes photodimerization upon UV irradiation. During photodimerization, two CF_3CO_2H are eliminated because of the proton transfer from bpe-H^+ to CF_3COO^- ligand bonded to the Pb(II), resulting in [Pb(*rctt*-tpcb)$(CF_3CO_2)_2$] (tpcb = tetrakis(4-pyridyl)cyclobutane). Crystallization of dimerized product from MeOH yielded a highly corrugated 1D CP with cyclobutane bridging in *rctt* steoreochemistry (Figure 132b).[382] However, the pyridyl rings in the 1,2-positions of the cyclobutane ring are involved in the connectivity rather than the expected 1,3-positions based on the structure of the polymer. Since the structure, composition, connectivity, etc., of the coordination polymers are greatly influenced by the recrystallization conditions, it is not surprising that the connectivity in the resulted polymer is different from that of the irradiated product.

6.1.2.3. 1D → 1D Ladders. A linear CP of $[Ag(bpe)(H_2O)](CF_3CO_2)\cdot CH_3CN$ is found as hydrogen-bonded 2D brick-wall-like network with single Ag(I) polymeric strands. There are no Ag···Ag interactions, and further, the trifluoroacetate is not bridging the 1D strands. Therefore olefins are separated by 5.17 Å, and the geometry is not suitable for reaction based on the Schmidt's criteria. Nonetheless, irradiation of the desolvated compound gave rise to complete photodimerized

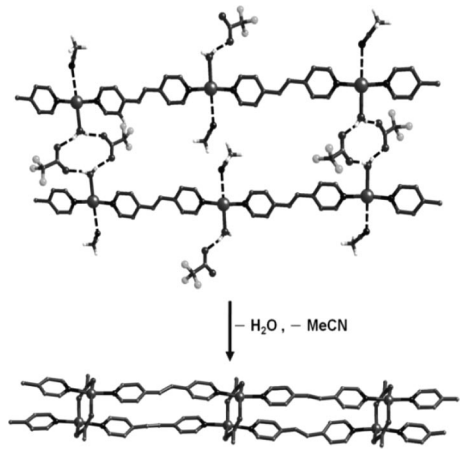

Figure 133. Anisotropic movements of linear polymeric chains to ladderlike structure resulting from solvent removal.

product as monitored by ^1H NMR. Photodimerization observed in a related compound $[\{(CF_3CO_2)Ag\}_2(bpe)_2]\cdot H_2O$, which displays ladder structure with well-aligned bpe ligand and Ag···Ag interactions (3.15 Å) as determined by X-ray crystallography further supports the formation of ladder structure by the free movements of the CP in the desolvation process. In other words, the anisotropic movements of polymeric chains, resulting from solvent removal, allow the transformation of a linear 1D structure to a ladderlike structure and, more importantly, reorient the C═C bonds for photodimerization (Figure 133).[158]

In $[Cd(bpe)(CH_3CO_2)_2(H_2O)]$, the linear 1D CP strands are aligned in parallel to form a hydrogen-bonded 2D network. The closest contact between the C═C bond is 4.33 Å, and further, these double bonds are aligned in antiparallel fashion suggesting unfavorable condition for [2 + 2] cycloaddition reaction. On the other hand, this CP can lose the aqua ligand unusually at the lower temperature range 67−106 °C. The oxygen atom of the acetate ligand is hydrogen-bonded to the aqua ligand of the adjacent neighbors such that the nonbonding Cd···O distance is 4.44 Å. The loss of aqua ligand leads to the formation of new bonds between oxygen atom of the acetato ligand and Cd(II) and results in a ladder structure, but the single crystallinity is not maintained during this process. However, 100% photodimerization of this dehydrated product as monitored by ^1H NMR spectroscopy confirms the ladder structure.[383]

6.1.2.4. 1D Ladder → 1D Ladder. Complexes $[\{(CH_3CO_2)(\mu\text{-}O_2CCH_3)Zn\}_2(bpe)_2]$ and $[\{(CF_3CO_2)(\mu\text{-}O_2CCH_3)Zn\}_2(bpe)_2]$ exhibit ladderlike structures with two bridging acetates as rungs. Perfect alignment of the bpe ligands and close proximity of pairs of C═C bonds (3.63 Å) in both compounds allow complete photodimerization and hence structural transformation. Nonetheless, the former compound loses its single crystallinity upon UV irradiation and hence precludes SCSC transformation. When 50% of the acetate ions were replaced by trifluoroacetate, the latter compound undergoes topochemical photodimerization in a SCSC manner (Figure 134). It is postulated that fluorine atoms in the anion is responsible for the crystal to withstand the strain generated during photodimerization.[384] The 1D ladderlike CP containing dinuclear Zn(II) units, $[Zn_2(bpefmp)(OH)(bpe)_2](ClO_4)_2\cdot 4H_2O$ (bpefmp = 2,6-bis[*N*-(2-pyridylethyl) formimidoyl]-4-methylphenol), has also been shown to undergo complete [2 + 2] cycloaddition upon UV irradiation. Though

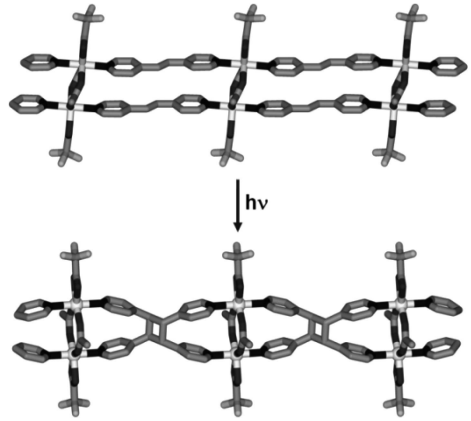

Figure 134. SCSC photoreactivity in ladder CPs.

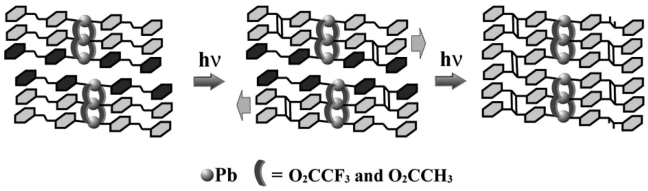

Figure 135. Schematic diagram showing the structural transformation of triple-stranded CP to 2D CP under UV light.

the single crystallinity is lost during transformation, ^{1}H NMR of the final product confirms the photodimerization process.[159]

6.1.2.5. Other Transformations. An unusual photochemical reactivity of a three-stranded CP $[Pb_3(bpe)_3(O_2CCF_3)_4(O_2CCH_3)_2]$ is reported, wherein the C═C bonds in bpe ligands are perfectly aligned one below another satisfying Schmidt's photochemical criteria for [2 + 2] cycloaddition reaction. However, only a pair of bpe ligands is expected to react to form *rctt*-tetrakis(4-pyridyl)cyclobutane (*rctt*-tpcb) but yielded 100% *rctt*-tpcb on exposure to UV light as monitored by ^{1}H NMR spectroscopy, instead of the expected 67% dimerized product. This photodimerization has been observed to occur in two steps as shown in Figure 135. The Schmidt's topochemical postulate has been used as a guide to rationalize the observed photoreactive behavior. The photodimerization in the first step is proposed to occur between the bpe pairs of the triple-stranded CP and accompanied by movements of the adjacent strands cooperatively to establish $\pi-\pi$ interactions between the unreacted bpe pairs. Although anisotropic movements of CPs have been observed before,[158,383] such movements of 1D coordination polymers induced during the photochemical reaction appear to be unique and highlight a new paradigm of the cooperativity among the polymeric strands during photochemical reactions.[385]

6.2. Structural Transformation in Solution during Synthesis

Several structural transformation reactions have already been covered indirectly in the sections 4 and 5 on the influence of various factors on the CP architectures and supermolecular isomerism, respectively. In many occasions, this arises from the lability of the M−L bonds, which leads to dissociation of the CPs into oligomeric species and solvation of the metal ions leads to the isolation of more kinetically favored products during synthesis. In other words, the conversion and eventual isolation of different products

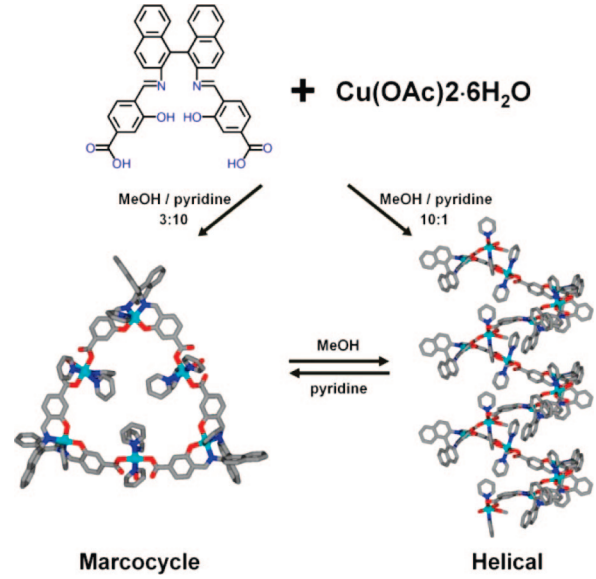

Figure 136. Solvent-induced interconversion between triangular macrocycle and helical CP.

are controlled by the experimental conditions used.[386] This section further supplements sections 4 and 5 with few more examples.

6.2.1. Transformation Induced by Solvent

Mirkin et al. have reported a spontaneous and reversible solvent-induced transformation between a triangular macrocycle and a helical CP. Reaction of (*S*)-4,4′-1,1′-binaphthalene-2,2′-diylbis-nitrilomethylidyne-bis-3-hydroxybenzoic acid (L is shown in the Figure 136) and $Cu(CH_3COO)_2$ in a mixture of pyridine and methanol at room temperature has resulted two types of structures, depending upon the solvent ratio. A 3:10 mixture of methanol and pyridine gave a triangular macrocyle complex with 3-fold rotational symmetry of $Cu_2L\cdot 6py$ as dark green cubic crystals with Cu···Cu distance of 16.7 Å. Interestingly, a 10:1 methanol and pyridine mixture has afforded rod-shaped crystals, $[Cu_2L(py)_2(MeOH)]\cdot 4MeOH\cdot 1.5H_2O$ as helical CP. It is noted that the chirality of the ligand precursors dictates the helicity of the resulting polymer. Closer examinations on both structures reveal that such transformation is feasible through the sequential breaking and reforming of the Cu−O carboxylate bond. As shown by PXRD, the transformation between two compounds can be achieved by soaking the compound in pyridine or methanol.[387] This work demonstrates how the solvent can direct the self-assembly of the molecules.

Structural transformation also has been observed by the controlled replacement of the solvent bonded to the cation. The complex $[Y(DMF)_8][Cu_4(\mu_3\text{-}I)_2(\mu\text{-}I)_3I_2]$ can be converted into 1D zigzag and 2D sheet polymers by progressive substitution of the DMF ligands by water molecules in a confined environment. Partial substitution of the DMF ligands of the $[Y(DMF)_8]^{3+}$ cation in the precursor by water in paratone after one week afforded 1D polymer $[Y(DMF)_6(H_2O)_2]$-$[Cu_7(\mu_4\text{-}I)_3(\mu_3\text{-}I)_2(\mu\text{-}I)_4(I)]$. The coordination number and geometry due to the solvents bonded to the cation influence the structure of the counterion. The initial discrete tetranuclear cluster $[Cu_4(\mu_3\text{-}I)_2(\mu\text{-}I)_3I_2]$ is transformed into a zigzag chain made up of heptanuclear $[Cu_7(\mu_4\text{-}I)_3(\mu_3\text{-}I)_2(\mu\text{-}I)_4(I)]$ units linked through bridging iodides. Further introduction of water into the cation led to formation of

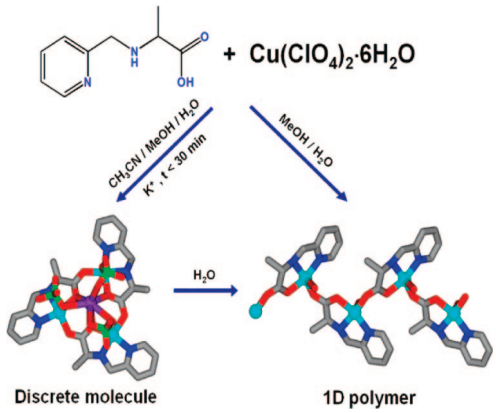

Figure 137. Solvent-dependent conversion from metallocrown into 1D CP.

$[Y(DMF)_6(H_2O)_3][Cu^I_7Cu^{II}_2(\mu_3\text{-}I)_8(\mu\text{-}I)_6]$ with mixed-valence copper iodide building blocks. Three $[Cu_9I_{14}]^{3-}$ building block units form a ring structure, which encapsulates the templating yttrium cation. There are six neighboring rings around each ring, and thus, a 2D sheetlike structure is obtained.[388]

Reaction of $Cu(ClO_4)_2$ with Hpala in the presence of KOH in methanol/acetonitrile has resulted in a potassium ion incorporated tricopper metallamacrocyclic compound, $[K(ClO_4)_3Cu_3(pala)_3](ClO_4)$. The cation comprised of a trimer formed by cyclization of Cu(pala) moiety through bridging of carboxylate group in the pala. Interestingly, in the absence of KOH, a 1D CP compound, $[Cu(pala)(H_2O)]\cdot ClO_4$, was obtained. It is worthwhile to mention that the former complex can be easily converted to the latter by prolong stirring the reactants in methanol/acetonitrile/water solution mixture. It has been shown that the formation of 1D CP is solely depending on the presence of water while the potassium ion has no influence. Figure 137 displays the schematic flowchart conversion of metallocrown into 1D CP.[389] Complex $[Cu(H_2O)_4Cu(azpy)_2(OTs)_2\ (H_2O)_2](OTs)_2\cdot 2H_2O\cdot 2EtOH$ (azpy = *trans*-4,4′-azobispyridine) exhibits a complete structure-restoration effect with a mechanism involving layering of molecular "bricks" of water and solvent molecules.[390]

CPs in solution are likely to exist as oligomers because of dissociation or solvation of the metal ions, where metal ions and the bridging spacer ligands are labile. An exchange between cyclic and open chain oligomers in solution is possible depending on the flexibility and preferred conformation of the bridging ligands, and this may result in high molecular weight CPs on crystallization. Macrocyclic complexes and 1D CPs have been isolated previously, but the isolation of the ring-opened oligomer is unprecedented and can be considered as a missing link in the ring-opening polymerization process. In the self-assembly of CPs containing Au(I), Puddephatt et al. provided evidence for the dynamic exchange between oligomers in solution was provided by the isolation of an intermediate decagold(I) oligomer.[391] They further show that the conversion of silver(I)-diphosphine complexes having ring and sheet structures to 1D polymeric chain has been proceeded by ring-opening polymerization of cyclic precursors.[392]

6.2.2. Transformation Induced by Temperature and Resolvation

Reaction of $CoCl_2$ and 1,3-bis(pyrid-4-ylthio)-propan-2-one (bptp) in a molar ratio of 1:2 in methanol/acetone gave

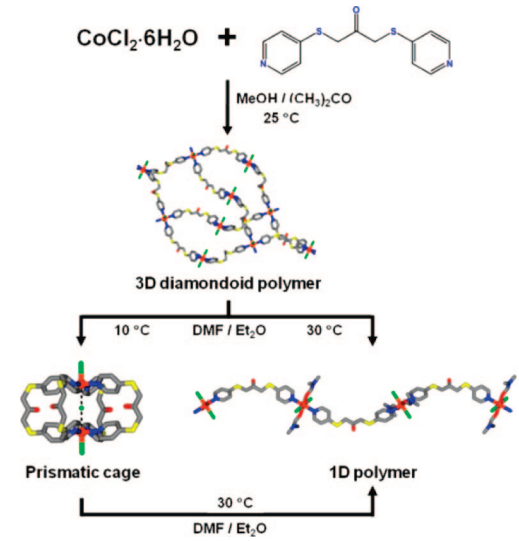

Figure 138. Structural transformation in response to changes in the solvent systems and temperatures.

rise to a 6-fold-interpenetrating diamondoid 3D polymer, $[Co(bptp)_2Cl_2]\cdot Me_2CO$ as orange crystals. Recrystallization of the compound in DMF/diethyl ether exhibits an interesting solvent-assisted temperature-dependent dynamic formation of 1D polymer and discrete cages (Figure 138). At 30 °C, the slow diffusion of diethyl ether into the blue DMF solution of freshly prepared compound for 2 weeks furnished red prismatic crystals of a 1D polymer, $[Co(bptp)Cl_2(DMF)_2]$. However, at a lower temperature of 10 °C, the diffusion process first created green jelly, which then changed into purple prismatic crystals of a dimeric cage, $[Co_2(bptp)_4Cl_2]\text{-}Cl_2\cdot Et_2O\cdot DMF\cdot 2MeOH\cdot 4H_2O$ in 3 weeks. At 30 °C, the slow diffusion of diethyl ether into a blue DMF solution of dimer produced the 1D polymer in 2 weeks. The transformation of 3D polymer into 1D polymer is accompanied with a change of ligand conformation, which is easily carried out in solution because of the lower steric energies of about 5−22 kJ/mol according to theoretical calculations. The authors rationalize the result that the fast assembly of reactants tend to produce the 3D diamondoid framework, while the stronger polar solvent DMF not only decomposes 3D network but also takes part in coordination with metal centers, thereby limiting structural extension and finally resulting in the 1D chain polymer.[393]

Braga, Grepioni, and co-workers demonstrated an alternative method for preparation of coordination polymers, by manual grinding of solid reactants, while single crystals that are suitable for X-ray diffraction are obtained by conventional crystallization from solution assisted by seeding. For instance, 1D CPs of $[Ag(dabco)_2(CH_3COO)]\cdot 5H_2O$ and $[Zn(dabco)Cl_2]$ (dabco = 1,4-diazabicyclooctane) obtained from cogrinding in the solid state.[394] Furthermore, they have found that $[CuCl_2(dace)]\cdot DMSO$ (dace = *trans*-1,4-diaminocyclohexane), a 1D CP that can undergo the mechanochemical transformation and readily absorb and release small molecules. The parallel 1D coordination chains form layers, which host, in intercalation fashion, the cocrystallized DMSO molecules. Interestingly, thermal and mechanochemical treatment on this material leading to the first example of a 1D coordination network with reversible intercalation property.[395]

A violet and binuclear complex of $[Cu(chxn)_2][Ni(CN)_4]\cdot 2H_2O$ (chxn = *trans*-cyclohexane-(1*R*,2*R*)-diamine) has been found to convert into a purple, 1D CP {$[Cu(chxn)_2]$-

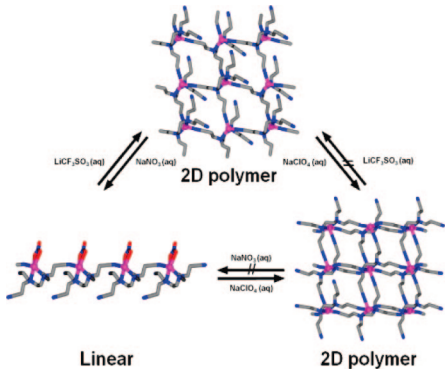

Figure 139. Schematic diagram showing the interconversion parthway induced by anion exchange.

$[Ni(CN)_4]\}$ upon thermal dehydration. The structure of 1D is evidenced from high-resolution powder X-ray diffraction patterns. The immersion the 1D CP in water allows the rehydration, and the color of the compounds also changes accordingly.[396]

6.2.3. Transformation Induced by Anion Exchange

Self-assembly of AgX (X = NO_3, CF_3SO_3, and ClO_4) with ethylenediamine tetrapropionitrile (edtpn) afforded 1D linear CP, 2D layer, and boxlike 2D network, respectively, depending on the counteranion. Interestingly, these CPs undergo structural transformation in crystalline state with anion exchange. Figure 139 summarizes the interconversion pathway and proposed mechanism for the structural transformation. When the NO_3^- anion in linear CP is exchanged with $CF_3SO_3^-$, the linear chains are linked together by using one of the three free cyano groups of an edtpn of the neighboring chain, which gives rise to a 2D layer. Such bridging is dissociated when the $CF_3SO_3^-$ is exchanged with NO_3^-. Furthermore, when the $CF_3SO_3^-$ is exchanged with ClO_4^-, two free cyano groups of an edtpn bind two neighboring Ag(I) ions, one in its own chain and the other in the adjacent chain, which leads to the boxlike 2D structure. When the NO_3^- is exchanged with the ClO_4^-, three free cyano groups bind three Ag(I) ions, one Ag(I) ion in its own chain and two Ag(I) ions in two different neighboring chains, which also gives rise to the boxlike 2D structure. It is postulated that the structural transformations are possible in the crystalline state, just by the coordination or uncoordination of polynitrile arms of the ligand without significant changes of the location of Ag(I) ions and edtpn ligands.[397]

Jung and co-workers have demonstrated the first example of fine-tuning the pitch of the self-assembled helical spring through the reversible incorporation of guest anions. Reactions of 3,3′-oxybispyridine (Py_2O) with AgX (X = NO_3, BF_4, ClO_4, and PF_6) have resulted a series of helical CPs through the skewed conformation of ligands and potential linear geometry of the N−Ag−N bond. The helices have similar skeletal structures and counteranions are pinched in two columns inside the helix. Interestingly, the helices reversibly stretch via counteranion exchange without destruction of the helical skeleton.[398] The Ag(I) complexes of the related ligand, 3,3′-thiobispyridine (Py_2S) also show structural transformation induced by anion exchange. Complexes $[Ag(Py_2S)]X$ (X = BF_4, ClO_4 and PF_6) exhibit single stranded helical structures with counteranions residing in two columns between/inside the helical pitch,, while the corresponding NO_3^- complex exhibit a 2D polymer. The BF_4^- anions within the helix are completely exchanged with PF_6^- anions, while exchange of ClO_4^- with BF_4^-, NO_3^-, or PF_6^- occurs scarcely or slightly. Fascinatingly, the 2D polymer with NO_3^- anions are easily converted into the helices via the anion exchange with PF_6^-, but the reverse anion exchange proceeds slightly (Figure 140). This indicates that the weakly bonded NO_3^- is labile enough to be exchanged with PF_6^- in aqueous suspension. The overall anion exchangeability seems to be governed by the nature of the anions rather than the skeletal structure.[399]

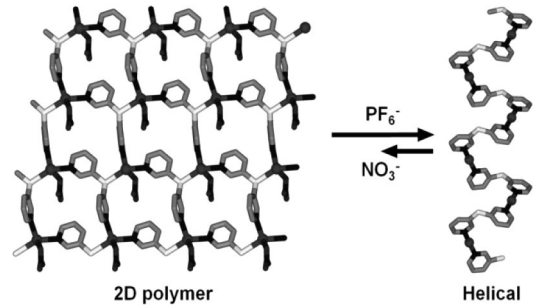

Figure 140. Conversion of 2D polymer into helical polymer.

A ribbon-like CP, $[Cu(bpcab)_2(H_2O)_2]\cdot(ClO_4)_2\cdot 2H_2O]\cdot 4$(guest) (bpcab = *N*,*N*′-bis(3-pyridinecarboxamide)-1,4-butane) features rectangular cavities having dimensions of 10.0 × 13.8 Å with naphthalene guest molecules are sandwiched between four amide moieties of the ligands via $\pi-\pi$ interactions. The adjacent 1D chains are joined together through hydrogen bonding interactions between the ClO_4^- anions, amide, and aqua ligand to furnish channels that can accommodate several aromatic guest molecules such as toluene, xylene, anisole, nitrobenzene, and ethylbenzene. Moreover, exchange of ClO_4^- anions with PF_6^- anions afforded a pseudodiamondoid 3D polymer, which cannot prepare directly from ligand and $Cu(PF_6)_2$. Reaction with $Zn(ClO_4)_2$ give rise to a similar 1D chain that contains a smaller guest molecule, such as acetonitrile in cavities.[400]

Reaction of $LaCl_3$ or $La(NO_3)_3$ with pyridine-2,6-dicarboxylic acid (H_2pdc) resulted in the formation of long bunched nanotubes with hexanuclear metal rings as building blocks. It is worthwhile to mention that the Cl^- anion can be readily replaced by NO_3^- anion with structural framework retained. Furthermore, exchange with BF_4^- broke down the tubular structure and afforded a linear CP, $[La(pdc)(Hpdc)(H_2O)_2]\cdot 4H_2O$. The linear CP also can be obtained from hydrothermal reaction of $La(CH_3COO)_3$ and H_2pdc in 1:2 molar ratio. The breakdown of the tubular structure in the presence of the BF_4^- or CH_3COO^- ion is due to the lack of hydrogen bonding interactions between aqua ligands and these anions, which is crucial for the construction of tubular structure.[401]

6.2.4. Transformation Induced by Other Factors

A 1D polymer of Cu(I) cubanes, $[Cu_4Br_4(ttt)_2]$ (ttt = triallyl-1,3,5-triazine-2,4,6(1H,3H,5H)-trione) has been found to transform into a 2D CP $[Cu_4Br_4(ttt)_2]$ (Figure 141). The 1D polymer is obtained from reaction of CuBr and ttt in methanol by heating with CuBr at 50−60 °C in a sealed tube. The open-cubane Cu_4Br_4 units are linked by two of the three arms of ttt ligands to form a polymeric chain. Reaction of CuBr and ttt in ethanol at 90 °C has resulted in a 2D polymer. Each Cu_6Br_6 clusters are attached to six tridentate ttt ligands, each of which is attached to three prismane clusters to form the 2D polymeric structure. Further, the 1D polymer is converted into 2D polymer by heating

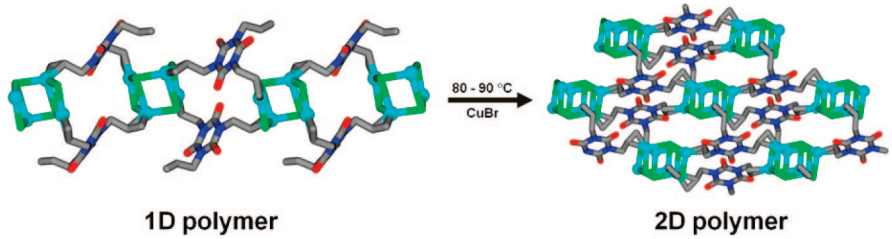

Figure 141. Cluster rearrangement of an open cubane (Cu_4Br_4) in 1D CP to a prismane (Cu_6Br_6) in a 2D CP.

the former compound with CuBr in ethanol. This may be attributed to the lower thermal stability of the open-cubane structure than the prismane structure.[402]

A 2D CP, $[Mn_2(salen)_2(H_2O)_2][(Mn(salen))_2(Nb_6Cl_{12}(CN)_6)]$, transformed into hydrogen-bonded structure and 1D CP when soaked in methanol solution of different guest molecules or ions. When microcrysalline powder of the 2D CP is mixed with a MeOH solution of Et_4N^+, a 3D hydrogen-bonded framework based on heterotrimers $[(Mn(salen)(H_2O)]_2$-$Nb_6Cl_{12}(CN)_6]$ is obtained. Whereas, soaking the microcrystalline powder in a MeOH solution of dpyo afforded a 1D CP, $\{[Mn(salen)(MeOH)]_2(dpyo)\}\{(dpyo)[Mn(salen)_2$-$Nb_6Cl_{12}(CN)_6\}\cdot$dpyo. The complex consists of anionic chains in which dypo ligands bridge the heterotrimer cluster into a sinusoidal wavelike structure. The structural transformations described here are solvent-mediated, and the overall process is expected to involve slow and partial dissociation of 2D CP in methanol solutions containing different guest molecules or ions. In the presence of cations, such as Et_4N^+, the original 2D frameworks cannot be reformed; a heterotrimer is formed, and the solubility equilibrium is shifted until complete depletion of 2D CP. This process is further supported by the formation of 1D CP when the 2D CP is left in contact in methanol solution containing the bridging ligand dpyo.[403]

Rao et al. have reported the reversible transformation of 3D−1D ladder network under acidic conditions. When a 3D zinc phosphate is treated with different amount of H_3PO_4 under hydrothermal conditions at 150 °C for 24 h, 3D network, 1D ladder, and 2D layer structures can be obtained in a facile manner. Further the ladder structure can undergo a transformation to the 2D layer compound on acid treatment and transform into the 3D network on heating with water without/with amine.[404]

The same research group also have demonstrated the building up of the three-dimensional structure emerged from the lower-dimensional structures through transformation involving hydrolysis and condensation. Thermal treatment on a 0D dinuclear compound, $(pip)_3[Zn_2(ox)_5]\cdot 8H_2O$ (pip = piperazine) in the presence of pip at different temperatures afforded 1D, pseudo-2D, and 3D coordination network (Figure 142). Heating at 100 °C resulted in a single-stranded helical chain. Higher temperature led to the condensation of the 1D single-stranded zinc oxalate chains to form a pseudo-2D zinc oxalate structure, with a honeycomb aperture. Further increase in temperature generated a 3D network with interconnected channels. The overall dimensionality of the product increases as the reaction temperature is increased, accompanied by decrease in the water content and removal of oxalic acid. Similarly, another dinculear compound $[Ni(pro)_2(H_2O)]$ (pro = propionic acid) with four bridging propionate groups in a paddlewheel-type architecture transforms into a 1D chain structure $[Ni(pro)_2]$ at 25 °C within 24 h, followed by the elimination of water.[405]

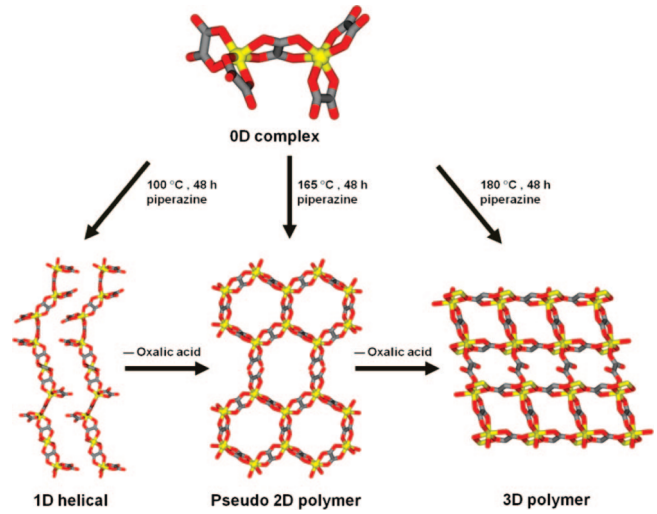

Figure 142. Temperature-driven formation of higher dimensionality framework by hydrolysis/condensation.

Reaction of metal acetates with di-*tert*-butyl phosphate (Hdtbp) results in the formation of tetrameric phosphates $[M_4(\mu_4\text{-O})(dtbp)_6]$ (M = Zn, Co, Mn).[406] Addition of strong donor ligands to this reaction breaks these tetramers to monomeric species, while the use of weak Lewis bases leads to the isolation of 1D CPs. Thus, the reaction of cobalt acetate with Hdtbp in the presence of 3,5-dimethylpyrazole (dmp) yields the monomeric $[Co(dmp)_2(dtbp)_2]$; 1D CPs $[M(dtbp)_2]$ (M = Mn or Cu) and $[Cd(dtbp)_2(OH_2)]$ are isolated from the same reaction in the presence of very weak Lewis bases.[407] On the other hand, complexes $[M(dtbp)_2]$ (M = Mn, Co), which exist as 1D molecular wires, transform to noninterpenetrating 2D rectangular grid structures $[M(dtbp)_2(4,4'\text{-bpy})_2\cdot 2H_2O]$ by the addition of 4,4′-bpy.[408]

Self-assembly between CuI and 2-(cyclohexylthio)-1-thiomorpholinoethanone (chttme) afforded $[Cu_2I_2(chttme)_2]$, $[Cu_4I_4(chttme)_2]$, and $[\{Cu_4I_4(chttme)_2\}\cdot MeCN\cdot nC_6H_{14}]$ under different experimental conditions (Figure 143). In the first CP, rhombohedral Cu_2I_2 clusters are linked by the ligands to form a 1D polymeric loop chain, and it is nonluminescent. The second polymer exhibits a 2D undulating polymeric network with Cu_4I_4 cluster nodes with orange luminescent property. The third polymer is a 1D zigzag loop-chain polymer with Cu_4I_4 cluster nodes and displays green luminescent. Interestingly, these CPs can be interconverted by heating and reacting with excess CuI or solvent. However, it is not clear that this transformation can be considered to be taking place in the solid state. The solid-state emission properties of CPs are attributed to the combination of ligand-to-metal charge-transfer and d−s transitions because of Cu···Cu interaction within Cu_4I_4 clusters. Hence, the temperature-dependent variation of Cu···Cu distance in the second and third CPs resulted in luminescence thermochromism behavior.[234d]

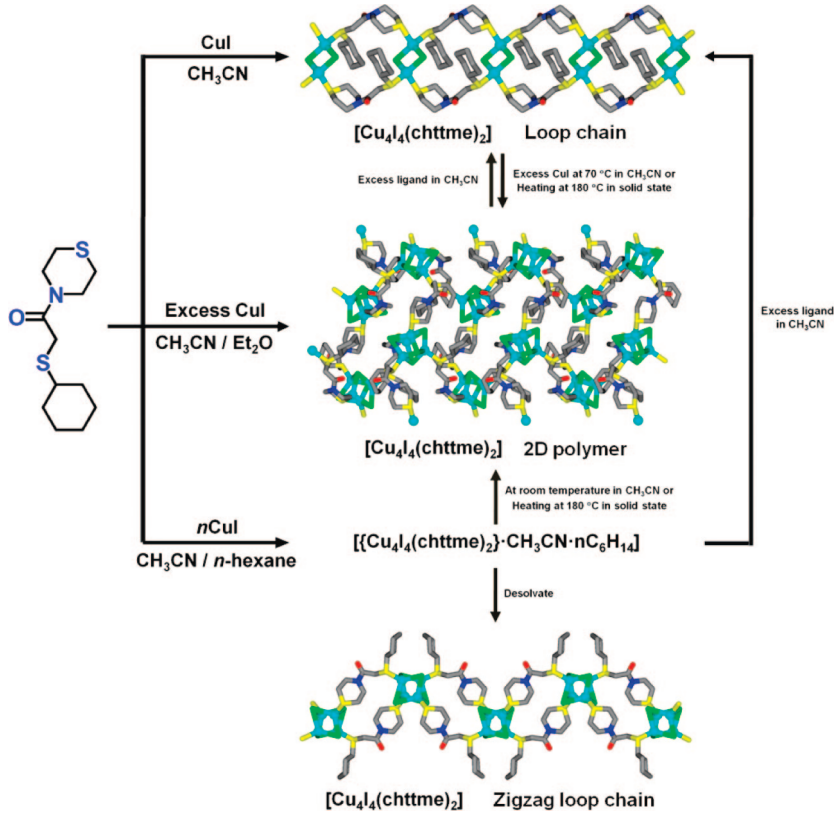

Figure 143. Schematic diagram of transformation of loop chains and 2D CP.

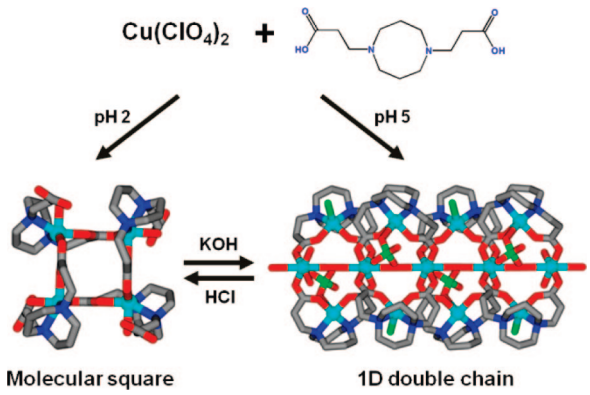

Figure 144. pH controlled interconversion between discrete molecular square and 1D double chain structures.

Bu and co-workers have shown an interesting pH-controlled reversible interconversion between an achiral molecular square and a spontaneously resolved chiral double chain (Figure 144). Reaction of $Cu(ClO_4)_2 \cdot 6H_2O$ and bis(3-propionyloxy)-1,5-diazacyclooctane (H_2bpdaco) at pH 2 afforded a molecular square, $[Cu(Hbpdaco)(H_2O)_{0.5}]_4 \cdot (ClO_4)_4$. At pH 6, a chiral 1D double chain, $[Cu_3(bpdaco)_2Cl] \cdot (ClO_4)_2 \cdot (H_3O)_2 \cdot Cl$, has been obtained with interlinked adjacent tetranuclear Cu_4 subunits that share the common Cu(II) center, forming a 1D chain with a cavity. The polymer also can be considered as two almost perpendicular 1D chains linked through the common Cu(II) ions to form a unique interpenetrated double-chain topology. Furthermore, the pH dependence of the electronic spectra confirmed that the molecular square and 1D double chain can be interconverted by changing the pH.[409]

7. Hosts for Water Clusters and Chains

The availability of hydrogen donor and acceptor groups in the cavities, along with their shape and size in the packing of organic and inorganic molecules, may influence various solvents including water to aggregate in the crystal lattices. On the other hand, the presence of water molecules during crystallization process can also play a significant role in influencing the molecules to adopt a particular packing in the crystals through supramolecular interactions. Hence it is not surprising that a plethora of 1D coordination polymers have been found to host a variety of water clusters and chains in their crystal lattices. In any case, such coordination polymers hosting water aggregates would certainly provide new insights into the properties and behavior of bulk water where the water molecules interact with the surface of the containers through weak interactions. A few 1D CPs containing water clusters and chains have been described already in a different context. This section is devoted to highlight the presence of some selected water aggregates hosted by 1D CPs but is not intend to cover the literature extensively. Such comprehensive literature may be found only in CSD-based reviews, such as those of Infante and Motherwell.[410]

7.1. Water Clusters

It has been shown that water cluster is distributed between the opposite handedness of the CP chains in *cis*-[Ni(*f*-rac-hmtactd)][$Ni(CN)_4$]$\cdot 3H_2O$ (hmtactd = 5,5,7,12,12,14-hexamethyl-1,4,8,11-tetraazacyclotetradecane). The $(H_2O)_6$ cluster linked the left- and right-handed helical chains through four hydrogen bonds with cyano N atoms in both chains. The $(H_2O)_6$ cluster functions as "mirror plane" to generate an adjacent chain with opposite chirality and further leads

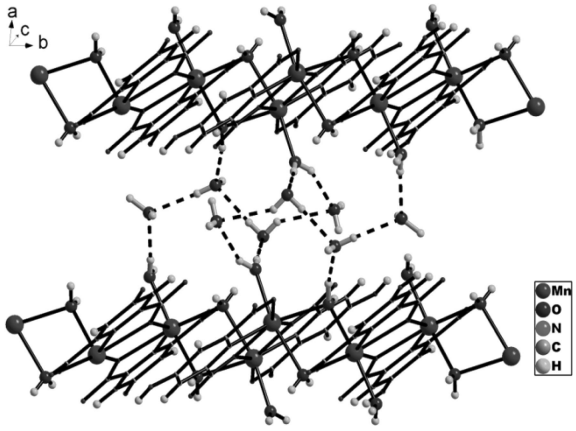

Figure 145. Perspective view of the $(H_2O)_{14}$ cluster linking two chains.

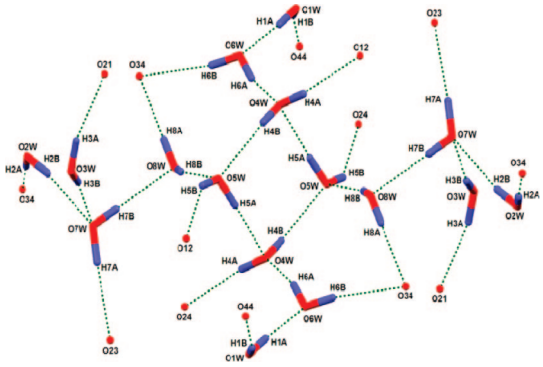

Figure 146. View of $(H_2O)_{16}$ water cluster in $[Zn(H_2O)_4Ce(dipic)_3]\cdot 8H_2O$.

to a meso or racemic structure. This is an unique example of the intermolecular water-cluster-induced chirality transfer.[71f]

Complex $[Mn_2(cda)_2\cdot 4H_2O]\cdot 4H_2O$ (H_2cda = chelidamic acid or 4-hydroxypyridine-2,6-dicarboxylic acid) displays a stairlike CP chain structure through aqua ligand bridging the dimeric building blocks. In addition, one bridging and two nonbridging axial water molecules of a polymeric chain are connected to a similar set of water molecules belonging to another chain through eight other intervening water molecules, forming an overall tetradecameric cluster (Figure 145), while other $(H_2O)_{14}$ clusters extend the polymeric chain in the crystallographic *c*-axis to form an overall 3D structure.[411]

A heterobimetallic complex, $[Zn(H_2O)_4Ce(dipic)_3]\cdot 8H_2O$ (H_2dipic = dipicolinic acid), has been reported as neutral 1D zigzag polymer. Because of the unusual zigzag arrangement in the triclinic lattice, a large empty space exists between the alternating polymeric chains that has been filled by a $(H_2O)_{16}$ water cluster. This $(H_2O)_{16}$ water cluster comprises one planar tetramer, two approximately pyramidal tetramers, and two dimers (Figure 146). Thermal dehydration on this compound leads to structurally related $[Cd(H_2O)_4Ce(dipic)_3]\cdot 3H_2O$ analogue with linear chains. Interestingly, upon addition of drops of water, the dehydrated powder is readily converted back to previous structure without much loss of crystallinity.[412]

In a double-stranded helix of $[Cd_4(bpa)_4(suc)_2(H_2O)_4](suc)_2\cdot 17H_2O$ (bpa = *N*,*N*′-bis(picolinamide)azine, H_2suc = succinic acid), the adjacent polymeric chains with different chiralities are linked to each other through interchain hydrogen bonds between the aqua ligands and the carboxylate groups into 2D host frameworks. Interestingly, an unprecedented $(H_2O)_{32}$ water cluster containing a central cyclic $(H_2O)_4$ is observed here. The uncoordinated suc and $(H_2O)_{32}$ cluster link each other via hydrogen bonds into a 2D guest network, which further alternately packed with the 2D host layers. The interlayer hydrogen bonds between the suc and the aqua ligands, lattice waters, as well as those between amino groups and free suc constructed a 3D hydrogen-bonded network. When glutaric acid is used as coligand, glutarate ligands linked the $[Cd_2(bpa)_2]$ units with different chiralities alternatively into a ladder-like meso-chiral chain with intrachain hydrogen bonds between the oxygen atoms of glu and the amino groups of bpa. The water chain is encapsulated in the empty channel along *c*-axis with a pore size of ~10.0 × 5.7 Å. In the structure, each water chain is hydrogen bonded to four different chains, and each host chain is, in turn, bonded to four water chains. The ladder polymeric chains act as a template for the formation of the water chains and stabilizes them through hydrogen-bonding interactions.[413]

Complex $Zn_3(Hapmdp)_2(2,2'\text{-bpy})_3\cdot 18H_2O$ (H_4apmdp = 1-amino-1-phenylmethane-1,1-diphosphonic acid) features an interesting vertical interpenetration of 1D water column and 1D zigzag CP chain. The salient feature is that there is a huge water column formed by 36 lattice water molecules with two $(H_2O)_6$ clusters self-assembled into the $(H_2O)_{14}$ cluster through another bridging water molecule, which further connects via other four water molecules to form a $(H_2O)_{18}$ water cage. Then symmetrical hydrogen bond joins the two $(H_2O)_{18}$ water cages with a 70.7° rotation to generate the $(H_2O)_{36}$ repeating unit and interconnect via the hydrogen bond to construct a 1D infinite column. The 1D water column and the zigzag CP chain intersect vertically with hydrogen-bonding interactions between water molecules and phosphonate groups of Hapmdp ligand. In addition, the adjacent 2,2′-bpy rings in the CP chains show strong $\pi-\pi$ stacking interactions (3.285 Å), which creates a large channel of ~11 × 7 Å, where the water aggregate occupied.[414] There are more examples on water cluster encapsulated in 1D CPs in literature.[415]

7.2. Water Chains

Among the helical CPs, only a staircase CP is able to host stream of water molecules inside its channel to furnish water chain structures. In complex $[(H_2O)_2\subset\{Ni(HSglu)(H_2O)_2\}]\cdot H_2O$ (H_3sglu = *N*-(2-hydroxybenzyl)-L-glutamic acid), of the two carboxylate groups in the $HSglu^{2-}$ ligand, one is chelating intramolecularly, while the other carboxylate coordinates to a neighboring Ni(II) atom to furnish staircase CP. Of the six lattice water molecules present in the asymmetric unit, four are inside the helical pore, while two are outside. Furthermore, two water molecules in the pore are hydrogen-bonded to produce a 1D helical polymer. This helical water chain is stabilized by hydrogen bonding interactions with aqua ligands. Another two water molecules reside along both the helical water chain and the aqua ligands through hydrogen bonding interactions as well. Figure 147 displays the hydrogen-bonded helical water chain inside the staircase CP.[416] Herein, the cooperative assembly and recognition of water molecules in the CP host is clearly exemplified.

A helical CP, $[Cu(L\text{-trp})(phen)]\cdot(ClO_4)\cdot 3H_2O$ (L-trp = L-tryptophan) has been reported to entrap left-handed water chain between the CP strands. The adjacent helical strands within the interhelical space force the trimeric acyclic water

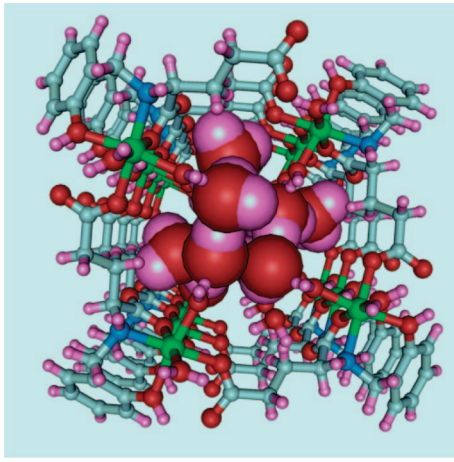

Figure 147. Helix inside helix: Hydrogen-bonded water chains inside staircase coordination polymer.

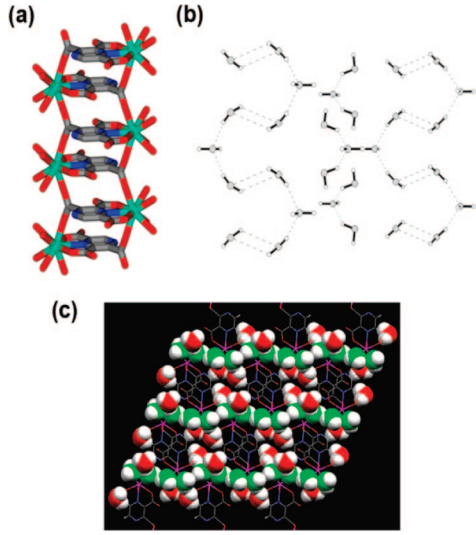

Figure 148. (a) Portion of ladder structure in $[Ln(pzta)(H_2O)_4]\cdot 2H_2O$. (b) Two types of water clusters formed by the coordinated and uncoordinated water molecules. (c) Packing diagram showing the intercalation of 1D ladder into the coordinated water molecules (shown in green color) and uncoordinated water molecules (shown in red color). Adapted with permission from ref 418. Copyright 2009 The Royal Society of Chemistry.

molecules through their contact mediated via C−H···O, N−H···O, and O−H···O hydrogen bonds and stabilize them in the helical arrangement.[417]

Molecular ladders $[Ln(pzta)(H_2O)_4]\cdot 2H_2O$ (Ln = Eu, Gd; H_3pzta = pyrazinetricarboxylic acid) (Figure 148a) contain hydrophilic environment because of the uncoordinated oxygen and nitrogen atoms which makes it feasible to attract uncoordinated or coordinated water molecules via hydrogen bonding. In this compound, two aqua ligands and two lattice water molecules furnish a 1D water chain and trimeric water cluster, as shown in Figure 148b. The packing diagram of the water molecules forms honeycomb-like channels and the polymeric strands reside in channels (Figure 148c).[418]

In 1D CP $[Co(tar)(2,2'\text{-bpy})\cdot 5H_2O]$ (H_2tar = tartaric acid), five lattice water molecules assembled to form a water chain, which consists of a edge-sharing cyclic water pentamer and a dimer water cluster. It is noted that four water chains and four polymeric chains interact to form a 1D channel, where the 2,2′-bpy molecules occupied. It is proposed that 2,2′-bpy molecules function as a template for the formation of the overall 3D network.[419] In the 1D CP complex

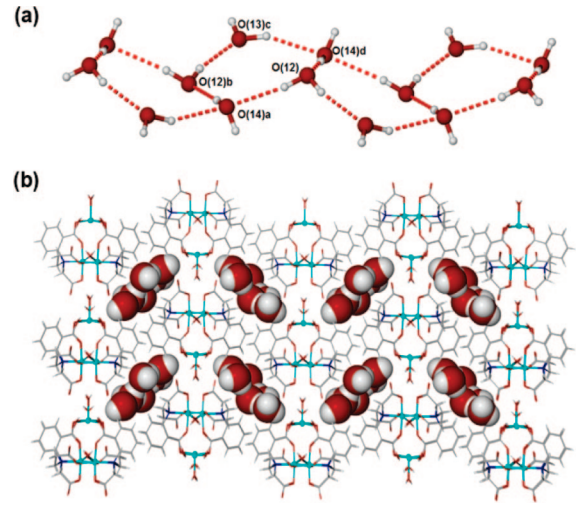

Figure 149. (a) Five-membered water cluster and the water tape. (b) 3D hydrogen-bonded network. Adapted with permission from ref 422. Copyright 2009 The Royal Society of Chemistry.

$[Cu(iqc)_2]\cdot(H_2O)_4$ (Hiqc = isoquinoline-3-carboxylic acid), the lattice water moieties formed a 1D infinite water tape consisting of edge-sharing tetrameric subunits. Furthermore, the 1D water chain interlinked the adjacent polymeric chains via intermolecular hydrogen bonds between the water molecules and carboxylates to form a 2D layer sheet.[420] A helix water chain has been observed in linear polymer of Cu(II) sugar alcohol $Li_2[Cu(Hdulc)]\cdot 10H_2O$ (Hdulc = galactitol). The water molecules are arranged in helical 2_1 axis by coordinating to both Li(I) and Cu(I) ions.[421]

Water molecules have been found to link to trinuclear units into 1D chain in $\{[Cu_3(cpiap)_2(H_2O)_3](\mu\text{-}H_2O)\}\cdot 7H_2O$ (H_3cpiap = 2-(carboxyphenyl)iminoacetic propanoic acid). Moreover, five lattice water molecules are arranged in a nonplanar cyclic pentamer, and the adjacent pentamers are fused together by sharing one edge, forming a T5(2) water tape (Figure 149a). The polymeric chains are linked by the adjacent water chains to form a 3D supramolecular architecture by various O−H···O hydrogen bonding and C−H···π interactions (Figure 149b). The related ligand, 2-(carboxyphenyl)iminodipropanoic acid forms a 1D zigzag CP.[422]

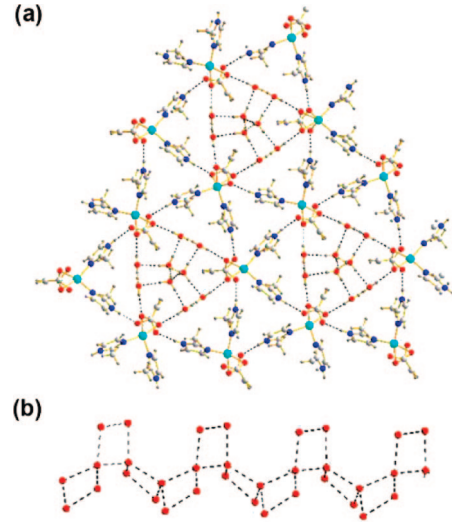

Figure 150. (a) Packing diagram along *c*-axis of $[Cu(mim)_2(mal)]\cdot(H_2O)_3$. (b) Perspective view of hydrogen-bonded infinite water chain.

A 1D linear CP, $[Cu(mim)_2(mal)]\cdot(H_2O)_3$ (H_2mal = maleic acid), contains infinite 1D water chains containing cyclic water tetramers (Figure 150).[423]

In a 1D zigzag polymer of $[Cu(4\text{-pytz})(NH_3)]\cdot 4H_2O$ (4-pytz = 3,5-di(4-pyridyl)-1,2,4-triazole), a novel hydrogen-bonded water−ammonia ribbon composed of fused $(H_2O)_5$ and $(H_2O)_4(NH_3)$ pentagons were found. The polymeric chains are arranged in alternate stacking and antiparallel fashion. It is worth mentioned that the hydrogen bonding donors and acceptors are exposed on the layer surface. Such packing of layered structure has allowed the formation of water ribbon comprises fused water pentamers within the 1D channels. The water ribbon is further interacted with ammonia ligand via N−H···O bonds to generate $(H_2O)_4(NH_3)$ pentagons.[424] On the other hand, complex $[\{Cu(phen)(H_2O)\}_2(muco)](NO_3)_2$ (H_2muco = muconic acid) contains hydrogen-bonded $H_2O\cdots NO_3^-$ aggregates with helical conformation.[425]

8. Application of 1D CP as Materials

Processability of organic polymers to fibers, sheets, and objects of a desired shape with varying mechanical and physical properties has been attributed to its enormous growth as materials. On the contrary, CPs or MOFs are not suitable for making materials similar to organic polymers as they are different in several aspects. The nonprocessability of these CPs may be attributed to insolubility, often melting with degradation, etc. Hence making CPs in any form in macroscopic scale is certainly a major step forward toward the technological applications of these new materials.

CPs exist in highly crystalline one-, two-, and three-dimensional architectures in the solid state, whereas processable organic polymers exclusively have one-dimensional structures. Hence it is logical to assume that 1D CPs are suitable candidates to mimic the properties of processable organic polymers. To make use of 1D CPs for this purpose, the first step is to make them amorphous. It is obvious that the CP gels are the key precursors to achieve this goal. This section aims to highlight the recent advances to make the 1D CPs into gels, fibers, nanocrystals, microspheres, etc.

8.1. Coordination Polymeric Gels

Though gel formation by organic molecules has been widely reported in the literature, metallogels and CP gels have only been of recent interest. Metallogels with various features of metal ions have been reported to show unusual functional properties, such as redox responsiveness, catalysis, phosphorescence behavior, spin-crossover phenomenon, and so on. Furthermore, binding of metal ion to gelator molecule can affect self-assembly modes and allow the gelation ability to be fine-tuned.[426] The gelation of CP stemmed from the basic of supramolecular chemistry and rational design of ligands as gelators and suitable coordination geometry of metals to generate scaffolds that contain void space, which can accommodate solvent molecules to form gel. Multidimensional CPs have been considerably employed in the formation of gel-phase materials.[427]

Recently, 1D CPs also have been exploited for their gelation properties. Lee et al. have shown an interesting reversible sol−gel interconversion of CPs in aqueous media triggered by anion exchange (Figure 151). The folded helical $[Ag(L)]BF_4$ (L is shown in Figure 151) CPs undergo spontaneous gelation at concentration above 2.5 wt %.

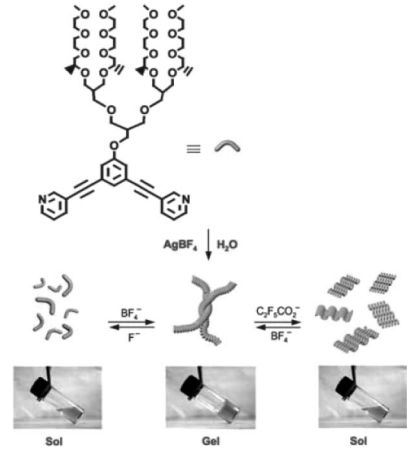

Figure 151. Schematic representation of reversible sol−gel transition with anion exchange. Reproduced with permission from ref 428. Copyright 2005 Wiley Interscience.

Interestingly, anion exchange to F^- or $C_2F_5CO_2^-$ has been found to drive the depolymerization of CP, and the gels transformed into fluid solution. The sol−gel transition process can be rationalized by the self-assembly of Ag(I) with pyridine derivatives and BF_4^- anions. The Ag(I) polymeric chains adopt a folded helical conformation in which the BF_4^- ions are coordinated in cis-like conformation such that the size of BF_4^- ion is compatible with the internal cavity. This helical secondary structure is responsible to form entangled fibrillar network that immobilize water molecules. Anion exchange with F^- or $C_2F_5CO_2^-$ ion has transformed the polymeric chains into trans conformation, that is, unfolded zigzag structure, which could not form entangled network to facilitate gelation. It is noted that the sol−gel transition is reversible by addition of BF_4^- ions. These results demonstrate that variation of size of counteranions influence the self-assembled structure significantly, which provides useful strategy to fabricate stimuli responsive smart materials.[428]

Clérac et al. have demonstrated that the known polymeric Fe(II)−triazole system can be modified into CP gels by functionalizing the triazole ligands with long alkyl chains. Because of the spin-crossover behavior of the materials, the resulting CP gels show interesting properties at the crossover temperatures, such as thermoreversible magnetism (i.e., the diamagnetic metal ions become paramagnetic) and optical and rheological switching.[429] The similar strategy has been adopted in other CP gels.[430] These gels highlight a new approach of transferring the unusual physical properties of solids into a soft-matter phase and polyfunctional materials successfully.

Kimizuka and co-workers reported the first example of thermally reversible, heat-set-gel-like networks in organic media. When the lipophilic Co(II) complex of 4-(3-lauryloxy)propyl)-1,2,4-triazole is dissolved in chloroform, a blue gel is obtained at room temperature and the Co(II) has tetrahedral geometry. Interestingly, when the gel is cooled down below 25 °C, the gel turns into a pale pink solution, which suggests octahedral geometry for Co(II). It is worth mentioning that the sol−gel and thermochromic transition is reversible upon changing of temperature (Figure 152).[430b]

These CP gels containing long chain appended groups can be termed as "first generation CP gels" in which the entanglement of such long chain groups generated the cross-link network that entraps solvent molecules. Nonetheless,

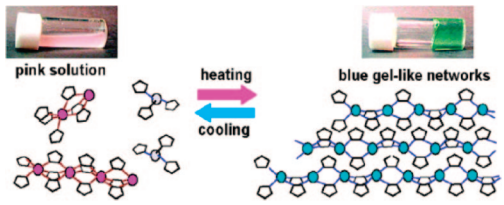

Figure 152. Schematic representation of sol−gel transition and thermochromic behavior of CP gel. Reproduced with permission from ref 430b. Copyright 2004 American Chemical Society.

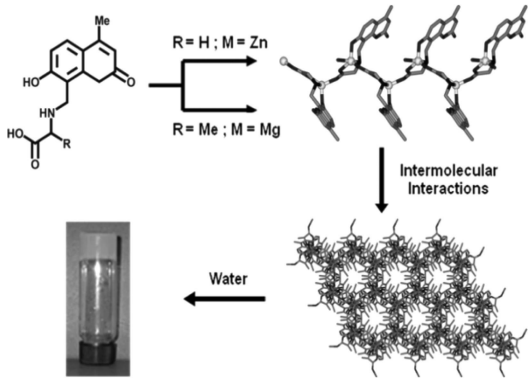

Figure 153. Schematic diagram of formation of coordination polymeric gels with *N*-(7-hydroxy-4-methyl-8-coumarinyl)-amino acid ligands.

gelation of metal complexes and CP also has been observed in the absence of long chain appended groups in gelators. For instance, a metallogel has been reported by mixing $LaCl_3$ and 1*H*-5-(2-pyridyl)tetrazole in the presence of triethylamine. It is postulated that triethylamine and triethylammonium cation, as well as concomitant formation of anionic La(III) complex promote the formation of a 3D hydrogen-bonded architecture in the presence of water.[431] Hence, one can envisage that CPs can be functionalized into gelators by themselves even in the absence of long chain groups. Such CP gels have been called as "second generation CP gels".

Recently, few more interesting examples for second generation CP gels have been reported. The Mannich base of *N*-(7-hydroxyl-4-methyl-8-coumarinyl)-amino acids have been shown as hydrogelators with Zn(II) and Mg(II) (Figure 153). The hydrogels are weak gels in nature as evidenced from rheological studies and are stimuli responsive to pH and mechanical stress. Structural investigation of the corresponding $[Zn(muala)(H_2O)]\cdot 0.5H_2O$ (H_2muala = *N*-(7-hydroxy-4-methyl-8-coumarinyl)-L-alanine) shows that the 1D zigzag chains are arranged in a criss-crossed fashion to form hydrophobic pockets with extensive hydrogen bonding interactions and provided evidence for the structure of gel formed by mugly^{2-} anion (H_2mugly = *N*-(7-hydroxy-4-methyl-8-coumarinyl)-glycine). It is proposed that the water molecules are entrapped in the cavities in the case of hydrogels formation. The interesting feature of these hydrogels is that they display strong blue emission and the fluorescence properties are enhanced dramatically as compared to free ligands upon the gelation.[432]

Furthermore, achiral imidazole derivatives also have been reported as gelators to generate nonracemic CP gel with Ag(I) in the absence of chiral influences and appended groups. Self-assembly of Ag(I) and rigid bridging imidazole ligand facilitated the formation of helical coordination polymer, which further led to chirality through chiral symmetry breaking process (Figure 154).[433]

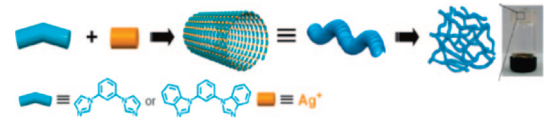

Figure 154. Schematic representation of the self-assembly process of the CP gels. Reproduced with permission from ref 433. Copyright 2008 The Royal Society of Chemistry.

8.2. Coordination Polymeric Fibers

A similar second generation CP gel was obtained from Ni(II), tba (Htba = 4-trifluoromethylbenzoic acid) and bpe/4,4′-bpy in different reactant ratios. Strutural investigations on the related complexes of $[Ni(tba)_2(H_2O)_2(bpe)]\cdot 2bpe$ and $[Ni(tba)_2(MeOH)_2(4,4'\text{-bpy})]\cdot 4,4'\text{-bpy}$ disclose the 1D linear and helical CP structures respectively. Because of the high viscosity nature, the diluted gels have been found to be suitable for making nanofiber bundles by electrospinning process in centimeter scale and in gram quantities. Usually electrospinning method yield either amorphous or very poor crystalline materials. Microscopic morphological studies indicate that these nanofibers are in diameters of ∼100 nm and aspect ratio of 10^7 (Figure 155). It is likely that these fine nanofibers are formed by the self-assembly of 1D CP chains. More interestingly, these nanofibers are good field emitter with turn-on field of 4.5−6.3 V/μm and current density of 0.14−0.18 μ-Amp/cm^2.[434]

Earlier Lu and co-workers demonstrated that 1D CPs can be fabricated into nanofibers by electrospinning process. Complex $[Zn(H_2O)_2(4,4'\text{-bipy})(bpe)_2]\cdot(bpe)_{1.75}\cdot(4,4'\text{-bpy})_{0.25}(NO_3)_2\cdot(H_2O)_{4.45}$ (Figure 156a) features a 1D linear CP structure and extends into 2D network through $\pi\cdots\pi$ stacking interactions between side arms of bpe ligands and hydrogen bonding interactions between aqua ligand and noncoordinated nitrogen atoms of bpe ligands. The free bpe ligands, nitrates, and water molecules are included in the 2D nets with extensive hydrogen bonding. It is important to note that the inclusion capability and the hydrogen bonding interactions contribute to the solubility of the complex. It has allowed the preparation for saturated DMF solution of CP for electrospinning, although it is not clear that this can be produced in large quantity. The diameters of the fibers

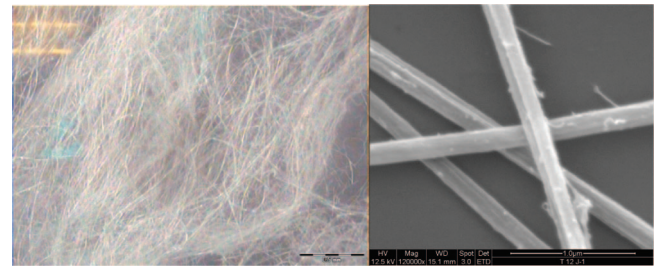

Figure 155. Optical and SEM images of electrospun fibers.

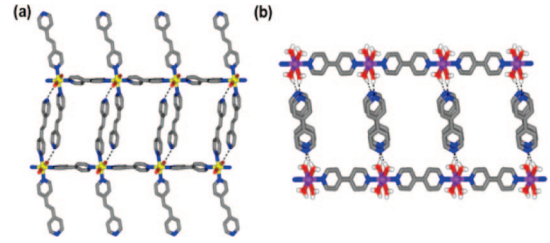

Figure 156. (a) View of linear CP chains linked into 2D networks by hydrogen bonding and $\pi\cdots\pi$ stacking interactions. (b) View of double hydrogen-bonded 2D sheet.

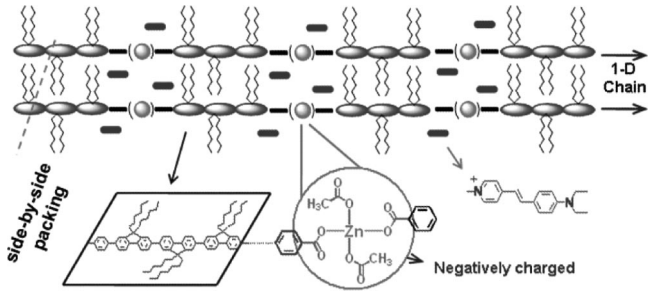

Figure 157. Proposed 1D CP structure of the nanofibers. Reproduced with permission from ref 437. Copyright 2009 American Chemical Society.

range from 60 nm to 4 μm.[435] Another linear CP $[Co(H_2O)_4(4,4'\text{-bpy})(4,4'\text{-bpy})_2]\cdot(NO_3)_2\cdot(H_2O)_{3.5}$ (Figure 156b) with double hydrogen-bonded 2D network structure also is soluble in DMF and can be fabricated into nanofibers by electrospinning.[436]

Thus these findings demonstrate that 1D CPs are suitable for processing just like their organic counterparts. Further, the metal ions and the spacer ligands can be tailored to modify the magnetic, electric, and electronic properties of the fiber produced for technological applications.

Loh and co-workers have demonstrated Zn((II) coordination-assisted self-assembly of 1-D nanostructured light-harvesting antenna and showed that efficient florescence resonance energy transfer (FRET) is favored in the assembled 1D nanostructure (Figure 157). The nanowires of 1D CPs can form stable dispersion and are not disassembled by organic solvents, thus affording the possibility of spin-coating for further applications. The coordination-assisted assembly strategy is expected to accelerate the development of new generation of photofunctional materials by rational tuning of the optical properties of the chromophores and proper selection of the metal species.[437]

The self-aggregation between charge-neutral and positively charged Pt(II) species through Pt···Pt or ligand−ligand interactions has effectively used to synthesize organoplatinum-based crystalline nanostructures by Che and co-workers. For example, Che's laboratory have demonstrated that $[Pt(CN^tBu)_2(CN)_2]$ molecules can form linear CP and micrometer- and nanometer-scale luminescent wires through weak Pt(II)···Pt(II) interactions. The $[Pt(CN^tBu)_2(CN)_2]$ units stack in pairs and propagate into infinite linear stacks of square planar Pt(II) molecules with Pt(II)···Pt(II) distances of 3.354 Å. Fascinatingly, the molecules can function as building block for the construction of 1D micrometer- and nanometer-sized wires and fibers based on Pt(II)···Pt(II) interactions. The wires can be obtained by evaporation or injection reprecipitation of a solution of $[Pt(CN^tBu)_2(CN)_2]$ in acetonitrile only or acetonitrile solution in water on a silicon substrate. More interestingly, these coordination wires exhibit temperature dependent and vapochromic emission behavior. This is attributed to the fact that subtle environmental changes can perturb the weak Pt(II)···Pt(II) interactions and subsequently affect the $^3[5d_\sigma^*,6p_\sigma]$ emissive properties.[438] Further this Pt(II)···Pt(II) interactions have been presumed to be responsible in the organization of discrete molecular platinum(II) complexes into gels and nanowires.[439]

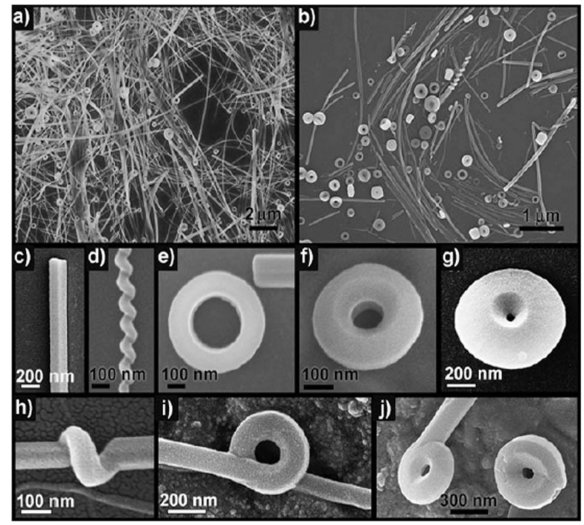

Figure 158. SEM images of the superstructures prepared by precipitating Pt(II) complex from acetonitrile into water at (a) 25 °C and (b) 70 °C. SEM images of freestanding (c) wires, (d) springs, (e−g) wheels, and (h−j) various intermediate structures formed. Reproduced with permission from ref 441. Copyright 2008 Wiley Interscience.

8.3. Coordination Polymeric Nanostructures

The Pt(II)···Pt(II) or ligand−ligand interactions are also responsible for the self-aggregation between charge-neutral and positively charged Pt(II) species in formation of organoplatinum-based nanowires.[440] The organoplatinum(II) complexes have been assembled into a number of crystalline superstructures with diverse morphologies such as rods, wires, helices, wheels, donuts, etc., shown below in Figure 158 under various conditions using metal−metal and ligand−ligand interactions.[441]

Oh and co-workers synthesized fluorescent hexagonal-tubes and ring-shaped CPs by the simple solvothermal reaction by reacting a salen ligand (salen = *N,N'*-phenylenebis (salicylideneimine)dicarboxylic acid) and 1,4-H_2bdc in a 1:5 molar ratio and $Zn(CH_3COO)_2$, in DMF. Furthermore, calcinations of these CPs generated metal oxide particles that maintain the morphology of the precursors used.[442]

8.4. Amorphous 1D CP Nanospheres and Microspheres

Micro- and nanoscale miniaturization is an important advancement in the area of MOF materials,[443] and this subject area was recently reviewed by Lin and co-workers,[443d] as well as Mirkin's group.[443e] According to Oh and Mirkin amorphous spherical micro- and nanoparticles composed of 1D CPs can be synthesized by the coordination-chemistry-induced assembly of metal ions and homochiral carboxylate-functionalized binapthyl bis-metallotridentate Schiff base (BMSB) building blocks (Figure 159), followed by the fast precipitation with a poor solvent.[444] These spherical particles with an average diameter of 1.60 μm are amorphous and are highly fluorescent. The particle size can be controlled by the rate of addition and type of initiation solvent used. Indeed, rapid addition of diethylether produce nanoparticle size of ~190 nm. The Zn(II) metal can easily be exchanged with Cu(II), Mn(II), and Pd(II) without affecting the size or morphology of the particles.[445] A similar strategy was used by Lin's laboratory to synthesize NCPs composed of the

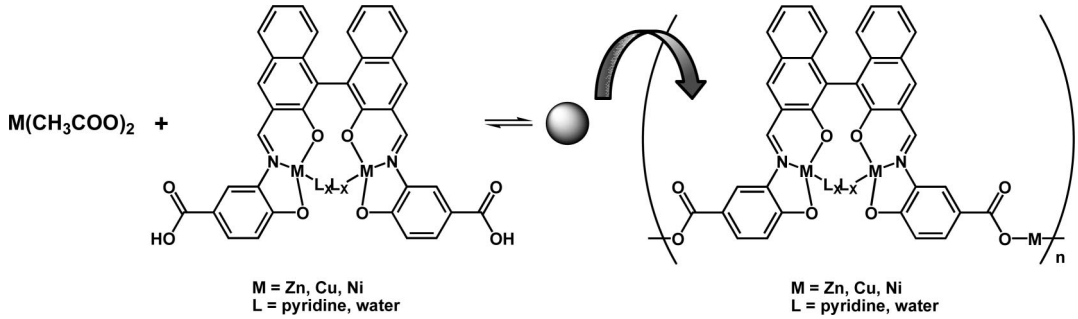

Figure 159. Schematic diagram showing the formation of colloidal particles (sphere) by precipitation method.

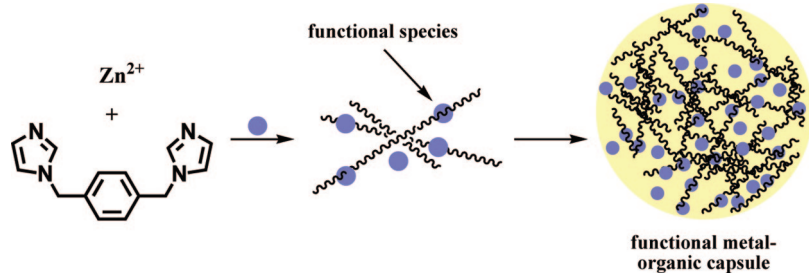

Figure 160. Schematic representation of the formation of Zn(bix) spheres and concomitant encapsulation of guest species.

anticancer drug disuccinatocisplatin (DSCP) and Tb(III).[446] Successful and reproducible synthesis of NCPs in this system depends on the careful control of the pH of the aqueous precursor solution.

Similarly the 1D CP formed between $PtCl_6^{2-}$ and *p*-phenylelediamine has been made into submicrometer-scale, monodispersed amorphous spherical colloids by fast precipitation under vigorous stirring. It has been observed that neither *o*-phenylenediamine nor *m*-phenylenediamine produce such colloidal particles, suggesting the importance of bridging nature of the ligands. Hence it is termed as coordination-induced assembly.[447] A number of amorphous CP nano and mircrospheres have been synthesized in this way.[448] Interestingly such CP micro- and nanospheres have been shown to be selective cation-exchange[445] and hydrogen-storage properties.[449]

Maspoch et al. developed a new and versatile coordination polymeric micro- and nanospheres for encapsulating nanocrystals and fluorescent organic dyes.[450] In this method, micro- and nanospheres of 1D CP are formed by reacting Zn(II) ions and bix, followed by a fast precipitation method as displayed in Figure 160. Several types of functional species, including magnetic nanoparticles, organic dyes, and luminescent quantum dots (QDs) have been encapsulated.

The surfactants on the surface of Fe_3O_4 NPs has been selectively replaced by organometallic 1D CP $[M(qmtc)_2(DMSO)_2]$ (M = Mn, Cd; qmtc = [(η^5-semiquinone)$Mn(CO)_3$].[451] Incorporation of nanosized functional materials into the coordination polymers may open new doors in terms of applications. There are few more literature on the nanospheres[452] and nanotubes[453] but it is not clear whether they belong to 1D CPs. While 1D CPs form amorphous micro- and nanoshapes, crystalline nano-MOFs are generally formed by 2D and 3D MOFs as well as 1D CPs.[443d,e]

8.5. Soluble 1D CPs

The coordination polymers are in general insoluble in common solvents and many show solubility because of the dissociation into oligomers and solvation of metal ions. In this section, unusual 1D CPs that are freely soluble and still maintain their connectivity are discussed.

The soluble nanoribbon CPs reported is based on a combination of a biosynthetic peptide polymer and an oppositely charged organometallic supramolecular polymer.[454] Ultrasound has been used to mechanically induce ligand dissociation from a 1D CP, thus making it a novel method for studying and controlling the degree of polymerization in toluene solution.[455] A double-stranded helical CP consisting of two complementary metallopolymer strands that are intertwined through chiral amidinium-carboxylate salt bridges shown in Figure 161 has been found to be stable in solution as characterized by ^{1}H NMR spectroscopy, circular dichroism (CD) and atomic force microscopy (AFM).[456]

The coordination polymers based on Ag(I) ion complexed with ditopic bridging ligands, based on phenanthrene and pyridine units with a bent conformation, have been investigated by Lee and co-workers for their dynamic self-assembling behavior in aqueous solution. These helical CPs are shown to display reversible extension-contraction mo-

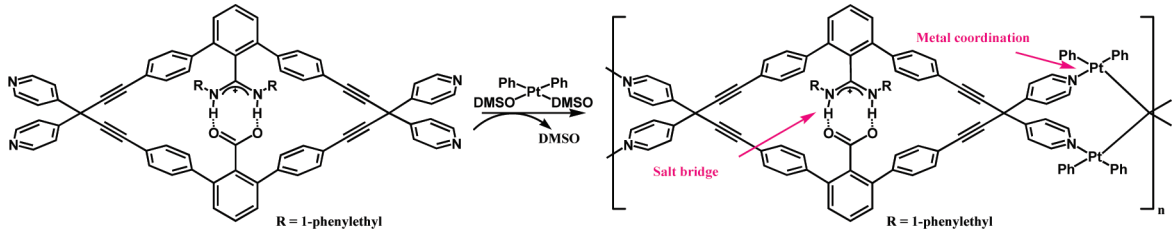

Figure 161. Formation of the double-stranded metallosupramolecular helical polymers.

tions, triggered by temperature. Further the aqueous solutions of the coordination polymers were shown to reversibly transform from transparent to translucent states above certain temperatures. Subsequent studies revealed that a fluorescence switching between the fluorescent stretched and nonfluorescent compressed states of the supramolecular springs occur due to this dynamic conformational change. Such mechanical motions of the supramolecular spring may be promising applications in the areas of dynamic nanodevices, optical modulators, and fluorescent thermometers.[457]

Ultrasonic degradation of polymers is a relatively slow process but highly selective, and the rate of scission is chain-length dependent. In this respect, a coordination polymer formed between silver(I) and *N*-heterocyclic carbene (NHC) ligand has been found to undergo an efficient ultrasonic scission and quantitatively broken in minutes to give highly reactive free carbenes. In the presence of water, scission is irreversible. The mechanochemical process that generates carbenes have been shown to catalyze organic transformations such as transesterification and polymerization of lactides.[458]

Another soluble 1D CP is obtained by reacting dendron-functionalized ligand based on a rigid 4,4′-bpy as a monomeric ligand with Pd(II) in organic solvents. The AFM studies show the interconnection of the fourth-generation poly(amidoamine) dendrimers individually immobilized on mica.[459]

8.6. 1D Polymers on the Surfaces

Controlled assembly of CPs on the solid surfaces has potential applications in molecular information storage and processing devices, and these are commonly referred as MMX polymers. Various methods have been used to self-assemble the 1D CP nanostructures on the surfaces. They are (i) deposition from solution, (ii) self-assembled monolayer formation, (iii) deposition by coevaporation of organic ligands and metal atoms, (iv) evaporation of organic ligands and reaction with metal atoms of the surface, and (v) sublimation of monomers. Recently, Zamora and co-workers published an excellent review on molecular wires based on coordination polymers.[460] The 1D CP $[Ru_2Br(\mu\text{-}O_2CEt)_4]$ has the repeating unit based on paddle wheel structures bridged by bromide ions. The single chains of this polymer have been aligned on different surfaces, such as mica and graphite, by drop casting the aqueous solution of the compound in sodium dodecyl sulfate.[461] Welte et al. have used ultrasound to break the coordination bonds in the 1D CP $[Ru_2I(\mu\text{-}O_2CEt)_4]$ to produce reactive species that self-organize in solution yielding a rich variety of structures. These activated building blocks have been assembled as MMX polymer when adsorbed on surfaces, as demonstrated by the AFM images. The observed structures reproduce those present in the solution.[462a] A similar MMX polymer has been self-assembled on the surfaces using $[Co(ox)(Htrz)_2]\cdot 2H_2O$ by sublimination method.[462b]

The antiferromagnetic $[Mn(ox)(4atr)_2]$ (4atr = 4-amine-1,2,4-triazole) has coordination polymeric structure determined by X-ray crystallography has been made into nanospheres and single chains on the graphite and mica surfaces by ultrasound or deprotonation of the coordinated 4atr ligands and characterized by AFM and scanning tunneling microscopy (STM).[463] A number of similar 1D CPs have been reported in the literature.[453,464]

Rational design of conductive coordination polymers based on the DFT calculations yielded two linear coordination polymers $[Ni(6\text{-}mp)_2]\cdot 2H_2O$ and $[Ni(6\text{-}thioG)_2]\cdot 2H_2O$ (6-mp = 6-mercaptopurinato and 6-thioG = 6-thioguanine). These two 1D CPs show electrical conduction at room temperature with some remarkable differences between them and those of the Cd(II) analogue, which have been rationalized by new DFT calculations. Preliminary surface studies show that it is possible to isolate single chains on surfaces.[465a,b] Similarly, the work by Mitsumi et al. and Calzolari et al. have also highlighted the use of theoretical calculations in assisting the interpretations of physical properties and reactivity.[465c,d] Welte et al. found the self-assembled electrically conductive 1D CP $[Pt_2I(S_2CCH_3)_4]$ on an insulating substrate by direct sublimation of polymer crystals exhibit significant electrical transport properties. Their theoretical calculations based on density functional theory, confirm coordination polymers as candidate materials for applications in molecular electronics.[465e] A similar work by Zamora et al. on $[Pt_2(n\text{-pentyl}CS_2)_4I]$ nanostructures adsorbed on an insulating surface show electrical conductivity suggesting that that MMX-polymer-based nanowires could be suitable for device applications.[465f]

8.7. Coordination Polymer as a Template for Nanocrystals Synthesis

The coordination polymers can be used as templates[28] and sacrificial templates to fabricate desired nanostructures. In the sacrificial template method, insoluble macroscopic crystalline materials can be employed where the crystal structure will guide the shape and size of the nanoparticles formed. On the other hand, the CPs can be made into nanoform first and then converted to nanoinorganic materials. Here the morphology of the CP precursor determines the shape of the final inorganic materials.

A unique method of making ZnO hexagonal tubes and rings was reported by Oh and co-workers. First they have generated fluorescent hexagonal tube and ring shaped CPs by solvothermal method. A unique particle-growth mechanism called self-template directed growth has been proposed for the formation of hexagonal tubes from hexagonal rods. Furthermore, these CPs acted as sacrificial templates for growth ZnO hexagonal tubes and rings by calcinations (Figure 162). This simple method will provide a new paradigm in the manufacture of customized metal oxide nanoparticles.[442,466]

Dandelion-like architectures of 1D CP Pb-cysteine have been assembled from well-aligned nanowires in the aqueous solution of L-cysteine and $Pb(OAc)_2$. They were further converted to spherical and various flowerlike PbS microstructures by conventional hydrothermal conditions.[467]

Xia et al. reported an interesting method for preparing ultrathin Au nanowires using 1D CP [(oleylamine)AuCl] chains made up of Au−Au interactions. The Au(I) is converted to Au(0) by slow reduction and the nucleation and growth of Au can be mediated by the 1D polymer strands to produce ultrathin nanowires. Here Ag nanoparticles are used as a reducing agent and the Au nanowires obtained in hexane solution have average diameter of 1.8 nm. If chloroform is used instead of hexane, only spherical nanocrystals (∼15 nm) were obtained with or without the addition of Ag nanoparticles at 60 °C. The change in the morphology has been attributed to different configuration of the polymer in the solvents.[468]

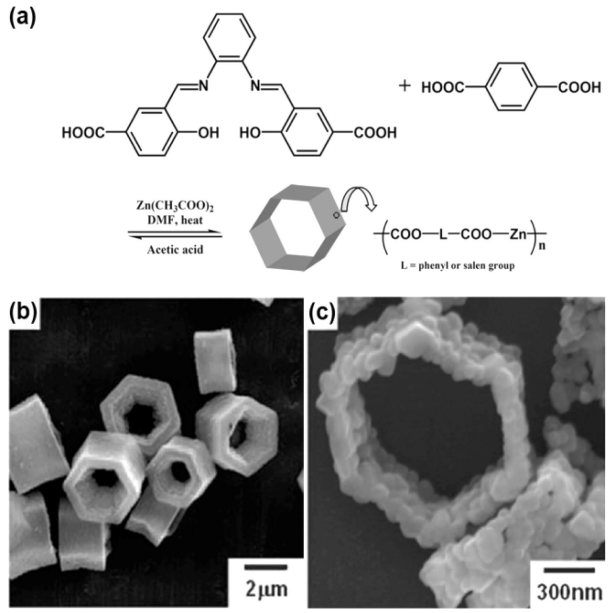

Figure 162. (a) Formation of hexagonal-tube coordination-polymer particles from coordination polymers. (b) SEM image of the fully formed hexagonal tubes. (c) High-magnification SEM image. Adapted with permission from ref 442. Copyright 2009 Wiley Interscience.

Here the nanowires of $[Cu(tu)]Cl \cdot 0.5H_2O$ (diameter 100 nm) were prepared just by mixing $CuCl_2$ solution with thiourea (tu). The as-prepared $[Cu(tu)]Cl \cdot 0.5H_2O$ nanowire precursors were used to prepare the black porous CuS nanotubes in alkaline aqueous solution under ambient conditions.[469]

The insoluble nature of a coordination polymer with predetermined arrangement of metal atoms and ligands can be used as a precursor, as well as a sacrificial template to synthesize copper sulfide with predefined shape. Recently the hydrogen-bonded 1D zigzag CP $[Cu(HSglu)(H_2O)] \cdot H_2O$ has been used to generate copper sulfide nanocrystals using solvothermal reactions. The reaction conditions have been optimized to obtain petal bedlike, flowerlike, and rice-ball morphologies. The investigation demonstrates that the orderly arrangement of metal atoms in the coordination polymer can be transferred to the nanomaterials by fine-tuning the reaction conditions.[470]

There are very few reports which utilize 1D, 2D, and 3D coordination polymers to synthesize metal oxides; zinc oxide and γ-manganese oxide using hydrothermal synthesis, cadmium oxide by thermal degradation, and microwave-assisted synthesis of nickel nanowires.[471] There are several reports available dealing with the use of 1D, 2D, and 3D CPs in the synthesis of inorganic nano- and microarchitectures.[472]

9. Concluding Remarks

More than four decades after the first review on coordination polymers written by Bailar Jr., this field has grown enormously and this class of CPs has been developed from "inorganic polymers" to coordination polymers and MOFs. This review addressed the major progress that has been accomplished from structural curiosity into multifaceted CP materials since Chen and Suslick's review appeared in 1993. From this manuscript, it may be noted that the field has come a long way from the perception that 1D CPs are less interesting compared to 2D and 3D systems.

The competition between the kinetically favored and thermodynamically stable products, as well as among various kinetic products makes the predictability of the 1D CP, the simplest of all the CPs, is difficult if not impossible. Hence, the statement by Maddox,[473] "*One of the continuing scandals in the physical sciences is that it remains in general impossible to predict the structure of even the simplest crystalline solids from a knowledge of their chemical composition*", which has been frequently quoted by Zaworotko in the context of crystal engineering,[1] is also true in the case of 1D CPs to a smaller extent. The influence of experimental conditions on the formation of 1D CPs discussed in this review (section 4) will exemplify this fact. The conformation of the 1D CPs', especially zigzag, spiral, or helical, nature can easily be manipulated by the anions, solvents, and packing. Although these irrational and unpredictable structures hinder our understanding and progress, such unexpected reactivity, fascinating architectures, interesting packing, and serendipitous new properties of these polymers keep the researchers more excited than ever.

Furthermore, this research area is witnessing its next phase of growth. Apart from discovering intriguing new structural features, for the past few years researchers are interested in unraveling new properties of these polymers, and these include mechanical, electrical (conductivity, semiconductivity, pyro- and piezo-electricity, etc), optoelectronic, magnetic, optical (luminescence, birefringence, nonlinear, etc), chiral separation, and catalytic properties. It is also interesting to find that 1D CPs exhibit permanent porosity and gas/solvent storage properties just like MOFs. Although majority of coordination polymers shows physical properties different from the organic polymers, new coordination polymers that are soluble in common organic solvents have been discovered. A number of CPs has been successfully processed into micro- and nanospheres, rods, fibers, etc. Such explorations in new directions make the coordination polymers as truly coordination polymeric materials. Because of the ease of formation by self-assembly process, these coordination polymers are very attractive as future advanced functional materials. However, the ultimate challenge in this field still remains to be addressed is the control of the conformation, connectivity and packing of the coordination polymers.

10. Acknowledgments

We gratefully acknowledge the Ministry of Education, Singapore, for the financial support through NUS FRC grant R-143-000-371-112. We sincerely thank a number of researchers for providing the figures in this review. J.J.V. would like to thank the Ministry of Education, Science & Technology (S. Korea) for the World Class University Chair Professorship and Prof. Shim Shung Lee for his excellent hospitality during his stay at Department of Chemistry, Gyeongsang National University, Jinju, S. Korea.

11. References

(1) Moulton, B.; Zaworotko, M. J. *Chem. Rev.* **2001**, *101*, 1629.
(2) (a) Lehn, J. M. *Supramolecular Chemistry: Concepts and Perspectives*; VCH: Weinheim, Germany, 1995. (b) Zaworotko, M. J., Seddon, K. R., Eds. *Crystal Engineering: The Design and Application of Functional Solids*; Kluwer: Dordrecht, The Netherlands, 1999. (c) Tiekink, E. R. T., Vittal, J. J., Eds. *Frontiers in Crystal Engineering*; Wiley: Chichester, U.K., 2006. (d) Batten, S. R.; Neville, S. M.; Turner, D. R. *Coordination Polymers: Design, Analysis and Application*; Royal Society of Chemistry: Cambridge, U.K., 2009. (e) Atwood, J. L., Steed, J. W., Eds. *Encyclopedia of Supramolecular*

Chemistry; Dekker: New York, 2004; Vol. 6. (f) Atwood, J. L., Steed, J. W., Eds. *Encyclopedia of Supramolecular Chemistry*; Dekker: New York, 2004; Vol. 7. (g) Steed, J. W.; Atwood, J. L. *Supramolecular Chemistry*, 2nd ed.; Wiley: Chichester, U.K., 2009.

(3) (a) Yaghi, O. M.; Li, H.; Davis, C.; Richardson, D.; Groy, T. L. *Acc. Chem. Res.* **1998**, *31*, 474. (b) Janiak, C. *Dalton Trans* **2003**, 2781. (c) Long, J. R.; Yaghi, O. M. *Chem. Soc. Rev.* **2009**, *38*, 1213. (d) Robson, R. *Dalton Trans* **2008**, 5113. (e) Blake, A. J.; Champness, N. R.; Hubberstey, P.; Li, W.-S.; Withersby, M. A.; Schröder, M. *Coord. Chem. Rev.* **1999**, *183*, 117. (f) Swiegers, G. F.; Malefetse, T. J. *Chem. Rev.* **2000**, *100*, 3483. (g) Kitagawa, S.; Uemura, K. *Chem. Soc. Rev.* **2005**, *34*, 109. (h) Robin, A. Y.; Fromm, K. M. *Coord. Chem. Rev.* **2006**, *250*, 2127.

(4) Bailar, Jr. In *Preparative Inorganic Reactions*; Jolly, W. L., Eds.; Wiley Interscience: New York, 1964; Vol. 1, pp 1−27.

(5) (a) Chen, C.-T.; Suslick, K. S. *Coord. Chem. Rev.* **1993**, *128*, 293. (b) Khlobystov, A. N.; Blake, A. J.; Champness, N. R.; Lemenovskii, D. A.; Majouga, A. G.; Zyk, N. V.; Schröder, M. *Coord. Chem. Rev.* **2001**, *222*, 155. (c) Han, L.; Hong, M. *Inorg. Chem. Commun.* **2005**, *8*, 406. (d) Serrano, J. L.; Sierra, T. *Coord. Chem. Rev.* **2003**, *242*, 73. (e) Sokolov, A. N.; MacGillivray, L. R. *Cryst. Growth Des.* **2006**, *6*, 2615. (f) Hartgerink, J. D.; Zubarev, E. R.; Stupp, S. I. *Curr. Opin. Solid State Mater. Sci.* **2001**, *5*, 355. (g) Chen, C.-L.; Kang, B.-S.; Su, C.-Y. *Aust. J. Chem.* **2006**, *59*, 3. (h) Biradha, K.; Sarkar, M.; Rajput, L. *Chem. Commun.* **2006**, 4169.

(6) (a) Noshiranzadeh, N.; Ramazani, A.; Morsali, A.; Hunter, A. D.; Zeller, M. *Inorg. Chem. Commun.* **2007**, *10*, 738. (b) Xie, Y.-B.; Li, J.-R.; Bu, X.-H. *Aus. J. Chem.* **2006**, *59*, 34. (c) Zheng, Y.; Li, J.-R.; Du, M.; Zou, R.-Q.; Bu, X.-H. *Cryst. Growth Des.* **2005**, *5*, 215. (d) Hu, T.-L.; Li, J.-R.; Xie, Y.-B.; Bu, X.-H. *Cryst. Growth Des.* **2006**, *6*, 648. (e) Wang, J.-J.; Liu, C.-S.; Hu, T.-L.; Chang, Z.; Li, C.-Y.; Yan, L.-F.; Chen, P.-Q.; Bu, X.-H.; Wu, Q.; Zhao, L.-J.; Wang, Z.; Zhang, X.-Z. *CrystEngComm* **2008**, *10*, 681. (f) Liu, F.-C.; Zeng, Y.-F.; Zhao, J.-P.; Hu, B.-W.; Bu, X.-H.; Ribas, J.; Cano, J. *Inorg. Chem.* **2007**, *46*, 1520. (g) Li, D.; Zheng, L.; Zhang, Y.; Huang, J.; Gao, S.; Tang, W. *Inorg. Chem.* **2003**, *42*, 6123. (h) Shek, I. P. Y.; Wong, W.-T.; Gao, S.; Lau, T.-C. *New J. Chem.* **2002**, *26*, 1099. (i) Costin-Hogan, C. E.; Chen, C.-L.; Hughes, E.; Pickett, A.; Valencia, R.; Rath, N. P.; Beatty, A. M. *CrystEngComm* **2008**, *10*, 1910. (j) Dan, M.; Rao, C. N. R. *Chem.−Eur. J.* **2005**, *11*, 7102. (k) Dan, M.; Cheetham, A. K.; Rao, C. N. R. *Inorg. Chem.* **2006**, *45*, 8227. (l) Li, Y.; Huang, J.-S.; Xu, G.-B.; Zhu, N.; Zhou, Z.-Y.; Che, C.-M.; Wong, K.-Y. *Chem.−Eur. J.* **2004**, *10*, 3486. (m) Zuo, J.-L.; Fun, H.-K.; Chinnakali, K.; You, X.-Z.; Che, C.-M. *New J. Chem.* **1998**, 923. (n) Murugavel, R.; Sathiyendiran, M.; Pothiraja, R.; Walawalkar, M. G.; Mallah, T.; Riviere, E. *Inorg. Chem.* **2004**, *43*, 945. (o) Draper, N. D.; Batchelor, R. J.; Leznoff, D. B. *Cryst. Growth Des.* **2004**, *4*, 621. (p) Mund, G.; Vidovic, D.; Batchelor, R. J.; Britten, J. F.; Sharma, R. D.; Jones, C. H. W.; Leznoff, D. B. *Chem.−Eur. J.* **2003**, *9*, 4757. (q) Munakata, M.; Kuroda-Sowa, T.; Maekawa, M.; Hirota, A.; Kitagawa, S. *Inorg. Chem.* **1995**, *34*, 2705. (r) Ouyang, X.; Campana, C.; Dunbar, K. R. *Inorg. Chem.* **1996**, *35*, 7188. (s) Ye, Q.; Wang, X.-S.; Zhao, H.; Xiong, R.-G. *Tetrahedron-Asymmetr.* **2005**, *16*, 1595. (t) Groeneman, R. H.; MacGillivray, L. R.; Atwood, J. L. *Inorg. Chem.* **1999**, *38*, 208. (u) Brandys, M.-C.; Puddephatt, R. J. *J. Am. Chem. Soc.* **2001**, *123*, 4839. (v) Cunha-Silva, L.; Ahmad, R.; Hardie, M. J. *Aus. J. Chem.* **2006**, *59*, 40. (w) Szczepura, L. F.; Galloway, C. P.; Zheng, Y.; Han, P.; Rheingold, A. L.; Wilson, S. R.; Rauchfuss, T. B. *Angew. Chem., Int. Ed.* **1995**, *34*, 1890. (x) Shieh, M.; Hsu, M. H.; Sheu, W.-S.; Jang, L.-F.; Lin, S.-F.; Chu, Y.-Y.; Miu, C.-Y.; Lai, Y.-W.; Liu, H.-L.; Her, J. L. *Chem.−Eur. J.* **2007**, *13*, 6605.

(7) (a) Jouaiti, A.; Hosseini, M. W.; Kyritsakas, N. *Eur. J. Inorg. Chem.* **2003**, 57. (b) Mislin, G.; Graf, E.; Hosseini, M. W.; Cian, A. D.; Kyritsakas, N.; Fischer, J. *Chem. Commun.* **1998**, 2545.

(8) Schmaltz, B.; Jouaiti, A.; Hosseini, M. W.; Cian, A. D. *Chem. Commun.* **2001**, 1242.

(9) Jouaiti, A.; Hosseini, M. W.; Cian, A. D. *Chem. Commun.* **2000**, 1863.

(10) Ferlay, S.; Jouaiti, A.; Löi, M.; Hosseini, M. W.; Cian, A. D.; Turek, P. *New J. Chem.* **2003**, *27*, 1801.

(11) Feller, R. K.; Cheetham, A. K. *Dalton Trans.* **2008**, 2034.

(12) Carlucci, L.; Ciani, G.; Macchi, P.; Proserpio, D. M.; Rizzato, S. *Chem.−Eur. J.* **1999**, *5*, 237.

(13) Hagrman, D.; Hammond, R. P.; Haushalter, R.; Zubieta, J. *Chem. Mater.* **1998**, *10*, 2091.

(14) Withersby, M. A.; Blake, A. J.; Champness, N. R.; Hubberstey, P.; Wan-Sheung, Li; Schröder, M. *Angew. Chem., Int. Ed.* **1997**, *36*, 2327.

(15) Zaman, M. B.; Smith, M. D.; Loye, H.-C. z. *Chem. Mater.* **2001**, *13*, 3534.

(16) Choi, H. J.; Suh, M. P. *Inorg. Chem.* **1999**, *38*, 6309.

(17) Sun, C.-Y.; Zheng, X.-J.; Gao, S.; Li, L.-C.; Jin, L.-P. *Eur. J. Inorg. Chem.* **2005**, 4150.

(18) Kato, M.; Sah, A. K.; Tanase, T.; Mikuriya, M. *Inorg. Chem.* **2006**, *45*, 6646.

(19) Hagrman, D.; Zubieta, C.; Rose, D. J.; Zubieta, J.; Haushalter, R. C. *Angew. Chem., Int. Ed.* **1997**, *3*, 873.

(20) Kawata, S.; Kitagawa, S.; Kumagai, H.; Kudo, C.; Kamesaki, H.; Ishiyama, T.; Suzuki, R.; Kondo, M.; Katada, M. *Inorg. Chem.* **1996**, *35*, 4449.

(21) Leong, W. L.; Vittal, J. J. *Inorg. Chim. Acta* **2009**, *362*, 2189.

(22) Leong, W. L.; Vittal, J. J. *Cryst. Growth Des.* **2007**, *7*, 2112.

(23) Biradha, K.; Fujita, M. *Dalton Trans.* **2000**, 3805.

(24) ManuelQuesad; Prins, F.; Bill, E.; Kooijman, H.; Gamez, P.; Roubeau, O.; Spek, A. L.; Haasnoot, J. G.; Reedijk, J. *Chem.−Eur. J.* **2008**, *14*, 8486.

(25) Xiong, K.; Wu, M.; Zhang, Q.; Wei, W.; Yang, M.; Jiang, F.; Hong, M. *Chem. Commun.* **2009**, 1840.

(26) Matsuda, K.; Takayama, K.; Irie, M. *Chem. Commun.* **2001**, 363.

(27) Lee, E. Y.; Suh, M. P. *Angew. Chem., Int. Ed.* **2004**, *43*, 2798.

(28) Moon, H. R.; Kim, J. H.; Suh, M. P. *Angew. Chem., Int. Ed.* **2005**, *44*, 1261.

(29) (a) Takamizawa, S.; Nakata, E.-I.; Yokoyama, H.; Mochizuki, K.; Mori, W. *Angew. Chem., Int. Ed.* **2003**, *42*, 4331. (b) Takamizawa, S.; Nakata, E.-I.; Saito, T. *Angew. Chem., Int. Ed.* **2004**, *43*, 1368.

(30) Hu, S.; He, K.-H.; Zeng, M.-H.; Zou, H.-H.; Jiang, Y.-M. *Inorg. Chem.* **2008**, *47*, 5218.

(31) Cingolani, A.; Galli, S.; Masciocchi, N.; Pandolfo, L.; Pettinari, C.; Sironi, A. *J. Am. Chem. Soc.* **2005**, *127*, 6144.

(32) Brandon, E. J.; Rogers, R. D.; Burkhart, B. M.; Miller, J. S. *Chem.−Eur. J.* **1998**, *4*, 1938.

(33) Rittenberg, D. K.; Sugiura, K.-I.; Sakata, Y.; Guzei, I. A.; Rheingold, A. L.; Miller, J. S. *Chem.−Eur. J.* **1999**, *5*, 1874.

(34) (a) Sesto, R. E. D.; Arif, A. M.; Miller, J. S. *Inorg. Chem.* **2000**, *39*, 4894. (b) Mikami, S.; Sugiura, K.-I.; Maruta, T.; Maeda, Y.; Ohba, M.; Usuki, N.; Ōkawa, H.; Akutagawa, T.; Nisihara, S.; Nakamura, T.; Iwasaki, K.; Miyazaki, N.; Hino, S.; Asato, E.; Miller, J. S.; Sakata, Y. *J. Chem. Soc., Dalton Trans.* **2001**, 448. (c) Dawe, L. N.; Miglioi, J.; Turnbow, L.; Taliaferro, M. L.; Shum, W. W.; Bagnato, J. D.; Zakharov, L. N.; Rheingold, A. L.; Arif, A. M.; Fourmigué, M.; Miller, J. S. *Inorg. Chem.* **2005**, *44*, 7530. (d) Pokhodnya, K. I.; Bonner, M.; DiPasquale, A. G.; Rheingold, A. L.; Her, J.-H.; Stephens, P. W.; Park, J.-W.; Kennon, B. S.; Arif, A. M.; Miller, J. S. *Inorg. Chem.* **2007**, *46*, 2471.

(35) Sun, X.-R.; Liang, J.-L.; Che, C.-M.; Zhu, N.; Zhang, X. X.; Gao, S. *Chem. Commun.* **2002**, 2090.

(36) Yuan, M.; Zhao, F.; Zhang, W.; Pan, F.; Wang, Z.-M.; Gao, S. *Chem.−Eur. J.* **2007**, *13*, 2937.

(37) Genre, C.; Matouzenko, G. S.; Jeanneau, E.; Luneau, D. *New J. Chem.* **2006**, *30*, 1669.

(38) Murray, K. S. *Aust. J. Chem.* **2009**, *62*, 1081.

(39) (a) Gütlich, P.; Goodwin, H. A. *Spin Crossover in Transition Metal Compounds I*; Topics in Current Chemistry, Vol. 233; Springer: Berlin, 2004. (b) Gütlich, P.; Goodwin, H. A. *Spin Crossover in Transition Metal Compounds I*; Topics in Current Chemistry, Vol. 234; Springer: Berlin, 2004.

(40) Takaishi, S.; Yamashita, M.; Matsuzaki, H.; Okamoto, H.; Tanaka, H.; Kuroda, S.-I.; Goto, A.; Shimizu, T.; Takenobu, T.; Iwasa, Y. *Chem.−Eur. J.* **2008**, *14*, 472.

(41) (a) Yamashita, M.; Takaishi, S.; Kobayashi, A.; Kitagawa, H.; Matsuzaki, H.; Okamotoc, H. *Coord. Chem. Rev.* **2006**, *250*, 2335. (b) Yamashita, M.; Yokoyama, K.; Furukawa, S.; Manabe, T.; Ono, T.; Nakata, K.; Kachi-Terajima, C.; Iwahori, F.; Ishii, T.; Miyasaka, H.; Sugiura, K.; Matsuzaki, H.; Kishida, H.; Okamoto, H.; Tanaka, H.; Hasegawa, Y.; Marumoto, K.; Ito, H.; Kuroda, S. *Inorg. Chem.* **2002**, *41*, 1998. (c) Takaishi, S.; Miyasaka, H.; Sugiura, K.-I.; Yamashita, M.; Hiroyuki, M.; Kishida, H.; Okamoto, H.; Tanaka, H.; Marumoto, K.; Ito, H.; Kuroda, S.-I.; Takami, T. *Angew. Chem., Int. Ed.* **2004**, *43*, 3171. (d) Wu, H.; Kawakami, D.; Sasaki, M.; Xie, J.; Takaishi, S.; Kajiwara, T.; Miyasaka, H.; Yamashita, M.; Matsuzaki, H.; Okamoto, H. *Inorg. Chem.* **2007**, *46*, 7410.

(42) Vaughn, A. E.; Barnes, C. L.; Duval, P. B. *Angew. Chem., Int. Ed.* **2007**, *46*, 6622.

(43) Katz, M. J.; Kaluarachchi, H.; Batchelor, R. J.; Bokov, A. A.; Ye, Z.-G.; Leznoff, D. B. *Angew. Chem., Int. Ed.* **2007**, *46*, 8804.

(44) Amiri, M. G.; Mahmoudi, G.; Morsali, A.; Hunter, A. D.; Zeller, M. *CrystEngComm* **2007**, *9*, 686.

(45) Banfi, S.; Carlucci, L.; Caruso, E.; Ciani, G.; Proserpio, D. M. *J. Chem. Soc., Dalton Trans.* **2002**, 2714.

(46) Ma, C.-B.; Chen, C.-N.; Liu, Q.-T. *CrystEngComm* **2005**, *7*, 650.

(47) Muthu, S.; Ni, Z.; Vittal, J. J. *Inorg. Chim. Acta* **2005**, *358*, 595.

(48) (a) Horikoshi, R.; Mochida, T.; Maki, N.; Yamada, S.; Moriyama, H. *J. Chem. Soc., Dalton Trans.* **2002**, 28. (b) Jin, C.-M.; Chen, Z.-F.; Mei, H.-F.; Shi, X.-K. *J. Mol. Struct.* **2009**, *921*, 58.

(49) Qin, Z.; Jennings, M. C.; Puddephatt, R. J. *Chem. Commun.* **2002**, 354.
(50) Zhang, X.-M.; Tong, M.-L.; Gong, M.-L.; Chen, X.-M. *Eur. J. Inorg. Chem.* **2003**, 138.
(51) Carlucci, L.; Ciani, G.; Gramaccioli, A.; Proserpio, D. M.; Rizzato, S. *CrystEngComm* **2000**, *2*, 154.
(52) Li, Y.-H.; Su, C.-Y.; Goforth, A. M.; Shimizu, K. D.; Gray, K. D.; Smith, M. D.; Loye, H.-C. z.616 *Chem. Commun.* **2003**, 1630.
(53) Han, L.; Zhou, Y. *Inorg. Chem. Commun.* **2008**, *11*, 385.
(54) Peedikakkal, A. M. P.; Vittal, J. J. *Cryst. Growth Des.* **2008**, *8*, 375.
(55) Cheng, A.-L.; Liu, N.; Yue, Y.-F.; Jiang, Y.-W.; Gao, E.-Q.; Yan, C.-H.; He, M.-Y. *Chem. Commun.* **2007**, 407.
(56) Cheng, A.-L.; Ma, Y.; Zhang, J.-Y.; Gao, E.-Q. *Dalton Trans.* **2008**, 1993.
(57) Ma, Y.; Cheng, A.-L.; Zhang, J.-Y.; Yue, Q.; Gao, E.-Q. *Cryst. Growth Des.* **2009**, *9*, 867.
(58) Wang, X.-L.; Qin, C.; Wang, E.-B.; Xu, L. *Cryst. Growth Des.* **2006**, *6*, 2061.
(59) Li, G.; Zhu, C.; Xi, X.; Cui, Y. *Chem. Commun.* **2009**, 2118.
(60) Brown, K.; Zolezzi, S.; Aguirre, P.; Venegas-Yazigi, D.; Paredes-García, V.; Baggio, R.; Novak, M. A.; Spodine, E. *Dalton Trans.* **2009**, 1422.
(61) Tang, Y.-Z.; Huang, X.-F.; Song, Y.-M.; Chan, P. W. H.; Xiong, R.-G. *Inorg. Chem.* **2006**, *45*, 4868.
(62) Huang, X.-F.; Li, Y.-H.; Wu, Q.; Ye, Q.; Xiong, R.-G. *Inorg. Chim. Acta* **2005**, *358*, 2097.
(63) Matouzenko, G. S.; Perrin, M.; Guennic, B. L.; Genre, C.; Molnár, G.; Bousseksou, A.; Borshch, S. A. *Dalton Trans.* **2007**, 934.
(64) (a) Teo, P.; Koh, L. L.; Hor, T. S. A. *Chem. Commun.* **2007**, 4221. (b) Teo, P.; Koh, L. L.; Hor, T. S. A. *Inorg. Chem.* **2008**, *47*, 9561. (c) Teo, P.; Koh, L. L.; Hor, T. S. A. *Inorg. Chem.* **2008**, *47*, 6464. (d) Bu, X.-H.; Liu, H.; Du, M.; Wong, K. M.-C.; Yam, V. W.-W.; Shionoya, M. *Inorg. Chem.* **2001**, *40*, 4143. (e) Chen, D.; Lai, C. S.; Tiekink, E. R. T. *CrystEngComm* **2006**, *8*, 51. (f) Biradha, K.; Fujita, M. *J. Incl. Phenom. Macro.* **2001**, *49*, 201. (g) Rajput, L.; Biradha, K. *Polyhedron* **2008**, *27*, 1248. (h) Stephenson, M. D.; Hardie, M. J. *Cryst. Growth Des.* **2006**, *6*, 423. (i) Cunha-Silva, L.; Ahmad, R.; Carr, M. J.; Franken, A.; Kennedy, J. D.; Hardie, M. J. *Cryst. Growth Des.* **2007**, *7*, 658. (j) Liu, Y.-J.; Xiong, R.-G.; You, X.-Z.; Che, C.-M. *Z. Anorg. Allg. Chem.* **2004**, *630*, 2761. (k) Jin, Y.; Lee, H.-I.; Pyo, M.; Lah, M. S. *Dalton Trans.* **2005**, 797. (l) Murugavel, R.; Korah, R. *Inorg. Chem.* **2007**, *46*, 11048. (m) Miyasaka, H.; Campos-Fernández, C. S.; Galán-Mascarós, J. R.; Dunbar, K. R. *Inorg. Chem.* **2000**, *39*, 5870. (n) Chen, Z.-F.; Zhang, Z.-L.; Tan, Y.-H.; Tang, Y.-Z.; Fun, H.-K.; Zhou, Z.-Y.; Abrahams, B. F.; Liang, H. *CrystEngComm* **2008**, *10*, 217. (o) Kim, H. J.; Jin, Y.; Seo, J.; Lee, J.-E.; Lee, J. Y.; Lee, S. S. *Inorg. Chem. Commun.* **2006**, *9*, 1040. (p) Brandys, M.-C.; Puddephatt, R. J. *Chem. Commun.* **2001**, 1508. (q) Hou, L.; Li, D.; Shi, W.-J.; Yin, Y.-G.; Ng, S. W. *Inorg. Chem.* **2005**, *44*, 7825.
(65) (a) Albrecht, M. *Chem. Rev.* **2001**, *101*, 3457. (b) Piguet, C.; Bernardinelli, G.; Hopfgartner, G. *Chem. Rev.* **1997**, *97*, 2005.
(66) (a) Zheng, X.-D.; Lu, T.-B. *CrystEngComm* **2010**, *12*, 324. (b) Miguel, P. J. S.; Amo-Ochoa, P.; Castillo, O.; Houlton, A.; Zamora, F. Supramolecular chemistry of metal−nucleobase complexes. In *Metal Complex: DNA Interactions*; Hadjiliadis, N., Sletten, E., Eds.; Wiley: Chichester, U.K., 2009; pp 95−132.
(67) Biradha, K.; Seward, C.; Zaworotko, M. J. *Angew. Chem., Int. Ed.* **1999**, *38*, 492.
(68) Moulton, B.; Zaworotko, M. J. Rational design of polar solid. In *Crystal Engineering: From Molecules and Crystals to Materials*; Braga, D., Grepioni, F., Orphen, A. G., Eds.; Kluwer: Boston, 1999; pp 311−380.
(69) Ezuhara, T.; Endo, K.; Aoyama, Y. *J. Am. Chem. Soc.* **1999**, *121*, 3279.
(70) (a) Zhang, Q.; Bu, X.; Lin, Z.; Biasini, M.; Beyermann, W. P.; Feng, P. *Inorg. Chem.* **2007**, *46*, 7262. (b) Zhang, W.; Wang, Z.-Q.; Sato, O.; Xiong, R.-G. *Cryst. Growth Des.* **2009**, *9*, 2050. (c) Rueff, J.-M.; Caignaert, V.; Leclaire, A.; Simon, C.; Haelters, J.-P.; Jaffres, P.-A. *CrystEngComm* **2009**, *11*, 556. (d) Cordes, D. B.; Sharma, C. V. K.; Rogers, R. D. *Cryst. Growth Des.* **2007**, *7*, 1943. (e) Wang, Y.-T.; Tong, M.-L.; Fan, H.-H.; Wang, H.-Z.; Chen, X.-M. *Dalton Trans.* **2005**, 424. (f) Balamurugan, V.; Mukherjee, R. *CrystEngComm* **2005**, *7*, 337. (g) Caradoc-Davies, P. L.; Hanton, L. R. *Chem. Commun.* **2001**, 1098. (h) Hong, M.; Su, W.; Cao, R.; Fujita, M.; Lu, J. *Chem.−Eur. J.* **2000**, *6*, 427. (i) Gao, E.-Q.; Yue, Y.-F.; Bai, S.-Q.; He, Z.; Yan, C.-H. *J. Am. Chem. Soc.* **2004**, *126*, 1419.
(71) (a) Chen, J.-Q.; Cai, Y.-P.; Fang, H.-C.; Zhou, Z.-Y.; Zhan, X.-L.; Zhao, G.; Zhang, Z. *Cryst. Growth Des.* **2009**, *9*, 1605. (b) Jia, W.-G.; Huang, Y.-B.; Lin, Y.-J.; Wang, G.-L.; Jin, G.-X. *Eur. J. Inorg. Chem.* **2008**, 4063. (c) Mondal, R.; Basu, T.; Sadhukhan, D.; Chattopadhyay, T.; Bhunia, M. K. *Cryst. Growth Des.* **2009**, *9*, 1095. (d) Tong, M.-L.; Chen, X.-M.; Ye, B.-H.; Ng, S. W. *Inorg. Chem.* **1998**, *37*, 5278. (e) Colacio, E.; Ghazi, M.; Kiveks, R.; Moreno, J. M. *Inorg. Chem.* **2000**, *39*, 2882. (f) Jiang, L.; Feng, X.-L.; Su, C.-Y.; Chen, X.-M.; Lu, T.-B. *Inorg. Chem.* **2007**, *46*, 2637. (g) Song, X.; Zhou, X.; Liu, W.; Dou, W.; Ma, J.; Tang, X.; Zheng, J. *Inorg. Chem.* **2008**, *47*, 11501. (h) Wen, L.-L.; Dang, D.-B.; Duan, C.-Y.; Li, Y.-Z.; Tian, Z.-F.; Meng, Q.-J. *Inorg. Chem.* **2005**, *44*, 7161. (i) Qi, Y.; Wang, Y.; Hu, C.; Cao, M.; Mao, L.; Wang, E. *Inorg. Chem.* **2003**, *42*, 8519. (j) Kaes, C.; Hosseini, M. W.; Rickard, C. E. F.; Skelton, B. W.; White, A. H. *Angew. Chem., Int. Ed.* **1998**, *37*, 920. (k) Liang, J.; Wu, B.; Jia, C.; Yang, X.-J. *CrystEngComm* **2009**, *11*, 975. (l) Ni, W.-X.; Li, M.; Zhan, S.-Z.; Hou, J.-Z.; Li, D. *Inorg. Chem.* **2009**, *48*, 1433. (m) Ou, G.-C.; Jiang, L.; Feng, X.-L.; Lu, T.-B. *Inorg. Chem.* **2008**, *47*, 2710.
(72) Wheaton, C. A.; Puddephatt, R. J. *Angew. Chem., Int. Ed.* **2007**, *46*, 4461.
(73) (a) Li, X.-Z.; Li, M.; Li, Z.; Hou, J.-Z.; Huang, X.-C.; Li, D. *Angew. Chem., Int. Ed.* **2008**, *47*, 6371. (b) Tuna, F.; Hamblin, J.; Clarkson, G.; Errington, W.; Alcock, N. W.; Hannon, M. J. *Chem.−Eur. J.* **2002**, *8*, 4957. (c) Tabellion, F. M.; Seidel, S. R.; Arif, A. M.; Stang, P. J. *J. Am. Chem. Soc.* **2001**, *123*, 11982.
(74) (a) Vittal, J. J. Hydrogen-bonded coordination polymeric structures. In *Frontiers In Crystal Engineering*; Tiekink, E. R. T.; Vittal, J. J., Eds.; Wiley: Chichester, U. K., 2006; pp 297−320 and references therein. (b) Ganguly, R.; Sreenivasulu, B.; Vittal, J. J. *Coord. Chem. Rev.* **2008**, *252*, 1027. (b) Yang, X.; Wu, D.; Ranford, J. D.; Vittal, J. J. *Cryst. Growth Des.* **2005**, *5*, 41. (c) Yang, C.-T.; Vetrichelvan, M.; Yang, X.; Moubaraki, B.; Murray, K. S.; Vittal, J. J. *Dalton Trans.* **2004**, 113.
(75) Lü, Z.; Zhang, D.; Gao, S.; Zhu, D. *Inorg. Chem. Commun.* **2005**, *8*, 746.
(76) Chen, X.-D.; Mak, T. C. W. *Dalton Trans.* **2005**, 3646.
(77) Qi, Y.; Luo, F.; Batten, S. R.; Che, Y.-X.; Zheng, J.-M. *Cryst. Growth Des.* **2008**, *8*, 2806.
(78) Zhang, F.; Yajima, T.; Li, Y.-Z.; Xu, G.-Z.; Chen, H.-L.; Liu, Q.-T.; Yamauchi, O. *Angew. Chem., Int. Ed.* **2005**, *44*, 3402.
(79) (a) Chen, C.-L.; Zhang, Q.; Yao, J.-H.; Zhang, J.-Y.; Kang, B.-S.; Su, C.-Y. *Inorg. Chim. Acta* **2008**, *361*, 2934. (b) Becker, G.; Eschbach, B.; Seidler, O. M. U. N. *Z. Anorg. Allg. Chem.* **1994**, *620*, 1381. (c) Bartlett, R. A.; Olmstead, M. M.; Power, P. P. *Inorg. Chem.* **1986**, *25*, 1243. (d) Plasseraud, L.; Maid, H.; Hampel, F.; Saalfrank, R. W. *Chem.−Eur. J.* **2001**, *7*, 4007. (e) Zheng, X.-D.; Jiang, L.; Feng, X.-L.; Lu, T.-B. *Inorg. Chem.* **2008**, *47*, 10858.
(80) (a) Luan, X.-J.; Wang, Y.-Y.; Li, D.-S.; Liu, P.; Hu, H.-M.; Shi, Q.-Z.; Peng, S.-M. *Angew. Chem., Int. Ed.* **2005**, *44*, 3864. (b) Luan, X.-J.; Cai, X.-H.; Wang, Y.-Y.; Li, D.-S.; Wang, C.-J.; Liu, P.; Hu, H.-M.; Shi, Q.-Z.; Peng, S.-M. *Chem.−Eur. J.* **2006**, *12*, 6281.
(81) Jouaiti, A.; Hosseini, M. W.; Kyritsakas, N.; Grosshans, P.; Planeix, J.-M. *Chem. Commun.* **2006**, 3078.
(82) Mamula, O.; Zelewsky, A. V.; Bark, T.; Bernardinelli, G. *Angew. Chem., Int. Ed.* **1999**, *38*, 2945.
(83) Han, L.; Valle, H.; Bu, X. *Inorg. Chem.* **2007**, *46*, 1511.
(84) Lee, J. W.; Kim, E. A.; Kim, Y. J.; Lee, Y.-A.; Pak, Y.; Jung, O.-S. *Inorg. Chem.* **2005**, *44*, 3151.
(85) Chen, X.-M.; Liu, G.-F. *Chem.−Eur. J.* **2002**, *8*, 4811.
(86) Han, Z.-B.; Cheng, X.-N.; Chen, X.-M. *Cryst. Growth Des.* **2005**, *5*, 695.
(87) Zhang, L.-Y.; Liu, G.-F.; Zheng, S.-L.; Ye, B.-H.; Zhang, X.-M.; Chen, X.-M. *Eur. J. Inorg. Chem.* **2003**, 2965.
(88) Wang, R.; Xu, L.; Li, X.; Li, Y.; Shi, Q.; Zhou, Z.; Hong, M.; Chan, A. S. C. *Eur. J. Inorg. Chem.* **2004**, 1595.
(89) Wang, R.; Xu, L.; Ji, J.; Shi, Q.; Li, Y.; Zhou, Z.; Hong, M.; Chan, A. S. C. *Eur. J. Inorg. Chem.* **2005**, 751.
(90) Lee, H. Y.; Park, J.; Lah, M. S.; Hong, J.-I. *Cryst. Growth Des.* **2008**, *8*, 587.
(91) Chen, C.-Y.; Cheng, P.-Y.; Wu, H.-H.; Lee, H. M. *Inorg. Chem.* **2007**, *46*, 5691.
(92) Dong, Y.-B.; Sun, T.; Ma, J.-P.; Zhao, X.-X.; Huang, R.-Q. *Inorg. Chem.* **2006**, *45*, 10613.
(93) Carlucci, L.; Ciani, G.; Gudenberg, D. W. V.; Proserpio, D. M. *Inorg. Chem.* **1997**, *36*, 3812.
(94) Mohr, F.; Jennings, M. C.; Puddephatt, R. J. *Angew. Chem., Int. Ed.* **2004**, *43*, 969.
(95) Jouaiti, A.; Hosseini, M. W.; Kyritsakas, N. *Chem. Commun.* **2003**, 472.
(96) Peng, R.; Li, D.; Wu, T.; Zhou, X.-P.; Ng, S. W. *Inorg. Chem.* **2006**, *45*, 4035.
(97) Sarkar, M.; Biradha, K. *CrystEngComm* **2004**, *6*, 310.
(98) Bowyer, P. K.; Porter, K. A.; Rae, A. D.; Willis, A. C.; Wild, S. B. *Chem. Commun.* **1998**, 1153.
(99) Tian, Z.; Duan, H.; Xuan, F.; Ren, X. *Inorg. Chem. Commun.* **2009**, *12*, 417.
(100) Meng, X.; Li, J.; Hou, H.; Song, Y.; Fan, Y.; Zhu, Y. *J. Mol. Struct.* **2008**, *891*, 305.

(101) Cui, Y.; Ngo, H. L.; Lin, W. *Chem. Commun.* **2003**, 1388.
(102) Wu, C.-D.; Ngo, H. L.; Lin, W. *Chem. Commun.* **2004**, 1588.
(103) Wu, C.-D.; Lin, W. *Inorg. Chem.* **2005**, *44*, 1178.
(104) (a) Wu, C.-D.; Lin, W. *Dalton Trans.* **2006**, 4563. (b) Wu, C.-D.; Zhang, L.; Lin, W. *Inorg. Chem.* **2006**, *45*, 7278.
(105) (a) Cui, Y.; Ngo, H. L.; White, P. S.; Lin, W. *Chem. Commun.* **2003**, 994. (b) Cui, Y.; Ngo, H. L.; White, P. S.; Lin, W. *Inorg. Chem.* **2003**, *42*, 652.
(106) Grosshans, P.; Jouaiti, A.; Bulach, V.; Planeix, J.-M.; Hosseini, M. W.; Nicoud, J.-F. *Chem. Commun.* **2003**, 1336.
(107) Liu, J.-Q.; Wang, Y.-Y.; Liu, P.; Dong, Z.; Shi, Q.-Z.; Batten, S. R. *CrystEngComm* **2009**, *11*, 1207.
(108) Huang, X.-C.; Zhang, J.-P.; Lin, Y.-Y.; Chen, X.-M. *Chem. Commun.* **2005**, 2232.
(109) Hou, J.-Z.; Li, M.; Li, Z.; Zhan, S.-Z.; Huang, X.-C.; Li, D. *Angew. Chem., Int. Ed.* **2008**, *47*, 1711.
(110) (a) Ciurtin, D. M.; Pschirer, N. G.; Smith, M. D.; Bunz, U. H. F.; Loye, H.-C. z. *Chem. Mater.* **2001**, *13*, 2743. (b) Sailaja, S.; Rajasekharan, M. V. *Inorg. Chem.* **2000**, *39*, 4586. (c) Niu, C.-Y.; Wu, B.-L.; Zheng, X.-F.; Zhang, H.-Y.; Li, Z.-J.; Hou, H.-W. *Dalton Trans.* **2007**, 5710.
(111) Cui, Y.; Lee, S. J.; Lin, W. *J. Am. Chem. Soc.* **2003**, *125*, 6014.
(112) Byrne, P.; Lloyd, G. O.; Anderson, K. M.; Clarke, N.; Steed, J. W. *Chem. Commun.* **2008**, 3720.
(113) Wang, X.-L.; Qin, C.; Wang, E.-B.; Xu, L.; Su, Z.-M.; Hu, C.-W. *Angew. Chem., Int. Ed.* **2004**, *43*, 5036.
(114) Hirsch, K. A.; Wilson, S. R.; Moore, J. S. *Chem. Commun.* **1998**, 13.
(115) (a) Han, L.; Hong, M.; Wang, R.; Luo, J.; Lin, Z.; Yuan, D. *Chem. Commun.* **2003**, 2580. (b) Wang, X.-L.; Qin, C.; Wang, E.-B.; Li, Y.-G.; Su, Z.-M. *Chem. Commun.* **2005**, 5450. (c) Bu, X.-H.; Chen, W.; Du, M.; Biradha, K.; Wang, W.-Z.; Zhang, R.-H. *Inorg. Chem.* **2002**, *41*, 437. (d) Kaczorowski, T.; Justyniak, I.; Lipinska, T.; Lipkowski, J.; Lewinski, J. *J. Am. Chem. Soc.* **2009**, *131*, 5393. (e) Sun, Y.-Q.; Zhang, J.; Chen, Y.-M.; Yang, G.-Y. *Angew. Chem., Int. Ed.* **2005**, *44*, 5814. (f) Martin, D. P.; Staples, R. J.; LaDuca, R. L. *Inorg. Chem.* **2008**, *47*, 9754. (g) Carlucci, L.; Ciani, G.; Proserpio, D. M.; Rizzato, S. *Chem. Commun.* **2000**, 1319.
(116) Shyu, E.; Supkowski, R. M.; LaDuca, R. L. *Inorg. Chem.* **2009**, *48*, 2723.
(117) Xiao, D.-R.; Li, Y.-G.; Wang, E.-B.; Fan, L.-L.; An, H.-Y.; Su, Z.-M.; Xu, L. *Inorg. Chem.* **2007**, *46*, 4158.
(118) (a) Barnett, S. A.; Champness, N. R. *Coord. Chem. Rev.* **2003**, *246*, 145. (b) Khlobystov, A. N.; Blake, A. J.; Champness, N. R.; Lemenovskii, D. A.; Majouga, A. G.; Zyk, N. V.; Schröder, M. *Coord. Chem. Rev.* **2001**, *222*, 155.
(119) Losier, P.; Zaworotko, M. J. *Angew. Chem., Int. Ed.* **1996**, *35*, 2779.
(120) Hennigar, T. L.; MacQuarrie, D. C.; Losier, P.; Rogers, R. D.; Zaworotko, M. J. *Angew. Chem., Int. Ed.* **1997**, *36*, 972.
(121) Jung, O.-S.; Park, S. H.; Kim, K. M.; Jang, H. G. *Inorg. Chem.* **1998**, *37*, 5781.
(122) McManus, G. J.; Perry, J. J.; Perry, M.; Wagner, B. D.; Zaworotko, M. J. *J. Am. Chem. Soc.* **2007**, *129*, 9094.
(123) Ciurtin, D. M.; Dong, Y.-B.; Smith, M. D.; Barclay, T.; Loye, H.-C. z. *Inorg. Chem.* **2001**, *40*, 2825.
(124) Ohmori, O.; Kawano, M.; Fujita, M. *CrystEngComm* **2004**, *6*, 51.
(125) Min, D.; Cho, B.-Y.; Lee, S. W. *Inorg. Chim. Acta* **2006**, *359*, 577.
(126) Sui, B.; Zhao, W.; Ma, G.; Okamura, T.-a.; Fan, J.; Li, Y.-Z.; Tang, S.-H.; Sun, W.-Y.; Ueyama, N. *J. Mater. Chem.* **2004**, *14*, 1631.
(127) Withersby, M. A.; Blake, A. J.; Champness, N. R.; Paul, A.; Cooke; Hubberstey, P.; Li, W.-S.; Schröder, M. *Inorg. Chem.* **1999**, *38*, 2259.
(128) Wang, R.; Hong, M.; Yuan, D.; Sun, Y.; Xu, L.; Luo, J.; Cao, R.; Chan, A. S. C. *Eur. J. Inorg. Chem.* **2004**, 37.
(129) Lee, J. W.; Kim, E. A.; Kim, Y. J.; Lee, Y.-A.; Pak, Y.; Jung, O.-S. *Inorg. Chem.* **2005**, *44*, 3151.
(130) Yang, X.; Rivers, J. H.; McCarty, W. J.; Wiester, M.; Jones, R. A. *New J. Chem.* **2008**, *32*, 790.
(131) Venkataraman, D.; Lee, S.; Moore, J. S.; Zhang, P.; Hirsch, K. A.; Gardner, G. B.; Covey, A. C.; Prentice, C. L. *Chem. Mater.* **1996**, *8*, 2030.
(132) Knoeppel, D. W.; Shore, S. G. *Inorg. Chem.* **1996**, *35*, 5328.
(133) Lescouezec, R.; Vaissermann, J.; Toma, L. M.; Carrasco, R.; Lloret, F.; Julve, M. *Inorg. Chem.* **2004**, *43*, 2234.
(134) Zhang, Y.-Z.; Gao, S.; Wang, Z.-M.; Su, G.; Sun, H.-L.; Pan, F. *Inorg. Chem.* **2005**, *44*, 4534.
(135) Decurtins, S.; Gross, M.; Schmalle, H. W.; Ferlay, S. *Inorg. Chem.* **1998**, *37*, 2443.
(136) Domasevitch, K. V.; Guralskiy, I. A.; Solntsev, P. V.; Rusanov, E. B.; Krautscheid, H.; Howard, J. A. K.; Chernega, A. N. *Dalton Trans.* **2007**, 3140.
(137) Zheng, S.-L.; Tong, M.-L.; Yu, X.-L.; Chen, X.-M. *Dalton Trans.* **2001**, 586.
(138) Gong, Y.; Wang, R.; Yuan, D.; Su, W.; Huang, Y.; Yue, C.; Jiang, F.; Hong, M. *Polyhedron* **2007**, *26*, 5309.
(139) Sha, J.; Peng, J.; Zhang, Y.; Pang, H.; Tian, A.; Zhang, P.; Liu, H. *Cryst. Growth Des.* **2009**, *9*, 1708.
(140) Kobayashi, A.; Kitagawa, H. *J. Am. Chem. Soc.* **2006**, *128*, 12066.
(141) Akhriff, Y.; Server-Carrió, J.; Sancho, A.; García-Lozano, J.; Escrivá, E.; Folgado, J. V.; Soto, L. *Inorg. Chem.* **1999**, *38*, 1174.
(142) Batten, S. R.; Harris, A. R.; Jensen, P.; Murray, K. S.; Ziebell, A. *Dalton Trans.* **2000**, 3829.
(143) Yaghi, O. M.; Li, H.; Groy, T. L. *Inorg. Chem.* **1997**, *36*, 4292.
(144) Domasevitch, K. V.; Enright, G. D.; Moulton, B.; Zaworotko, M. J. *J. Solid State Chem.* **2000**, *152*, 280.
(145) Tong, M.-L.; Chen, H.-J.; Chen, X.-M. *Inorg. Chem.* **2000**, *39*, 2235.
(146) Zhang, L.-Y.; Zhang, J.-P.; Lin, Y.-Y.; Chen, X.-M. *Cryst. Growth Des.* **2006**, *6*, 1684.
(147) Hsu, G.-Y.; Chen, C.-W.; Cheng, S.-C.; Lin, S.-H.; Wei, H.-H.; Lee, C.-J. *Polyhedron* **2005**, *24*, 487.
(148) Jin, S.-W.; Chen, W.-Z. *Polyhedron* **2007**, *26*, 3074.
(149) Gamez, P.; Hoog, P. D.; Roubeau, O.; Lutz, M.; Driessen, W. L.; Spek, A. L.; Reedijk, J. *Chem. Commun.* **2002**, 1488.
(150) Song, X.-Q.; Liu, W.-S.; Dou, W.; Zheng, J.-R.; Tang, X.-L.; Zhang, H.-R.; Wang, D.-Q. *Dalton Trans.* **2008**, 3582.
(151) Beauchamp, D. A.; Loeb, S. J. *Dalton Trans.* **2007**, 4760.
(152) Ohi, H.; Tachi, Y.; Itoh, S. *Inorg. Chem.* **2004**, *43*, 4561.
(153) Ma, J.-F.; Yang, J.; Li, L.; Zheng, G.-L.; Liu, J.-F. *Inorg. Chem. Commun.* **2003**, *6*, 581.
(154) Plater, M. J.; Foreman, M. R. S. J.; Coronado, E.; Gómez-Garcia, C. J.; Slawin, A. M. Z. *Dalton Trans.* **1999**, 4209.
(155) (a) Kutasi, A. M.; Batten, S. R.; Harris, A. R.; Moubaraki, B.; Murray, K. S. *CrystEngComm* **2002**, *4*, 202. (b) Madalan, A. M.; Paraschiv, C.; Sutter, J.-P.; Schmidtmann, M.; Müller, A.; Andruh, M. *Cryst. Growth Des.* **2005**, *5*, 707.
(156) Field, L. M.; Morn, M. C.; Lahti, P. M.; Palacio, F.; Paduan-Filho, A.; Oliveira, N. F. *Inorg. Chem.* **2006**, *45*, 2562.
(157) Toh, N. L.; Nagarathinam, M.; Vittal, J. J. *Angew. Chem., Int. Ed.* **2004**, *44*, 2237.
(158) Nagarathinam, M.; Vittal, J. J. *Angew. Chem., Int. Ed.* **2006**, *45*, 4337.
(159) Papaefstathiou, G. S.; Georgiev, I. G.; Friscic, T.; MacGillivray, L. R. *Chem. Commun.* **2005**, 3974.
(160) Tong, M.-L.; Chen, X.-M.; Ng, S. W. *Inorg. Chem. Commun.* **2000**, *3*, 436.
(161) Lu, J.; Yu, C.; Niu, T.; Paliwala, T.; Crisci, G.; Somosa, F.; Jacobson, A. J. *Inorg. Chem.* **1998**, *37*, 4637.
(162) Conerney, B.; Jensen, P.; Kruger, P. E.; Moubaraki, B.; Murray, K. S. *CrystEngComm* **2003**, *5*, 454.
(163) Zhu, L.-G.; Kitagawa, S.; Miyasaka, H.; Chang, H.-C. *Inorg. Chim. Acta* **2003**, *355*, 121.
(164) Zhang, G.; Yang, G.; Ma, J. S. *Cryst. Growth Des.* **2006**, *6*, 1897.
(165) Sun, Y.; Wang, Z.; Zhang, H.; Cao, Y.; Zhang, S.; Chen, Y.; Huang, C.; Yu, X. *Inorg. Chim. Acta* **2007**, *360*, 2565.
(166) Chu, Q.; Swenson, D. C.; MacGillivray, L. R. *Angew. Chem., Int. Ed.* **2005**, *44*, 3569.
(167) Huang, X.-C.; Zhang, J.-P.; Chen, X.-M. *Cryst. Growth Des.* **2006**, *6*, 1194.
(168) Blake, A. J.; Baum, G.; Champness, N. R.; Chung, S. S. M.; Cooke, P. A.; Fenske, D.; Khlobystov, A. N.; Lemenovskii, D. A.; Li, W.-S.; Schröder, M. *Dalton Trans.* **2000**, 4285.
(169) Liu, C.-S.; Wang, J.-J.; Chang, Z.; Yan, L.-F.; Hu, T.-L. *Z. Anorg. Allg. Chem.* **2009**, *635*, 523.
(170) Blake, A. J.; Champness, N. R.; Khlobystov, A.; Lemenovskii, D. A.; Li, W.-S.; Schröder, M. *Chem. Commun.* **1997**, 2027.
(171) Withersby, M. A.; Blake, A. J.; Champness, N. R.; Paul, A.; Cooke; Hubberstey, P.; Schröder, M. *J. Am. Chem. Soc.* **2000**, *122*, 4044.
(172) Shi, Z.; Gu, X.; Peng, J.; Yu, X.; Wang, E. *Eur. J. Inorg. Chem.* **2006**, 385.
(173) Li, X.-J.; Cao, R.; Bi, W.-H.; Wang, Y.-Q.; Wang, Y.-L.; Li, X. *Polyhedron* **2005**, *24*, 2955.
(174) Carlucci, L.; Ciani, G.; Proserpio, D. M. *Dalton Trans.* **1999**, 1799.
(175) Carlucci, L.; Ciani, G.; Proserpio, D. M. *Chem. Commun.* **1999**, 449.
(176) (a) Fujita, M.; Kwon, Y. J.; Sasaki, O.; Yamaguchi, K.; Ogura, K. *J. Am. Chem. Soc.* **1995**, *117*, 7287. (b) Fujita, M.; Sasaki, O.; Watanabe, K.-y.; Ogura, K.; Yamaguchi, K. *New J. Chem.* **1998**, 189.
(177) Tao, J.; Yin, X.; Huang, R.; Zheng, L. *Inorg. Chem. Commun.* **2002**, *5*, 1000.
(178) Dong, Y.-B.; Layland, R. C.; Smith, M. D.; Pschirer, N. G.; Bunz, U. H. F.; Loye, H.-C. z. *Inorg. Chem.* **1999**, *38*, 3056.
(179) Wu, C.-D.; Ma, L.; Lin, W. *Inorg. Chem.* **2008**, *47*, 11446.
(180) Blake, A. J.; Li, W.-S.; Lippolis, V.; Schröder, M. *Chem. Commun.* **1997**, 1943.
(181) Moon, H. R.; Choi, C. H.; Suh, M. P. *Angew. Chem., Int. Ed.* **2008**, *47*, 8390.

(182) Song, R.-F.; Xie, Y.-B.; Li, J.-R.; Bu, X.-H. *CrystEngComm* **2005**, *7*, 249.
(183) (a) Su, C.-Y.; Goforth, A. M.; Smith, M. D.; Loye, H.-C. z. *Chem. Commun.* **2004**, 2158. (b) Zaman, M. B.; Udachin, K.; Ripmeester, J. A.; Smith, M. D.; Loye, H.-C. z. *Inorg. Chem.* **2005**, *44*, 5047.
(184) Carlucci, L.; Ciani, G.; Macchi, P.; Proserpio, D. M. *Chem. Commun.* **1998**, 1837.
(185) Huang, Z.; Song, H.-B.; Du, M.; Chen, S.-T.; Bu, X.-H. *Inorg. Chem.* **2004**, *43*, 931.
(186) Sun, B.-W.; Gao, S.; Wang, Z.-M. *Chem. Lett.* **2001**, *1*, 2.
(187) Ghoshal, D.; Mostafa, G.; Maji, T. K.; Zangrando, E.; Lu, T.-H.; Ribas, J.; Chaudhuri, N. R. *New J. Chem.* **2004**, *28*, 1204.
(188) Phuengphai, P.; Youngme, S.; Kongsaeree, P.; Pakawatchai, C.; Chaichit, N.; Teat, S. J.; Gamez, P.; Reedijk, J. *CrystEngComm* **2009**, *11*, 1723.
(189) Li, F.; Li, X.; Li, T.; Su, W.; Cao, R. *J. Mol. Struct.* **2006**, *782*, 116.
(190) (a) Ohba, M.; Fukita, N.; Okawa, H. *Dalton Trans.* **1997**, 1733. (b) Ohba, M.; Maruono, N.; Okawa, H.; Enoki, T.; Latour, J.-M. *J. Am. Chem. Soc.* **1994**, *116*, 11566.
(191) (a) You, Y. S.; Kim, D.; Do, Y.; Oh, S. J.; Hong, C. S. *Inorg. Chem.* **2004**, *43*, 6899. (b) Rodriguez-Dieguez, A.; Colacio, E. *Polyhedron* **2007**, *26*, 2859. (c) Fallah, M. S. E.; Ribas, J.; Solans, X.; Font-Bardia, M. *New J. Chem.* **2003**, *27*, 895. (d) Lim, J. H.; You, Y. S.; Yoo, H. S.; Yoon, J. H.; Kim, J. I.; Koh, E. K.; Hong, C. S. *Inorg. Chem.* **2007**, *46*, 10578.
(192) Zhang, L.; Tang, L.-F.; Wang, Z.-H.; Du, M.; Julve, M.; Lloret, F.; Wang, J.-T. *Inorg. Chem.* **2001**, *40*, 3619.
(193) (a) Sumby, C. J.; Fisher, J.; Prior, T. J.; Hardie, M. J. *Chem.—Eur. J.* **2006**, *12*, 2945. (b) Carruthers, C.; Ronson, T. K.; Sumby, C. J.; Westcott, A.; Harding, L. P.; Prior, T. J.; Rizkallah, P.; Hardie, M. J. *Chem.—Eur. J.* **2008**, *14*, 10286.
(194) Knaust, J. M.; Lopez, S.; Inman, C.; Keller, S. W. *Polyhedron* **2003**, *22*, 3015.
(195) Wang, Y.; Ding, B.; Cheng, P.; Liao, D.-Z.; Yan, S.-P. *Inorg. Chem.* **2007**, *46*, 2002.
(196) Huang, W.; Gou, S.; Hu, D.; Chantrapromma, S.; Fun, H.-K.; Meng, Q. *Inorg. Chem.* **2001**, *40*, 1712.
(197) Motokawa, N.; Oyama, T.; Matsunaga, S.; Miyasaka, H.; Sugimoto, K.; Yamashita, M.; Lopez, N.; Dunbar, K. R. *Dalton Trans.* **2008**, 4099.
(198) Yang, J.; Ma, J.-F.; Liu, Y.-Y.; Ma, J.-C.; Batten, S. R. *Cryst. Growth Des.* **2009**, *9*, 1894.
(199) Werff, P. M. v. d.; Batten, S. R.; Jensen, P.; Moubaraki, B.; Murray, K. S.; Tan, E. H.-K. *Polyhedron* **2001**, *20*, 1129.
(200) Rajput, L.; Biradha, K. *Cryst. Growth Des.* **2007**, *7*, 2376.
(201) Choudhury, A.; Natarajan, S.; Rao, C. N. R. *Inorg. Chem.* **2000**, *39*, 4295.
(202) Wagner, B. D.; McManus, G. J.; Moulton, B.; Zaworotko, M. J. *Chem. Commun.* **2002**, 2176.
(203) Zou, Y.; Liu, W.; Gao, S.; Xie, J.; Meng, Q. *Chem. Commun.* **2003**, 2946.
(204) Kawakami, D.; Yamashita, M.; Matsunaga, S.; Takaishi, S.; Kajiwara, T.; Miyasaka, H.; Sugiura, K.-I.; Matsuzaki, H.; Okamoto, H.; Wakabayashi, Y.; Sawa, H. *Angew. Chem., Int. Ed.* **2006**, *45*, 7214.
(205) (a) Beer, P. D.; Sambrook, M. R.; Curiel, D. *Chem. Commun.* **2006**, 2105. (b) Coronado, E.; Gaviña, P.; Tatay, S. *Chem. Soc. Rev.* **2009**, *38*, 1674. (c) Rescifina, A.; Zagni, C.; Iannazzo, D.; Merino, P. *Curr. Org. Chem.* **2009**, *13*, 448. (d) Harada, A. *Acc. Chem. Res.* **2001**, *34*, 456. (e) Silvi, S.; Venturi, M.; Credi, A. *J. Mater. Chem.* **2009**, *19*, 2279.
(206) (a) Suzaki, Y.; Taira, T.; Osakada, K.; Horie, M. *Dalton Trans.* **2008**, 4823. (b) Batten, S. R.; Robson, R. *Angew. Chem., Int. Ed.* **1998**, *37*, 1460. (c) Loeb, S. J. *Chem. Soc. Rev.* **2007**, *36*, 226. (d) Kim, K. *Chem. Soc. Rev.* **2002**, *31*, 96. (e) Carlucci, L.; Ciani, G.; Proserpio, D. M. *Coord. Chem. Rev.* **2003**, *246*, 247.
(207) Batten, S. R.; Robson, R. Catenane and rotaxane motifs in interpenetrating and self-penetrating coordination polymers. In *Molecular Catenanes, Rotaxanes and Knots*; Sauvage, J.-P., Dietrich-Buchecker, C., Eds.; Wiley: Weinheim, Germany, 2000; pp 77−106.
(208) (a) Whang, D.; Jeon, Y.-M.; Heo, J.; Kim, K. *J. Am. Chem. Soc.* **1996**, *118*, 11333. (b) Park, K.-M.; Whang, D.; Lee, E.; Heo, J.; Kim, K. *Chem.—Eur. J.* **2002**, *8*, 498.
(209) (a) Whang, D.; Heo, J.; Kim, C.-A.; Kim, K. *Chem. Commun.* **1997**, 2361. (b) Whang, D.; Kim, K. *J. Am. Chem. Soc.* **1997**, *119*, 451.
(210) Park, K.-M.; Roh, S.-G.; Lee, E.; Kim, J.; Kim, H.-J.; Lee, J. W.; Kim, K. *Supramol. Chem.* **2002**, *14*, 153.
(211) (a) Liu, Y.; Zhao, Y.-L.; Zhang, H.-Y.; Song, H.-B. *Angew. Chem., Int. Ed.* **2003**, *42*, 3260. (b) Yang, Y.-W.; Chen, Y.; Liu, Y. *Inorg. Chem.* **2006**, *45*, 3014. (c) Vidal, P. L.; Billon, M.; Divisia-Blohorn, B.; Bidan, G.; Kernb, J. M.; Sauvage, J. P. *Chem. Commun.* **1998**, 629. (d) Liu, Y.; Song, S.-H.; Chen, Y.; Zhao, Y.-L.; Yang, Y.-W. *Chem. Commun.* **2005**, 1702.
(212) Davidson, G. J. E.; Loeb, S. J. *Angew. Chem., Int. Ed.* **2003**, *42*, 74.
(213) Knight, L. K.; Vukotic, V. N.; Viljoen, E.; Caputo, C. B.; Loeb, S. J. *Chem. Commun.* **2009**, 5585.
(214) Gao, X.-M.; Li, D.-s.; Wang, J.-J.; Fu, F.; Wu, Y.-P.; Hu, H.-M.; Wang, J.-W. *CrystEngComm* **2008**, *10*, 479.
(215) Plater, M. J.; Foreman, M. R. S. J.; Gelbrich, T.; Hursthouse, M. B. *Cryst. Eng.* **2001**, *4*, 319.
(216) Hoskins, B. F.; Robson, R.; Slizys, D. A. *J. Am. Chem. Soc.* **1997**, *119*, 2952.
(217) Carlucci, L.; Ciani, G.; Proserpio, D. M. *Cryst. Growth Des.* **2005**, *5*, 37.
(218) Hoskins, B. F.; Robson, R.; Slizys, D. A. *Angew. Chem., Int. Ed.* **1997**, *36*, 2336.
(219) Kasai, K.; Sato, M. *Chem. Asian J.* **2006**, *1*, 344.
(220) Tong, M.-L.; Wu, Y.-M.; Ru, J.; Chen, X.-M.; Chang, H.-C.; Kitagawa, S. *Inorg. Chem.* **2002**, *41*, 4846.
(221) Yao, Q.-X.; Ju, Z.-F.; Jin, X.-H.; Zhang, J. *Inorg. Chem.* **2009**, *48*, 1266.
(222) Ng, M. T.; Deivaraj, T. C.; Klooster, W. T.; McIntyre, G. J.; Vittal, J. J. *Chem.—Eur. J.* **2004**, *10*, 5853.
(223) Wang, X.-L.; Qin, C.; Wang, E.-B. *Cryst. Growth Des.* **2006**, *6*, 439.
(224) Dobrzańska, L.; Lloyd, G. O.; Jacobs, T.; Rootman, I.; Oliver, C. L.; Bredenkamp, M. W.; Barbour, L. J. *J. Mol. Struct.* **2006**, *796*, 107.
(225) Noro, S.-i.; Horike, S.; Tanaka, D.; Kitagawa, S.; Akutagawa, T.; Nakamura, T. *Inorg. Chem.* **2006**, *45*, 9290.
(226) Noro, S.-i.; Tanaka, D.; Sakamoto, H.; Shimomura, S.; Kitagawa, S.; Takeda, S.; Uemura, K.; Kita, H.; Akutagawa, T.; Nakamura, T. *Chem. Mater.* **2009**, *21*, 3346.
(227) Zhang, Y.-Z.; Wei, H.-Y.; Pan, F.; Wang, Z.-M.; Chen, Z.-D.; Gao, S. *Angew. Chem., Int. Ed.* **2005**, *44*, 5841.
(228) Kasai, K.; Aoyagi, M.; Fujita, M. *J. Am. Chem. Soc.* **2000**, *122*, 2140.
(229) Wu, C.-D.; Lin, W. *Angew. Chem., Int. Ed.* **2005**, *44*, 1958.
(230) Uemura, K.; Saito, K.; Kitagawa, S.; Kita, H. *J. Am. Chem. Soc.* **2006**, *128*, 16122.
(231) (a) Cui, G.-H.; Li, J.-R.; Tian, J.-L.; Bu, X.-H.; Batten, S. R. *Cryst. Growth Des.* **2005**, *5*, 1775. (b) Lu, Z.; Wen, L.; Ni, Z.; Li, Y.; Zhu, H.; Meng, Q. *Cryst. Growth Des.* **2007**, *7*, 268. (c) Akhbari, K.; Morsali, A. *Cryst. Growth Des.* **2007**, *7*, 2024. (d) Yu, J.-H.; Mereiter, K.; Hassan, N.; Feldgitscher, C.; Linert, W. *Cryst. Growth Des.* **2008**, *8*, 1535. (e) Wen, L.-L.; Lu, Z.-D.; Ren, X.-M.; Duan, C.-Y.; Meng, Q.-J.; Gao, S. *Cryst. Growth Des.* **2009**, *9*, 227. (f) Kasai, K.; Fujita, M. *Chem.—Eur. J.* **2007**, *13*, 3089. (g) Carlucci, L.; Ciani, G.; Maggini, S.; Proserpio, D. M. *CrystEngComm* **2008**, *10*, 1191. (h) Gunning, N. S.; Cahill, C. L. *Dalton Trans.* **2005**, 2788. (i) Luo, J.; Hong, M.; Wang, R.; Yuan, D.; Cao, R.; Han, L.; Xu, Y.; Lin, Z. *Eur. J. Inorg. Chem.* **2003**, 3623. (j) Cui, Y.; Ngo, H. L.; Lin, W. *Inorg. Chem.* **2002**, *41*, 1033. (k) Draper, N. D.; Batchelor, R. J.; Aguiar, P. M.; Kroeker, S.; Leznoff, D. B. *Inorg. Chem.* **2004**, *43*, 6557. (l) Genuis, E. D.; Kelly, J. A.; Patel, M.; McDonald, R.; Ferguson, M. J.; Greidanus-Strom, G. *Inorg. Chem.* **2008**, *47*, 6184. (m) Zhao, Q.; Li, H.; Wang, X.; Chen, Z. *New J. Chem.* **2002**, *26*, 1709. (n) Li, Y.-X.; Li, Y.-H.; Zeng, X.-R.; Xiong, R.-G.; You, X.-Z.; Fun, H.-K. *Inorg. Chem. Commun.* **2003**, *6*, 1144. (o) Zhang, L.-Y.; Zeng, M.-H.; Sun, X.-Z.; Shi, Z.; Feng, S.-H.; Chen, X.-M. *J. Mol. Struct.* **2004**, *697*, 181. (p) MacDonald, M.-A.; Puddephatt, R. J. *Organometallics* **2000**, *19*, 2194. (q) Murugavel, R.; Shanmugan, S.; Kuppuswamy, S. *Eur. J. Inorg. Chem.* **2008**, 1508. (r) Leznoff, D. B.; Shorrock, C. J.; Batchelor, R. J. *Gold Bull.* **2007**, *40*, 36. (s) Geisheimer, A. R.; Katz, M. J.; Batchelor, R. J.; Leznoff, D. B. *CrystEngComm* **2007**, *9*, 1078.
(232) Chang, F.; Wang, Z.-M.; Sun, H.-L.; Gao, S.; Wen, G.-H.; Zhang, X.-X. *Dalton Trans.* **2005**, 2976.
(233) Hong, M.; Zhao, Y.; Su, W.; Cao, R.; Fujita, M.; Zhou, Z.; Chan, A. S. C. *Angew. Chem., Int. Ed.* **2000**, *39*, 2468.
(234) (a) Ma, L.-F.; Wang, L.-Y.; Lu, D.-H.; Batten, S. R.; Wang, J.-G. *Cryst. Growth Des.* **2009**, *9*, 1741. (b) Xu, Y.; Yuan, D.; Wu, B.; Han, L.; Wu, M.; Jiang, F.; Hong, M. *Cryst. Growth Des.* **2006**, *6*, 1168. (c) Kim, T. H.; Shin, Y. W.; Jung, J. H.; Kim, J. S.; Kim, J. *Angew. Chem., Int. Ed.* **2008**, *47*, 685–234. (d) Feng, S.; Zhu, M.; Lu, L.; Guo, M. *Chem. Commun.* **2007**, 4785.
(235) (a) Kahn, O. *Acc. Chem. Res.* **2000**, *33*, 647. (b) Černák, J.; Orendáč, M.; Potočňák, I.; Chomič, J.; Orendáčová, A.; Skoršepa, J.; Feher, A. *Coord. Chem. Rev.* **2002**, *224*, 51. (c) Miller, J. S. *Dalton Trans.* **2006**, 2742. (d) Andruh, M. *Chem. Commun.* **2007**, 2565. (e) Kurmoo, M. *Chem. Soc. Rev.* **2009**, *38*, 1353. (f) Andruh, M.; Costes, J.-P.; Diaz, C.; Gao, S. *Inorg. Chem.* **2009**, *48*, 3342. (g) Miyasaka, H.; Julve, M.; Yamashita, M.; Clérac, R. *Inorg. Chem.* **2009**, *48*, 3420. (h) Sun, H.-L.; Wang, Z.-M.; Gao, S. *Coord. Chem. Rev.* **2010**, *254*, 1081. (i) Winpenny, R., Ed. *Single-Molecule Magnets and Related Phenomena*; Springer: Berlin, 2006; Vol. 122.
(236) Ng, M. T.; Deivaraj, T. C.; Vittal, J. J. *Inorg. Chim. Acta* **2003**, *348*, 173.
(237) Jia, L.; Tang, N.; Vittal, J. J. *Inorg. Chim. Acta* **2009**, *362*, 2525.

(238) Alley, K. G.; Bircher, R.; Waldmann, O.; Ochsenbein, S. T.; Gudel, H. U.; Moubaraki, B.; Murray, K. S.; Fernandez-Alonso, F.; Abrahams, B. F.; Boskovic, C. *Inorg. Chem.* **2006**, *45*, 8950.
(239) Ma, C.-B.; Chen, C.-N.; Liu, Q.-T.; Liao, D.-Z.; Li, L.-C. *Eur. J. Inorg. Chem.* **2008**, 1865.
(240) Casarin, M.; Corvaja, C.; Nicola, C. D.; Falcomer, D.; Franco, L.; Monari, M.; Pandolfo, L.; Pettinari, C.; Piccinelli, F. *Inorg. Chem.* **2005**, *44*, 6265.
(241) Contaldi, S.; Nicola, C. D.; Garau, F.; Karabach, Y. Y.; Martins, L. M. D. R. S.; Monari, M.; Pandolfo, L.; Pettinari, C.; Pombeiro, A. J. L. *Dalton Trans.* **2009**, 4928.
(242) (a) Reddy, K. R.; Rajasekharan, M. V.; Tuchagues, J.-P. *Inorg. Chem.* **1998**, *37*, 5978. (b) Ko, H. H.; Lim, J. H.; Kim, H. C.; Hong, C. S. *Inorg. Chem.* **2006**, *45*, 8847. (c) Yuan, M.; Zhao, F.; Zhang, W.; Wang, Z.-M.; Gao, S. *Inorg. Chem.* **2007**, *46*, 11235. (d) Panja, A.; Shaikh, N.; Vojtíek, P.; Gao, S.; Banerjee, P. *New J. Chem.* **2002**, *26*, 1025.
(243) Han, L.; Zhou, Y.; Zhao, W.-N. *Cryst. Growth Des.* **2008**, *8*, 2052.
(244) Han, L.; Hong, M.; Wang, R.; Wu, B.; Xu, Y.; Lou, B.; Lin, Z. *Chem. Commun.* **2004**, 2578.
(245) (a) Yang, X.; Jones, R. A.; Wiester, M. J.; Oye, M. M.; Wong, W.-K. *Cryst. Growth Des.* **2010**, *10*, 970. (b) Zartilas, S.; Moushi, E. E.; Nastopoulos, V.; Boudalis, A. K.; Tasiopoulos, A. J. *Inorg. Chim. Acta* **2008**, *361*, 4100. (c) Kim, J.; Lim, J. M.; Do, Y. *Eur. J. Inorg. Chem.* **2003**, 2563.
(246) Peng, R.; Li, M.; Li, D. *Coord. Chem. Rev.* **2010**, *254*, 1.
(247) Lee, J. Y.; Kim, H. J.; Jung, J. H.; Sim, W.; Lee, S. S. *J. Am. Chem. Soc.* **2008**, *130*, 13838.
(248) Huang, X.-F.; Fu, D.-W.; Xiong, R.-G. *Cryst. Growth Des.* **2008**, *8*, 1795.
(249) Zhang, J.-J.; Zhou, H.-J.; Lachgar, A. *Angew. Chem., Int. Ed.* **2007**, *46*, 4995.
(250) Zhou, H.; Strates, K. C.; Muñoz, M. Á.; Little, K. J.; Pajerowski, D. M.; Meisel, M. W.; Talham, D. R.; Lachgar, A. *Chem. Mater.* **2007**, *19*, 2238.
(251) Feng, P.; Bu, X.; Zheng, N. *Acc. Chem. Res.* **2005**, *38*, 293–303.
(252) Xie, J.; Bu, X.; Zheng, N.; Feng, P. *Chem. Commun.* **2005**, 4916.
(253) Selby, H. D.; Roland, B. K.; Zheng, Z. *Acc. Chem. Res.* **2003**, *36*, 933.
(254) Selby, H. D.; Orto, P.; Zheng, Z. *Polyhedron* **2003**, *22*, 2999.
(255) Selby, H. D.; Orto, P.; Carducci, M. D.; Zheng, Z. *Inorg. Chem.* **2002**, *41*, 6175.
(256) Xu, L.; Kim, Y.; Kim, S.-J.; Kim, H. J.; Kim, C. *Inorg. Chem. Commun.* **2007**, *10*, 586.
(257) Zhang, W.-H.; Song, Y.-L.; Wei, Z.-H.; Li, L.-L.; Huang, Y.-J.; Zhang, Y.; Lang, J.-P. *Inorg. Chem.* **2008**, *47*, 5332.
(258) Zheng, N.; Bu, X.; Lu, H.; Chen, L.; Feng, P. *J. Am. Chem. Soc.* **2005**, *127*, 14990.
(259) (a) Awaleh, M. O.; Badia, A.; Brisse, F. *Inorg. Chem.* **2007**, *46*, 3185. (b) Delgado, S.; Miguel, P. J. S.; Priego, J. L.; Jiménez-Aparicio, R.; Gómez-García, C. J.; Zamora, F. *Inorg. Chem.* **2008**, *47*, 9128.
(260) Long, D.-L.; Köerler, P.; Farrugia, L. J.; Cronin, L. *Chem. Asian J.* **2006**, *1*, 352.
(261) Thomas, J.; Ramanan, A. *Cryst. Growth Des.* **2008**, *8*, 3390.
(262) Dai, L.; You, W.; Wang, E.; Wu, S.; Su, Z.; Du, Q.; Zhao, Y.; Fang, Y. *Cryst. Growth Des.* **2009**, *9*, 2110.
(263) Izarova, N. V.; Sokolov, M. N.; Samsonenko, D. G.; Rothenberger, A.; Naumov, D. Y.; Fenske, D.; Fedin, V. P. *Eur. J. Inorg. Chem.* **2005**, 4985.
(264) Liu, C.-M.; Zhang, D.-Q.; Zhu, D.-B. *Cryst. Growth Des.* **2006**, *6*, 524.
(265) Shivaiah, V.; Reddy, P. V. N.; Cronin, L.; Das, S. K. *Dalton Trans.* **2002**, 3781.
(266) Shivaiah, V.; Nagaraju, M.; Das, S. K. *Inorg. Chem.* **2003**, *42*, 6604.
(267) An, H.; Xu, T.; Jia, C.; Zheng, H.; Mu, W. *J. Mol. Struct.* **2009**, *933*, 86.
(268) Yao, S.; Zhang, Z.; Li, Y.; Wang, E. *Dalton Trans.* **2009**, 1786.
(269) Dong, B.; Peng, J.; Chen, Y.; Zhang, P.; Tian, A.; Chen, J. *J. Mol. Struct.* **2008**, *875*, 75.
(270) Xu, Z.-H.; Wang, X.-L.; Li, Y.-G.; Wang, E.-B.; Qin, C.; Si, Y.-L. *Inorg. Chem. Commun.* **2007**, *10*, 276.
(271) (a) Cui, X.-B.; Xu, J.-Q.; Meng, H.; Zheng, S.-T.; Yang, G.-Y. *Inorg. Chem.* **2004**, *43*, 8005. (b) Niu, J.-Y.; Wu, Q.; Wang, J.-P. *Dalton Trans.* **2002**, 2512. (c) Niu, J.-Y.; Wei, M.-L.; Wang, J.-P.; Dang, D.-B. *J. Mol. Struct.* **2003**, *655*, 171. (d) Niu, J.-Y.; Wei, M.-L.; Wang, J.-P. *J. Mol. Struct.* **2004**, *689*, 147. (e) Ma, Y.; Li, Y.; Wang, E.; Lu, Y.; Xu, X. *J. Mol. Struct.* **2006**, *791*, 10. (f) Han, Z.; Chai, T.; Zhai, X.; Wang, J.; Hu, C. *Solid State Sci.* **2009**, *11*, 1998.
(272) Winpenny, R. *Single-Molecule Magnets and Related Phenomena*; Springer: Berlin, 2006.
(273) (a) Eppley, H. J.; deVries, N.; Wang, S.; Aubin, S. M.; Tsai, H.-L.; Folting, K.; Hendriekson, D. N.; Christou, G. *Inorg. Chim. Acta* **1997**, *263*, 323. (b) Bai, Y.-L.; Tao, J.; Wernsdorfer, W.; Sato, O.; Huang, R.-B.; Zheng, L.-S. *J. Am. Chem. Soc.* **2006**, *128*, 16428. (c) Xu, H.-B.; Wang, B.-W.; Pan, F.; Wang, Z. M.; Gao, S. *Angew. Chem., Int. Ed.* **2007**, *46*, 7388. (d) Liu, C.-M.; Zhang, D.-Q.; Zhu, D.-B. *Inorg. Chem.* **2009**, *48*, 4980.
(274) Nakata, K.; Miyasaka, H.; Sugimoto, K.; Ishii, T.; Sugiura, K.-I.; Yamashita, M. *Chem. Lett.* **2002**, *31*, 658.
(275) Baca, S. G.; Malaestean, I. L.; Keene, T. D.; Adams, H.; Ward, M. D.; Hauser, J.; Neels, A.; Decurtins, S. *Inorg. Chem.* **2008**, *47*, 11108.
(276) Yoo, J.; Wernsdorfer, W.; Yang, E.-C.; Nakano, M.; Rheingold, A. L.; Hendrickson, D. N. *Inorg. Chem.* **2005**, *44*, 3377.
(277) Sauvage, J.-P., Dietrich-Buchecker, C. *Molecular Catenanes, Rotaxanes and Knots: A Journey through the World of Molecular Topology*; Wiley: Weinheim, Germany, 1999.
(278) Zaman, M. B.; Smith, M. D.; Loye, H.-C. z. *Chem. Commun.* **2001**, 2256.
(279) Carlucci, L.; Ciani, G.; Moret, M.; Proserpio, D. M.; Rizzato, S. *Angew. Chem., Int. Ed.* **2000**, *39*, 1506.
(280) Liao, J.-H.; Juang, J.-S.; Lai, Y.-C. *Cryst. Growth Des.* **2006**, *6*, 354.
(281) Mahmoudi, G.; Morsali, A. *CrystEngComm* **2009**, *11*, 50.
(282) Du, M.; Jiang, X.-J.; Zhao, X.-J. *Chem. Commun.* **2005**, 5521.
(283) Sagué, J. L.; Fromm, K. M. *Cryst. Growth Des.* **2006**, *6*, 1566.
(284) Mahmoudi, G.; Morsali, A. *Inorg. Chim. Acta* **2009**, *362*, 3238.
(285) Carlucci, L.; Ciani, G.; Proserpio, D. M. *Chem. Commun.* **2004**, 380.
(286) Carlucci, L.; Ciani, G.; Proserpio, D. M.; Spadacini, L. *CrystEngComm* **2004**, *6*, 96.
(287) Yang, E.; Zhang, J.; Li, Z.-J.; Gao, S.; Kang, Y.; Chen, Y.-B.; Wen, Y.-H.; Yao, Y.-G. *Inorg. Chem.* **2004**, *43*, 6525.
(288) He, X.; Lu, C.-Z.; Wu, C.-D.; Chen, L.-J. *Eur. J. Inorg. Chem.* **2006**, 2491.
(289) Biradha, K.; Fujita, M. *Chem. Commun.* **2002**, 1866.
(290) Hirsch, K. A.; Wilson, S. R.; Moore, J. S. *Inorg. Chem.* **1997**, *36*, 2960.
(291) (a) Wang, R.; Han, L.; Xu, L.; Gong, Y.; Zhou, Y.; Hong, M.; Chan, A. S. C. *Eur. J. Inorg. Chem.* **2004**, 3751. (b) Wang, X.-L.; Qin, C.; Wang, E.-B.; Su, Z.-M.; Hu, C.-W. *Angew. Chem., Int. Ed.* **2004**, *43*, 5036. (c) Ayyappan, P.; Evans, O. R.; Lin, W. *Inorg. Chem.* **2002**, *41*, 3328.
(292) Tabellion, F. M.; Seidel, S. R.; Arif, A. M.; Stang, P. J. *J. Am. Chem. Soc.* **2001**, *123*, 7740.
(293) Grosshans, P.; Jouaiti, A.; Hosseini, M. W.; Kyritsakas, N. *New J. Chem.* **2003**, *27*, 793.
(294) Duriska, M. B.; Neville, S. M.; Batten, S. R. *Chem. Commun.* **2009**, 5579.
(295) Uemura, K.; Maeda, A.; Kita, H. *Polyhedron* **2008**, *27*, 2939.
(296) Song, Y. J.; Kwak, H.; Lee, Y. M.; Kim, S. H.; Lee, S. H.; Park, B. K.; Jun, J. Y.; Yu, S. M.; Kim, C.; Kim, S.-J.; Kim, Y. *Polyhedron* **2009**, *28*, 1241.
(297) Sharma, C. V. K.; Broker, G. A.; Huddleston, J. G.; Baldwin, J. W.; Metzger, R. M.; Rogers, R. D. *J. Am. Chem. Soc.* **1999**, *121*, 1137.
(298) (a) Prater, M. E.; Pence, L. E.; Clérac, R.; Finniss, G. M.; Campana, C.; Auban-Senzier, P.; Jérome, D.; Canadell, E.; Dunbar, K. R. *J. Am. Chem. Soc.* **1999**, *121*, 8005. (b) Balamurugan, V.; Mukherjee, R. *Inorg. Chim. Acta* **2006**, *359*, 1376. (c) Zang, S.-Q.; Su, Y.; Lin, J.-G.; Li, Y.-Z.; Gao, S.; Meng, Q.-j. *Inorg. Chim. Acta* **2009**, *362*, 2440. (d) Chen, B.-L.; Mok, K.-F.; Ng, S.-C.; Drew, M. G. B. *New J. Chem.* **1999**, *23*, 877.
(299) Wang, X.-T.; Wang, X.-H.; Wang, Z.-M.; Gao, S. *Inorg. Chem.* **2009**, *48*, 1301.
(300) Wu, B.; Yuan, D.; Jiang, F.; Han, L.; Lou, B.; Liu, C.; Hong, M. *Eur. J. Inorg. Chem.* **2005**, 1303.
(301) Zheng, S.-L.; Tong, M.-L.; Yu, X.-L.; Chen, X.-M. *Dalton Trans.* **2001**, 586.
(302) Costes, J.-P.; Gheorghe, R.; Andruh, M.; Shova, S.; Juan, J.-M. C. *New J. Chem.* **2006**, *30*, 572.
(303) Branzea, D. G.; Guerri, A.; Fabelo, O.; Ruiz-Pérez, C.; Chamoreau, L.-M.; Sangregorio, C.; Caneschi, A.; Andruh, M. *Cryst. Growth Des.* **2008**, *8*, 941.
(304) (a) Huang, F.-P.; Tian, J.-L.; Chen, G.-J.; Li, D.-D.; Gu, W.; Liu, X.; Yan, S.-P.; Liao, D.-Z.; Cheng, P. *CrystEngComm* **2010**, *12*, 1269. (b) Lai, C. S.; Tiekink, E. R. T. *CrystEngComm* **2004**, *6*, 593. (c) Lai, C. S.; Liu, S.; Tiekink, E. R. T. *CrystEngComm* **2004**, *6*, 221. (d) Hu, T.-L.; Zou, R.-Q.; Li, J.-R.; Bu, X.-H. *Dalton Trans.* **2008**, 1302.
(305) Wang, X.; Vittal, J. J. *Inorg. Chem. Commun.* **2003**, *6*, 1074.
(306) Wang, X.; Ranford, J. D.; Vittal, J. J. *J. Mol. Struct.* **2006**, *796*, 28.
(307) Seward, C.; Chan, J.; Song, D.; Wang, S. *Inorg. Chem.* **2003**, *42*, 1112.
(308) (a) Lee, J. W.; Kim, E. A.; Kim, Y. J.; Lee, Y.-A.; Pak, Y.; Jung, O.-S. *Inorg. Chem.* **2005**, *44*, 3151. (b) Jung, O.-S.; Kim, Y. J.; Kim, K. M.; Lee, Y.-A. *J. Am. Chem. Soc.* **2002**, *124*, 7906.
(309) Jung, O.-S.; Kim, Y. J.; Lee, Y.-A.; Park, K.-M.; Lee, S. S. *Inorg. Chem.* **2003**, *42*, 844.

(310) Kang, Y.; Lee, S. S.; Park, K.-M.; Lee, S. H.; Kang, S. O.; Ko, J. *Inorg. Chem.* **2001**, *40*, 7027.
(311) Schultheiss, N.; Powell, D. R.; Bosch, E. *Inorg. Chem.* **2003**, *42*, 8886.
(312) Wu, H.-P.; Janiak, C.; Rheinwald, G.; Lang, H. *Dalton Trans.* **1999**, 183.
(313) Awaleh, M. O.; Badia, A.; Brisse, F. *Cryst. Growth Des.* **2006**, *6*, 2674.
(314) Park, K.-M.; Yoon, I.; Seo, J.; Lee, J.-E.; Kim, J.; Choi, K. S.; Jung, O.-S.; Lee, S. S. *Cryst. Growth Des.* **2005**, *5*, 1707.
(315) Jo, M.; Seo, J.; Lindoy, L. F.; Lee, S. S. *Dalton Trans.* **2009**, 6096.
(316) Kim, H. J.; Song, M. R.; Lee, S. Y.; Lee, J. Y.; Lee, S. S. *Eur. J. Inorg. Chem.* **2008**, 3532.
(317) (a) Halper, S. R.; Cohen, S. M. *Angew. Chem., Int. Ed.* **2004**, *43*, 2385. (b) Halper, S. R.; Cohen, S. M. *Inorg. Chem.* **2005**, *44*, 4139. (c) Halper, S. R.; Malachowski, M. R.; Delaney, H. M.; Cohen, S. M. *Inorg. Chem.* **2004**, *43*, 1242. (d) Delgado, S.; Barrilero, A.; Molina-Ontoria, A.; Medina, M. E.; Pastor, C. J.; Jiménez-Aparicio, R.; Priego, J. L. *Eur. J. Inorg. Chem.* **2006**, 2746.
(318) Zhang, X.; Zhou, X.-P.; Li, D. *Cryst. Growth Des.* **2006**, *6*, 1440.
(319) (a) Jouaiti, A.; Jullien, V.; Hosseini, M. W.; Planeix, J.-M.; Cian, A. D. *Chem. Commun.* **2001**, 1114. (b) Kumar, D. K.; Das, A.; Dastidar, P. *CrystEngComm* **2006**, *8*, 805. (c) Park, K.-M.; Moon, S.-T.; Kang, Y. J.; Kim, H. J.; Seo, J.; Lee, S. S. *Inorg. Chem. Commun.* **2006**, *9*, 671. (d) Tang, J.; Costa, J. S.; Pevec, A.; Kozlevčar, B.; Massera, C.; Roubeau, O.; Mutikainen, I.; Turpeinen, U.; Gamez, P.; Reedijk, J. *Cryst. Growth Des.* **2008**, *8*, 1005.
(320) Fromm, K. M.; Doimeadios, J. L. S.; Robin, A. Y. *Chem. Commun.* **2005**, 4548.
(321) Carlucci, L.; Ciani, G.; Proserpio, D. M.; Sironi, A. *J. Am. Chem. Soc.* **1995**, *117*, 4562.
(322) Dobrzanska, L.; Lloyd, G. O.; Esterhuysen, C.; Barbour, L. J. *Angew. Chem., Int. Ed.* **2006**, *45*, 5856.
(323) Dobrzańska, L.; Lloyd, G. O.; Barbour, L. J. *New J. Chem.* **2007**, *31*, 669.
(324) Zhu, L.-G.; Kitagawa, S.; Miyasaka, H.; Chang, H.-C. *Inorg. Chim. Acta* **2003**, *355*, 121.
(325) Dong, Y.-B.; Jiang, Y.-Y.; Li, J.; Ma, J.-P.; Liu, F.-L.; Tang, B.; Huang, R.-Q.; Batten, S. R. *J. Am. Chem. Soc.* **2007**, *129*, 4520.
(326) Go, Y.; Wang, X.; Anokhina, E. V.; Jacobson, A. J. *Inorg. Chem.* **2004**, *43*, 5360.
(327) Go, Y. B.; Wang, X.; Anokhina, E. V.; Jacobson, A. J. *Inorg. Chem.* **2005**, *44*, 8265.
(328) Dobrzańska, L.; Kleinhans, D. J.; Barbour, L. J. *New J. Chem.* **2008**, *32*, 813.
(329) Vittal, J. J.; Wang, X.; Ranford, J. D. *Inorg. Chem.* **2003**, *42*, 3390.
(330) Forster, P. M.; Burbank, A. R.; Livage, C.; Férey, G.; Cheetham, A. K. *Chem. Commun.* **2004**, 368.
(331) Livage, C.; Egger, C.; Férey, G. *Chem. Mater.* **2001**, *13*, 410.
(332) (a) Livage, C.; Egger, C.; Férey, G. *Chem. Mater.* **2000**, *11*, 1546. (b) Livage, C.; Egger, C.; Nogues, M.; Férey, G. *J. Mater. Chem.* **1998**, 2743. (c) Long, L.-S.; Chen, X.-M.; Tong, M.-L.; Sun, Z.-G.; Ren, Y.-P.; Huang, R.-B.; Zheng, L.-S. *Dalton Trans.* **2001**, 2888.
(333) Feazell, R. P.; Carson, C. E.; Klausmeyer, K. K. *Inorg. Chem.* **2006**, *45*, 2627.
(334) Chen, W.; Liu, F.; Xu, D.; Matsumoto, K.; Kishi, S.; Kato, M. *Inorg. Chem.* **2006**, *45*, 5552.
(335) Cordes, D. B.; Hanton, L. R.; Spicer, M. D. *Inorg. Chem.* **2006**, *45*, 7651.
(336) Chen, Y.; Li, H.-X.; Liu, D.; Liu, L.-L.; Li, N.-Y.; Ye, H.-Y.; Zhang, Y.; Lang, J.-P. *Cryst. Growth Des.* **2008**, *8*, 3810.
(337) Uemura, K.; Kumamoto, Y.; Kitagawa, S. *Chem.—Eur. J.* **2008**, *14*, 9565.
(338) Ghosh, S. K.; Savitha, G.; Bharadwaj, P. K. *Inorg. Chem.* **2004**, *43*, 5495.
(339) Ren, C.-X.; Ye, B.-H.; He, F.; Cheng, L.; Chen, X.-M. *CrystEngComm* **2004**, *6*, 200.
(340) Ren, C.-X.; Cheng, L.; Ye, B.-H.; Chen, X.-M. *Inorg. Chim. Acta* **2007**, *360*, 3741.
(341) Yang, E.-C.; Liu, Z.-Y.; Wang, X.-G.; Batten, S. R.; Zhao, X.-J. *CrystEngComm* **2008**, *10*, 1140.
(342) (a) Ghosh, S. K.; Azhakar, R.; Kitagawa, S. *Chem. Asian J.* **2009**, *4*, 870. (b) Lu, X.-M.; Li, P.-Z.; Wang, X.-T.; Gao, S.; Wang, X.-J.; Zhou, L.; Liu, C.-S.; Sui, X.-N.; Feng, J.-H.; Deng, Y.-H.; Jin, Q.-H.; Liu, J.; Liu, N.; Lian, J.-P. *Polyhedron* **2008**, *27*, 3669. (c) Wu, S.-T.; Long, L.-S.; Huang, R.-B.; Zheng, L.-S. *Cryst. Growth Des.* **2007**, *7*, 1746. (d) Yu, Q.; Zhang, X.; Bian, H.; Liang, H.; Zhao, B.; Yan, S.; Liao, D. *Cryst. Growth Des.* **2008**, *8*, 1140. (e) Ma, L.-F.; Wang, L.-Y.; Huo, X.-K.; Wang, Y.-Y.; Fan, Y.-T.; Wang, J.-G.; Chen, S.-H. *Cryst. Growth Des.* **2008**, *8*, 620. (f) Stamatatos, T. C.; Tangoulis, V.; Raptopoulou, C. P.; Terzis, A.; Papaefstathiou, G. S.; Perlepes, S. P. *Inorg. Chem.* **2008**, *47*, 7969.
(343) Abourahma, H.; Moulton, B.; Kravtsov, V.; Zaworotko, M. J. *J. Am. Chem. Soc.* **2002**, *124*, 9990.
(344) Su, C.-Y.; Goforth, A. M.; Smith, M. D.; Loye, H.-C. z. *Inorg. Chem.* **2003**, *42*, 5685.
(345) Jiang, L.; Lu, T.-B.; Feng, X.-L. *Inorg. Chem.* **2005**, *44*, 7056.
(346) Hernández-Ahuactzi, I. F.; Cruz-Huerta, J.; Barba, V.; Höpfl, H.; Zamudio-Rivera, L. S.; Beltrán, H. I. *Eur. J. Inorg. Chem.* **2008**, 1200.
(347) Lozano, E.; Nieuwenhuyzen, M.; James, S. L. *Chem.—Eur. J.* **2001**, *7*, 2644.
(348) Yang, X.; Ranford, J. D.; Vittal, J. J. *Cryst. Growth Des.* **2004**, *4*, 781.
(349) Muthu, S.; Yip, J. H. K.; Vittal, J. J. *Dalton Trans.* **2001**, 3577.
(350) Huang, X.-C.; Zhang, J.-P.; Chen, X.-M. *J. Am. Chem. Soc.* **2004**, *126*, 13218.
(351) Huang, X.-C.; Li, D.; Chen, X.-M. *CrystEngComm* **2006**, *8*, 351.
(352) Blake, A. J.; Brooks, N. R.; Champness, N. R.; Crew, M.; Deveson, A.; Fenske, D.; Gregory, D. H.; Hanton, L. R.; Hubberstey, P.; Schröder, M. *Chem. Commun.* **2001**, 1432.
(353) (a) Horikoshi, R.; Mochida, T.; Kurihara, M.; Mikuriya, M. *Cryst. Growth Des.* **2005**, *5*, 243. (b) Horikoshi, R.; Mochida, T.; Moriyama, H. *Inorg. Chem.* **2001**, *40*, 2430.
(354) Knaust, J. M.; Keller, S. W. *CrystEngComm* **2003**, *5*, 459.
(355) Zhang, J.-P.; Lin, Y.-Y.; Huang, X.-C.; Chen, X.-M. *Chem. Commun.* **2005**, 1258.
(356) Fujita, M.; Kwon, Y. J.; Miyazawaa, M.; Ogura, K. *J. Chem. Soc., Chem. Commun.* **1994**, 1977.
(357) Hennigar, T. L.; MacQuarrie, D. C.; Losier, P.; Rogers, R. D.; Zaworotko, M. J. *Angew. Chem., Int. Ed.* **1997**, *36*, 972.
(358) Lee, I. S.; Shin, D. M.; Chung, Y. K. *Chem.—Eur. J.* **2004**, *10*, 3158.
(359) Zimmer, B.; Bulach, V.; Hosseini, M. W.; Cian, A. D.; Kyritsakas, N. *Eur. J. Inorg. Chem.* **2002**, 3079.
(360) Masaoka, S.; Tanaka, D.; Nakanishi, Y.; Kitagawa, S. *Angew. Chem., Int. Ed.* **2004**, *43*, 2530.
(361) Manna, S. C.; Zangrando, E.; Ribas, J.; Chaudhuri, N. R. *Eur. J. Inorg. Chem.* **2008**, 1400.
(362) Carlucci, L.; Ciani, G.; Maggini, S.; Proserpio, D. M. *Cryst. Growth Des.* **2008**, *8*, 162.
(363) Gao, E.-Q.; Wang, Z.-M.; Liao, C.-S.; Yan, C.-H. *New J. Chem.* **2002**, *26*, 1096.
(364) Lu, X. L.; Leong, W. K.; Hor, T. S. A.; Goh, L. Y. *J. Organomet. Chem.* **2004**, *689*, 1746.
(365) Lu, X. L.; Leong, W. K.; Goh, L. Y.; Hor, A. T. S. *Eur. J. Inorg. Chem.* **2004**, 2504.
(366) Lefebvre, J.; Batchelor, R. J.; Leznoff, D. B. *J. Am. Chem. Soc.* **2004**, *126*, 16117.
(367) (a) Ring, D. J.; Aragoni, C.; Champness, N. R.; Wilson, C. *CrystEngComm* **2005**, *7*, 621. (b) Liu, P.-P.; Wang, Y.-Q.; Tian, C.-Y.; Peng, H.-Q.; Gao, E.-Q. *J. Mol. Struct.* **2009**, *920*, 459.
(368) Vittal, J. J. *Coord. Chem. Rev.* **2007**, *251*, 1781.
(369) Ranford, J. D.; Vittal, J. J.; Wu, D. *Angew. Chem., Int. Ed.* **1998**, *37*, 1114.
(370) Ranford, J. D.; Vittal, J. J.; Wu, D.; Yang, X. *Angew. Chem., Int. Ed.* **1999**, *38*, 3498.
(371) Libri, S.; Mahler, M.; Espallargas, G. M.; Daljit C. N. G., Singh; Soleimannejad, J.; Adams, H.; Burgard, M. D.; Rath, N. P.; Brunelli, M.; Brammer, L. *Angew. Chem., Int. Ed.* **2008**, *47*, 1693.
(372) Campo, J.; Falvello, L. R.; Mayoral, I.; Palacio, F.; Soler, T.; Tomás, M. *J. Am. Chem. Soc.* **2008**, *130*, 2932.
(373) Cai, Y.-P.; Zhou, X.-X.; Zhou, Z.-Y.; Zhu, S.-Z.; Thallapally, P. K.; Liu, J. *Inorg. Chem.* **2009**, *48*, 6341.
(374) Oliver, S.; Kuperman, A.; Lough, A.; Ozin, G. A. *Chem. Mater.* **1996**, *8*, 2391.
(375) Hu, C.; Englert, U. *Acc. Chem. Res.* **2005**, *44*, 2281.
(376) Müller-Buschbaum, K.; Mokaddem, Y. *Z. Anorg. Allg. Chem.* **2008**, *634*, 2360.
(377) Dikarev, E. V.; Li, B.; Chernyshev, V. V.; Shpanchenko, R. V.; Petrukhina, M. A. *Chem. Commun.* **2005**, 3274.
(378) Masciocchi, N.; Galli, S.; Tagliabue, G.; Sironi, A.; Castillo, O.; Luque, A.; Beobide, G.; Wang, W.; Romero, M. A.; Barea, E.; Navarro, J. A. R. *Inorg. Chem.* **2009**, *48*, 3087.
(379) Aslani, A.; Morsali, A. *Chem. Commun.* **2008**, 3402.
(380) Barnett, S. A.; Champness, N. R.; Wilson, C. *Eur. J. Inorg. Chem.* **2005**, 1572.
(381) (a) Nagarathinam, M.; Peedikakkal, A. M. P.; Vittal, J. J. *Chem. Commun.* **2008**, 5277. (b) Nagarathinam, M.; Vittal, J. J. *Macromol. Rapid Commun.* **2006**, *27*, 1091.
(382) Peedikakkal, A. M. P.; Koh, L. L.; Vittal, J. J. *Chem. Commun.* **2008**, 441.
(383) Nagarathinam, M.; Vittal, J. J. *Chem. Commun.* **2008**, 438.
(384) Toh, N. L.; Nagarathinam, M.; Vittal, J. J. *Angew. Chem., Int. Ed.* **2005**, *44*, 2237.
(385) Peedikakkal, A. M. P.; Vittal, J. J. *Inorg. Chem.* **2010**, *49*, 10.

(386) (a) Choudhury, A.; Neeraj, S.; Natarajan, S.; Rao, C. N. R. *J. Mater. Chem.* **2002**, *12*, 1044. (b) Thirumurugan, A.; Rao, C. N. R. *J. Mater. Chem.* **2005**, *15*, 3852.
(387) Heo, J.; Jeon, Y.-M.; Mirkin, C. A. *J. Am. Chem. Soc.* **2007**, *129*, 7712.
(388) Mishra, S.; Jeanneau, E.; Chermette, H.; Daniele, S. E.; Hubert-Pfalzgraf, L. G. *Dalton Trans.* **2008**, 620.
(389) Wang, X.; Vittal, J. J. *Inorg. Chem.* **2003**, *43*, 5135.
(390) Kondo, A.; Noguchi, H.; Kajiro, H.; Carlucci, L.; Mercandelli, P.; Proserpio, D. M.; Tanaka, H.; Kaneko, K.; Kanoh, H. *J. Phys. Chem. B* **2006**, *110*, 25565.
(391) Wheaton, C. A.; Jennings, M. C.; Puddephatt, R. J. *J. Am. Chem. Soc.* **2006**, *128*, 15370.
(392) Brandys, M.-C.; Puddephatt, R. J. *J. Am. Chem. Soc.* **2002**, *124*, 3946.
(393) Wu, B.; Yuan, D.; Lou, B.; Han, L.; Liu, C.; Zhang, C.; Hong, M. *Inorg. Chem.* **2005**, *44*, 9175.
(394) Braga, D.; Giaffreda, S. L.; Grepioni, F.; Polito, M. *CrystEngComm* **2004**, *6*, 458.
(395) Braga, D.; Curzi, M.; Johansson, A.; Polito, M.; Rubini, K.; Grepioni, F. *Angew. Chem., Int. Ed.* **2006**, *45*, 142.
(396) Sereda, O.; Neels, A.; Stoeckli, F.; Stoeckli-Evans, H. *Cryst. Growth Des.* **2008**, *8*, 3380.
(397) Min, K. S.; Suh, M. P. *J. Am. Chem. Soc.* **2000**, *122*, 6834.
(398) Jung, O.-S.; Kim, Y. J.; Lee, Y.-A.; Park, J. K.; Chae, H. K. *J. Am. Chem. Soc.* **2000**, *122*, 9921.
(399) Jung, O.-S.; Kim, Y. J.; Lee, Y.-A.; Chae, H. K.; Jang, H. G.; Hong, J. *Inorg. Chem.* **2001**, *40*, 2105.
(400) Sarkar, M.; Biradha, K. *Cryst. Growth Des.* **2007**, *7*, 1318.
(401) Ghosh, S. K.; Bharadwaj, P. K. *Inorg. Chem.* **2005**, *44*, 3156.
(402) Xue, X.; Wang, X.-S.; Xiong, R.-G.; You, X.-Z.; Abrahams, B. F.; Che, C.-M.; Ju, H.-X. *Angew. Chem., Int. Ed.* **2002**, *41*, 2944.
(403) Zhang, J.-J.; Zhao, Y.; Gamboa, S. A.; Lachgar, A. *Cryst. Growth Des.* **2008**, *8*, 172.
(404) (a) Choudhury, A.; Neeraj, S.; Natarajan, S.; Rao, C. N. R. *J. Mater. Chem.* **2001**, *11*, 1537. (b) Choudhury, A.; Rao, C. N. R. *Chem. Commun.* **2003**, 366.
(405) (a) Vaidhyanathan, R.; Natarajan, S.; Rao, C. N. R. *Dalton Trans.* **2001**, 699. (b) Dan, M.; Rao, C. N. R. *Angew. Chem., Int. Ed.* **2006**, *45*, 281.
(406) Murugavel, R.; Sathiyendiran, M.; Walawalkar, M. G. *Inorg. Chem.* **2001**, *40*, 427.
(407) Sathiyendiran, M.; Murugavel, R. *Inorg. Chem.* **2002**, *41*, 6404.
(408) Pothiraja, R.; Sathiyendiran, M.; Butcher, R. J.; Murugavel, R. *Inorg. Chem.* **2004**, *43*, 7585.
(409) Du, M.; Bu, X.-H.; Guo, Y.-M.; Ribas, J.; Diaz, C. *Chem. Commun.* **2002**, 2550.
(410) (a) Infantes, L.; Chisholm, J.; Motherwell, S. *CrystEngComm* **2003**, *5*, 480. (b) Infantes, L.; Motherwell, S. *CrystEngComm* **2002**, *4*, 454.
(411) Ghosh, S. K.; Ribas, J.; Fallah, M. S. E.; Bharadwaj, P. K. *Inorg. Chem.* **2005**, *44*, 3856.
(412) Prasad, T. K.; Rajasekharan, M. V. *Cryst. Growth Des.* **2008**, *8*, 1346.
(413) Cheng, L.; Lin, J.-B.; Gong, J.-Z.; Sun, A.-P.; Ye, B.-H.; Chen, X.-M. *Cryst. Growth Des.* **2006**, *6*, 2739.
(414) Chen, S.-P.; Yuan, Y.-X.; Pan, L.-L.; Yuan, L.-J. *J. Inorg. Organomet. Polym.* **2008**, *18*, 384.
(415) (a) Manna, S. C.; Zangrando, E.; Ribas, J.; Chaudhuri, N. R. *Eur. J. Inorg. Chem.* **2007**, 4592. (b) Li, P.; Qiu, Y.; Liu, J.; Ling, Y.; Cai, Y.; Yue, S. *Inorg. Chem. Commun.* **2007**, *10*, 705. (c) Ye, B.-H.; Sun, A.-P.; Wu, T.-F.; Weng, Y.-Q.; Chen, X.-M. *Eur. J. Inorg. Chem.* **2005**, 1230.
(416) Sreenivasulu, B.; Vittal, J. J. *Angew. Chem., Int. Ed.* **2004**, *43*, 5769.
(417) Selvakumar, P. M.; Suresh, E.; Subramanian, P. S. *Polyhedron* **2009**, *28*, 245.
(418) Wan, Y.-H.; Zheng, X.-J.; Wang, F.-Q.; Zhou, X.-Y.; Wang, K.-Z.; Jin, L.-P. *CrystEngComm* **2009**, *11*, 278.
(419) Lu, J.; Yu, J.-H.; Chen, X.-Y.; Cheng, P.; Zhang, X.; Xu, J.-Q. *Inorg. Chem.* **2005**, *44*, 5978.
(420) Du, M.; Zou, R.-Q.; Zhong, R.-Q.; Xu, Q. *Inorg. Chem. Commun.* **2007**, *360*, 3442.
(421) Klufers, P.; Schuhmacher, J. *Angew. Chem., Int. Ed.* **1994**, *33*, 1742.
(422) Abuhmaiera, R.; Lan, Y.; Ako, A. M.; Kostakis, G. E.; Mavrandonakis, A.; Klopper, W.; Clérac, R.; Anson, C. E.; Powell, A. K. *CrystEngComm* **2009**, *11*, 1089.
(423) Jin, Y.; Che, Y.; Batten, S. R.; Chen, P.; Zheng, J. *Eur. J. Inorg. Chem.* **2007**, 1925.
(424) Zhang, J.-P.; Lin, Y.-Y.; Huang, X.-C.; Chen, X.-M. *Cryst. Growth Des.* **2006**, *6*, 519.
(425) Mir, M. H.; Vittal, J. J. *Cryst. Growth Des.* **2008**, *8*, 1478.
(426) (a) Fages, F. *Angew. Chem., Int. Ed.* **2006**, *45*, 1680. (b) Lloyd, G. O.; Steed, J. W. *Nature Chem.* **2009**, *1*, 437. (c) Piepenbrock, M.-O. M.; Lloyd, G. O.; Clarke, N.; Steed, J. W. *Chem. Rev.* **2010**, *110*, 1960.
(427) (a) Beck, J. B.; Rowan, S. J. *J. Am. Chem. Soc.* **2003**, *125*, 13922. (b) Zhao, Y.; Beck, J. B.; Rowan, S. J.; Jamieson, A. M. *Macromolecules* **2004**, *37*, 3529. (c) Wei, Q.; James, S. L. *Chem. Commun.* **2005**, 1555. (d) Weng, W.; Beck, J. B.; Jamieson, A. M.; Rowan, S. J. *J. Am. Chem. Soc.* **2006**, *128*, 11663. (e) Weng, W.; Li, Z.; Jamieson, A. M.; Rowan, S. J. *Macromolecules* **2009**, *42*, 236. (f) Weng, W.; Li, Z.; Jamieson, A. M.; Rowan, S. J. *Soft Matter.* **2009**, *5*, 4647. (g) Xing, B.; Choi, M.-F.; Xu, B. *Chem.—Eur. J.* **2002**, *8*, 5028. (h) Xing, B.; Choi, M.-F.; Xu, B. *Chem. Commun.* **2002**, 362. (i) Hui, J. K.-H.; Yu, Z.; MacLachlan, M. J. *Angew. Chem., Int. Ed.* **2007**, *46*, 7980. (j) Yoon, S.; Kwon, W. J.; Piao, L.; Kim, S.-H. *Langmuir* **2007**, *23*, 8295. (k) Luisi, B. S.; Rowland, K. D.; Moulton, B. *Chem. Commun.* **2007**, 2802. (l) Vondrova, M.; McQueen, T. M.; Burgess, C. M.; Ho, D. M.; Bocarsly, A. B. *J. Am. Chem. Soc.* **2008**, *130*, 5563. (m) Zhang, S.; Yang, S.; Lan, J.; Tang, Y.; Xue, Y.; You, J. *J. Am. Chem. Soc.* **2009**, *131*, 1689.
(428) Kim, H.-J.; Lee, J.-H.; Lee, M. *Angew. Chem., Int. Ed.* **2005**, *44*, 5810.
(429) (a) Roubeau, O.; Colin, A.; Schmitt, V.; Clérac, R. *Angew. Chem., Int. Ed.* **2004**, *43*, 3283. (b) Grondin, P.; Roubeau, O.; Castro, M.; Saadaoui, H.; Colin, A.; Clérac, R. *Langmuir* **2010**, *26*, 5184.
(430) (a) Fujigaya, T.; Jiang, D.-L.; Aida, T. *Chem. Asian J.* **2007**, *2*, 106. (b) Kuroiwa, K.; Shibata, T.; Takada, A.; Nemoto, N.; Kimizuka, N. *J. Am. Chem. Soc.* **2004**, *126*, 2016.
(431) Andrews, P. C.; Junk, P. C.; Massi, M.; Silberstein, M. *Chem. Commun.* **2006**, 3317.
(432) (a) Leong, W. L.; Tam, A. Y.-Y.; Batabyal, S. K.; Koh, L. W.; Kasapis, S.; Yam, V. W.-W.; Vittal, J. J. *Chem. Commun.* **2008**, 3628. (b) Leong, W. L.; Batabyal, S. K.; Kasapis, S.; Vittal, J. J. *Chem.—Eur. J.* **2008**, *10*, 8822.
(433) Zhang, S.; Yang, S.; Lan, J.; Yang, S.; You, J. *Chem. Commun.* **2008**, 6170.
(434) Batabyal, S. K.; Peedikakkal, A. M. P.; Ramakrishna, S.; Sow, C. H.; Vittal, J. J. *Macromol. Rapid Commun.* **2009**, *30*, 1356.
(435) Lu, J. Y.; Runnels, K. A.; Norman, C. *Inorg. Chem.* **2001**, *40*, 4516.
(436) Lu, J. Y.; Norman, C.; Abboud, K. A.; Ison, A. *Inorg. Chem. Commun.* **2001**, *4*, 459.
(437) Zhang, X.; Chen, Z.-K.; Loh, K. P. *J. Am. Chem. Soc.* **2009**, *131*, 7210.
(438) Sun, Y.; Ye, K.; Zhang, H.; Zhang, J.; Zhao, L.; Li, B.; Yang, G.; Yang, B.; Wang, Y.; Lai, S.-W.; Che, C.-M. *Angew. Chem., Int. Ed.* **2006**, *45*, 5610.
(439) (a) Camerel, F.; Ziessel, R.; Donnio, B.; Bourgogne, C.; Guillon, D.; Schmutz, M.; Iacovita, C.; Bucher, J.-P. *Angew. Chem., Int. Ed.* **2007**, *46*, 2659. (b) Tam, A. Y.-Y.; Wong, K. M.-C.; Wang, G.; Yam, V. W.-W. *Chem. Commun.* **2008**, 2028.
(440) Lu, W.; Roy, V. A. L.; Che, C.-M. *Chem. Commun.* **2006**, 3972.
(441) Lu, W.; Chui, S. S.-Y.; Ng, K.-M.; Che, C.-M. *Angew. Chem., Int. Ed.* **2008**, *47*, 4568.
(442) Jung, S.; Cho, W.; Lee, H. J.; Oh, M. *Angew. Chem., Int. Ed.* **2009**, *48*, 1459.
(443) (a) Coronado, E.; Galán-Mascarós, J. R.; Monrabal-Capilla, M.; García-Martínez, J.; Pardo-Ibáñez, P. *Adv. Mater.* **2007**, *19*, 1359. (b) Rieter, W. J.; Taylor, K. M. L.; An, H.; Lin, W.; Lin, W. *J. Am. Chem. Soc.* **2006**, *128*, 9024. (c) Vaucher, S.; Li, M.; Mann, S. *Angew. Chem., Int. Ed.* **2000**, *39*, 1793. (d) Lin, W.; Rieter, W. J.; Taylor, K. M. L. *Angew. Chem., Int. Ed.* **2009**, *48*, 650. (e) Spokoyny, A. M.; Kim, D.; Sumrein, A.; Mirkin, C. A. *Chem. Soc. Rev.* **2009**, *38*, 1218.
(444) Oh, M.; Mirkin, C. A. *Nature* **2005**, *438*, 651.
(445) Oh, M.; Mirkin, C. A. *Angew. Chem., Int. Ed.* **2006**, *45*, 5492.
(446) Rieter, W. J.; Pott, K. M.; Taylor, K. M. L.; Lin, W. *J. Am. Chem. Soc.* **2008**, *130*, 11584.
(447) Sun, X.; Dong, S.; Wang, E. *J. Am. Chem. Soc.* **2005**, *127*, 13102.
(448) (a) Imaz, I.; Maspoch, D.; Rodriguez-Blanco, C.; Perez-Falcon, J. M.; Campo, J.; Ruiz-Molina, D. *Angew. Chem., Int. Ed.* **2008**, *47*, 1857. (b) Maeda, H.; Hasegawa, M.; Hashimoto, T.; Kakimoto, T.; Nishio, S.; Nakanishi, T. *J. Am. Chem. Soc.* **2006**, *128*, 10024. (c) Park, K. H.; Jang, K.; Son, S. U.; Sweigart, D. A. *J. Am. Chem. Soc.* **2006**, *128*, 8740.
(449) (a) Jeon, Y.-M.; Armatas, G. S.; Heo, J.; Kanatzidis, M. G.; Mirkin, C. A. *Adv. Mater.* **2008**, *20*, 2105. (b) Jeon, Y.-M.; Armatas, G. S.; Kim, D.; Kanatzidis, M. G.; Mirkin, C. A. *Small* **2009**, *5*, 46.
(450) (a) Imaz, I. J. H.; Ruiz-Molina, D.; Maspoch, D. *Angew. Chem., Int. Ed.* **2009**, *48*, 2325. (b) Champness, N. R. *Angew. Chem., Int. Ed.* **2009**, *48*, 2274.
(451) Kim, S. B.; Cai, C.; Sun, S.; Sweigart, D. A. *Angew. Chem., Int. Ed.* **2009**, *48*, 2907.
(452) (a) Shen, Z.-R.; Wang, J.-G.; Sun, P.-C.; Ding, D.-T.; Chen, T.-H. *Chem. Commun.* **2009**, 1742. (b) Johnson, K. T.; Gribb, T. E.; Smoak, E. M.; Banerjee, I. A. *Chem. Commun.* **2010**, *46*, 1757.
(453) Liu, B.; Qian, D.-J.; Chen, M.; Wakayama, T.; Nakamura, C.; Miyake, J. *Chem. Commun.* **2006**, 3175.

(454) Yan, Y.; Martens, A. A.; Besseling, N. A. M.; Wolf, F. A. D.; Keizer, A. D.; Drechsler, M.; Stuart, M. A. C. *Angew. Chem., Int. Ed.* **2008**, *47*, 4192.
(455) Paulusse, J. M. J.; Sijbesma, R. P. *Angew. Chem., Int. Ed.* **2004**, *43*, 4460.
(456) Ikeda, M.; Tanaka, Y.; Hasegawa, T.; Furusho, Y.; Yashima, E. *J. Am. Chem. Soc.* **2006**, *128*, 6806.
(457) Kim, H.-J.; Lee, E.; Park, H.-S.; Lee, M. *J. Am. Chem. Soc.* **2007**, *129*, 10994.
(458) Karthikeyan, S.; Potisek, S. L.; Piermattei, A.; Sijbesma, R. P. *J. Am. Chem. Soc.* **2008**, *130*, 14968.
(459) Tokuhisa, H.; Kanesato, M. *Langmuir* **2005**, *21*, 9728.
(460) Mas-Ballesté, R.; Castillo, O.; Miguel, P. J. S.; Olea, D.; Gómez-Herrero, J.; Zamora, F. *Eur. J. Inorg. Chem.* **2009**, 2885.
(461) Olea, D.; González-Prieto, R.; Priego, J. L.; Barral, M. C.; Pablo, P. J. D.; Torres, M. R.; Gómez-Herrero, J.; Jiménez-Aparicio, R.; Zamora, F. *Chem. Commun.* **2007**, 1591.
(462) (a) Welte, L.; González-Prieto, R.; Olea, D.; Torres, M. R.; Priego, J. L.; Jiménez-Aparicio, R.; Gómez-Herrero, J.; Zamora, F. *ACS Nano* **2008**, *2*, 2051. (b) Welte, L.; García-Couceiro, U.; Castillo, O.; Olea, D.; Polop, C.; Guijarro, A.; Luque, A.; Gómez-Rodríguez, J. M.; Gómez-Herrero, J.; Zamora, F. *Adv. Mater.* **2009**, *21*, 2025.
(463) García-Couceiro, U.; Olea, D.; Castillo, O.; Luque, A.; Román, P.; Pablo, P. J. D.; Gómez-Herrero, J.; Zamora, F. *Inorg. Chem.* **2005**, *44*, 8343.
(464) (a) Olea, D.; Alexandre, S. S.; Amo-Ochoa, P.; Guijarro, A.; Jesús, F. D.; Soler, J. M.; Pablo, P. J. D.; Zamora, F.; Gómez-Herrero, J. *Adv. Mater.* **2005**, *17*, 1761. (b) Olea, D.; Garcia-Couceiro, U.; Castillo, O.; Gomez-Herrero, J.; Zamora, F. *Inorg. Chim. Acta* **2007**, *360*, 48. (c) Amo-Ochoa, P.; Rodríguez-Tapiador, M. I.; Castillo, O.; Olea, D.; Guijarro, A.; Alexandre, S. S.; Gómez-Herrero, J. G.; Zamora, F. *Inorg. Chem.* **2006**, *45*, 7642. (d) Novokmet, S.; Alam, M. S.; Dremov, V.; Heinemann, F. W.; Muller, P.; Alsfasser, R. *Angew. Chem., Int. Ed.* **2005**, *44*, 803. (e) Mateo-Marti, E.; Welte, L.; Amo-Ochoa, P.; Miguel, P. J. S.; Gómez-Herrero, J.; Martin-Gago, J. A.; Zamora, F. *Chem. Commun.* **2008**, 945. (f) Alam, M. S.; Scheurer, A.; Saalfrank, R. W.; Müller, P. *Z. Naturforsch. B* **2008**, *63*, 1443.
(465) (a) Amo-Ochoa, P.; Castillo, O.; Alexandre, S. S.; Welte, L.; Pablo, P. J. D.; Rodríguez-Tapiador, M. I.; Gómez-Herrero, J.; Zamora, F. *Inorg. Chem.* **2009**, *48*, 7931. (b) Alexandrea, S. S.; Soler, J. M.; Miguel, P. J. S.; Nunes, R. W.; Yndurain, F.; Gómez-Herrero, J.; Zamora, F. *Appl. Phys. Lett.* **2007**, *90*, 193107. (c) Mitsumi, M.; Murase, T.; Kishida, H.; Yoshinari, T.; Ozawa, Y.; Toriumi, K.; Sonoyama, T.; Kitagawa, H.; Mitani, T. *J. Am. Chem. Soc.* **2001**, *123*, 11179. (d) Calzolari, A.; Alexandre, S. S.; Zamora, F.; Felice, R. D. *J. Am. Chem. Soc.* **2008**, *130*, 5552. (e) Welte, L.; Calzolari, A.; Felice, R. D.; Zamora, F.; Gómez-Herrero, J. *Nat. Nanotechnol.* **2010**, *5*, 110. (f) Guijarro, A.; Castillo, O.; Welte, L.; Calzolari, A.; Miguel, P. J. S.; Gómez-García, C. J.; Olea, D.; Felice, R. D.; Gómez-Herrero, J.; Zamora, F. *Adv. Funct. Mater.* **2010**, *20*, 1451.
(466) Liu, X. *Angew. Chem., Int. Ed.* **2009**, *48*, 3018.
(467) Shen, X.-F.; Yan, X.-P. *Angew. Chem., Int. Ed.* **2007**, *46*, 7659.
(468) Lu, X.; Yavuz, M. S.; Tuan, H.-Y.; Korgel, B. A.; Xia, Y. *J. Am. Chem. Soc.* **2008**, *130*, 8900.
(469) Mao, J.; Shu, Q.; Wen, Y.; Yuan, H.; Xiao, D.; Choi, M. M. F. *Cryst. Growth Des.* **2009**, *9*, 2546.
(470) Nagarathinam, M.; Chen, J.; Vittal, J. J. *Cryst. Growth Des.* **2009**, *9*, 2457.
(471) (a) Xiong, Y.; Li, Z.; Zhang, R.; Xie, Y.; Yang, J.; Wu, C. *J. Phys. Chem. B* **2003**, *107*, 3697. (b) Xiong, Y.; Xie, Y.; Li, Z.; Wu, C. *Chem.—Eur. J.* **2003**, *9*, 1645. (c) Su, C.-Y.; Goforth, A. M.; Smith, M. D.; Pellechia, P. J.; Loye, H.-C. z. *J. Am. Chem. Soc.* **2004**, *126*, 3576. (d) Li, Z.; Xiong, Y.; Xie, Y. *Nanotechnology* **2005**, *16*, 2303. (e) Zhang, F.; Bei, F.-L.; Cao, J.-M.; Wang, X. *J. Solid State Chem.* **2008**, *181*, 143. (f) Sahu, R. K.; Ray, A. K.; Pathak, T. M. C. *Cryst. Growth Des.* **2008**, *8*, 3754.
(472) (a) Banerjee, P.; Kar, S.; Bhaumik, A.; Lee, G.-H.; Peng, S.-M.; Goswami, S. *Eur. J. Inorg. Chem.* **2007**, 835. (b) Nagarathinam, M.; Saravanan, K.; Leong, W. L.; Balaya, P.; Vittal, J. J. *Cryst. Growth Des.* **2009**, *9*, 4461. (c) Aslani, A.; Morsali, A.; Zeller, M. *Solid State Sci.* **2008**, *10*, 1591. (d) Mohammadi, M.; Morsali, A. *Mater. Lett.* **2009**, *63*, 2349. (e) Haddadian, H.; Aslani, A.; Morsali, A. *Inorg. Chim. Acta* **2009**, *362*, 1805. (f) Soltanzadeh, N.; Morsali, A. *Polyhedron* **2009**, *28*, 1343. (g) Khanjani, S.; Morsali, A. *J. Mol. Struct.* **2009**, *935*, 27. (h) Khanjani, S.; Morsali, A. *J. Coord. Chem.* **2009**, *62*, 3642. (i) Khanjani, S.; Morsali, A. *J. Coord. Chem.* **2009**, *62*, 3343. (j) Bigdeli, F.; Morsali, A. *Mater. Lett.* **2010**, *64*, 4. (k) Bigdeli, F.; Morsali, A.; Retailleau, P. *Polyhedron* **2010**, *29*, 801. (l) Soltanzadeh, N.; Morsali, A. *Ultrason. Sonochem.* **2010**, *17*, 139. (m) Pramanik, A.; Das, G. *CrystEngComm.* **2010**, *12*, 401.
(473) Maddox, J. *Nature* **1988**, *335*, 201.

CR100160E